

ADVANCED BIOPOWER GENERATION VIA  
GASIFICATION OF BIOMASS AND MUNICIPAL  
SOLID WASTE

By

NATARIANTO INDRAWAN

Bachelor of Engineering in Gas and Petrochemical  
Engineering  
Universitas Indonesia  
Depok, Indonesia  
2002

Master of Engineering in Bioenergy and Biomaterials  
Engineering  
Chonnam National University  
Gwangju, Korea  
2012

Submitted to the Faculty of the  
Graduate College of the  
Oklahoma State University  
in partial fulfillment of  
the requirements for  
the Degree of  
DOCTOR OF PHILOSOPHY  
December, 2018

ADVANCED BIOPOWER GENERATION VIA  
GASIFICATION OF BIOMASS AND MUNICIPAL  
SOLID WASTE

Dissertation Approved:

Dr. Ajay Kumar

---

Dissertation Adviser

Dr. Raymond L. Huhnke

---

Dr. Scott Stoodley

---

Dr. Khaled A. Sallam

---

## ACKNOWLEDGEMENTS

With the completion of this dissertation, my school career finally comes to an end. This is a great moment that is worth being cherished forever in my life indeed. But more important, I owe my deepest gratitude to those who devote their time and effort to guide and help me to make this achievement.

First and foremost, I am deeply indebted to my advisor, Dr. Ajay Kumar, for his mentorship role during my whole doctoral work. I appreciate all his contributions of time, ideas, and assistantship funding to make my Ph.D. experience productive and stimulating. Dr. Kumar provided me with every bit of guidance, assistance, and expertise that I needed to improve my research skills and records.

I would like to thank Dr. Raymond L. Huhnke, from Biosystems and Agricultural engineering department, Oklahoma State University for supporting my research activities over my study. I gratefully extend my acknowledgement to Dr. Scott Stoodley, who accepted me as a Ph.D student under the Environmental Science and Graduate Program, Oklahoma State University. I would like to thank Dr. Khaled A. Sallam, for his devoted time and valuable advice over my Ph.D. research.

I am very thankful to Mr. Mark Gilstrap, lab manager of the bioenergy lab where most of my Ph.D. research activities occurred, for substantial guidance and comments on lab safety and handling and repairing of analytical instruments. I also appreciate the support from the staff in

BAE lab, Mr. Wayne R. Kiner, Mr. Mike Veldman, and Mr. Jason Walker, for supporting my work in the laboratory.

I have been blessed with a friendly and cheerful group of fellow students. Many thanks to Dr. Prakash Bhoi, Redemptus Tshikesho, Sunil Thapa, Dr. Kezhen Qian, Dr. Zixu Yang, Cody Collins and Hindu Negi for their assistance and collaboration on my Ph.D. research.

I also extend my gratitude for the Indonesian Endowment Fund for Education (LPDP), which has been a financial sponsor to support my study. I would like to express my deep gratitude to all staff in the National Energy Technology Laboratory (NETL) for giving me an opportunity to complete my research and be a part of one of the most productive research groups in the globe. Thank you to Dr. David Tucker, Dr. Lawrence J. Shadle, Dr. Farida Harun, Dr. Nana Zhou, Dr. Paolo Pezzini, Hao Chen, Harry Bonilla, and all summer intern students 2018.

Finally, I would like to express my heart-felt gratitude to my family for their love, patience and sacrifices. Without them, none of this would have been possible. I am grateful to my parents for their continuous support and encouragement of all my pursuits. Especially to my father, although he has been rest in peace, his life always motivates me in striving my academic endeavor. I am also thankful to my lovely kids, Hafidz, Afifah, and Fatih for accompanying me during the study. Their smiles always motivate me to beat all circumstances, and at the same time stimulate me to strive harder and take more responsibility in my future life. This last word of acknowledgment I have saved for my dearest wife, Yanthi Brihtsanthi, who has been with me throughout my whole Ph.D. pursuit and made this all one of the best gifts during the best years of my life.

Name: NATARIANTO INDRAWAN

Date of Degree: DECEMBER, 2018

Title of Study: ADVANCED BIOPOWER GENERATION VIA GASIFICATION OF BIOMASS AND MUNICIPAL SOLID WASTE

Major Field: ENVIRONMENTAL SCIENCE

Abstract: The overall goal of this study was to develop and analyze efficient power generation systems through the downdraft gasification of biomass and municipal solid waste (MSW) for distributed power applications. This goal was accomplished with the following major objectives that were focus of dissertation chapters. The literature review of power generation and emissions from gasification-based technologies was presented in Chapter 1. Performance and emission analyses of experimental of a 10-kW internal combustion (IC) engine running on syngas generated from gasification of a low density biomass was presented in Chapter 2. Engine performance was satisfactory with maximum load of 5 kW, resulting in an electrical efficiency of 21.3%. The only modification made to the engine was addition of a single venturi pipe in the air-intake system for adjusting flows and mixing of air and syngas. Chapter 3 focused on performance and emission analyses of the gasification-energy system when biomass mixed with MSW in various ratios was used as the feedstock (co-gasification). The air-intake system was further modified using a two series venturi pipe. The gasification and engine performance was stable with maximum MSW weight ratio of 40 wt.%, producing the maximum engine output power of 5 kW with an electrical efficiency of 19.5%. An increase in MSW ratio resulted in an increase of hydrocarbon and SO<sub>2</sub> engine emissions. An economic analysis of a 60-kW power plant based on the downdraft gasification system was presented in Chapter 4. The downdraft gasification power plant showed a payback period, an internal rate of return (IRR), a modified internal rate of return (MIRR), and a net present value (NPV) of 7.7 years, 10.9%, 7.7%, and \$84,550, respectively. Using sensitivity analysis, feed-in-tariff resulted in the greatest impact on the project's NPV, followed by the electricity selling price, the output power and the tipping fee, while the labor and feedstock cost and the tax rate generated a negative impact on the NPV. In comparison with a commercially available 250-kW downdraft gasification power generation, the downdraft gasification power plant performed a shorter payback period and a higher IRR. However, these results may vary significantly based on local economic factors and assumptions made. Modeling of low-temperature plasma gasification technology using MSW was the main focus of Chapter 5. At temperatures of 2,500, 2000, and 1,500°C, the energy consumption of the plasma torch decreased from 3,816 kW at conventional condition (4000°C) to 3,157, 2,775, and 2,358 kW, respectively, with corresponding gasification efficiency of 48.7%, 48.9%, and 49.2%. Finally, Chapter 6 focused on a simulation based on experimental data was used to investigate performance of a hybrid power generation (solid oxide fuel cell and gas turbine) using syngas generated from gasification of biomass and municipal solid waste mixture. At 40 wt.% MSW ratio, the syngas produced resulting in a total stack power of 307 kW, and a gas turbine output of 40 kW with a system electrical efficiency of 49.5%.

## TABLE OF CONTENTS

Chapter	Page
CHAPTER 1. INTRODUCTION AND LITERATURE REVIEW: ADVANCES AND CHALLENGES OF DISTRIBUTED POWER GENERATION VIA BIOMASS AND MUNICIPAL SOLID WASTE GASIFICATION.....	1
1.1. Introduction.....	3
1.2. Gasification versus direct combustion.....	5
1.3. Advancements in biomass and MSW gasification.....	9
1.3.1. Gasifier design.....	11
1.3.2. Feeding and auxiliary system.....	15
1.3.3. Syngas conditioning system.....	16
1.4. Advancement and challenges in distributed power generation from syngas.....	17
1.4.1. Combustion characteristics of syngas.....	19
1.4.2. IC engines.....	21
1.4.2.1. Key operational parameters of ICEs.....	21
1.4.2.2. Natural gas engine.....	23
1.4.2.3. Gasoline engine.....	25
1.4.2.4. Compressed ignition engine.....	27
1.4.3. Gas turbines.....	31
1.4.4. Micro gas turbine.....	34
1.4.5. Steam plant.....	35
1.4.6. Stirling engine.....	36
1.4.7. Organic Rankine Cycle generators.....	38
1.4.8. Fuel cells (FCs).....	39
1.4.8.1. Types of fuel cells and their characteristics.....	40
1.4.8.2. SOFC as distributed power generation.....	42
1.4.8.3. Recent status and challenges of FCs development in the U.S.....	45

Chapter	Page
1.4.9. Polygeneration based syngas.....	46
1.5. Economic analyses of power generation from biomass and MSW gasification....	48
1.5.1. Biomass .....	49
1.5.1.1. Economic potential of gasification of biomass and MSW.....	49
1.5.1.2. Lesson learned from Muzizi Plant, Uganda.....	53
1.5.2. MSW .....	57
1.5.2.1. Economic potential of plasma gasification .....	58
1.5.2.2. Lesson learned from Utashinai Plant, Japan .....	62
1.5.3. Techno-economic comparison of various technologies to generate power from syngas .....	63
1.6. Socio-environmental analyses of power generation based gasification of biomass and MSW .....	66
1.6.1. Social analysis .....	66
1.6.1.1. Creation of employment .....	66
1.6.1.2. Community development.....	67
1.6.2. Environmental analysis and its pertinent standard.....	69
1.6.2.1. Ash / slag.....	69
1.6.2.2. Particulates (PMs) / Fly ash .....	71
1.6.2.3. Flue Gas Emissions.....	71
1.6.2.3.1. Emission and its control strategy.....	72
1.6.2.3.2. Lesson Learned from Valmet Plant, Finland.....	81
1.6.2.3.3. MSW Gasification and its Pertinent Standards .....	83
1.6.2.4. Wastewater.....	85
1.7. Conclusions.....	86
<b>CHAPTER 2. ENGINE POWER GENERATION AND EMISSION PERFORMANCE OF SYNGAS GENERATED FROM LOW DENSITY BIOMASS .....</b>	<b>89</b>
2.1. Introduction.....	92
2.2. Material and Methods .....	94
2.2.1. Materials.....	94
2.2.2. Gasifier specification.....	95
2.2.3. Gasification efficiency .....	95

Chapter	Page
2.2.4. Syngas cleaning system.....	96
2.2.5. Power generation unit and emissions analysis .....	97
2.2.6. Method of operating the engine on syngas and natural gas .....	98
2.2.7. Power performance and emission analyses .....	101
2.2.8. Statistical analysis .....	101
2.3. Results and discussion .....	102
2.3.1. Gasification operation and condition .....	102
2.3.2. Syngas quality .....	103
2.3.3. The characteristics of power generation.....	105
2.3.3.1. Effect on engine performance and operation .....	105
2.3.3.2. Power de-rating.....	108
2.3.4. Emissions characteristics.....	109
2.3.4.1. CO <sub>2</sub> emission .....	112
2.3.4.2. CO emission.....	113
2.3.4.3. NO <sub>x</sub> emission .....	113
2.3.4.4. Hydrocarbon emission .....	114
2.3.4.5. SO <sub>2</sub> emission.....	115
2.4. Conclusions.....	115
<b>CHAPTER 3. POWER GENERATION FROM CO-GASIFICATION OF MUNICIPAL SOLID WASTES AND BIOMASS: ELECTRICITY GENERATION AND EMISSION PERFORMANCE.....</b>	<b>118</b>
3.1. Introduction.....	120
3.2. Materials and method.....	124
3.2.1. Materials .....	124
3.2.2. Gasifier description .....	126
3.2.3. Syngas cleaning system.....	127
3.2.4. Gasifier operation .....	127
3.2.5. Power generation unit and emissions analysis .....	130
3.2.6. Statistical analysis .....	131
3.3. Results and discussion .....	132
3.3.1. Gasifier performance .....	132

Chapter	Page
3.3.2. Syngas quality .....	133
3.3.3. The characteristics of power generation.....	135
3.3.3.1. Effect on engine performance and operation .....	135
3.3.3.2. Power de-rating.....	139
3.3.4. Emissions characteristics.....	139
3.3.4.1. CO emission.....	142
3.3.4.2. NO <sub>x</sub> emission .....	143
3.3.4.3. Hydrocarbon (HC) emission.....	145
3.3.4.4. SO <sub>2</sub> emission.....	145
3.3.4.5. CO <sub>2</sub> emission .....	146
3.4. Conclusions.....	146
<b>CHAPTER 4. ECONOMICS OF DISTRIBUTED POWER GENERATION VIA GASIFICATION OF BIOMASS AND MUNICIPAL SOLID WASTES .....</b>	<b>149</b>
4.1. Introduction.....	152
4.2. Economic assets of gasification technologies.....	156
4.3. Methodology .....	157
4.3.1. Gasifier characteristics .....	159
4.3.2. Basic key economic inputs .....	160
4.4. Results and discussion .....	167
4.4.1. Downdraft gasification power system.....	168
4.4.2. Comparison to other downdraft gasification power plant .....	172
4.5. Conclusions.....	174
<b>CHAPTER 5. MODELLING LOW-TEMPERATURE PLASMA GASIFICATION OF MUNICIPAL SOLID WASTE .....</b>	<b>176</b>
5.1. Introduction.....	178
5.2. Material and Methods .....	180
5.2.1. Plasma gasification model.....	180
5.2.2. Model comparison.....	185
5.2.3. System performance.....	186
5.2.4. Sensitivity analysis .....	187
5.3. Results and Discussion .....	188

Chapter	Page
5.3.1. Model comparison .....	188
5.3.2. The energy consumption .....	189
5.3.3. Gasification efficiency .....	190
5.3.4. Effect on syngas characteristics .....	191
5.3.5. System performance .....	193
5.3.6. Sensitivity analysis .....	195
5.4. Conclusions .....	196
<b>CHAPTER 6. PERFORMANCE ANALYSIS OF SOFC/GT HYBRID POWER GENERATION FROM GASIFICATION OF MUNICIPAL SOLID WASTE .....</b>	
	<b>197</b>
6.1. Introduction .....	200
6.2. Materials and Method .....	205
6.2.1. Gasification performance .....	207
6.2.2. Syngas requirement .....	208
6.2.3. SOFC/GT hybrid power generation system .....	209
6.2.3.1. System description .....	209
6.2.3.2. System performance .....	214
6.3. Results and discussion .....	216
6.3.1. Gasification performance .....	216
6.3.2. SOFC/GT performance .....	216
6.3.2.1. SOFC/GT operating performance .....	217
6.3.2.1.1. Current density .....	218
6.3.2.1.2. Degradation rate .....	219
6.3.2.1.3. Fuel cell solid and gas temperature .....	220
6.3.2.1.4. Syngas composition changes .....	222
6.3.2.1.5. Activation loss .....	226
6.3.2.1.6. Ohmic loss .....	227
6.3.2.1.7. Nernst potential .....	228
6.4. Conclusions .....	229
<b>CHAPTER 7. SUMMARY AND RECOMMENDATIONS FOR FUTURE WORK... 231</b>	
7.1. Summary .....	232
7.2. Future work .....	235

Chapter	Page
References.....	238
Appendices.....	255

## LIST OF TABLES

Table	Page
Table 1.1. Major differences between gasification and direct combustion (incineration)..	6
Table 1.2. Major chemical reactions involved in the biomass and MSW gasification .....	8
Table 1.3. Advanced gasifiers and their main characteristics available worldwide .....	14
Table 1.4. Typical gas quality requirements for power generation .....	17
Table 1.5. Performances of state-of-the-art engines running on 100% syngas for distributed power generation .....	29
Table 1.6. Comparison of fuel cells intended for distributed power generation.....	41
Table 1.7. Several polygeneration systems available in the current market .....	47
Table 1.8. Power production cost from gasification technology using various feedstock	52
Table 1.9. Proximate and ultimate analysis of different MSW and biomass.....	58
Table 1.10. List of power generation plants using plasma technology for treating MSW	59
Table 1.11. Techno-economic comparison of various technologies to generate power from syngas .....	64
Table 1.12. Leaching test and acid extraction test of ash disposed from MSW gasification power plant .....	70
Table 1.13. The possible elemental pollutants generated from gasification of biomass and MSW and fundamental abatement strategies to reduce their levels.....	72
Table 1.14. The emission performance of 2 x 80 MW CFB gasifier for steam power plant using wood biomass at Lahti Energia, Finland .....	82
Table 1.15. Comparative analyses of emissions performance of MSW gasification and incineration plants .....	84
Table 2.1. The properties of switchgrass used in the experiment.....	94
Table 2.2. The SI engine and generator specification.....	97
Table 2.3. The experimental conditions.....	100
Table 2.4. P-values of interaction between the load increment and the emission level.	112

Table	Page
Table 3.1. The proximate and ultimate analyses of MSW and SG.....	125
Table 3.2. The experimental conditions.....	130
Table 4.1. The equipment and materials of the downdraft gasifier .....	161
Table 4.2. The operation and maintenance costs of the 60–kW downdraft gasifier.....	162
Table 4.3. The depreciation with the 50% first-year bonus depreciation .....	165
Table 4.4. Basic key economic inputs .....	166
Table 4.5. The worse, baseline and best scenario that can occur during operation .....	172
Table 4.6. The comparison of economics performance between two gasification power plants .....	173
Table 5.1. Main blocks description in AspenPlus <sup>TM</sup> plasma gasification model.....	181
Table 5.2. The model comparison with previous studies using equilibrium techniques	189
Table 5.3. Performance of the plasma gasification and conventional air gasification of MSW .....	194
Table 6.1. Major composition of syngas derived from co-gasification of MSW and switchgrass .....	208
Table 6.2. Syngas compositions at STRC=2.0 used in the hybrid system .....	209
Table 6.3. SOFC/GT parameters and operating condition .....	214
Table 6.4. The overall operating performance of SOFC/GT at steady state.....	217

## LIST OF FIGURES

Figure	Page
Figure 1.1. The steps of gasification and temperature profile .....	10
Figure 1.2. Synopsis of the efficiency data of various power generation units .....	19
Figure 1.3. Comparison of flame characteristics (PLIF fluorescence signal) of (a) methane, and various syngas fuels generated from (b) bituminous coal , (c) wood residue, (d) corn core, and (e) wheat straw .....	21
Figure 1.4. Efficiency of a natural gas ICE versus load .....	23
Figure 1.5. Sketch of an IGCC in principle . .....	31
Figure 1.6. The modification of the GTs burner from: a) regular multi burner natural gas, to b) syngas type .....	33
Figure 1.7. The Lahti Energia Plant, with the plant description: 1) fuel handling, 2) gasifier, 3) gas cooling, 4) gas filter, 5) gas boiler and flue gas cleaning ....	36
Figure 1.8. The thin layer of dust in the boiler after operating for 13000h with syngas ..	36
Figure 1.9. An updraft gasifier connected with a Stirling engine .....	38
Figure 1.10. Schematics of a typical SOFC flow sheet using (a) various fuel types, and (b) a possible GT/SOFC integrated plant .....	44
Figure 1.11. A schematic diagram of a 250 kW gasification based power generating system in Muzizi tea plant, Uganda.....	56
Figure 1.12. Typical composition of MSW in the world (2009) and in the U.S. (2013)..	57
Figure 1.13. Samples of ash/slag collected from the ash collector from co-gasification of MSW and biomass, with a detailed performance of power generation reported by Indrawan et al. ....	70
Figure 1.14. WDP advanced syngas cleaning system at Tampa Electric Company (TECO) .....	81
Figure 2.1. The process diagram of the power generation system with a modified air-fuel regulator coupled with a 60 kW of gasifier .....	99

Figure	Page
Figure 2.2. Flame characteristics of syngas observed at flare stack at (a) initial stage and (b) steady-state condition.....	104
Figure 2.3. The engine speed and AFR with varying load for engine using syngas and natural gas (note that load on natural gas fuel continued to increase until 9 kW) .....	106
Figure 2.4. The electrical efficiency and specific fuel consumption of engine run syngas and natural gas .....	107
Figure 2.5. Emissions levels (ppm) of the engine operated on syngas and natural gas at varying load (kW): (a) CO <sub>2</sub> , (b) CO, (c) NO <sub>x</sub> , (d) HC, and (e) SO <sub>2</sub> .....	112
Figure 3.1. (a) Gasification system with total capacity of 60 kW and (b) detail experimental set-up with a modified air-fuel regulation.....	129
Figure 3.2. Gas composition of syngas generated at various MSW ratio (0, 20, and 40 wt.%) at maximum load (5 kW) .....	134
Figure 3.3. Speed of engine running on syngas generated at various MSW ratio (0, 20, and 40 wt.%) .....	136
Figure 3.4. Air fuel ratio (AFR) of engine running on syngas generated at various MSW ratio (0, 20, and 40 wt.%) .....	137
Figure 3.5. Electrical efficiencies of engine running on syngas generated at various MSW ratio (0, 20, and 40 wt.%) .....	138
Figure 3.6. Emission profile (variation with change in load applied) of (a) CO, (b) NO <sub>x</sub> , (c) HC, (d) SO <sub>2</sub> , and (e) CO <sub>2</sub> of engine running on syngas generated at various MSW ratio (0, 20, and 40 wt.%).....	142
Figure 3.7. Exhaust gas temperature (EGT) with variable load .....	144
Figure 4.1. People without access to electricity worldwide: nine of ten people are located in sub-Saharan Africa in 2030 .....	153
Figure 4.2. Gasifier technology versus capacity range .....	160
Figure 4.3. A schematic diagram of power generation derived from downdraft gasifier	160
Figure 4.4. Major operating costs of the downdraft gasification power system at OSU	163

Figure	Page
Figure 4.5. The major factors impacting on the project's NPV of the downdraft gasification power system with MSW 40 wt.% .....	169
Figure 4.6. The impact of output power on the NPV, IRR, and PP of the downdraft gasification power plant .....	172
Figure 5.1. Types of plasma discharge based on voltage and current density .....	181
Figure 5.2. Process diagram of MSW plasma gasification .....	182
Figure 5.3. Tar yields in generic gasification process at different temperatures .....	188
Figure 5.4. Effect of plasma temperature on energy consumption for generating plasma gas .....	190
Figure 5.5. Effect of plasma temperature on plasma gasification efficiency (PGE) .....	191
Figure 5.6. Syngas composition on different plasma temperatures .....	192
Figure 5.7. Effect of plasma temperature on syngas heating values .....	193
Figure 5.8. The effect of mass flow of plasma gas on syngas composition at 1,500°C .	196
Figure 6.1. Basic diagram of an SOFC unit .....	203
Figure 6.2. Schematic process of experiment: a) gasification plant at OSU, b) SOFC/GT hybrid power generation system at NETL .....	206
Figure 6.3. Schematic process of gasification plant, consisting of belt conveyor, air lock, biomass stirrer, downdraft reactor, grate, ash scrapper, ash conveyor, ash drum, and cyclone separator. ....	207
Figure 6.4. Simplified process diagram of SOFC/GT hybrid power generation system	211
Figure 6.5. A one-dimensional (1D) real-time distributed SOFC model: a) unit cell PEN geometry, and b) model discretization .....	212
Figure 6.6. Current density profile across the fuel cells .....	219
Figure 6.7. Degradation rate profile across the fuel cells .....	220
Figure 6.8. Fuel cell solid temperature across the fuel cells .....	221
Figure 6.9. Fuel cell gas temperature across the fuel cells .....	222
Figure 6.10. H <sub>2</sub> profile across the fuel cells .....	223
Figure 6.11. CO profile across the fuel cells .....	223
Figure 6.12. CH <sub>4</sub> profile across the fuel cells .....	224
Figure 6.13. H <sub>2</sub> O profile across the fuel cells .....	225

Figure	Page
Figure 6.14. CO <sub>2</sub> profile across the fuel cells .....	225
Figure 6.15. Activation loss profile across the fuel cells .....	227
Figure 6.16. Ohmic loss profile across the fuel cells .....	228
Figure 6.17. Nernst potential across the fuel cells .....	229

## CHAPTER 1

### INTRODUCTION AND LITERATURE REVIEW: ADVANCES AND CHALLENGES OF DISTRIBUTED POWER GENERATION VIA BIOMASS AND MUNICIPAL SOLID WASTE GASIFICATION

Part of this chapter was published as:

“Indrawan, N., Kumar, A., & Kumar, S. (2018). Recent Advances in Power Generation Through Biomass and Municipal Solid Waste Gasification. *In Coal and Biomass Gasification: Recent Advances and Future Challenges* (pp. 369-402). Singapore: Springer”.

**Abstract:** This chapter focuses on the fundamentals, recent technology development, economics, socio-environmental analyses, and commercialization of power generation by gasification of municipal solid waste and biomass for distributed power application. Design and operational factors affecting the performance and emission characteristics of power generation systems using syngas are reviewed. Performance characteristics include maximum power output, engine efficiency, and specific fuel consumption of various technologies. Emissions characteristics including levels of carbon dioxide (CO<sub>2</sub>), carbon monoxide (CO), nitrogen oxides (NO<sub>x</sub>), unburned hydrocarbon (HC), sulfur dioxide (SO<sub>2</sub>), and polychlorinated dibenzo-p-dioxins and dibenzofurans (PCDD/PCDF) are discussed. Biopower generation from state-of-the-art power generation technologies (i.e. internal combustion engines, gas turbines, Stirling engines, organic rankine cycle generators, and fuel cells) using 100% syngas generated from gasification of biomass and municipal solid waste with capacities ranging between 50 and 20,000 kW is presented. The economic, social and environmental aspects of the distributed biopower generation are discussed in detail.

**Keywords:** Municipal Solid Waste; Biomass; Gasification; Power Generation Technologies; Emissions; Economic and Socio-environmental Analysis

## 1.1. Introduction

Universal access to electricity is critical for human productivity and development of global economy. Access to electricity has increased worldwide, growing from 60 million of additional consumers per year in 2000-2012 to 100 million per year in 2012-2016. However, this progression is still slow since, at this rate, around 675 million people will still be without access to electricity by 2030 (90% in sub-Saharan Africa). Moreover, 2.3 billion people are expected to still use traditional biomass, coal, and kerosene for cooking by 2030, remaining vulnerable to harmful indoor air pollution that potentially causes lethal poisoning to humans that is currently linked to 2.8 million premature deaths per year [1]. The projected expansion of global population from the current 7.4 billion to more than 9 billion people in 2040 will create additional challenges if coal and other non-renewable resources remain dominant energy sources. Indeed, since 2000, coal based power plant additions have totaled nearly 900 gigawatts (GW), increasing the global CO<sub>2</sub> emissions by 3% per year from about 24.5 in 2000 to nearly 40 Giga tons today [2, 3].

Natural gas use in power generation has been growing and is considered a cleaner energy source compared to coal [4]. However, the increasing use of Liquefied Natural Gas (LNG) in natural gas pipelines has raised the price of natural gas to the end-customers due to the mixing process in the pipeline. In some developed and developing economies, such as China, Japan, South Korea, Indonesia, and other southeast Asian countries, the final price of natural gas can reach \$10-15/MMBtu for end-customers [5, 6]. This consequently shifts gas-fired power plants from a baseload role towards a peak-saving role [4], decreasing the economic attractiveness of natural gas as an investment for future clean power generation.

The use of gasification to produce power from different energy sources, such as coal, biomass, and solid wastes, has been gaining attention worldwide. Recent syngas production costs reached \$5-7/MMBtu [5, 7, 8], which makes syngas favorably competitive with natural gas. Coal gasification has been well known since 1984, when the Lurgi gasifier was installed in the Great Plains (North Dakota, U.S.). It consumed 16,000 tons per day (tpd) of lignite coal and produced pipeline quality gas until 1985. The plant then discontinued operation due to a drastic drop in oil prices [9, 10]. Meanwhile, biomass gasification is well known and has been used since the 1920s and was especially popular during World War II, when approximately one million downdraft “gas producers” were used to power cars, trucks, boats, trains and electric generators in Europe [11]. In contrast, MSW gasification is relatively new but has huge potential since the global production of MSW is projected to increase from 1.3 billion tons (1.2 kg per person per day) in 2012 to over 2.2 billion tons (1.42 kg per person per day) in 2025 [12].

Syngas for distributed power generation (with generator’s size < 20 MW) has the potential to meet future electricity demand. The total electric capacity of distributed and dispersed (independently operating) generation (with generator’s size < 1 MW) in the U.S. reached 5,407 MW in 2015 [13]. Meanwhile, the global net electricity generation is projected to increase from 23.4 trillion kilowatt hours (kWh) in 2015 to 34.0 trillion kWh in 2040 [14, 15]. Among power generation units deploying syngas, the internal combustion engine (ICE) and the gas turbine (GT) are currently the most prevalent units for distributed application. Recent advancements in ICEs and natural gas-fired gas turbine combined cycles (GTCCs) have enabled efficiencies up to 41% [16] and more than 60% [17], respectively. Thus, the prospects of using syngas in ICE have become more attractive,

driven by the quest for lower emissions, mainly sulfur dioxide (SO<sub>x</sub>) and nitrogen oxides (NO<sub>x</sub>) [18].

Report on operational performance, including economic and socio-environmental analysis of power generation systems running on pure syngas generated from gasification of biomass and MSW is limited in the literature. This chapter aims to detail advancements and developments made in syngas based power plants for distributed applications. Advantages and challenges from the technical, operational, and environmental standpoints, including system efficiency, hardware modification requirements, and emission performances are discussed in detail. Economic and socio-environmental analyses are included to further investigate the viability of the power generating system in practical application. The outcome of this chapter is to support and accelerate the global development of power generation through the gasification of biomass and MSW with low capital and operating cost.

## **1.2. Gasification versus direct combustion**

In the U.S., more than 70 mass-burn incineration facilities in 21 states utilize about 13% of the nation's total household refuses, generating about 2.5 gigawatts (GW) of power [19]. 10-12% of those refuse streams contain plastic, which, when incinerated, can create complex health problems in humans due to the emission of toxic gases, including polychlorinated dibenzo-p-dioxins (PCDDs/dioxins), polychlorinated dibenzo-p-furans (PCDFs/furans), mercury, and polychlorinated biphenyls (PCBs) [20].

By contrast, gasification is still a relatively new alternative, and there are several misunderstandings about the differences between gasification and direct combustion

(incineration), even by regulatory bodies [21]. To date, only around 33 gasification plants have been operated, planned or constructed in the U.S. [22]. Gasification using bio or residual resources offers more sustainable investment with better flexibility than direct incineration technology [23]. Gasification can also be integrated with other advanced power generation technologies (i.e. gas turbines and fuel cells) to improve performance efficiency (to over 60%) [24]. Because its main product is syngas (considered as the intermediate product), the economic value of gasification can further be increased by applying it to the production of petrochemicals, such as ammonia, methanol, and hydrogen [25]. These products contributed to the largest syngas market industry in 2016, creating markets of 180, 84, and 40 million tons per year, respectively [26]. Because gasification occurs at lower temperatures (600-1,000°C) than incineration (>1,500°C) with a limited oxygen environment, the potential is low to generate dioxin and furans (PCDDs/PCDFs) and volatilize harmful emissions, such as heavy metals and alkali, at the flue stack (differences summarized in Table 1.1).

**Table 1.1. Major differences between gasification and direct combustion (incineration)**

Category	Gasification	Direct Combustion
Process		
Temp.	Typically occurs at 600 – 1000°C [27].	Typically occurs at over 1500°C [28].
O <sub>2</sub> level	Limited (5-20% of stoichiometric) [29].	Excess (more than stoichiometric) [28].
Products	Mainly syngas, which can be used for energy generation or liquid fuels and chemicals production [30]. Others products are biochar, tar, and ash [31].	Flue gas, fly ash, and fixed carbon [32].

Category	Gasification	Direct Combustion
Emissions	Syngas can be suitable for applications in small scale power generation [30, 33]	Direct combustion of solids is not convenient because of the need for advanced gas cleaning [30].
	Low levels of alkali volatilization, fouling, slagging, heavy metal volatilization and bed agglomeration (for fluidized bed reactors) [30].	High level of alkali and heavy metal volatilization [30].
	Dioxin and furans (PCDDs/PCDFs) emission levels for MSW are low (~0.28 ng/Nm <sup>3</sup> ) [32].	High level of PCDDs/PCDFs emission (up to 0.02 mg/Nm <sup>3</sup> ) [34].
System Efficiency	Syngas-based power generation emits low emissions (NO <sub>x</sub> , CO <sub>2</sub> , HC, SO <sub>2</sub> ) [29, 30].	Emissions are high and must be reduced after combustion [21].
	The deficit of air (instead of an excess) reduces heat losses at the stack and thus increases energy recovery efficiency [30].	High heat loss at the stack [30].
	Overall system efficiency is higher than 60%, if integrated with an advanced power system (e.g., fuel cells) [24].	Overall system efficiency of a steam power plant is ~30-35% [35].

**Table 1.2. Major chemical reactions involved in the biomass and MSW gasification**

[36, 37]

<i>Main reaction*:</i>		
$CH_xO_y + aO_2 + wH_2O + 3.76aN_2$ $= n_1H_2 + n_2CO + n_3CO_2 + n_4H_2O + n_5CH_4 + n_6N_2 + n_7C (char) + tar$		
<i>Oxidation reaction:</i>		
1. $C + \frac{1}{2} O_2 \rightarrow CO$	-111 MJ/kmol	Carbon partial oxidation
2. $CO + \frac{1}{2} O_2 \rightarrow CO_2$	-283 MJ/kmol	Carbon monoxide
3. $C + O_2 \rightarrow CO_2$	-394 MJ/kmol	Oxidation
4. $H_2 + \frac{1}{2} O_2 \rightarrow H_2O$	-242 MJ/kmol	Carbon oxidation
5. $CH_4 + 1/2 O_2 \rightarrow CO + 2H_2$	-36 MJ/kmol	Hydrogen oxidation
6. $CH_4 + 2O_2 \rightarrow CO_2 + 2 H_2O$	-803 MJ/kmol	CH <sub>4</sub> partial oxidation Oxidation
<i>Gasification reactions involving steam:</i>		
7. $CH_4 + H_2O \rightarrow CO + 3H_2$	206 MJ/kmol	Steam methane reforming
8. $CO + H_2O \rightarrow CO_2 + H_2$	-41 MJ/kmol	Water-gas shift reaction
9. $C + H_2O \rightarrow CO + H_2$	131 MJ/kmol	Water-gas reaction
10. $C_nH_m + n H_2O \rightarrow nCO + (n+m/2) H_2$	Endothermic	Steam reforming
<i>Gasification reactions involving hydrogen:</i>		
11. $C + 2H_2 \rightarrow CH_4$	-75 MJ/kmol	Hydrogasification
12. $CO + 3H_2 \rightarrow CH_4 + H_2O$	-227 MJ/kmol	Methanation
13. $2CO + 2H_2 \rightarrow CH_4 + CO_2$	247 MJ/kmol	Methanation
14. $CO_2 + 4H_2 \rightarrow CH_4 + 2H_2O$	165 MJ/kmol	Methanation
<i>Gasification reactions involving carbon dioxide:</i>		
15. $C + CO_2 \rightarrow 2CO$	172 MJ/kmol	Boudouard reaction
16. $C_nH_m + nCO_2 \rightarrow 2nCO + m/2 H_2$	Endothermic	Dry reforming
<i>Decomposition reactions of tars and hydrocarbons:</i>		
17. $pC_xH_y \rightarrow qC_nH_m + rH_2$	Endothermic	Dehydrogenation
18. $C_nH_m \rightarrow nC + m/2 H_2$	Endothermic	Carbonization

\*notes: where  $a$  is the amount of oxygen per kmol of waste,  $w$  is the amount of water per kmol of waste materials,  $n_1$ ,  $n_2$ ,  $n_3$ ,  $n_4$ ,  $n_5$ ,  $n_6$ , and  $n_7$  are the coefficients of the gaseous products and soot.

By far the most eminent factors that make gasification more attractive than incineration for treating biomass and MSW are low emissions of PCDDs/PCDFs and high system efficiency, as compared in Table 1.1. PCDDs/PCDFs are classified as

persistent organic pollutants (POP) with carcinogenic and mutagenic characteristics [38]. The low emission of PCDDs/PCDFs is due to low operating temperatures and limited oxygen in the gasification environment, which restricts the combination of carbon, oxygen, and chlorine – three main precursors in PCDD/PCDF formation [38]. The high efficiency of gasification (> 60%) may further be complemented by the promising integration of gasification with gas turbines and fuel cell technologies that are not compatible with incineration technology [24]. Integration of gasification system with other advanced technologies will likely be emerging in the near future.

### **1.3. Advancements in biomass and MSW gasification**

Biomass gasification is a well-known technology and has been used since the 1920s when about one million downdraft “gas producers” were used to drive cars, trucks, boats, trains and electric generators in Europe [11]. Biomass gasification generates syngas, a mixture of CO, H<sub>2</sub>, CO<sub>2</sub>, CH<sub>4</sub>, H<sub>2</sub>O, hydrocarbons, H<sub>2</sub>S, tar and other trace species. Syngas compositions generally depend on the operational variables of the gasifier, such as raw material characteristics, gasification medium (steam, air, oxygen, CO<sub>2</sub>, plasma), temperature/pressure and catalyst type, if used. Currently, syngas is converted into major chemical commodities: 180 MM tons for ammonia and 85 MMT for methanol, in 2016 [26], with coal and natural gas used as the primary feedstocks.

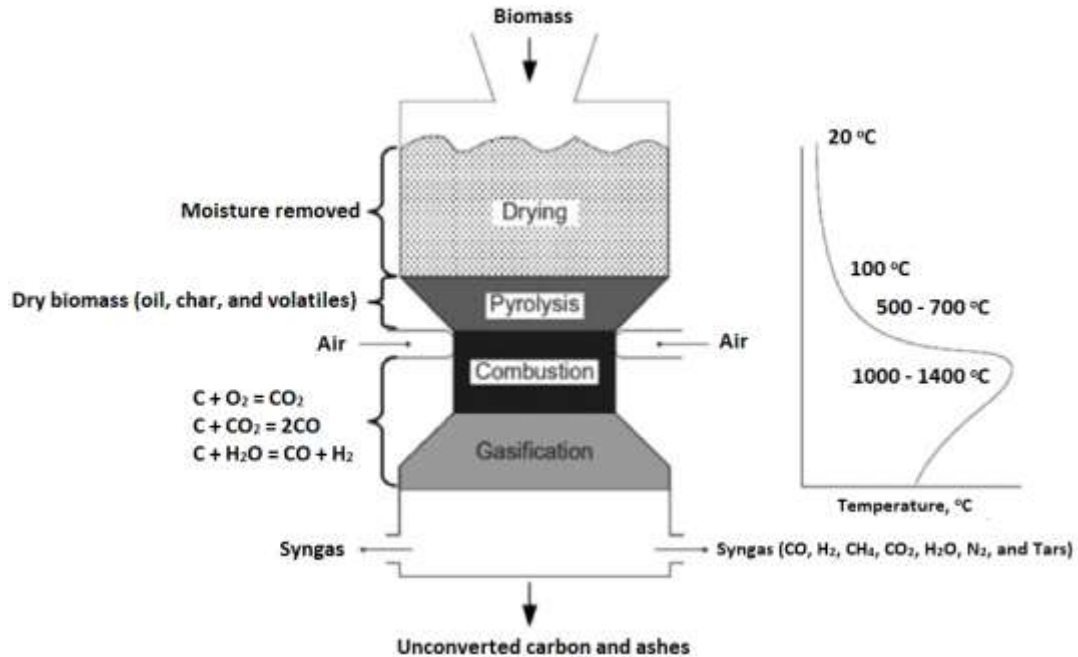


**Figure 1.1. The steps of gasification and temperature profile [27]**

Syngas is produced from biomass gasification through the following processes: drying, pyrolysis (which includes a devolatilization step) and partial oxidation. Feedstock dehydration generally occurs until 120°C, while pyrolysis occurs within 120-700°C, and volatile species are released below 500°C [39]. The pyrolysis products are charcoal, oil and syngas. Since biomass is richer in volatile components (70-86% on a dry basis) than coal (around 30%), pyrolysis of biomass produces more syngas than pyrolysis of coal. The solid product mainly consists of char and ash. Syngas is released at a temperature to 1400°C [37] and mainly contains CO and H<sub>2</sub> as combustible fraction. Table 1.2 and Figure 1.1 illustrate the overall gasification reactions and sequence as well as the corresponding temperature profile. Over these processes, the carbon fraction of biomass is converted into syngas with an efficiency of 80 to 95% [30, 40].

MSW is heterogeneous and is containing a great variety of compounds, such as metals, plastics, and possibly hazardous materials, including medical wastes. Gasification of MSW is significantly more challenging than gasification of biomass because of various composition of MSW (i.e. high ash content); thus, the selection of appropriate technology and operating conditions is paramount. Slags made of potassium-rich ash on the bottom of gasifiers can occur especially when biomass is mixed with MSW, because the resulting ash mixture has a lower melting point. This may lead to clogging of the lower part of the gasifier [41, 42]. However, paper, wood, yard trimmings, food, and plastic represent over 70% of the global MSW, indicating a high fraction of organic compounds, thus becoming a huge potential to be transformed into syngas and various valuable products (e.g., ammonia, methanol, hydrogen – three major final products of syngas in 2016) [43]. Advanced MSW gasification can play a critical role in increasing local economics while minimizing environmental concerns; currently the most proven technology in treating MSW (e.g. incineration) is still environmentally problematic due to fly ash generation [44]. Compared to biomass, MSW is characterized by low carbon, lower heating value and higher ash content, resulting in a more challenging and complex gasification process, as mentioned earlier. Therefore, to improve the technical and economic reliability of biomass and MSW gasification, advances have been made in design and optimization of gasifiers, feeding and other auxiliary systems, and syngas conditioning systems [6, 45].

### **1.3.1. Gasifier design**

The gasifier design plays a critical role in the way the reagents, biomass and gasifying agent come into contact and react, thereby influencing the reaction kinetics, residence time, syngas lower heating value (LHV), and eventually power generation performance. Current

commercially available biomass gasifier designs include fixed-bed reactors (downdraft and updraft), fluidized bed (bubbling and circulating), entrained flow bed reactors, and plasma reactors. Advantages and drawbacks of these gasifier designs have been previously reported by Indrawan et al. [33]. In power generation, selecting the appropriate gasifier technology to fit the size of the targeted power generation is critical. For power units up to 1 MW, corresponding to feedstock inputs up to about 10 tons/day, downdraft gasifiers are generally used because these can generate syngas with high energy content (4.5-6.5 MJ/Nm<sup>3</sup>) while producing less tar (0.01-3 mg/Nm<sup>3</sup>) than other types (0.01-150 mg/Nm<sup>3</sup>). At higher feedstock inputs, pressurized fluidized bed and entrained flow gasifiers are preferred. Moreover, gasifiers that can operate at high temperatures (>800°C) will not only produce high gasification efficiency and maximize the fraction of gaseous syngas produced, they will also reduce tar content in the syngas [46]. For high temperature gasification, advanced plasma gasifiers are well known for their capability in MSW processing to generate nearly tar-free syngas due to their high operation temperatures (above 5,000°C) [30, 47]; tars are thermally decomposed into H<sub>2</sub> and CH<sub>4</sub> and ash is converted into some vitrified and inert slag [47, 48]. Advances in the design of MSW gasification systems include increased reliability and availability of gasifiers, advanced refractory gasifiers, refractory durability, mitigation of fouling, control of ash in IGCC, the capability to mix low rank coals with biomass and MSW, improvement of hardware, development of sensors and controls, and reduction in fouling and slagging [6, 45]. Although plasma gasification is considered the most reliable technique in treating an MSW stream, its high operating temperature can require complex construction and high capital costs (up to 13,000 \$/kW), which are the major challenges in commercial application [49,

50]. A pictorial guideline for selecting a gasifier based on the feed rate is available elsewhere [51].

Table 1.3 summarizes several recent advanced gasifiers along with their main characteristics. As shown, each gasifier has certain advantages, depending upon its design. For distributed power generation, besides their simple and reliable operation, gasifiers producing syngas with high calorific value and less tar are highly desired.

**Table 1.3. Advanced gasifiers and their main characteristics available worldwide**

Gasifier	Main characteristics	Advantages	Ref.
UNIQUE gasifier	Integrates gasification, gas cleaning (catalytic filter candle in the freeboard) and conditioning in one reactor unit	Reduced footprint, investment costs and syngas particulates, tar level of 11-18 g/Nm <sup>3</sup> and syngas LHV of 10.9-13.5 MJ/Nm <sup>3</sup> .	[52, 53]
Milena gasifier	The combustion and pyrolysis reactions are performed in two separate, sequential reactors that are integrated in one refractory lined vessel.	The gasification rate of carbon is close to 100% and the dilution of the syngas by N <sub>2</sub> (from the air stream) and CO <sub>2</sub> and H <sub>2</sub> O (from the combustion products) is minimized. LHV of the syngas is three to four times higher than that of syngas from a typical air-blown gasifier and even 60% higher than with an oxygen/steam blown gasifier.	[54, 55]
Internal cyclonic downdraft gasifier	The gasifier has an internal separate combustion section where turbulent, swirling high-temperature combustion flows are generated	Capable of treating various low density biomass and MSW (up to 40 wt.%), generating syngas with high LHV (~6.0-6.8 MJ/Nm <sup>3</sup> ) and tar content (300-400 mg/Nm <sup>3</sup> ).	[33, 56]
Multi-stage gasifier (Viking gasifier)	Separate and combine pyrolysis and gasification in single controlled stages	Low tar content (<15 mg/Nm <sup>3</sup> ), with syngas LHV ~6.1 MJ/Nm <sup>3</sup> , CGE 93% and an electrical efficiency ~25%.	[57]
Güssing fluidized bed gasifier	Use nickel-based catalytic filters inserted in the gasifier freeboard, and use steam as gasifying agent	Less tar and particulate matter, generating syngas with LHV of 12 MJ/Nm <sup>3</sup>	[52, 58]
LT-CFB gasifier	Consisting of two stages of gasification run at an elevated temperature: the first used circulating fluidized bed (630°C) and the second used bubbling fluidized bed (730°C).	Capable to treat difficult biomass feedstocks (straw, manure fibers, sewage sludge), producing syngas with LHV of 5.2-7 MJ/Nm <sup>3</sup> and CGE of 87-93%.	[52]

Gasifier	Main characteristics	Advantages	Ref.
Supercritical water gasifier	Gasification is performed in supercritical water (above P = 22.12 MPa and T = 374.12°C)	Capable of treating wet and high moisture content biomass, without pre-drying	[52]
Plasma gasifier	Gasification is performed in plasma, generally occurs at high temperature (> 5000°C)	Decomposes organic materials into elemental molecules. Low tar content, and inert slag. Syngas with 50-55% H <sub>2</sub> and 40-44% CO is achievable (LHV ~11.5 MJ/Nm <sup>3</sup> )	[47]

### 1.3.2. Feeding and auxiliary system

The feeding system plays a critical role in biomass gasification. Biomass types, such as bagasse, sugar cane trash, rice husk, rice straw, coir pith, and groundnut shell, have densities below 200 kg/m<sup>3</sup> and LHVs between 12 and 16 MJ/kg (dry basis) [39], with moisture contents ranging from 10 to 20% [51]. Specific feed preparation strategies are needed in commercial gasification plants to accept feedstock with diverse characteristics. The feed preparation strategies include sizing, drying, pyrolysis, and low temperature gasification. Advantages and drawbacks of each strategy are reported elsewhere [51]. A relatively new strategy is torrefaction, which uses a mild, oxygen-free thermal treatment, lasting approximately 30 min at 200-300°C. This strategy offers several benefits, including increased energy density (from 2-3 to 15-20 GJ/m<sup>3</sup>), increased hydrophobic characteristics that allow open air transport and storage, and the ability to convert raw feed and wastes into energy commodities [59]. Advanced feeding systems have been investigated, including a high pressure solid feed capable of improving efficiency and expanding fuel flexibility in gasification of coal, biomass and MSW [45]. Low-cost O<sub>2</sub> separation, production of O<sub>2</sub>-enriched air and pure O<sub>2</sub> via contactor or sorbent-based techniques are also being investigated to produce high LHV syngas [6].

Unlike biomass gasification, which is a relatively more mature technology, MSW gasification faces serious challenges due to the heterogeneity of the raw materials, which include plastics, metals, and organics compounds, and may require exacting plant supporting systems. These complex mixtures of MSW result in challenges in feeding the materials into the reactor; a pelletized form of the materials, therefore, is extremely necessary to achieve a stable operation of the gasifier because it has a high density and reduces moisture content [60]. In addition, only a few MSW gasification plants are operating worldwide and these are still evolving to become economically viable. Currently, more than 938 commercial gasifiers are now operating worldwide, but those using biomass/waste mixtures represent less than 200 units [22].

### **1.3.3. Syngas conditioning system**

A major focus on syngas processing systems is the abatement of multiple contaminants including tar and particulate char to extremely low levels, as required both by emission regulations and the anticorrosion protection of the power units [45, 61, 62]. The technologies are often classified according to the temperature of the syngas exiting the clean-up device: hot, cold, and warm, which have been described in detail elsewhere [6, 61]. Other purification technologies include advanced acid gas separation, chemical looping, advanced water gas shift reactor design and improvement, catalytic gasification and candle-based filtration, H<sub>2</sub>/CO<sub>2</sub> membranes, syngas cooler fouling mitigation, and integrated CO<sub>2</sub> removal [6, 7].

A general guideline of syngas requirements for power generation units is presented in Table 1.4. In terms of tar, particulate, and alkali metals, internal combustion engines (ICEs) are more tolerant than gas turbines (GTs) and fuel cells (FCs). However, GTs have

additional requirements, including limits on sulfur and nitrogen, generally set by the manufacturers. Since the use of syngas as the primary fuel in boilers is still limited, the respective standards are still evolving. Overall, FCs have the most stringent requirement to maintain performance and lifetime [63].

**Table 1.4. Typical gas quality requirements for power generation** [33, 39, 61, 63-68]

Parameter	Boiler	ICEs	GTs	FCs
LHV, MJ/Nm <sup>3</sup>	> 4	> 4	> 4	-
Particulate, mg/Nm <sup>3</sup>	-	< 5 – 50 (PM 10)	< 5 – 30 (PM 5)	-
Tars, mg/Nm <sup>3</sup>	-	< 10 – 100	< 5	< 1
Alkali metals, ppm	-	< 1 – 2	< 0.2 – 1	-
Sulfur (H <sub>2</sub> S, COS), μL/L	-	-	< 20	< 5-10 ppm <sup>a,b</sup> , < 3% <sup>b</sup>
Nitrogen (NH <sub>3</sub> , HCN), μL/L	-	-	< 50	-
Halides (mainly HCL), μL/L	-	-	< 1	-
Carbon monoxide, CO	-	-	-	< 10 ppm <sup>a</sup> , < 3% <sup>b</sup>
Chlorine, Cl <sub>2</sub>	-	-	-	< 5 ppm
Siloxane, [SiO (CH <sub>3</sub> ) <sub>2</sub> ] <sub>n</sub>	-	-	-	< 10 ppm

Notes: <sup>a</sup> applied for low temperature polymer electrolyte membrane fuel cell (LT-PEMFC) and solid oxide fuel cell (SOFC) [63, 68], <sup>b</sup> applied for high temperature polymer electrolyte membrane fuel cell (HT-PEMFC) and phosphoric acid fuel cell (PAFC) [68].

#### 1.4. Advancement and challenges in distributed power generation from syngas

Recent developments in power generation have rendered more efficient use of syngas derived from biomass and waste. This applies to most prime movers and especially to ICEs, GTs and micro GTs, FCs, boilers/steam plants, and hybrid systems with a typical range of electrical efficiency from 10 to 60%. When used as a modular electric power source close to an end-user, the power generation suppresses the capital expenditure (CAPEX) of grid expansion and the operational expenditure (OPEX) related to line losses, thereby offering cost savings. When connected to the grid, the bi-directional transactions between the local

generation unit and the grid enhance grid capacity, which reduces the risks of supply interruption and allows for improved energy pricing due to versatile use/buy/sell options [69]. Although no recognized global standard defines the maximum capacity of distributed power generation, 1.5-10 MW is commonly considered typical capacity in countries such as UK, Sweden, and New Zealand [69]. In this study, an upper limit of 20 MW is used, allowing the application of an aeroderivative GT, such as LM 2500 General Electric (GE) and A-20 Siemens GT [70].

FCs, including solid oxide fuel cells (SOFC), polymer electrolyte membrane fuel cells (PEMC), phosphoric acid fuel cells (PAFC), and molten carbonate fuel cells (MCFC), boast high electrical efficiency (40-60%) but still have limited power outputs (0.005-1 MW), as shown in Figure 1.2. Integrating a FC in a gas turbine combined cycle (GTCC) to create a “hybrid system” can drastically increase overall power output, which can reach up to 100 MW. In comparison, ICEs offer a wider range of capacity (0.005-6.5 MW) [16] with a moderately high electrical efficiency (30-50%), while GTs offer high capacities (1-250 MW) along with electrical efficiencies ranging from 20 to 50%, depending on their size and configuration (simple cycle, combined cycle or cogeneration). Similarly, steam power plants are capable of a high capacity (up to nearly 1,000 MW) with an efficiency of 40-45%. The combustion behavior of syngas when used in power generation units, including ICEs, GTs, microturbines (MGTs), boiler and steam turbines (STs), Stirling engines, ORC generators, and FCs is presented below.

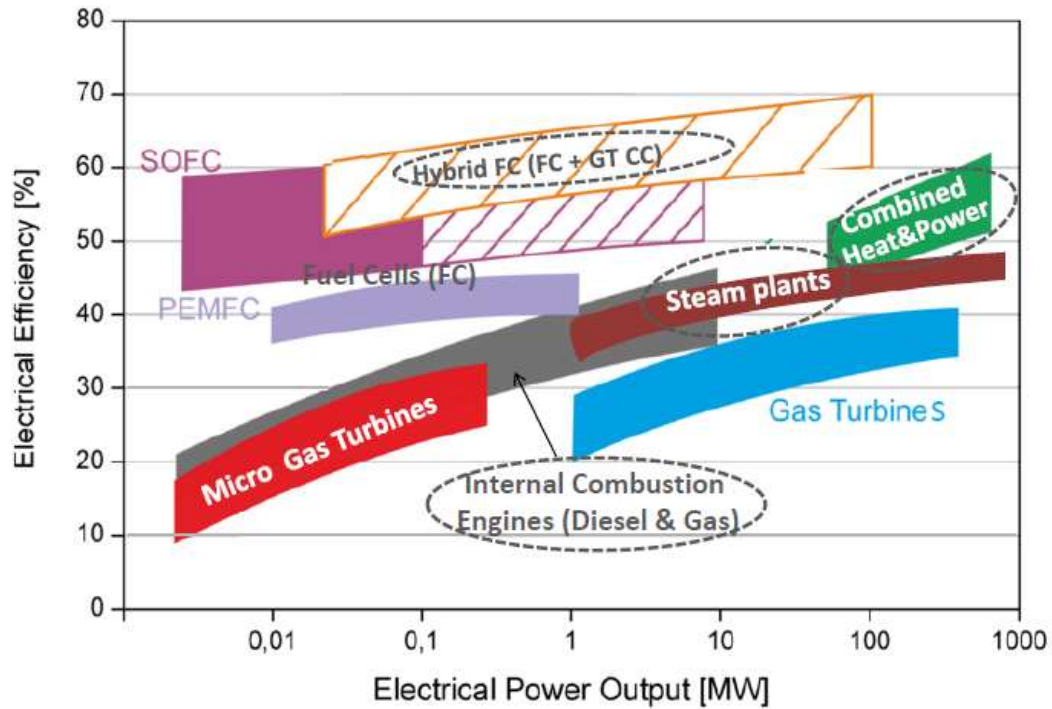


**Figure 1.2.** Synopsis of the efficiency data of various power generation units [23, 71, 72]

#### 1.4.1. Combustion characteristics of syngas

To characterize syngas fuels, LHV is used more commonly than higher heating value (HHV), because the water generated by combustion is released as vapor at the exhaust and its latent heat of condensation is lost. Generally, LHV of syngas (4-15 MJ/m<sup>3</sup>) is approximately one-third to one-eighth that of natural gas (35-40 MJ/m<sup>3</sup>) [64, 73, 74].

Understanding combustion behavior and flame characteristics of syngas fuels is a key requisite to enhance the efficiency of power generation from syngas. Using advanced planar laser induced fluorescence (PLIF), flame characteristics of pure methane, as well as the flame characteristics of a series of air-blown gasification syngas fuels generated from bituminous coal, wood residue, corn core and wheat straw, have been reported (Figure 1.3). The LHVs of syngas derived from bituminous coal, wood residue, corn core and wheat

straw are 35.6; 6.3; 5.5; 5.0 and 4.7 MJ/Nm<sup>3</sup>, respectively [75]. Bituminous coal syngas appears to have the strongest OH fluorescence signal intensity and the narrowest region of low reactivity (along the chamber axis), while wheat straw syngas has the lowest signal intensity and the widest unburned region. Despite its high LHV, methane displays a lower OH signal intensity and a wider region of low reactivity than syngas. Therefore, bituminous coal syngas shows a better burn-out behavior due to its high H<sub>2</sub> content.

In contemporary combustion facilities, such as GTs and ICEs, lean premixed dry low emission (i.e. NO<sub>x</sub>) (DLE/DLN) systems are the best achievable technology for high energy fuels such as methane. However, these systems are sensitive to (i) “flashback” issues, which consist of unwanted retro-propagations of the flame from the combustion zone to the premix zone, and (ii) “spontaneous ignition” events that occur when the residence time in the premix zone exceeds the auto ignition delay of the fuel. DLN systems cannot accommodate high H<sub>2</sub> fuels due to increased flashback risks but, fortunately, the low BTU character of syngas fuels yields very low NO<sub>x</sub> emissions, generally below 25 ppm [76].

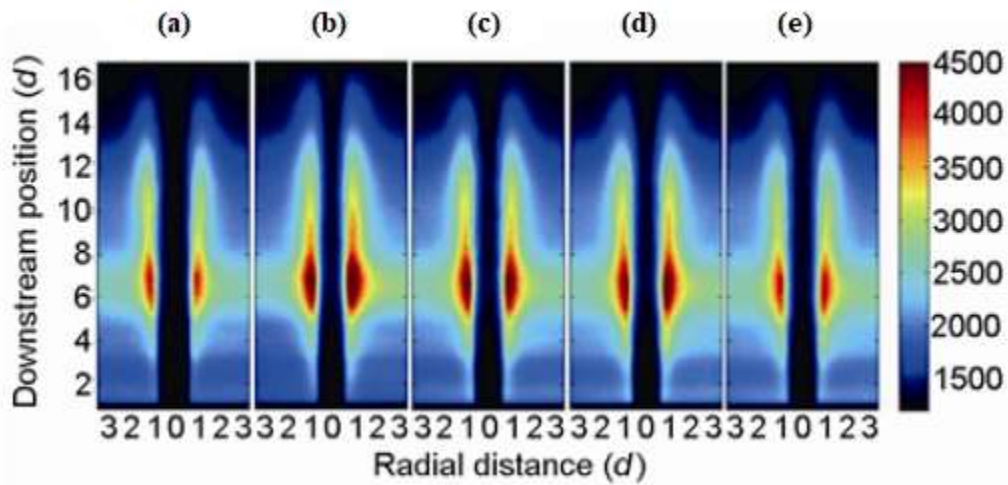


**Figure 1.3. Comparison of flame characteristics (PLIF fluorescence signal) of (a) methane, and various syngas fuels generated from (b) bituminous coal , (c) wood residue, (d) corn core, and (e) wheat straw [75]**

#### **1.4.2. IC engines**

Syngas can feed various power generation technologies, including ICEs, GTs, boilers, STs and FCs after moderate hardware modifications. Among these technologies, generally ICEs and GTs are predominant in existing plants. With ICEs, an electrical efficiency can be achieved in the range of 20-35% [67, 77, 78] and latest developments promise unit power levels up to 6,500 kW that potentially bring higher economic return, a long interval maintenance (6,000 hours, about every one to two years), a low noise level (about 44 dB at 3 ft.), and satisfactory emission performances [16]. In distributed power generation, to date, ICEs are often preferred to other novel technologies such as MGTs and FCs, as these offer simple set-up requiring minimum modification [29], proven performance, rapid start-up and shutdown, high generation efficiency (33-41% on LHV basis) and moderate capital cost (\$700-1,000/kW) [16].

##### **1.4.2.1. Key operational parameters of ICEs**

The major performance parameters of a syngas-fueled ICE include thermal efficiency, specific fuel consumption, compression ratio, power output after power de-rating (when necessary), Wobbe index, heat release, and cylinder pressure.

The unit power and thermal efficiency of an ICE are especially critical for distributed power applications. These parameters are functions of the engine compression ratio (CR), which will be described later in this section. Engine thermal efficiency, also commonly called “brake thermal efficiency”, is the ratio between the brake shaft power output and the rate of energy expanded. Engine efficiency varies considerably depending on the type of

fuel and the equivalence ratio, as reported elsewhere [79-82]. A gasoline engine with a displaced volume of 5.73 L and a CR of 16 potentially generates a brake thermal efficiency of about 39% [83]. Methane-rich fuels generally feature higher brake thermal efficiency than hydrogen-rich fuels [79]. However, high hydrogen content expands the flammability range of the syngas and stabilizes its combustion [84]. The efficiency of an ICE could be increased by making its expansion ratio greater than its CR [85]. Specific fuel consumption (*SFC*), another parameter to evaluate engine performance, is defined as a ratio of fuel consumption and power produced. For distributed power application (<100 kW), ICEs running on syngas generated from the gasification of biomass and solid waste generally result in *SFC* ranging from 0.5-5.8 kg/kWh [29, 33, 57, 86-92].

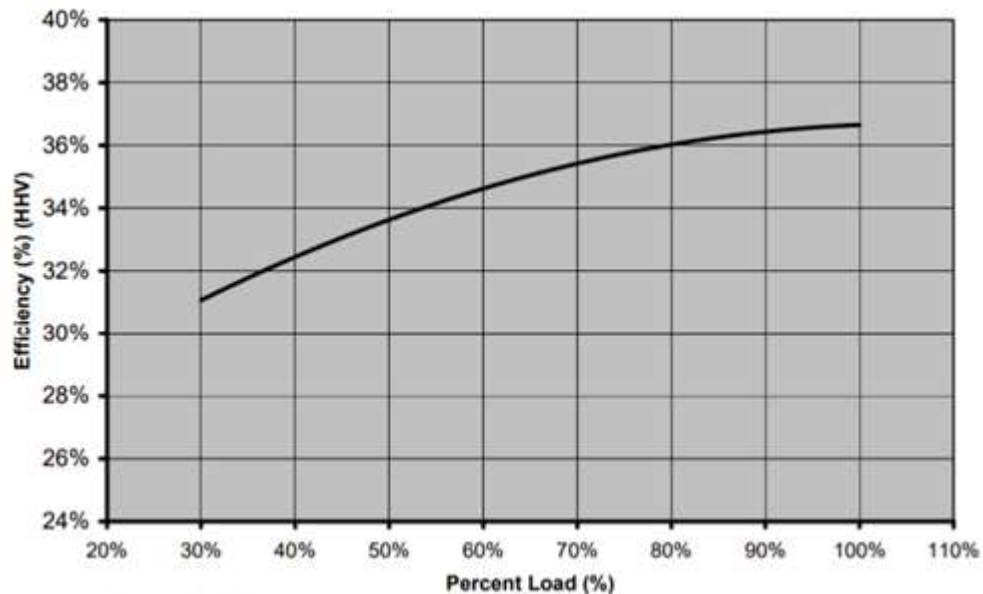
Another key design parameter of ICE is its CR, which is the ratio between the maximum volume and the minimum volume developed by the piston-cylinder assembly. Higher CRs result in higher cylinder pressures [83]. In syngas operation, modified gasoline ICEs can achieve a CR of 4.5-20 [91]; however, due to the low LHVs of common syngas fuels, high CRs do not increase engine efficiency substantially.

ICEs generally experience power de-rating when their fuel has a lower calorific value than NG (38-40 MJ/Nm<sup>3</sup>), gasoline (44-46 MJ/kg), and diesel oil (45 MJ/kg) [93], which is the case with a syngas (LHV of 4-15 MJ/Nm<sup>3</sup>) [64, 73]. The power de-rating is defined as the ratio between the actual power output with new fuel and rated power output. On syngas, ICE features typical power de-rating of 22-55% [29, 77, 84, 94, 95]. Heat release and cylinder pressure are also important operational parameters for ICE. A spark ignition (SI) engine with a rated power of 4.7 kW and rated speed of 3,400 rpm showed a decrease

in its heat release and cylinder pressure (drop from 31.6 to ~29 bar) using various syngas fuels [86] compared with those using propane.

#### 1.4.2.2. Natural gas engine

NG engines are SI engines. Compared to gasoline and diesel engines, they offer several advantages: they produce lower NO<sub>x</sub> and CO emissions, they offer low first cost and fast start up, they are excellent load-following characteristics, and they are considerably more efficient [96]. At maximum load, a natural gas engine can achieve an efficiency of more than 36% (Figure 1.4).



Source: Caterpillar, EEA/ICF

**Figure 1.4. Efficiency of a natural gas ICE versus load [97]**

Another advantage of the NG engines is its odorless exhaust gas [98]. Sridhar et al. [89] fed syngas with a density of 1.7 kg/Nm<sup>3</sup> into a 101 kW NG engine. By modifying the carburetor, they found that the maximum brake power output and electrical efficiency were about 60 kW and 24.7%, and CO and NO<sub>x</sub> emissions generated were 1.4-6.5 g/kWh and 0.7-2.5 g/kWh.

Raman and Ram [64] fed 100% syngas with a density of  $1.05 \text{ kg/m}^3$  into a 100 kW NG engine. A series of gas cleaning system equipment comprised of a venturi scrubber, chiller, fabric filter and paper filter, was used to reduce syngas tar from 350 to  $35 \text{ mg/m}^3$ . Having a compression ratio of 12, the engine ran using an air fuel-ratio of 1.2, producing a maximum power output of 73 kW and an efficiency of 21%. However, emission performance was not reported.

Tsiakmakis et al. [86] fed syngas generated from fluidized bed gasification of olive, peach and grape kernels into a 4.7 kW, unmodified, NG engine. The syngas energy contents ranged from  $4.52\text{-}6.96 \text{ MJ/Nm}^3$ . Authors also used propane to increase the energy content of the syngas mixture to about  $23.7\text{-}24.4 \text{ MJ/Nm}^3$ . The maximum engine power output ranged from 3.55-3.68 kW and the engine efficiency varied from 23.2-26.2%. However, emissions were not reported.

Margaritis et al. [99] used a syngas derived from downdraft gasification of olive kernels, containing 53.1-55%  $\text{N}_2$ , 23.6-24.1%  $\text{H}_2$ , 3.8-4.1%  $\text{CH}_4$  and 9.5-10.6%  $\text{CO}$ . Tar and particulates were removed from this syngas using a venturi scrubber, a heat exchanger with chiller, a mist eliminator and a series of fine filters. A gas blower was also used to ensure a stable input flow of the syngas into the gas engine. The research team burned this gas in a 135 kW NG engine with a power setting of 70 kW. The cold gas and electric efficiency data were 75% and 16.1%, respectively. However, the air-fuel ratio and potential operational issues were not reported.

Henriksen et al. [57] tested a two-stage gasifier in which the pyrolysis and char gasification processes were performed in two separate reactors and produced syngas that contained 32-35%  $\text{H}_2$ , 28-30%  $\text{N}_2$ , 20%  $\text{CO}_2$ , 15-18%  $\text{CO}$ , and 2-3%  $\text{CH}_4$ . The syngas was

injected into a 75 kW NG engine, which performed stably for approximately 410 h. The engine produced 20 kW of power as compared to 25 kW when it ran on NG, resulting a de-rating factor of 20%. The efficiency from gas to mechanical power (engine efficiency) was around 28%. Operational issues were observed including a failure of one of the engine cylinders to ignite.

Indrawan et al. [29, 33] fed syngas generated from a downdraft gasifier into 10 kW NG engine. The maximum power of 5 kW on syngas and 9 kW on propane was generated. The authors also ran the gasifier with MSW (up to 40 wt.%) mixed with switchgrass and generated a syngas with LHV of 6.7-7.7 MJ/Nm<sup>3</sup> and an output power of 5 kW [60]. Agglomeration of bed materials in the gasifier was observed with a higher fraction of MSW (40 wt.%). Only the air/fuel-intake system required modifications to obtain a more homogenous mixing of syngas and air. A single venturi pipe was used for SG syngas [29], while a two series of venturi pipe was used for MSW/SG syngas [60].

#### **1.4.2.3. Gasoline engine**

Gasoline engines are also a type of SI engine. Several authors have investigated performance of gasoline engine running on 100% syngas. Shah et al. [87] modified the engine by adding two air venturi devices in series in the gas feed line to adjust and stabilize the syngas flow delivered from a storage tank. The engine was first cranked on gasoline before being progressively transferred to 100% syngas. On syngas, the engine efficiency was about 19% and the CO emission decreased by 30-96% as compared to gasoline. The higher CO emission on gasoline might be due to the richer operation conditions and higher carbon content of gasoline (88.7% w/w versus 16.9% w/w of syngas) [100]. However, the exhaust CO<sub>2</sub> was 10.6-13.1% using syngas as compared to 4.9-8.1% using gasoline. The

33-167% higher CO<sub>2</sub> emission on syngas can be attributed to a high conversion of CO to CO<sub>2</sub>. HC emission was less than 40 ppm for almost all the load variation, probably due to the very low HC content (1.2-6.4%) of the syngas. Syngas operation resulted in 54-84% lower NO<sub>x</sub> emission than for gasoline operation. Indeed, the generation of thermal NO<sub>x</sub> is governed by the Zeldovich mechanism in which the combustion temperature has an exponential effect on the NO<sub>x</sub> formation rate. Because syngas has a lower LHV than gasoline (5.6 MJ/Nm<sup>3</sup> versus 44.4 MJ/kg), it develops a lower flame front temperature, resulting in remarkably lower NO<sub>x</sub> emissions [86].

Mustafi et al. [91] tested a gasoline engine using a syngas fuel with a LHV of 15 MJ/Nm<sup>3</sup>. The CO emissions with syngas were low, indicating complete combustion in the engine; the CO<sub>2</sub> emissions with syngas were higher (19% v/v) than with gasoline (15% v/v). The HC emissions with syngas were very low (about 0-20 ppm) compared to gasoline (90-225 ppm) and natural gas (20-106 ppm). However, NO<sub>x</sub> emissions with syngas were higher (~4500 ppm) than with gasoline operation (~1500 ppm).

Lee et al. [101] assessed engine performance using syngas generated from a trailer-scale downdraft gasifier. The engine, originally designed for gasoline and natural gas, achieved an output power of 28.3 and 17 kW at 1800 rpm while running on gasoline and propane, respectively. Syngas was generated from several biomass and waste sources with a flowrate of 13-25 ft<sup>3</sup>/min and a LHV of 4.53 (pine), 5.06 (red oak), 5.22 (horse manure), and 4.21 (cardboard) MJ/Nm<sup>3</sup>, respectively. The maximum output power and overall efficiencies achieved were 11.8 kW at 23% (Pine), 13.1 kW at 20.6% (Red oak), 10.1 kW at 21.3% (horse manure), and 9.6 kW at 15.8% (cardboard). However, the required hardware modifications and the emission performances of the engine were not available.

#### 1.4.2.4. Compressed ignition engine

The diesel engine is another type of reciprocating ICE, also known as a compression ignition engine (CIE), and in which the ignition is not spark triggered but occurs spontaneously (auto-ignition). The specificity of CIE is that the combustion air is compressed first and the fuel is subsequently injected in the CIE, allowing designs with high compression ratios. In the following sections, we discuss several studies reporting the performance of diesel engines running on syngas after minor engine modifications.

Modifications made by Homdoun [88] to a diesel engine included some changes to the combustion chamber, a reduction of the compression ratio, the mounting of an ignition system in place of the injector nozzle and the addition of an air-gas mixer. The tar content of the syngas (LHV of  $4.64 \text{ MJ/Nm}^3$ ) was reduced to below  $50 \text{ mg/Nm}^3$  using a specific gas cleaning system. The highest engine efficiency attained was about 24% producing 3.5 kW.

Sridhar et al. [89] investigated the performance of a modified 28 kW diesel engine that ran on syngas with tar content of  $60 \text{ mg/m}^3$ . A new carburetor was developed to maintain gas pressure close to air pressure, aiming at ensuring the air-fuel ratio was adjusted regardless of the total air-fuel flowrate. The uniformity of the fuel-air mixture entering the engine was controlled using a long interconnecting duct featuring several bends with a large diameter for keeping pressure losses between the gas carburetor and the intake manifold to a minimum. Using a compression ratio of 17:1, the maximum power achieved was 20 kW with engine efficiency of 27.6%, and power de-rating of 20-30%).

Nataraj et al. [90] tested a single-cylinder diesel engine with a compression ratio of 17.5, running on 100% syngas with energy content of  $5.0\text{-}5.6 \text{ MJ/Nm}^3$  and tar content

below 60 mg/m<sup>3</sup>. The maximum power output and engine efficiency were achieved at 2.96 kW and 18.9%. No engine modification was reported. CO, NO<sub>x</sub> and HC emissions were in the ranges of 0.3 to 0.4%, 40 to 100 ppm, and 20 to 50 ppm, respectively. A summary of recent research on these engines (NG, gasoline, and compressed ignition) is presented in Table 1.5.

**Table 1.5. Performances of state-of-the-art engines running on 100% syngas for distributed power generation**

References	Feed type	Reactor type, capacity and condition	Syngas LHV, MJ/Nm <sup>3</sup>	Original engine fuel type, # of cylinder, rated power, rated speed, displacement, compression ratio	Modified	Air-Fuel ratio (AFR)	Max. Brake Power produced, Specific Fuel Cons., Engine Efficiency	Emissions				
								HC	CO	NO <sub>x</sub>	CO <sub>2</sub>	SO <sub>2</sub>
[88]	Charcoal longan tree	Downdraft, 5 - 6 kg/h	4.64	Diesel, 1 cylinder, 8.2 kW, 1800 rpm, 0.6 L, 14	Combustion chamber and ignition system	-	3.17 kW, 5.53 kg/kWh, 23.5%	3.5 - 10 ppm	3,000 - 4,000 ppm	n/a	n/a	n/a
[89]	n/a	Downdraft, 75 kg/h	4.90	Diesel, 3 cylinder, 28 kW, 1500 rpm, 3.3 L, 17	Converted to SI engine, carburetor	1.2 - 1.5	20 kW, 4.52 kg/kWh, 27.6%	n/a	14.4 - 57.6 g/kWh	0.1 - 0.7 g/kWh	n/a	n/a
[89]	n/a	Downdraft, 75 kg/h	4.90	Natural gas, 6 cylinder, 101 kW, 1500 rpm, 12.1 L, 10	Carburetor	1.2 - 1.5	60 kW, 5.06 kg/kWh, 24.7%	n/a	1.4 - 6.5 g/kWh	0.7 - 2.5 g/kWh	n/a	n/a
[87]	n/a	No gasifier	5.79 <sup>2)</sup>	Gasoline, 1 cylinder, 5.5 kW, 3600 rpm, n/a, n/a	Air venturies: two in series	n/a	1.39 kW, 5.53 kg/kWh, 19% (electric)	n/a	45.3 - 51 g/kWh <sup>1)</sup>	0.5 g/kWh <sup>1)</sup>	254 g/kWh <sup>3)</sup>	n/a
[91]	n/a	n/a	15.3	Gasoline, 1 cylinder, n/a, 2000 rpm, 0.5 L, 4.5 - 20	n/a	4.25:1	4.6 kW, 1.1 kg/kWh, 36%	0 - 20 ppm	n/a	4,500 ppm	190,000 ppm	n/a
[64]	Wood chips	Downdraft, 87 kg/h, 0.35 ER and 88% CGE	5.6	Natural gas, 6 cylinder, 100 kW, 1500 rpm, 12.3 L, 12	Fuel intake manifold & hydraulic governor	1.2	73 kW, 3.21 kg/kWh, 21%	n/a	n/a	n/a	n/a	n/a
[92]	Sawdust, Sugarcane	Downdraft	4.4	Producer gas, n/a, 100 kW, 1500 rpm, n/a, n/a	none	n/a	98 kW, 4.9-5.7 kg/kWh, 24.3-28.2%	n/a	n/a	n/a	n/a	n/a
[57]	Wood chips	Downdraft	6.2	Natural gas, 3 cylinder, n/a, n/a, n/a, n/a	none	n/a	20 kW, 3.5 kg/kWh, 28%	n/a	n/a	n/a	n/a	n/a
[86]	Peach kernels	Bubbling fluidized bed	6.9	Natural gas, 1 cylinder, 4.7 kW, 3400 rpm, 0.3 L, 10	none	1.7	3.68 kW, 0.49 kg/kWh, 26.2%	n/a	n/a	n/a	n/a	n/a

References	Feed type	Reactor type, capacity and condition	Syngas LHV, MJ/Nm <sup>3</sup>	Original engine fuel type, # of cylinder, rated power, rated speed, displacement, compression ratio	Modified	Air-Fuel ratio (AFR)	Max. Brake Power produced, Specific Fuel Cons., Engine Efficiency	Emissions				
								HC	CO	NO <sub>x</sub>	CO <sub>2</sub>	SO <sub>2</sub>
[90]	Rice bran oil methyl ester	Downdraft	5.60	Diesel, 1 cylinder, 3.7 kW, 1500 rpm, 0.7 L, 17.5	n/a	n/a	2.96 kW, 5.78 kg/kWh, 18.9%	20 - 50 ppm	3,000 - 4,000 ppm	40 - 100 ppm	n/a	n/a
[29]	Switchgrass	Downdraft, 100 kg/h, 0.25 ER and 68% CGE	6 - 7	Natural gas, 2 cylinder, 10 kW, 3600 rpm, 0.6 L, n/a	Air fuel intake	1.2 - 1.6	5 kW, 1.9 kg/kWh, 21.3% (electric)	0 - 262 ppm	4,000 ppm	21.5 - 32.5 ppm	75,000 ppm	429 - 768 ppm
[101]	Red oak	Downdraft, 0.55 ER and 85% CGE	5.1 - 6.0	Gasoline, 4 cylinder, 28.3 kW, 1800 rpm, 2.26 L, 9.7	Timing and engine control module	n/a	13.1 kW, n/a, 25.6%	n/a	n/a	n/a	n/a	n/a
[33]	MSW (40 wt.%) and Switchgrass	Downdraft, 100 kg/h, 0.20 ER and 49-62% CGE	6.7 - 7.7	Natural gas, 2 cylinder, 10 kW, 3600 rpm, 0.6 L, n/a	Air fuel intake with two venturies	0.7 - 1.0	5 kW, 3.0 kg/kWh, 19.5-22% (electric)	1.2 - 90 ppm	2867 - 16533 ppm	4.4 - 27.3 ppm	33785 - 68367 ppm	30 - 95 ppm

Note: 1) Calculated, 2) Syngas LHV based on purchased based, 3) Calculated based on AFR 1.2

### 1.4.3. Gas turbines

Contrary to ICEs, GTs are continuous-flow engines that develop steady aerodynamics and flame kinetics, providing a considerable margin for devising clean combustion designs and relaxing the constraints placed on fuel properties for performing combustion. This is why gas turbines can accommodate a broad range of primary energies (NG, liquid fuels, LPG, syngas etc.). Compared to ICEs, GTs offer comparable electrical efficiency, high availability/reliability, and low maintenance, making this technology a strong candidate for new distributed power generation units. Contemporary GTs using conventional fuels (NG or No 2 diesel oil) offer thermal efficiencies as high as 33 to 42+% in open cycle and 52 to 60+% in GTCC, on a LHV basis [67, 102]. In a combined cycle operation, advanced combustion research of GTs has targeted an efficiency of 65% through several strategies, including pressure gain combustion, increased aerothermal and heat transfer, and supercritical CO<sub>2</sub> cycle [103].

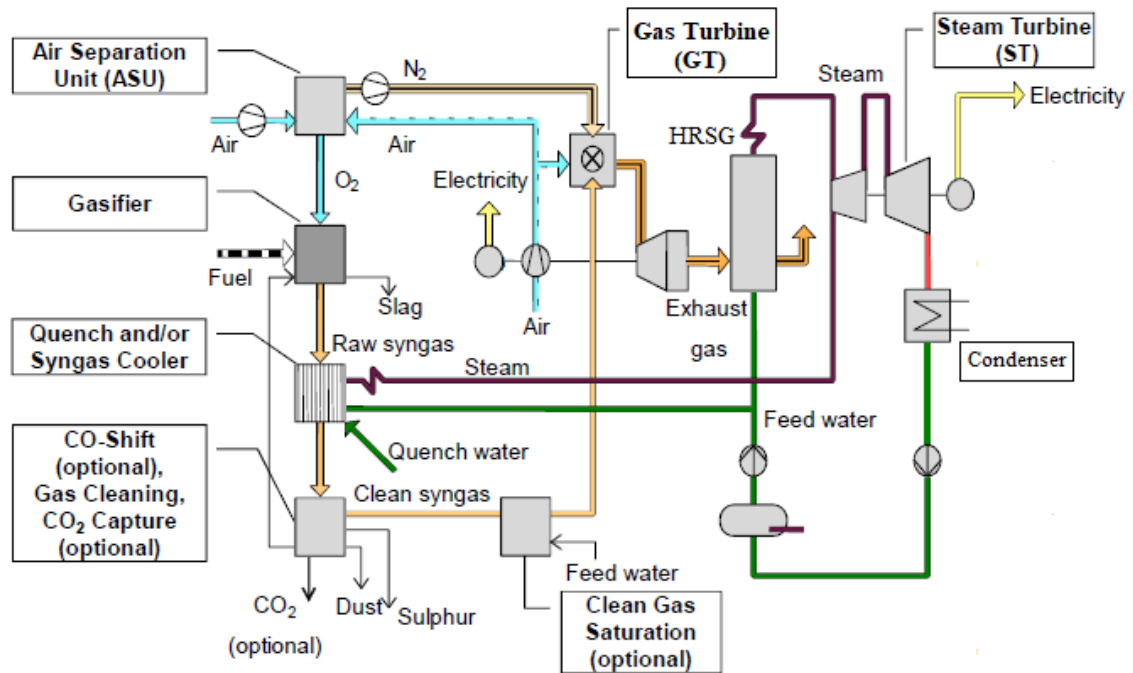
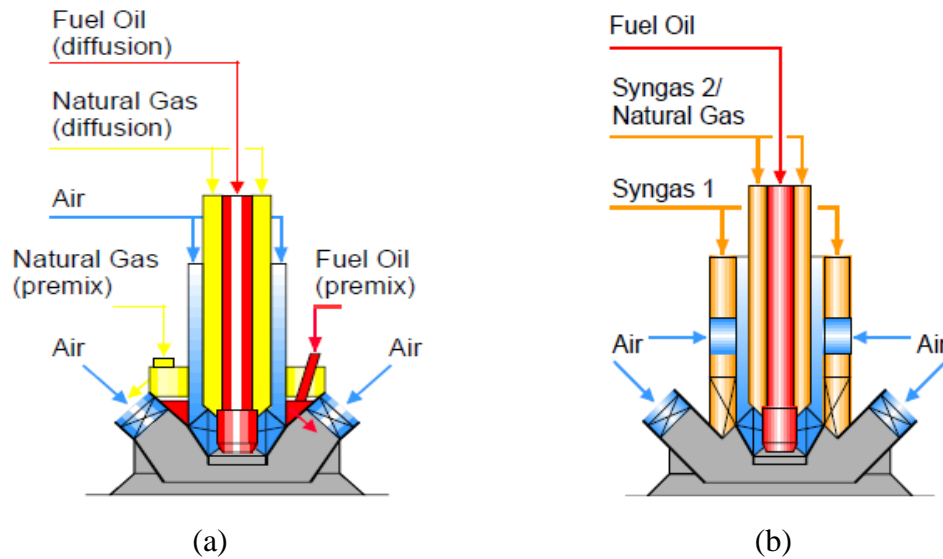


Figure 1.5. Sketch of an IGCC in principle [104].

IGCC plant solutions (Figure 1.5) require proper integration design for the interfaces and a robust plant design implementing lessons learned. In this context, the Brayton and Rankine cycles, also called the “topping” and “bottoming” cycles, are the most critical factors for IGCC plant performance. The simple cycle performances of aeroderivative GTs typically exceed those of heavy-duty GTs; however, in the combined cycle both aeroderivative and heavy duty GTs show improved performance because they have higher exhaust temperatures, which boosts the efficiency of the bottoming cycle. Other factors influencing the performance of IGCC are feedstock properties, the gasification process (i.e. dry vs slurry fed system), concepts for syngas heat recovery (quench vs syngas cooler), the syngas purification process, CO<sub>2</sub> capture level (0 to 90%), strategies for syngas dilution and NO<sub>x</sub> reduction, and air and nitrogen integration and air supplying unit (ASU) processes [104].

In the last two decades, modifications have been made among three major parts in GTs (compressor, combustor, and fuel system) to enable the use of low btu syngas (including blast furnace gas and liquefaction tail gas). The turbine does not require any modification. The prime goal of these modifications is to improve efficiency, fuel flexibility and DLE (dry low emissions), namely with the advent of DLN (dry low NO<sub>x</sub>) combustion as the BAT (best achievable technology) [104, 105]. These advancements have transformed modern F and H-class gas turbines into very clean and efficient power generation tools. Figure 1.6 displays Siemen’s modified burner for syngas application [104]. For syngas application, the modified burner allows the air to diffuse uniformly along the burners and dilute the syngas fuel for controlled NO<sub>x</sub> and flame speed [104].



**Figure 1.6. The modification of the GTs burner from: a) regular multi burner natural gas, to b) syngas type [104].**

Nevertheless, GTs are relatively sensitive to gas quality and tolerate only low levels of contaminants including tar, alkali metals and sulfur compounds (as shown previously in Table 1.4). Erosion of the GT buckets typically occurs if the syngas is not completely cleaned and still has contaminants (i.e.  $H_2S$ ) that may erode the bucket materials in long term [106]. In addition to these fuel requirements, other general considerations for industrial application of syngas as gas turbine fuel include the following: syngas must be combusted in diffusion-type burners; dilution with nitrogen and/or steam may be required for reactivity and/or control of  $NO_x$  emissions; natural gas may be needed to increase fuel btu; the lower LHV design limits must be checked in relation to fuel composition and fuel reactivity regarding combustion [104].

The use of syngas in small-sized GTs has been reported in previous studies. Fortunato et al. [107] investigated a very specific power unit design in which a circulating fluidized

bed (CFB) gasifier was fed with a stream of pomace having a moisture content below 15%, at a feeding rate of 4.3 to 21.6 tpd. The gasifier was coupled with a GT that was installed in a regenerative, external combustor configuration: the air exiting the GT compressor was reheated through a heat exchanger that was fed with the hot combustion gas of a biomass combustor burning a feedstock of olive trees. A fraction of the biomass combustion gas and the combustion gas of the gas turbine fed the main heat recovery steam generator (HRSG). Steam generated by an auxiliary HRSG was used as gasification medium. The resulting syngas had an LHV of about 15.2 MJ/Nm<sup>3</sup> and contained some tar [107]. The authors reported that a total power output of 2.0 MW and an overall efficiency of 36 to 48% could be achieved in a GTCC.

#### **1.4.4. Micro gas turbine**

Running syngas in a micro gas turbine (MGT) is an alternative option to support distributed power generation. MGTs are compact electricity generators, typically with rated capacities in the range of 25-300 kW [108]. Compared to ICEs, MGTs will run on syngas characterized by a higher level of contamination [109]. However, experimental studies on MGTs run on syngas are still limited. Delattin et al. [108] reported that an experimental set-up was prepared to run a MGT on natural gas and two syngas/natural gas mixtures with a CCD camera installed to observe the combustion regime. After running for nearly 1.5h, they found that the MGT produced a maximum power of 500 kW on natural gas, and less than 200 kW on syngas. The blue color resulting from a natural gas premix flame was observed to change to red when the MGT relied solely on syngas for operation. The CO and NO<sub>x</sub> emissions observed were very low (< 5ppm) during syngas operation.

Rabou et al. [110] tested a 30 kW MGT that ran on a mixture of natural gas and biomass syngas generated from a CFB gasifier with a LHV of 6 MJ/Nm<sup>3</sup> (with syngas composition of 7% H<sub>2</sub>, 17% CO, 15% CO<sub>2</sub>, 4% CH<sub>4</sub>, 2% other hydrocarbons). No modifications of the MGT were reported. They found that the maximum output powers of 30 kW and 8 kW were achieved when the MGT ran on a gas mixture with a LHV of 15 and 8 MJ/Nm<sup>3</sup>, respectively. Above 20 kW, the emissions of CO, unburned hydrocarbons, and NO were 5, 20 and 30 ppm, respectively.

#### **1.4.5. Steam plant**

An electrical efficiency of 31.5% was achieved by feeding syngas with an LHV of 9-20 MJ/kg in the steam power plant at Valmet (Lahti Energia, Finland) [35]. The plant used pre-sorted household and industrial wastes, demolition wood and industrial waste wood, with a moisture content below 40%; the plant is illustrated in Figure 1.7. The plant was based on a 2 x 80 MW CFB gasifier operating at 5-30 kPa (g) and 750-900°C using air as the gasification medium, while the steam cycle ran at 120 bar and 550°C and generated an electrical efficiency of nearly 32%. The plant operated for 6967 h and generated 241 GWh of electricity that was delivered to the grid as well as 514 GWh of heat for district heating in 2014 [35].

The plant achieved nearly 80% operational availability in 2014 with no major issue in maintenance, including no indications of corrosion or erosion of the boiler tubes. The marking of tube manufacturing was still visible after 13,000 h of operation. However, a small amount of dust/slag in the gas cooler and a thin dust layer in the boiler were observed [35] (Figure 1.8). The plant's emission control included DeNO<sub>x</sub> catalyst, sodium

bicarbonate injection, activated carbon injection and bag house filters, allowing PMs and other pollutants to be substantially reduced.

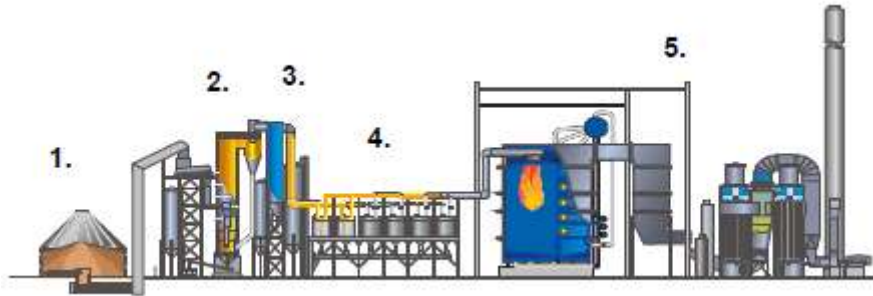


**Figure 1.7. The Lahti Energia Plant, with the plant description: 1) fuel handling, 2) gasifier, 3) gas cooling, 4) gas filter, 5) gas boiler and flue gas cleaning [35]**

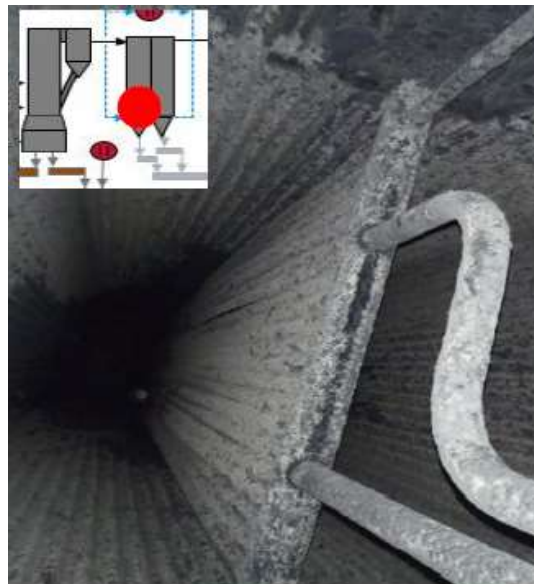


**Figure 1.8. The thin layer of dust in the boiler after operating for 13000h with syngas [35]**

#### **1.4.6. Stirling engine**

The use of Stirling engines integrated within biomass and MSW gasification systems is a relatively new concept [111-114]. This type of prime-mover generally uses the residual

energy contained in flue gas streams. Although the experimental works in this area are still few, the concept is highly promising for clean power generation in the future. These engines use pressurized gas, which expands when heated, driving a piston to perform work. The expanded gas volume, having released the major fraction of its energy, is then cooled and compressed before the next heating cycle [113]. Contrary to ICEs, the Stirling engines use a working gas (e.g. air, helium, hydrogen), rather than fuel, contained in a sealed circuit; therefore, combustion does not occur in the engine, so only a low level of noise and vibration and zero emissions are created [113]. The engines generally have a good performance at partial load and fuel flexibility [115]. The heat consumed by the engines can be provided by any thermal heat source or energy conversion devices, such as solar power, geothermal, biomass, MSW, and others [114]. Several additional advantages include high efficiency (typically 30% of electrical efficiency and 85-95% of overall efficiency based on LHV operating in a cogeneration mode), and low maintenance costs (~\$0.008/kWh) [112]. Nevertheless, the following concerns must be addressed to improve Stirling engine performance and encourage their use in today's market: high pressure operation (min. 15 MPa) [112], reduced capital cost (current commercial cost is about \$5,000/kW [115]), increased lifespan, faster rate-up and response to load changes, and augmented power output level (>1 MW) [113].

An attempt to use this technology was reported by Leu [112]. An updraft fixed-bed gasifier was connected to a 25 kW Stirling engine that used hydrogen as working gas rotating at a speed of 1,800 rpm (Figure 1.9). A flue gas stream generated from the gasifier (with temperature 980°C and flowrate 730 g/sec) was used to heat the engine. The gas stream allowed the working gas to transfer back and forth between the hot and cold portions

of the machine by the movement of the engine's pistons, generating a stable output power of 24.5 kW after 25-30 min from start-up.

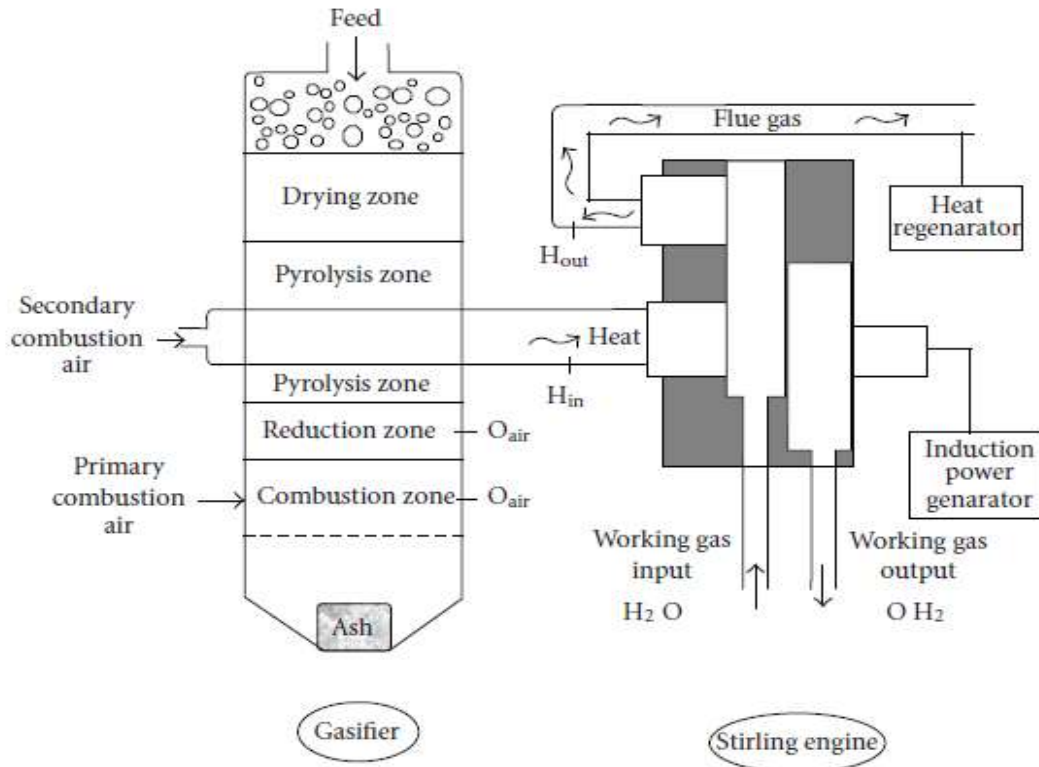


**Figure 1.9. An updraft gasifier connected with a Stirling engine [112]**

### 1.4.7. Organic Rankine Cycle generators

Organic Rankine Cycles (ORCs) rely on the same principle as a conventional steam (or Rankine) cycle, but, instead of water, the working fluid is an organic compound with a lower boiling point, thus decreasing the temperature and heat rate needed in the evaporator [116]. As this working fluid must meet certain criteria relating to environmental health and safety (non-toxicity, non-corrosiveness, fire safety, etc.), cycle thermodynamics, and cost, its selection is always a challenge. Among the most interesting working fluids are n-pentane, R245fa, and R134a, which can drive ORCs with

power output capacities in the range of 0.01-5 MW and electrical efficiencies ranging from 17 to 23% [116-118].

Experimental studies on ORCs coupled with gasification systems are limited. Most of the studies relied on modelling, energy and exergy balance [118-120], such as the one reported by Kelina (2011) [121]. A theoretical model of a downdraft gasifier producing an output energy of 1 MW using air as the gasification medium was coupled with an ICE and an ORC generator. With three possible configurations, the gasifier-ICE-ORC system potentially offers an overall electrical efficiency of 23.6-28.3%. As of 2016, the total global ORC CHP system using waste heat recovery from biomass accounted for 301 MW, generated from 332 small-to-medium-scale plants [122].

#### **1.4.8. Fuel cells (FCs)**

Considering the limited efficiency performances of ICEs and steam plants, and the limited choices of convenient ORC working fluids, FCs offer promising alternatives for distributed power generation. FCs consume hydrogen, a zero carbon energy vector that can be produced from renewable energy sources and convert it into electricity without direct combustion. FCs are gaining in popularity as recent technological advancements have put on the market small-sized FCs (50-200 W) showing higher tolerance to typical impurities such as H<sub>2</sub>S (up to 200 ppm) [123]. Typical outputs are 10 to 300 kW for transportation propulsion, and 200 to 1,000 kW for stationary applications [24, 124]. In addition, the use of hydrogen-rich syngas in a MCFC can generate an electrical efficiency up to 45% [67], while a SOFC can reach 45-60% [24, 125, 126]. However, the low durability of FCs has hindered this technology's entry into the commercial market [126].

#### **1.4.8.1. Types of fuel cells and their characteristics**

Fuel cells are generally classified according to the nature of the solid or liquid electrolyte that transports the ions towards the electrodes on which the electrochemical reactions occurs. These media comprise phosphoric acid, molten carbonate, solid oxide, and polymer electrolyte membrane [127]. Generally, PEMFCs are suited for small capacities (2 to 200 kW) and residential heating systems (1-3 kW thermal), while PAFCs and MCFCs are suited for high capacities of 50 kW to 10 MW and 200 kW to 100 MW, respectively [126]. Compared to other types, SOFCs are more attractive for stationary distributed power generation because they can cover a wide range of capacities ranging from 2 kW to 100 MW, with electrical efficiencies of 23-60%, depending on the power rating and the configuration of the overall system (e.g., standalone, combined heat and power, and combined generation configurations) [24, 127]. SOFCs can also use a wide range of fuels, including syngas, natural gas, and biogas, with relatively high resistance to contaminants, such as sulfur [72]. Future SOFC power generation using syngas for stationary application is targeted to achieve a low capital cost (<1,000 \$/kW) with high durability (>80,000 hours) [72]. Table 1.6 provides a detailed comparison of the advantages and drawbacks of the various types of FCs.

**Table 1.6. Comparison of fuel cells intended for distributed power generation [68, 124]**

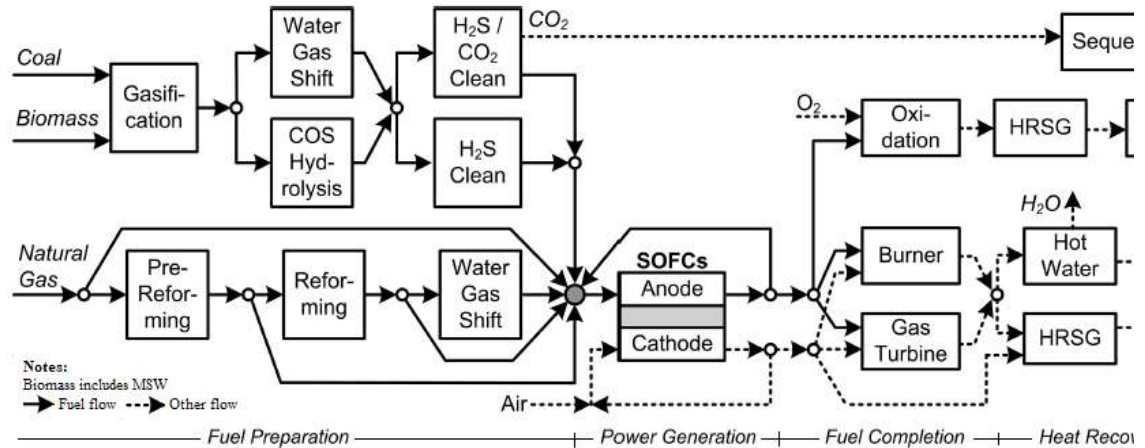
Fuel cell type	Operating Temp., °C	Fuel	Electrical efficiency, %	Major advantageous	Major disadvantageous
LT-PEMFC	65 – 85	H <sub>2</sub>	40 – 60	Highly modular, high power density, rapid start-up, compact structure, fast dynamic response,	High sensitivity to contaminants, low-grade heat, and expensive catalyst
HT-PEMFC	140 – 200	H <sub>2</sub>	50 – 60	High-grade heat, high tolerance to contaminants	Accelerated stack degradation, expensive catalyst, humidification issues
MCFC	600 – 700	H <sub>2</sub> , CO, CH <sub>4</sub>	55 – 65	High-grade heat, high tolerance to contaminants, fuel flexible, high electrical efficiency, inexpensive catalyst	Slow start-up, low power density, cathode carbon injection requirement
PAFC	160 – 220	H <sub>2</sub>	36 – 45	High-grade heat, high tolerance to contaminants, mature technology, reliable	Low electrical efficiency, low power density, expensive catalyst
SOFC	500 – 1000	H <sub>2</sub> , CO,	55 – 65	High-grade heat, high electrical efficiency, high tolerance to contaminants, low cost catalyst, fuel flexible	Slow start-up, high manufacturing cost, high thermal stress

#### 1.4.8.2. SOFC as distributed power generation

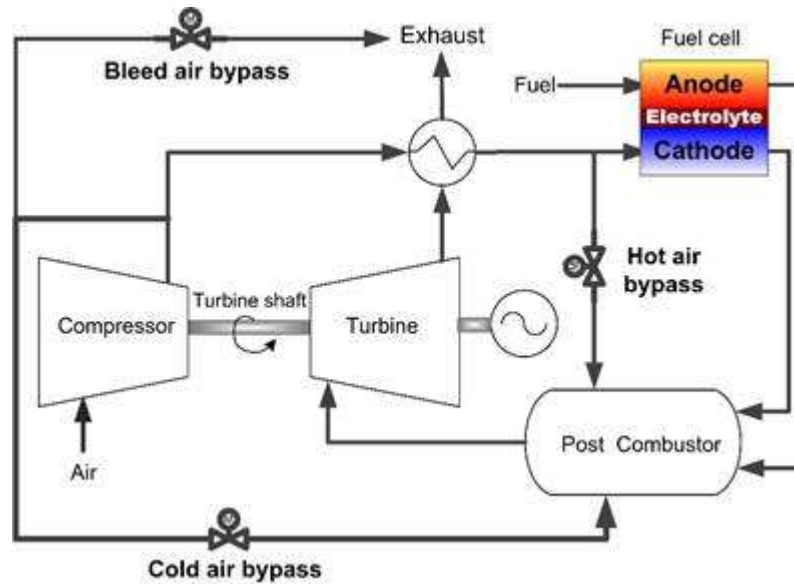
SOFCs are an attractive option for distributed power generation [24, 68]. Unlike PEMFCs that require relatively pure hydrogen and low operating temperatures ( $< 90^{\circ}\text{C}$ ), SOFCs are more resistant to contaminants, including to poisoning by CO. This increases the variety of fuel sources possible to produce electricity, including coal-derived syngas, biomass, NG, methanol, and diesel [24, 128]. Prominent additional advantages of SOFCs are high electrical efficiency, high operating temperature (between  $500$  and  $1,000^{\circ}\text{C}$ ), which enables SOFC to be integrated within thermal generation systems, such as gas turbines and gasifiers, and fuel flexibility [24, 129, 130]. An SOFC unit consists of three main solid layers called the anode, the electrolyte and the cathode. On the upper section of an SOFC, channels are constructed to deliver the fuel along the anode and oxidant along the cathode. The open-circuit potential difference resulting from the anodic and cathodic reactions follows the Nernst potential as law [128]. Figures 1.10 (a) & (b) illustrate an SOFC potential development from various feedstock (e.g. coal, biomass/MSW, and natural gas), and its possible integration within a gas turbine cycle. Figure 1.10a shows several process pathways of an SOFC system intended for distributed power generation. The pathway comprises four stages: 1) fuel preparation, 2) SOFC power generation, 3) fuel combustion/oxidation, and 4) heat recovery [24]. Integrating high-temperature SOFC within a gas turbine engine (Figure 1.10b), such as the unit developed in National Energy Technology Laboratory (NETL), is a promising technology for supporting distributed power generation. In this configuration both the anodic gas stream (unreacted  $\text{H}_2 + \text{H}_2\text{O}$ ) and the cathodic gas stream (unreacted  $\text{O}_2 + \text{N}_2 + \text{H}_2\text{O}$ ) leaving the SOFC are directed to the gas turbine combustors to perform a direct combustion ( $\text{H}_2/\text{O}_2$  reaction) [128].

The NETL system involves a virtual gasifier, a gas turbine and a real-time SOFC model, running on a dSpace hardware-in-the-loop-simulation platform [128, 130-132]. The hardware used to simulate the fuel cell is incorporated with a 120 kW Garret Series 85 auxiliary power unit (APU) for a gas turbine with a rotational speed of 40,500 rpm and compressor system. In this configuration both the anodic gas stream (unreacted  $H_2 + H_2O$ ) and the cathodic gas stream (unreacted  $O_2 + N_2 + H_2O$ ) leaving the SOFC are directed to the gas turbine combustors to perform a direct combustion ( $H_2/O_2$  reaction) [128].

In this configuration, the hybrid SOFC/GT system can reach a bottoming cycle efficiency of more than 60% [133] and enables optimization of the overall system flexibility when dealing with changing feedstock streams [129]. However, remaining challenges still exist, including control of cathode air flow, and compressor stall and surge [133]. The SOFC/GT hybrid system offers an economical return because the FC's lifetime can be extended in a hybrid generation [130]. Since SOFCs operate at temperature greater than  $600^\circ C$ , their system is appropriately run on various fuels (e.g. natural gas, syngas, biogas, ethanol, and biodiesel), as mentioned earlier, making them more economical for distributed power generation. A previous study showed that the net present value (NPV) of a polygeneration plant for power and chemical production could improve up to 63% if the system is switchable from power production to chemical production or vice versa [130]. The primary benefit of the SOFC/hybrid system is that the parasitic electric load on the power system from the required cathode air blower can be eliminated [24].



(a)



(b)

**Figure 1.10. Schematics of a typical SOFC flow sheet using (a) various fuel types, and (b) a possible GT/SOFC integrated plant [24, 128]**

From a thermodynamic standpoint, FCs represent one of the most efficient power generation technologies because they boast better exergy and thermal efficiency than the other technologies. A comparison of the exergy efficiency between FCs and other main power generation technologies, such as gas and diesel engines, gas turbines, photovoltaic panels, thermal solar power plants, waste incineration, wind turbines, hydroelectric plants,

and nuclear power plants has been reported elsewhere [134]. The study reported that the FC boasts a high energy efficiency, surpassing small hydroelectric and NG-based power plants (35-45%), that is close to large hydroelectric power plants (70-90%) [134].

#### **1.4.8.3. Recent status and challenges of FCs development in the U.S.**

In the U.S., since the late 1990s, the progress of FCs intended for distributed power generation, including SOFCs, has been led by the Solid State Energy Conversion Alliance (SECA) under the U.S. Department of Energy, which focuses on the development of commercially relevant and robust FC systems [24, 128, 135]. The efforts aim to reduce stack costs, increase cell efficiency, and extend cell longevity. A detailed report regarding the major FC development for distributed power generation in the U.S. has been provided elsewhere [136].

On August 3, 2015, the U.S. Environmental Protection Agency released its new source performance standard (NSPS) that required new coal power plants in the U.S. to emit less than 636 kg of CO<sub>2</sub> per megawatt hours (MWh) of gross power produced [137]. This new stringent limit was created considering the deployment of CCS (carbon capture and storage). Among the power plant candidates, an integrated gasification fuel cell (IGFC) was identified capable of achieving the stringent limit with a projected emission of about 603 kg CO<sub>2</sub>/MWh. The emission of an IGFC can be even lower if it would resort to a catalytic gasifier or a pressurized SOFC, resulting in a reduced emission level of 501 and 498 kg CO<sub>2</sub>/MWh, respectively [137]. Other types of power plants featuring CO<sub>2</sub> emission lower than the foreseen limit include IGCC power plants with high quality coal (627 kg CO<sub>2</sub>/MWh), Integrated Gasification Supercritical CO<sub>2</sub> Brayton Cycle Plants (603 kg CO<sub>2</sub>/MWh), Advanced Ultra Supercritical (USC) Plants with 25% steam (568 kg

CO<sub>2</sub>/MWh), IGCC plants with 1700°C Combustion Turbine (567 kg CO<sub>2</sub>/MWh), Integrated Gasification Triple Cycle Plants (527 kg CO<sub>2</sub>/MWh), Advanced USC Plants with 50% steam (465 kg CO<sub>2</sub>/MWh), and IGFC plants with catalytic gasifier and pressurized SOFC (430 kg CO<sub>2</sub>/MWh). Although this standard is currently under a repeal process [138], it has constituted a high level recognition of the fact that SOFCs are promising prime-movers for clean power generation in the future. An SOFC can be more economical than a pulverized coal and an IGCC when carbon capture storage (CCS) is required, and even more economical than a natural gas CCGTs if the natural gas prices exceed \$6.5/MMBtu [24].

Significant challenges relating to commercial SOFC plants can be summarized as following: improved system operation dynamic [129], reduced capital cost, increased unit capacity, and extended reliability and lifetime [137]. Severe fuel cell damages can occur in IGFCs due to thermal stresses, unbalanced pressures between anode and cathode, GT shaft over speeds, and compressor surges and stalls. These disturbances are likely to occur if the operational transients are very fast, such as in a fuel-flexible operation [130]. According to Electric Power Research Institute (EPRI)'s analysis, a megawatt-scale module of SOFC power plants with a capability to run more than 1,600 hours without any technical issue will be commercially available in the market after the year 2020 [137].

#### **1.4.9. Polygeneration based syngas**

Polygeneration is a strategy to improve the economics, sustainability, and overall conversion effectiveness of organic materials, including coal, biomass, and organic wastes. Instead of relying on a single product, polygeneration can generate distinct products in parallel, namely heat, electricity and liquid or gaseous chemicals, thanks to the dual nature

of syngas as a fuel or chemical feedstock [52, 128]. During operation, the polygeneration system must have a maximum flexibility and capability to switch from one product to another. For instance, if the local electricity selling price is high, the operator will only convert biomass into power. In turn, if prices of petrochemical commodities (such as ammonia and methanol) are elevated, the operator can produce liquid ammonia or methanol as the final product of the syngas.

**Table 1.7. Several polygeneration systems available in the current market**

System	Main characteristics
Combined heat and power production (CHP)	Generates heat and power (electricity) that can be used locally. Typical CHP with gas engines generates an electrical efficiency of 25-31%, while using an ORC and gas engines potentially offers biomass to electrical efficiency of 40% [52]. If an IGCC were used, an electrical efficiency of up to 53% can be achieved [139], while using a MGT and an SOFC theoretically could generate an electrical efficiency of 58-60% [140]. Above all, using an SOFC and biomass gasifiers potentially increases the electrical efficiency up to 65% [24].
Synthetic natural gas (SNG), heat and power production	To generate syngas that can be injected into natural gas pipeline. A polygeneration plant producing SNG can achieve an overall efficiency of 90% [52]. A high economic return of producing SNG can be obtained in the 20 MW-scale of the plant [141].
Biofuels, heat and power production	Biofuels generated from biomass gasification have significantly influenced today's world energy economic [26]. Methanol, DME, and FT diesel can be used for transportation and heating fuels. With a polygeneration plant, producing these fuels will be more cost-effective than stand-alone production [142, 143], including reducing more carbon footprints and GHG emissions [144, 145].
Hydrogen (H <sub>2</sub> ), heat and power production	H <sub>2</sub> is mainly used for FC power generation (commonly known as hydrogen economy). A high H <sub>2</sub> content with syngas LHV of 18-20 and 10-15 MJ/Nm <sup>3</sup> can be generated from biomass gasification using steam and oxygen, respectively [33, 40]. Instead of using oxygen and steam, an air blown gasifier can also generate a high hydrogen content (up to 6-7 MJ/Nm <sup>3</sup> ) by using several advanced gasifiers as described earlier.

Therefore, to continuously optimize the operational scenario, the polygeneration system must be able to respond in a fast and reliable way to requested changes. Major challenges can include storage strategy, integration with local power network, and control strategy due to integrated power network [146]. A leading institution that has been investigating this important control aspect for years is the National Energy Technology Laboratory (NETL). The control strategy is based on a cyber-physical system, which includes a virtual gasifier, a gas turbine and an SOFC, and secures a close numeric/hardware integration model [128, 130-132]. The system is able to simulate dynamic performances of a SOFC/GT hybrid power plant and optimize the overall system flexibility when dealing with various feedstocks. Table 1.7 presents the main characteristics of several polygeneration systems available worldwide.

### **1.5. Economic analyses of power generation from biomass and MSW gasification**

Studies of economics and socio-environmental analysis of power generation derived from gasification of biomass and MSW are still limited. Evans et al. [147] described the prices of generating electricity and the respective efficiencies of biomass gasification, compared with pyrolysis and combustion. Full life-cycle carbon dioxide emissions data from biomass power production was also included. The study highlighted the emissions from alternate fuels and technologies, such as straw combustion, short rotation crops, woodchip gasification, and forest residue woodchip gasification. However, the study did not discuss social impacts. Kirkels and Verbong [148] reviewed the development of biomass gasification since the 1980's using an extensive literature study (the most

significant part from IEA bioenergy) and science and technology indicators (i.e., patents). They found biomass gasification has not yet matured enough to be applied in the market and is hardly ready to compete with other technologies (especially the use of natural gas and biomass combustion). However, the economic and socio-environmental considerations were not discussed.

The following sections discuss economic and socio-environmental analysis on power generation derived from gasification of biomass and MSW. The discussion uses practical experiences of several operating gasification-based power plants worldwide that support distributed power generation (< 20 MW). The outcomes of the discussion are to support and accelerate the global development of power generation based on bio- and residual energies through the gasification of biomass and MSW.

### **1.5.1. Biomass**

Economic analysis of power generation from biomass syngas is greatly influenced by feedstock price and capital expenditures, with plant capacity also being a key parameter [149, 150]. Renewable energy policies, such as renewable portfolio standard (RPS) and renewable fuel standard (RFS), are also important to accelerate the deployment of power generation from gasification of biomass and MSW in the commercial market [151]. The economics performance of biomass gasification is discussed next.

#### **1.5.1.1. Economic potential of gasification of biomass and MSW**

Syngas production costs are critical for the economics of gasification technology. Syngas production costs may vary depending on the feedstock. According to a recent report [152], syngas derived from gasification of biomass and agricultural residues can reach \$5.5-6.0/MMBtu, while the cost of syngas produced from MSW may vary depending

on the plant capacity and tipping fee rates. A plant having 1,000 tons/day of treated MSW with zero tipping fees can potentially generate syngas with production cost of 2 cents per kWh (~\$5.9/MMBtu), while at tipping fee of \$60/ton, a syngas production cost can be nearly to zero [153]. In comparison, the production cost of syngas generated from natural gas (NG) lies generally in the range \$5-7/MMBtu (with NG base price of \$3/MMBtu) [7]. Therefore, due to the presence of tipping fees, generating syngas from gasification of MSW brings more economic potential than that from biomass. However, current challenges on MSW gasification remain. One of the major challenges is the high capital cost since current commercial technology of MSW gasification still relies on a high thermal plasma system that requires large amounts of energy for plasma generation (up to 5,000 °C) [47].

An important challenge in biomass gasification is the net cost of the feedstock, which includes harvesting, transportation, and additional processes (e.g., trimming, chopping, etc.) that require additional energy and increase the operational costs of the plant. In addition to organic domestic wastes and sludge, the use of residual biomass feedstocks, such as verge grass and demolition wood, can become beneficial due to their negative costs [154]; negative fuel costs are obtained when current costs for waste treatment can serve as income to the facility, which can ultimately reduce the power production costs; similarly MSW dumping provides tipping fees to the municipalities. However, the presence of verge grass and demolition wood is not likely to be sufficient to ensure the sustainable operation of the plant, so that a biomass power generation system is always smaller than coal-based power plants [155].

The availability of dedicated crops for energy purposes is essential to sustain the future primary energy demand. So far, switchgrass and short rotation crops (SRCs), such as

hybrid poplar, willow, Eucalyptus, and non-woody perennial grasses, such as Miscanthus, are ideally suited as renewable primary energies; however, their presence is also likely insufficient to support continuous operation of the plant [147]. As comparison, switchgrass generally has a maximum production rate of 8 dry metric ton/ha/annum, while poplar and willow have an equivalent production rate of 15 dry metric ton/ha/annum [156]. A typical biomass gasification plant with a feeding rate of 1,000 tons/day has generating capacity of 25 MWe [149]. At this condition, the plant can only sustain operation for a single day if the dedicated area provided were about 67 ha (without considering the harvesting time).

Table 1.8 presents the power production costs from gasification technology using biomass, waste and agricultural residues (i.e., demolition wood and organic domestic waste). Biomass gasification plants at a minimum scale of 0.5 MW generally pose sufficient economic feasibility [157], even though a 20 MW plant is largely accepted for commercial operation [158]. As the transportation fees greatly impacted the production cost [147, 155], lowest production costs were achieved using wastes (i.e., forestry residues and demolition wood) due to minimum transportation cost and possible tipping fees. Thus, using wastes as the gasifier feedstock is preferable to achieve a greater economic return, as mentioned earlier. However, current technologies for processing wastes (such as MSW) in the gasifier with sustainable operation are still limited and generally require high energy input (such as thermal plasma gasification), making the viability of the project difficult to maintain [33]. Besides the feedstock type, the plant capacity next most substantially affects the power production cost, as can be seen from the wood processing feedstock (i.e. 18 cents/kWh at 250 kW and 6 cents/kWh at 60 MW versus 4.2 cents/kWh at 300 MW). Thus, larger plants will be more economically competitive with current conventional available

technologies treating biomass and MSW (i.e. gas turbine and combustion system) than small plants. Power production cost from biomass must be competitive with fossil fuel to easily penetrate the market and get public acceptance [159].

**Table 1.8. Power production cost from gasification technology using various feedstock**

Authors	Year	Power production cost, cent \$/kWh	Capacity, MW	Fuel	Refs.
Elliot	1993	7.8	25	Low cost plantation	[160]
Bridgwater	1995	6.0	60	Wood	[161]
Craig and Mann	1996	6.5 – 8.2	56 – 132	Wood	[162]
Faaij et al.	1997	-7.5 – 9.6	30	Wastes and residues	[154]
Faaij et al.	1998	7.7	30	Willow	[163]
McKendry	2003	16.4	2.5	Energy crops	[40]
Hamelinck et al.	2005	4.2	300	Wood	[155]
Gan and Smith	2006	5.0	10	Poplar	[164]
Bain and Amos	2003	8.1 (7.4)	75 (150)	Forest residues, mill residues, agricultural residues, urban wood wastes	[165]
Marbe et al.	2004	4.6 – 5.3	50 – 60	Wood chips and wood pellets	[166, 167]
Afgan et al.	2007	3.0	75	Disintegrated wooden mass, sawdust	[168]
Susanto et al.	2017	8.4 – 18.0 <sup>a</sup>	0.5	Palm biomass	[169]
Wei et al.	2011	11.0 <sup>b</sup> – 18.0 <sup>c</sup>	0.5	Switchgrass	[158]
Arena et al.	2010	9.3 <sup>d</sup> – 12.6 <sup>e</sup>	0.2	Beechwood	[170]
Buchholz et al.	2012	18	0.25	Eucalyptus wood	[171]

Notes: <sup>a</sup> with 24 hours' operation; <sup>b</sup> with counting heat and <sup>c</sup> without counting heat; <sup>d</sup> using gas engine, while <sup>e</sup> using gas turbine with 1.18 \$/Euro.

### **1.5.1.2. Lesson learned from Muzizi Plant, Uganda**

A good example of a small-scale biomass gasification power plant that benefited the local economic community was the Muzizi Tea Estate processing utility in Uganda [171]. The estate is in Kibaale District, western Uganda, comprising 371 ha under tea (*Camellia sinensis*) and 99 ha under eucalyptus (*Eucalyptus grandis*). The estate produces around 1200 tons of black tea annually and employs approximately 400 tea pickers and 70 factory workers [171].

A 250-kW downdraft gasifier system was provided by Ankur Scientific, India and installed to replace one of the diesel generators (200 kW in capacity) that had previously been used to support the factory processes. The gasifier used fuelwood (cut 10 x 10 x 10 cm) with a feed rate of 320-400 kg/h. The fuelwood had a moisture content of more than 40 percent at the plant gate and, with air-drying within six months (uncovered), the moisture was reduced to approximately 15 percent. The gasifier reactor had a name plate capacity of 400 kW thermal output and was equipped with an automated fuelwood feeder, a charcoal removal, and a cyclone filter separating ash. The syngas cleaning system consisted of a syngas water-cooling and a scrubbing unit containing 20 m<sup>3</sup> water, two parallel filtering units with a coarse filter (wood chips) and two fine filters (sawdust) (each to allow switching filter units), and one cloth bag filter. The power generation unit used a three-phase 250 kW Cummins India syngas engine with a generator having an electrical efficiency of 16-20 percent. A blower was used to supply air into the gasifier and heat recovery units on the engine's exhaust pipes and the engine's water cooling cycle, and to connect to the tea drier (as shown in Figure 1.11) [171].

A 100 kW diesel generator was used to support a 30 kW internal consumption for running the pumps, blower, fuelwood feeder, and control units. The system ran continuously for about 12 h/day, supplying electricity to the withering troughs with demand load variations between 50 and 170 kW; the mean and the peak electricity output were 85 and 175 kW, respectively.

Several disturbances causing the gasifier to only produce 150 kW (of 250 kW capacity) were reported. Missing control units, low electricity demand (only 87 kW on average), and rapid changes of load (causing sudden pressure drop and eventually shut off of the gas engine) were several operational challenges during the plant run.

The gasification system successfully replaced the use of a 200-kW diesel fuel generator, saving 71,000 liter of diesel fuel per year. Total capital, operating and labor costs were \$459,198 (\$2087/kW), \$48,030/year, and \$17,275/year, respectively. With the feedstock price of \$22/dry-ton, the gasification power system provided an internal rate of return (IRR) of 13 percent. Electricity production costs and avoided diesel costs saved were about \$0.29/kWh and \$44,733/year. However, instead of using the diesel generator to supply the internal load, an improved system was proposed where the output power of the gasification power plant directly supplied the internal load. In this case, the gasification power system offered an internal rate of return (IRR) and payback period of 11 percent and 8 years, with the diesel fuel savings of 149,000 liters/year. In this case, the electricity production costs correspondingly decreased to \$0.18/kWh and avoided diesel costs increased to \$93,631/year [171].

Excluding the fuelwood supply chain beyond the plant gate, the plant generated employment from the local community. A group of at least 12 workers was involved to run

the entire gasification and power generation system, comprising two skilled and four unskilled workers and six employees (two shifts working) to treat the fuelwood feedstock. Moreover, under the improved system, the gasifier saved the use of diesel fuel and offered CO<sub>2</sub> emission reduction of about 771 tons/year [171]. The water from the cooling and scrubbing unit was discharged monthly and pumped into the tea fields to serve as fertilizer.

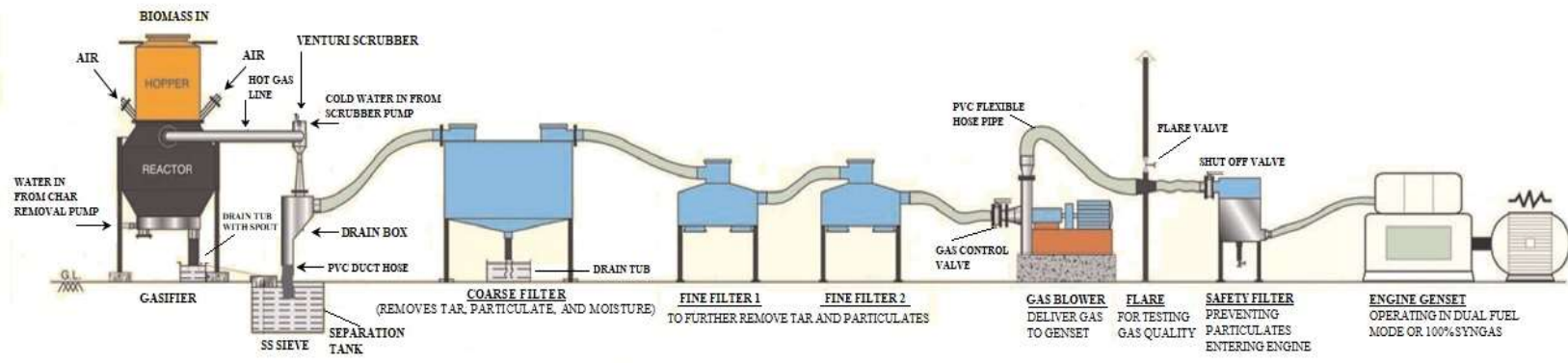
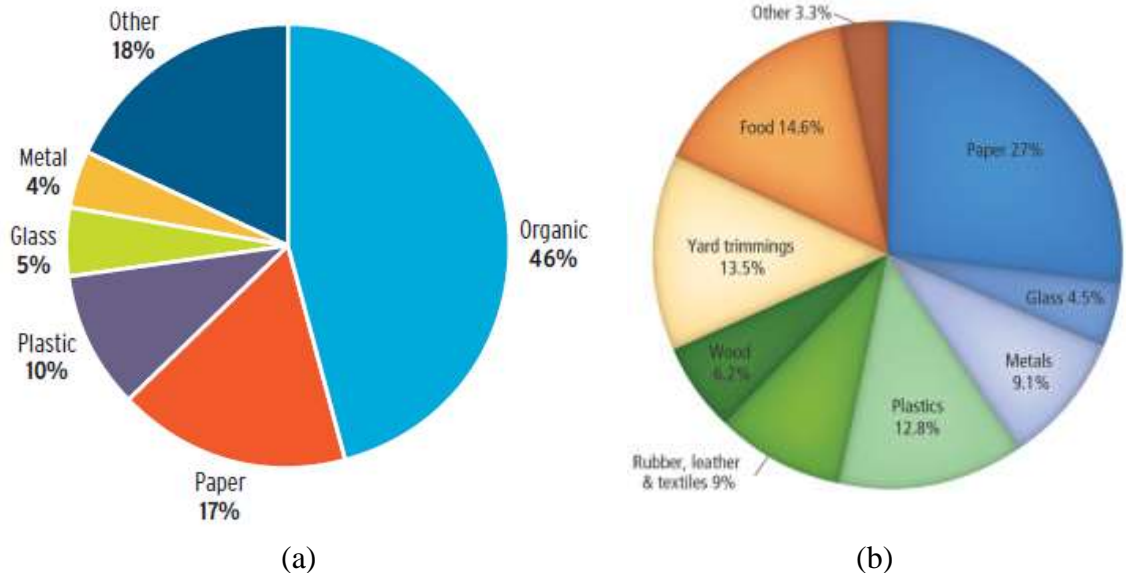


Figure 1.11. A schematic diagram of a 250 kW gasification based power generating system in Muzizi tea plant, Uganda [171]

### 1.5.2. MSW

Organic domestic waste and sludge are potential feedstocks that can improve the economic competitiveness of gasification technology but they can complicate the gasification process due to their low heating value and high ash content. Figure 1.12 illustrates the comparison composition of MSW in the U.S. and the world, which shows similar characteristics where the organic materials (i.e. paper, organic, wood, yard trimmings) are dominant (61-63%).



**Figure 1.12. Typical composition of MSW in the world (2009) [12] and in the U.S. (2013) [172]**

Compared to biomass, MSW relatively has a higher fraction of ash, as shown in Table 1.9. Gasification feedstocks with high ash contents are conducive to the formation of abundant and sometimes adherent deposits inside the gasifiers (commonly known as “ash agglomeration”) that can restrict (or ultimately block) the gasifier throughput and impair the cold gas efficiency [41, 42]. Moreover, the agglomeration eventually blocks the syngas

entering the downstream processes of power generation. Corresponding to this, plasma gasification to now has been considered as the most promising pathway to deal with MSW and its economic consideration will further be presented in the section below.

**Table 1.9. Proximate and ultimate analysis of different MSW and biomass**

Biomass type / References	MSW-1 [173]	MSW-2 [173]	MSW-3 [60]	SG [29]	Wood chips [174]	Red cheddar [56]
<b>Proximate (wt.%, dry basis)</b>						
Moisture content (wet basis)	51.7	44.0	20	7.69	7.50	10.39
Volatile matter	44.2	46.9	75.95	78.60	82.20	78.31
Fixed carbon	-	-	10.23	17.47	17.60	20.42
Ash	4.1	9.1	13.81	3.93	0.20	1.27
<b>Ultimate (wt.%, dry basis)</b>						
Carbon, C	21.2	24.7	48.23	49.63	52.13	54.44
Hydrogen, H	3.0	3.3	6.37	5.72	6.36	5.80
Oxygen, O	23.1	18.3	28.48	40.37	41.23	38.28
Nitrogen, N	0.3	0.33	1.22	0.30	0.07	0.20
Sulphur, S	0.03	0.03	0.76	0.05	0.01	0.01
Lower heating value, MJ/kg	6.80	9.10	16.30	16.49	20.17	18.44
Higher heating value,	7.14*	9.55*	20.20	17.73*	21.24	19.69
Bulk density (kg/m <sup>3</sup> )			1,095	91	660	122

\*Note: calculated using 1.05\*LHV; SG = Switchgrass

### 1.5.2.1. Economic potential of plasma gasification

The data on the economics of commercial-scale gasification plants for MSW are still scarce. In general, gasification technology has not yet been applied for treating MSW at commercial scale, including in the U.S. However, available data from pilot and demonstration-scale facilities shows that the cost of gasification systems varies significantly depending on the type of feedstock, the type of gasification technology, the type of outputs and location [175].

**Table 1.10. List of power generation plants using plasma technology for treating MSW**

Plants	Location	Descriptions	Status	Ref
The Maharashtra Enviro Power Ltd. (“MEPL”) plant / SMSIL Plant	Pune, India	Syngas is used to generate electricity which is exported to the grid. 40 to 60 waste streams including hazardous and medical waste with total capacity of 72 tpd are simultaneously treated during the year. Approximately 1.6 MW of electricity is exported to the grid.	Plant has been in operation since 2008	[47, 176]
Tees Valley Plant	Northeast of UK	With 1,000 tpd of feedstock, the Tees Valley project could be the biggest plasma gasification power plant with total power output capacity of 2 x 50 MW. Two units of gasifier have been delivered to site on May 2013. The technology provider was Westinghouse Plasma Corporation (WOC) using plasma torches, while the owner of the project was Air Product. The project cost reached \$13,000/kW. However, due to technical difficulty and hard economic return, Air Liquid exit from this project.	Project suspended since April 2016	[47, 49]
Eco-Valley Plant	Utashinai, Japan	The plant began into operation in 2003 with total capacity of 165 tpd for treating MSW and auto shredder residue (ASR) (50:50 mixture). The project’s sponsor was supported by Hitachi and Westinghouse Corporation. The plant used plasma	Plant ceased operation in 2013 due to unsustainable feedstock input	[177]

Plants	Location	Descriptions	Status	Ref
		torches that operated at above 5,500°C, and could generate syngas with LHV and cold gas efficiency of around 11.9 MJ/Nm <sup>3</sup> and 79%, respectively. The electricity was produced through steam (Rankine) cycle. Torch power requirement is about 2.4% of energy input, while syngas production is 78% of energy output. During operation, plant delivered 1.5 MW of electricity to the grid.		
Shanghai Chengtou hazardous waste facility	Shanghai, China	The plant owner is GTS Energy, while the technology provider is WPC. The facility was built to treat 30 tpd of medical wastes. The commissioning was successfully run in 2014. The electricity generation was performed by using steam cycle.	Plant has been in operation since 2014.	[47]
Plasco Plant	Ottawa, Ontario, Canada	The plant treats 85 tpd of post-recycle MSW. The facility uses gas engine to generate the electricity with total generation of 4 MW (net).	The plant has been in operation since 2008	[176]
Morcenx Plant	Morcenx, France	The technology provider is Europlasma. The plant was built to run on 100 tpd of industrial waste combined with 41 tpd of wood chips. Total electricity generation is nearly 12 MW. The plant also produces 18 MW of hot water. The plant uses two plasma torches and the syngas	The plant has been in operation since 2014	[176]

Plants	Location	Descriptions	Status	Ref
		generated is directly used to run the gas engine.		
Bijie Plant	Bijie, China	The project owner is Greenworld Energy Solutions Corp. (GES). The plant is designed to treat 600 tpd of MSW from the city, and to generate 15 MW of electricity. WPC is the provider of plasma technology.	The project is preparing for the commissioning.	[176]

Gasification facilities must offset capital costs with product revenues and tipping fees. The amount of fuels, chemicals, or energy produced per ton is affected by the management of the heat produced by the gasification process and whether it is captured and/or used at the facility to provide heat and/or energy to the system. Estimated capital costs derived from MSW gasification facilities using plasma technology from different companies (e.g. Enerkem, AlterNRG, Plasco, and Europlasma) range from \$40 to \$86 per ton with operating costs vary from \$42 to \$63 per ton [175]. Table 1.10 lists several plants that have been operated throughout the world since 2008.

A key factor that increases the economics of a plasma gasification power plant is the tipping fee. The tipping fees of landfills across regions in the U.S. have significantly increased, from averagely \$28.8/ton (in 1992) to \$43.6/ton (in 2011). In 2011, the most lucrative tipping fees could be found in the Northeast (~\$70/ton), followed by the Pacific (~\$58/ton), making these regions greatly attractive for plasma gasification power plants [175]. Conversely, states where tipping fees are low may not be locations where a gasification facility will be competitive because charging a tipping fee will not be sufficient to cover its operating costs. According to a previous report [153], at a feeding rate of 1,000

tons/day, syngas production cost from MSW gasification could be zero if a tipping fee of \$60/ton were applied; however, a syngas production cost of \$6/MMBtu would be generated when no tipping fee was applied (\$0/ton). A recent report presents that the tipping fee has had a steady average 7% percent increase nationally from 2016 through 2018, with a national average reaching \$55.1/ton; the largest tip fee increases are observed in the Midwest (18.3% percent), Northeast (15.8% percent), and Pacific (11.9% percent) regions over this period [178]

#### **1.5.2.2. Lesson learned from Utashinai Plant, Japan**

An existing plasma gasification plant, namely the Eco-Valley Waste to Energy (WTE) facility (Utashinai, Japan), has provided successful operational records and useful lessons for future WTE plants. The plant was operated at above 5,500°C to treat MSW at capacity of 220 to 300 ton/day using four 300-kW plasma torches and hot air as the gasification medium [177, 179]. The technology used at Eco-Valley is a result of a successful collaboration between Westinghouse Plasma Corp. (Alter NRG) and Hitachi Metals. The plant was constructed in 2002 and reached full operation in April 2003. The facility was originally designed to process a 50/50 mixture of auto shredder residues and MSW [177]. With a design capacity of 165 tons per day (tpd), this plant succeeded in producing syngas with a high fraction of CO and H<sub>2</sub>. The syngas generated was burned in a boiler to produce steam that powered a steam turbine, resulting in a total output power of 8 MW (about 1.5 MW exported to the grid [177]). However, nearly half of total power output was consumed to operate the plant operation, ultimately reducing its economic performance [179]. For operating the plant, there was no available data of tipping fees found in the literature. Due to the insufficient supply of feedstock, the plant operation was ceased in 2013 [177].

In addition to the Eco-Valley WTE facility, Hitachi Metals had another smaller plant, Mihama Mikata, that processed 17.2 tpd of MSW and 4.8 tpd of sewage sludge. The plant had been in full operation since 2003 without having issue with feed stream supply [177]. Based on operational experiences of the Utashinai and Mihama Mikata plant, AlterNRG developed the plasma reactor (namely G65) to have a capability to proceed seven times the amount of feedstock as each of the gasifiers at Eco-Valley. This plasma reactor was initially to be employed in the Tees Valley project of UK; however, the project was discontinued by Air Products in mid-2016 due to mostly technical and economic constraints [49].

### **1.5.3. Techno-economic comparison of various technologies to generate power from syngas**

Thermal equipment systems, such as internal combustion engines (ICEs), gas turbines (GTs) and steam units, rely on proven technologies and represent qualified candidates for future distributed power generation. However, fuel cells (FCs) enjoy several advantages: (i) they boast better standalone efficiencies; (ii) they can be directly fed with syngas fuels derived from biomass or solid wastes and (iii) they are static devices exempt of wear issues and run with almost no noise nor vibrations. The high efficiency advantage of FCs is tied to the fact that they are not constrained by the Carnot efficiency, unlike ICE's, GTs and Rankine cycles. However, advanced research is still emerging to minimize their degradation due to the carbon deposition and other possible contaminants of syngas

Instead of relying on individual technology, a hybrid gasifier concept integrating a fuel cell with a gas turbine is a promising alternative to increase the economics of power generation from gasification of biomass and MSW (including coal). The hybrid concept can support distributed power generation because of moderate capacity of the power

generation (in the range 100 kW to MW-scale), while it can increase the system efficiency (over 60 percent) [131, 180].

One of the worldwide leading facilities focusing on investigating the performance of this hybrid system is the hyper facility in the National Energy Technology Laboratory (NETL), USA. The hyper facility consists of a virtual gasifier, a gas turbine, and a real-time solid oxide fuel cell (SOFC), running on a dSpace hardware-in-the-loop-simulation platform. The system is capable of investigating system transient characteristics that are associated with feasible dynamic operating ranges, coupling effects between fuel cell subsystem and recuperated gas turbine cycle, and highly complex dynamic control strategies. Studies on detailed performance of this hybrid power generation system have been reported previously [128, 129, 181].

A summary of techno-economic comparison of power generation technologies, covering thermal equipment systems and FCs that can be fed with syngas is presented in Table 1.11 [124].

**Table 1.11. Techno-economic comparison of various technologies to generate power from syngas**

Stationary power	Power level, MW	Electrical Efficiency, %	Lifetime, years	Capital cost, \$/kW	Capacity factor, %
PAFC	0.2 – 10	30 – 45	5 – 20	1,500	< 95
MCFC + GT	0.1 - 100	55 – 65	5 – 20	1,000	< 95
SOFC + GT	0.1 – 100	55 – 65	5 – 20	1,000	< 95
Coal steam PP	10 – 1,000	33 – 40	> 20	1,300 – 2,000	60 – 90
IGCC	10 – 1,000	43 – 47	> 20	1,500 – 2,000	75 – 90

Stationary power	Power level, MW	Electrical Efficiency, %	Lifetime, years	Capital cost, \$/kW	Capacity factor, %
NG open cycle GT	0.03 – 1,000	30 – 40	> 20	500 – 800	< 95
NG combined cycle GT	50 – 1,000	45 – 60	> 20	500 – 1,000	< 95
Microturbine	0.01 – 0.5	15 – 30	5 – 10	800 – 1,500	80 – 95

Notes: PAFC = phosphoric acid fuel cell; MCFC = molten carbonate fuel cell; SOFC = solid oxide fuel cell; GT = gas turbine; PP = power plant; IGCC = integrated gasification combined cycle; NG = natural gas;

As shown, the hybrid power generation system offers a higher electrical efficiency than other types of power generation technologies with moderate power levels (0.1 – 100 MW). Because the hybrid power generation system is not commercially available yet in the market, simple and combined cycle gas turbine power plants are still leading technology with robust and proven performance; thus, these power plants are considered the second most efficient technology for generating power from syngas.

In addition, among the various processes of biomass and MSW gasification, the processes using air as a gasification medium promise a higher economic viability. A system study conducted in the U.S., taking as reference a plant capacity of 250 tpd shows that air gasification systems appeared more attractive than incineration, pyrolysis and thermal plasma. In term of CAPEX and OPEX, an air gasification system offers a greater economic return (\$120,000/ton/day and \$125/MWh) than incineration (\$240,000/ton/day and \$348/MWh), pyrolysis (\$160,000/ton/day and \$222/MWh), and thermal plasma (\$960,000/ton/day and \$1000/MWh) [182].

## **1.6. Socio-environmental analyses of power generation based gasification of biomass and MSW**

### **1.6.1. Social analysis**

The production of electricity from biomass and MSW raises many issues. The use of biomass for electricity production interferes with many social aspects, such as land issues, the actual renewal of harvested vegetation and a potential competition with food usages. To minimize the land issues and potential competition with food usage, growing biomass in the marginal lands is good alternative [147]. In addition, crops having a high maintenance requirement due to the use of watering, fertilizer and pest and disease control are not suitable for the electricity generation as they reduce environmental benefits, and increase carbon emissions and costs [147]. The actual renewal of harvested vegetation should be short and the crops must have a high energy yield that consequently reduces the necessary land-take. Also, the crops must not be edible to avoid the issue of food competition. However, all these issues disappear when using MSW as feedstock. These social aspects including potential job creation are discussed next.

#### **1.6.1.1. Creation of employment**

Direct labor inputs for wood biomass are considered as two to three times greater per unit energy than for coal [147]. The employment generated by the production of electricity from fuel oil is about 15 person.year/MW.year, while 32 person.year/MW.year for biomass. For underdeveloped and partly developing countries, where the auto-machineries for harvesting the biomass are still not well used, the need of employment generally follows the production rate of the biomass. A 10 MW biomass-based electricity generating plant can generate 20 jobs on-site and 80 jobs in the countryside and woodlands, transport,

catering, etc. [157]. Among other biomass crops (i.e. wheat, poplar, willow, switchgrass), Miscanthus has the largest potential energy that can be converted into syngas as it contains a high energy yield (up to 555 GJ/ha) and offers a higher crop yields than other crops (reaching 30 dmt/ha/a). It is also a non-edible feedstock and can be planted in non-arable areas, providing more potential employment opportunities for the local community [156]. Moreover, the value of Miscanthus as an energy crop at a 20 t/ha yield of dry matter would be about GBP 620/ha (~\$794/ha), which is equivalent to a value of one third that of oil and about half that of coal [156].

The sector of management of waste also represents a huge employment potential. In 2015, more than 40,600 people were employed in 297 waste transfer facilities, 104 recycling facilities, 43 organic processing facilities and 244 active solid waste landfills in the United States [183]. These figures refer to the overall waste management business, including the gasification of waste, and seem to be likely increasing in the near future reflecting the increased waste disposal by 2025 [12].

#### **1.6.1.2. Community development**

In emerging regions, such as Asian and African countries, the creation of distributed biomass and MSW based power units and the resulting economic activities, including materials transportation and erection of power units, will entail structuring or reinforcing effects on the societies. The generation of new employment opportunities, employee training, and technology transfers are examples of direct effects on the societies where local people can receive benefits from the presence of distributed power plants. Moreover, conscious gasification processes of biomass and wastes can have health benefits in the local community due to reduction of uncontrolled landfilling and noxious emissions, promoting

cleaner air in the atmosphere and preserving ground water from contaminations. Besides economic gain, education and health benefit, the presence of distributed power generation expands opportunities for supporting women productive endeavors (e.g. women and girls can collect fuel resources and improve efficiency of cooking processes through use of electric appliances). Also, maternal mortality rates can be significantly decreased due to the electrification of rural clinics [184].

Besides, the plant in Muzizi Tea Estate processing utility, Uganda, as discussed earlier (section 1.5.1.2), another successful project employing a decentralized biomass gasification-based power generation system benefiting the local community occurred in an un-electrified Indian village called Hosahalli village in Karnataka province, India [39]. The project emphatically reflects the promising nature of gasification systems. Power derived from a biomass gasification system provided lighting, drinking water supply via pipes, irrigation water supply and flour milling. A 20-kW gasifier-engine generator system with all the accessories for fuel processing and electricity distribution was installed in 1988 and operated until 2004. It satisfied all the electricity needs of the entire village. Cost of fuel, operation and maintenance costs were calculated as 5.85 INR/kWh (~\$9.2 cents/kWh<sup>1</sup>) at a load of 5 kW and 3.34 INR/kWh (\$5.3 cents/kWh) at a load of 20 kW, proving the economic potential of the system and its viability to be implemented in other part of the world [39].

An MSW treating facility (ENVIA plant), sponsored by Velocys, has recently been commissioned in Oklahoma City and produces synthetic hydrocarbons. The plant uses a Fischer-Tropsch process to convert MSW (~200,000 tons/year) into syngas and

---

<sup>1</sup> With exchange rate of 63.53 INR/\$

hydrocarbon jet fuel and is likely to cut the lifecycle GHG emission by 60 percent. The throughput of syngas is in the order of 28 million scf per day and hydrocarbon output is 1,000 barrels per day (bpd). This installation is currently considered as a model of modern biorefinery and has become a positive actor in the local economy and contributor to improved environmental stewardship [185, 186].

### **1.6.2. Environmental analysis and its pertinent standard**

In environmental terms, the gasification of biomass and MSW is considered superior to the incineration processes. Gasification allows possible raw materials contaminants (e.g., heavy metals, sulfur, etc.) to be easily collected in the ash drum together with the ash generated from the reactor, significantly reducing their presence in the product gas (syngas). Incineration simply releases all raw materials contaminants in the product stream together with the heat. Therefore, gasification is always considered as a cleaner technology, minimizing release of harmful pollutants to the atmosphere.

Consistent syngas facility designs will include extensive gas clean-up systems able to suppress particulate matter (PM) and tar residues. The possible environmental concerns can be divided into four main categories, which are (i) ash/slag residues, (ii) particulates (fly ash) gas, (iii) flue gas emissions, and iv) wastewater, as presented next.

#### **1.6.2.1. Ash / slag**

The disposal of the ash generated from biomass and MSW gasification must meet the pertinent standards. Leaching tests and acid extraction are common methods to evaluate the risks of ground water contamination. When these tests are performed on the ash from a 50-MSW gasification power plant and compared to the pertinent standard, the results are presented in Table 1.12 to have consistently met the targeted values [33, 173]. Because of

this ash material's low impurity levels and good homogeneity, it can be sold for various uses, such as an aggregate for asphalt paving. The metal oxides recovered from the melting section can be also separated during chemical treatment of the fly ash. This oxide fraction will be then deduced from the total output of ash, which will substantially reduce the amount of solid residues that must be disposed in landfills. Figure 1.13 shows ash/slag samples collected from co-gasification of MSW and biomass.



**Figure 1.13. Samples of ash/slag collected from the ash collector from co-gasification of MSW and biomass, with a detailed performance of power generation reported by Indrawan et al. [60]**

**Table 1.12. Leaching test and acid extraction test of ash disposed from MSW gasification power plant**

Pollutants	Leaching test		Acid-extraction test	
	Measured	JIS standard	Measured	JIS standard
Cd	< 0.001 mg/L	< 0.01 mg/L	< 5 mg/kg	< 150 mg/kg
Pb	< 0.005 mg/L	< 0.01 mg/L	18 mg/kg	< 150 mg/kg
Cr <sup>6+</sup>	< 0.02 mg/L	< 0.05 mg/L	< 5 mg/kg	< 250 mg/kg
As	< 0.001 mg/L	< 0.01 mg/L	< 5 mg/kg	< 150 mg/kg
Total Hg	< 0.0005 mg/L	< 0.0005 mg/L	< 0.05 mg/kg	< 15 mg/kg

Pollutants	Leaching test		Acid-extraction test	
	Measured	JIS standard	Measured	JIS standard
Se	< 0.001 mg/L	< 0.01	< 5 mg/kg	< 150 mg/kg
CN	-	-	< 1 mg/kg	< 50 mg/kg
F	-	-	172 mg/kg	< 4000 mg/kg
B	-	-	260 mg/kg	< 4000 mg/kg
Metal Fe	-	-	0.18 mg/kg	< 1.0%

### 1.6.2.2. Particulates (PMs) / Fly ash

Biomass and MSW gasification processes for power production often result in much lower emissions of pollutants compared to conventional incineration plants. The gasification process provides an inherent capability to remove most PMs like ash as slag or bottom ash. The presence of limited oxygen inhibits combustions and generates syngas containing high-density contaminants, which are easy to remove. Most gasification plants use a wet scrubbing technique to remove syngas contaminants [18]. As a comparison, in incineration plants, since air contains a large amount of nitrogen along with trace amounts of other gases that are not necessary in the combustion reaction, combustion gases are much less dense than syngas produced from the same fuel. Therefore, pollutants in the combustion exhaust are at much lower concentrations than in the syngas, resulting in a more complex system of air pollution control. The intrinsic advantages in removing syngas contaminants have been presented in detail by Ratafia-Brown et al. [18].

### 1.6.2.3. Flue Gas Emissions

In power generation, the control of noxious emissions such as CO<sub>2</sub>, black smoke, VOCs, ozone, poly-aromatic hydrocarbons, PMs, toxic metals, SO<sub>x</sub> and NO<sub>x</sub> will remain a main challenge that needs to be addressed by all stakeholders, including authorities [187].

The acid gases SO<sub>2</sub>, SO<sub>3</sub>, HCl, and HF are commonly considered as a group because they are all removed by the same kind of control equipment, such as dry or wet scrubbers [188]. Emissions generated from gasification of biomass and MSW, including their control strategies and associated standards, are presented in the following sections.

### 1.6.2.3.1. Emission and its control strategy

Several major pollutants generated from gasification of biomass and MSW, including fundamental abatement strategies to reduce their levels, are summarized in Table 1.13. Among major pollutants, heavy metal pollutants (such as cadmium, Cd) are found to be more risky for carcinogenic exposure than PCDDs/PCDFs [189]. Compared to gasification plants, PCDDs/PCDFs generally have a higher concentration in the flue gas of incineration plants [21, 34]. Thus, the emission control in a gasification power plant should focus on heavy metals in order to reduce the carcinogenic risk [189].

**Table 1.13. The possible elemental pollutants generated from gasification of biomass and MSW and fundamental abatement strategies to reduce their levels**

Pollutants	Production precursor	Reduction method
<i>Major elements</i>		
Chlorine, Cl	Observed only in Fly ash/flue gas [173], due to feedstock (esp. MSW) containing chlorine	Flue gas desulphurization (FGD) technology: once-through (wet and dry) and regenerable (wet and dry) technique [190]
Sulfur, S	Distributed in slag and flue gas (dominant), due to feedstock containing sulfur.  Together with oxygen, sulfur forms sulfur dioxide (SO <sub>2</sub> ).	Slag: Cyclone, ash/slag removal system [173].  Flue gas: Flue gas desulphurization (FGD) technology: once-through (wet and dry) and regenerable (wet and dry) technique [8]
Calcium, CaO	Equally distributed in slag and flue gas, due to feedstock (esp. MSW) containing calcium [173].	Slag: Cyclone, ash/slag removal system.

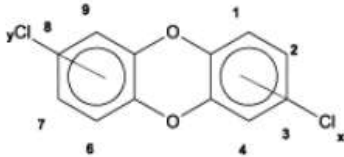
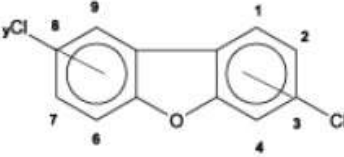
<b>Pollutants</b>	<b>Production precursor</b>	<b>Reduction method</b>
		Flue gas: Flue gas desulphurization (FGD) technology: once-through (wet and dry) and regenerable (wet and dry) technique [190]
Silica, SiO <sub>2</sub>	Equally distributed in slag and flue gas, due to feedstock (e.g. MSW) containing silica	Slag: Cyclone, ash/slag removal system  Flue gas: Flue gas desulphurization (FGD) technology: once-through (wet and dry) and regenerable (wet and dry) technique [190]
Aluminum, Al <sub>2</sub> O <sub>3</sub>	Fairly distributed in slag and flue gas (slightly more dominant) [173], due to feedstock (esp. MSW) containing Aluminum	Slag: Cyclone, ash/slag removal system [173]  Flue gas: Flue gas desulphurization (FGD) technology: once-through (wet and dry) and regenerable (wet and dry) technique [190]
Sodium, Na <sub>2</sub> O	Fairly distributed in slag and flue gas [173], due to feedstock (esp. MSW) containing sodium	Slag: Cyclone, ash/slag removal system [173].  Flue gas: Flue gas desulphurization (FGD) technology: once-through (wet and dry) and regenerable (wet and dry) technique [190]
Potassium, K <sub>2</sub> O	Fairly distributed in slag and flue gas (slightly more dominant) [173], due to feedstock (esp. MSW) containing potassium.	Slag: Cyclone, ash/slag removal system [173].  Flue gas: Flue gas desulphurization (FGD) technology: once-through (wet and dry) and regenerable (wet and dry) technique [190]
Magnesium, MgO	Equally distributed in slag and flue gas [173], due to feedstock (esp. MSW) containing magnesium	Slag: Cyclone, ash/slag removal system [173].  Flue gas: Flue gas desulphurization (FGD) technology: once-through (wet and dry) and regenerable (wet and dry) technique [190]

<b>Pollutants</b>	<b>Production precursor</b>	<b>Reduction method</b>
<i>Heavy metals</i>		
Lead, Pb	Distributed in slag and fly ash/flue gas (majority) due to feedstock (esp. MSW) containing lead.	Slag: Cyclone, ash/slag removal system [173].  Flue gas: (1) Selective Catalytic Reduction (SCR) with Flue-gas Desulfurization (FGD) [191], (2) Activated Carbon Injection (ACI) [191], (3) ACI with Fabric Filter (FF) [191], (4) Electrostatic Precipitators (ESP) [191], (5) Baghouse filter [173].
Ferrous, Fe	Distributed in slag (dominant) and flue gas, due to feedstock (esp. MSW) containing ferrous.	Slag: Cyclone, ash/slag removal system.  Flue gas: (1) Selective Catalytic Reduction (SCR) with Flue-gas Desulfurization (FGD) [191], (2) Activated Carbon Injection (ACI) [191], (3) ACI with Fabric Filter (FF) [191], (4) Electrostatic Precipitators (ESP) [191]. (5) Baghouse filter [173]
Copper, Cu	Distributed in slag (dominant) and flue gas, due to feedstock (esp. MSW) containing copper	Slag: Cyclone, ash/slag removal system [173].  Flue gas: (1) Selective Catalytic Reduction (SCR) with Flue-gas Desulfurization (FGD) [191], (2) Activated Carbon Injection (ACI) [191],

<b>Pollutants</b>	<b>Production precursor</b>	<b>Reduction method</b>
		(3) ACI with Fabric Filter (FF) [191], (4) Electrostatic Precipitators (ESP) [191].
Zinc, Zn	Distributed in slag and flue gas (dominant), due to feedstock (esp. MSW) containing zinc	Slag: Cyclone, ash/slag removal system [173].  Flue gas: (1) Selective Catalytic Reduction (SCR) with Flue-gas Desulfurization (FGD) [191], (2) Activated Carbon Injection (ACI) [191], (3) ACI with Fabric Filter (FF) [191], (4) Electrostatic Precipitators (ESP) [191], (5) Baghouse filter [173]
Mercury, Hg	Distributed in slag and flue gas, due to feedstock (esp. MSW) containing mercury	Slag: Cyclone [192], Ash/slag removal system.  Flue gas: (1) Selective Catalytic Reduction (SCR) with Flue-gas Desulfurization (FGD) [191, 192], (2) Activated Carbon Injection (ACI) [191], (3) ACI with Fabric Filter (FF) [191], (4) Electrostatic Precipitators (ESP) [191], (5) Baghouse filter [173], (6) Spray dryer absorber/fabric filter [192].
Nickel, Ni	Distributed in flue gas [193] due to feedstock (esp. MSW) containing mercury	(1) Selective Catalytic Reduction (SCR) with Flue-gas Desulfurization (FGD) [191, 192], (2) Activated Carbon Injection (ACI) [191],

<b>Pollutants</b>	<b>Production precursor</b>	<b>Reduction method</b>
		(3) ACI with Fabric Filter (FF) [191], (4) Electrostatic Precipitators (ESP) [191], (5) Baghouse filter [173], (6) Spray dryer absorber/fabric filter [192].
Arsenic, As	Distributed in flue gas [193] due to feedstock (esp. MSW) containing mercury	(1) Selective Catalytic Reduction (SCR) with Flue-gas Desulfurization (FGD) [191, 192], (2) Activated Carbon Injection (ACI) [191], (3) ACI with Fabric Filter (FF) [191], (4) Electrostatic Precipitators (ESP) [191], (5) Baghouse filter [173], (6) Spray dryer absorber/fabric filter [192].
Cadmium, Cd	Distributed in flue gas [193] due to feedstock (esp. MSW) containing mercury	(1) Selective Catalytic Reduction (SCR) with Flue-gas Desulfurization (FGD) [191, 192], (2) Activated Carbon Injection (ACI) [191], (3) ACI with Fabric Filter (FF) [191], (4) Electrostatic Precipitators (ESP) [191], (5) Baghouse filter [173], (6) Spray dryer absorber/fabric filter [192].
<b><i>Emissions</i></b>		
Dust / particulates	Gasification process [173].	Cyclone, Baghouse filter [173]

<b>Pollutants</b>	<b>Production precursor</b>	<b>Reduction method</b>
Carbon Dioxide, CO <sub>2</sub>	<p>(1) Mostly due to the oxidation reactions of gasification:</p> <ol style="list-style-type: none"> <li>1. <math>\text{CO} + \frac{1}{2} \text{O}_2 \rightarrow \text{CO}_2</math></li> <li>2. <math>\text{C} + \text{O}_2 \rightarrow \text{CO}_2</math></li> <li>3. <math>\text{CH}_4 + 2\text{O}_2 \rightarrow \text{CO}_2 + 2 \text{H}_2\text{O}</math></li> </ol> <p>(2) The engine combustion <math>\text{CH}_4 + \text{O}_2 \rightarrow \text{CO}_2 + \text{H}_2\text{O}</math></p>	<p><u>Primary method:</u></p> <p>(1) The reduced use of coal as the input of gasification</p> <p><u>Secondary method:</u></p> <p>(2) CO<sub>2</sub> sequestration: amine based sorbent [8]. Carbon capture</p>
Sulfur Dioxide, SO <sub>2</sub>	A high temperature combustion of the internal combustion (IC) engine converts sulfur in the fuel into SO <sub>2</sub> and SO <sub>3</sub> [194]	<p>(1) Sulfur removal from the fuel.</p> <p>(2) Flue gas desulphurization (FGD) technology: once-through (wet and dry) and regenerable (wet and dry) technique [190].</p>
Nitrogen Oxides, NO <sub>x</sub>	<p>The high combustion of syngas/natural gas occurring at temperature higher than 1,200°C following the Zeldovich mechanism develops the formation of NO<sub>x</sub> [194]:</p> $\text{N}_2 + \text{O} = \text{NO} + \text{N}$ $\text{N} + \text{O}_2 = \text{NO} + \text{O}$ $\text{N} + \text{OH} = \text{NO} + \text{H}$	<p>(1) Selective catalytic reduction (SCR) method can be used prior to the stack [173].</p> <p>(2) Flue Gas Recirculation (FGR) [194].</p> <p>(3) Low NO<sub>x</sub> Burners (LNB) [194].</p> <p>(4) Combustion optimization [194].</p> <p>(5) Less Excess Air (LEA) [194].</p> <p>(6) Water/steam injection [194].</p> <p>(7) Air preheat reduction [194].</p> <p>(8) The use of Ultra-Low Nitrogen Fuel [194].</p> <p>(9) The use of Non-Thermal Plasma Reactor [194].</p> <p>The use of Oxygen Instead Of Air [194].</p>
Carbon monoxides, CO	<p>(1) Oxidation, water-gas and Boudouard reactions of gasification process [37]:</p> <ol style="list-style-type: none"> <li>1. <math>\text{C} + \frac{1}{2} \text{O}_2 \rightarrow \text{CO}</math></li> <li>2. <math>\text{C} + \text{H}_2\text{O} \rightarrow \text{CO} + \text{H}_2</math></li> <li>3. <math>\text{C} + \text{CO}_2 \rightarrow 2\text{CO}</math></li> </ol> <p>(2) The incomplete combustion of the syngas engine</p>	<p><u>From viewpoint of Gasification:</u></p> <p>(1) Lowering the temperature of gasification can reduce the amount of CO in syngas [36], however, a high CO concentration of syngas is expected as it can increase the lower heating value (LHV) of the syngas.</p> <p><u>From viewpoint of engine operation:</u></p>

Pollutants	Production precursor	Reduction method
		The use of lean operation (high Air-Fuel-Ratio/AFR) [195].
PCDDs/PCDFs	<p>(1) Feedstock (esp. MSW) containing trace amount of chlorine [196-199], creates de novo synthesis, a reaction of the oxidative breakdown and transformation of macromolecular carbon structures to aromatic compounds [199-201].</p> <p>(2) Since PCDD has two oxygen atoms, and PCDF has one oxygen atom, a rich oxygen environment is preferred to accelerate the formation of PCDDs/PCDFs [21, 199, 201].</p> <div style="text-align: center;">  <p>PCDD</p>  <p>PCDF</p> </div>	<p><u>Primary method (preventing the PCDDs/PCDFs formation):</u></p> <ol style="list-style-type: none"> <li>(1) Oxygen starving process such as gasification [21, 199-202].</li> <li>(2) Proper selection of raw materials, avoiding as possible the addition of chlorine into the process [199].</li> <li>(3) The use of inhibitor for preventing de novo synthesis such as triethanolamine [199]. Another is ammonia, however, it is not effective for large-scale plant [199, 201, 203-205].</li> <li>(4) Lowering hydrocarbon and dust emission [199].</li> <li>(5) Accelerated cooling of the flue gas into temperature of 600-200°C [199, 206].</li> </ol> <p><u>Secondary method (providing measures to limit the emission of PCDDs/PCDFs to the atmosphere):</u></p> <ol style="list-style-type: none"> <li>(1) Cyclone [206].</li> <li>(2) Electrostatic precipitator [206].</li> <li>(3) Baghouse filter, catalytic baghouse filter [206].</li> <li>(4) Flue gas desulphurization (FGD) technology: once-through (wet scrubber) [206].</li> <li>(5) Selective Catalytic Reduction (SCR) [206].</li> <li>(6) Dry absorption in resins (carbon particles dispersed in a polymer matrix) [206].</li> <li>(7) Adsorption with activated carbon or open hearth coke [206].</li> <li>(8) Fabric filter [206].</li> </ol>

Pollutants	Production precursor	Reduction method
		<p>(9) The use of entrained flow reactor [199, 206]</p> <p>(10) UV mediated dechlorination [196, 198], ionization device [199], and electron irradiation process [198].</p> <p>(11) Pulse corona-induced plasma [207].</p> <p>(12) Catalytic dechlorination through metal chloride [196].</p> <p>(13) Incineration above 1,200°C [196].</p> <p>(14) Plasma gasification [208].</p> <p><i><u>Fly ash treatment (providing a safe handling of fly ash residues):</u></i></p> <p>(15) Thermal treatment at temperature &gt;300°C [198], using thermal treatment equipment such as electrical, oven, coke-bed melting furnace, rotary kiln with electric heater, sintering in LPG burning furnace, plasma melting furnace, etc. [198, 201].</p> <p>(16) Non-thermal plasma [198, 209-211].</p> <p>(17) Chemical reaction using metallic calcium in ethanol [198, 212].</p> <p>(18) Supercritical water oxidation (SCWO) [198].</p>
Hydrogen Fluoride, HF	Feedstock (esp. MSW) containing Fluoride [193].	<p><i><u>Flue gas:</u></i></p> <p>(1) Flue gas desulphurization (FGD) technology: once-through (wet and dry) and regenerable (wet and dry) technique [190].</p> <p>Adsorbent (e.g. CaO) [208].</p>
<i>Tars</i>	Thermal or partial-oxidation regimes (gasification) of any organic material	<p>(1) Dry gas cleaning [62, 213].</p> <p>(2) Wet gas cleaning [29, 213].</p> <p>(3) Nickel-based catalyst catalytic cracking [213].</p> <p>(4) Non-nickel metal catalyst catalytic cracking [213].</p> <p>(5) Alkali metal catalyst catalytic cracking [213].</p>

Pollutants	Production precursor	Reduction method
		(6) Basic catalyst catalytic cracking [213]. (7) Acid catalyst catalytic cracking [213]. (8) Activated carbon catalytic cracking [213]. (9) Thermal cracking [213]. (10) Plasma cracking [213].

In incineration plants, a complex control strategy, namely the Maximum Allowable Control Technology (MACT), to keep the emissions below the limits is generally used [34]. MACT generally consists of dry scrubber, fabric filter baghouses, activated carbon injection, selective non-catalytic reduction of NO<sub>x</sub> and other measures [34]. Using MACT, levels of Hg, Cd, Pb, polychlorinated dibenzo-p-dioxins (dioxins/PCDDs)/dibenzofurans (furans/PCDFs), particulate matters, NO<sub>x</sub> and SO<sub>2</sub> from U.S. incineration facilities (88 surveyed by the EPA) has reduced on average by over 96 percent (from 4,400 to 15 tons/year (tpy)), 96 percent (from 9.6 to 0.4 tpy), 97 percent (170 to 5.5 tpy), 99 percent (from 4,400 to 15 tpy), 96 percent (18,600 to 780 tpy), 24 percent (64,900 to 49,500 tpy), and 88 percent (38,300 to 4,600 tpy), respectively during 1990-2005 [214]. Since gasification allows heavy metals to settle down by gravity in the ash drum, levels of heavy metals in syngas are much lower than in the flue gas of incineration, creating a simpler emission control and syngas cleaning system. Syngas clean-up is still a major cost driver in gasification technology.

Another pollutant commonly found in the gasification process is sulfur. In general, sulfur is naturally present in coals, but it is also commonly found in solid wastes [60]. One of recent advanced technologies that has substantially reduced sulfur (e.g., H<sub>2</sub>S and COS) at 99.9 percent removal efficiency and syngas temperature of 600-650°C is warm

desulphurization process (WDP) developed by Research Triangle Institute [7, 8]. The process involves dual transport reactor loops and regenerable, high-capacity, rapid acting, attrition-resistant sorbents. Using WDP, a slide stream of syngas containing H<sub>2</sub>S (7,500-10,800 ppmv) and COS (450-650 ppmv) can achieve 99.9 percent removal efficiency [8]. A process flow diagram of a WDP syngas cleaning system, which is applied in Tampa Electric Company (TECO) with funding by the U.S. Department of Energy, is presented in Figure 1.14. The WDP syngas clean-up system has been considered as offering lower capital costs (20-50 percent), lower non-labor and non-feedstock operating costs (30-50 percent), and improved overall system efficiency by 10 percent [8].

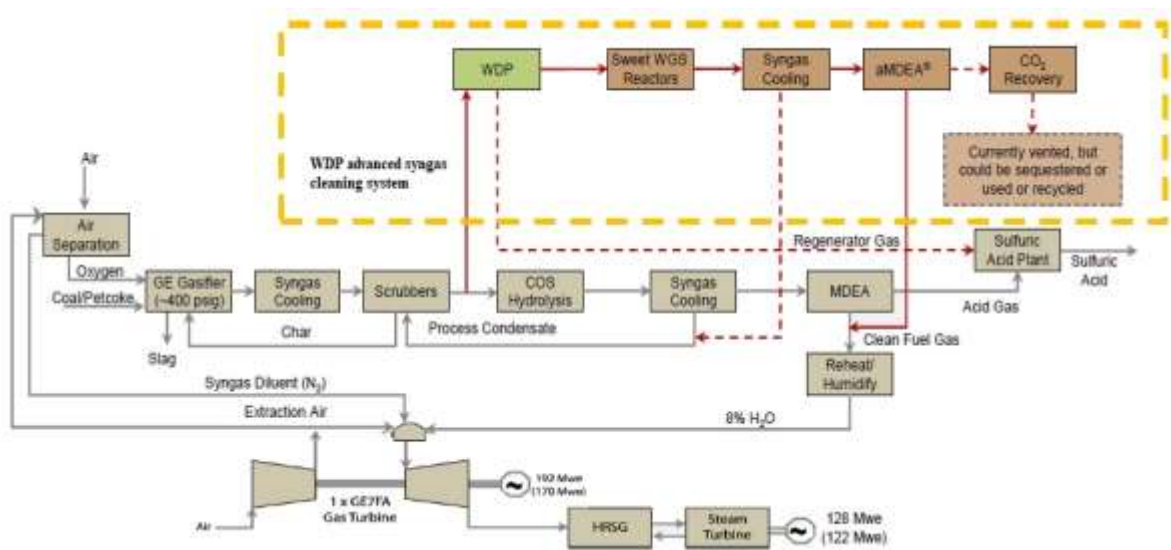


**Figure 1.14. WDP advanced syngas cleaning system at Tampa Electric Company (TECO) [8]**

### 1.6.2.3.2. Lesson Learned from Valmet Plant, Finland

A steam power plant at Valmet (Lahti Energia, Finland) is an example of successful plant showing the compliance of its emission performance with local regulation emission

standards as presented earlier in the previous section (section 1.4.5); a process diagram is also shown earlier in Figure 1.7 [35].

**Table 1.14. The emission performance of 2 x 80 MW CFB gasifier for steam power plant using wood biomass at Lahti Energia, Finland [35]**

Emissions	Measured	EU standard [34, 35, 215]	US EPA standard [34, 215]
NO <sub>x</sub>	161 mg/Nm <sup>3</sup>	200 mg/Nm <sup>3</sup>	264 mg/Nm <sup>3</sup>
SO <sub>2</sub>	7 mg/Nm <sup>3</sup>	50 mg/Nm <sup>3</sup>	63 mg/Nm <sup>3</sup>
CO	< 2 mg/Nm <sup>3</sup>	50 mg/Nm <sup>3</sup>	45 mg/Nm <sup>3</sup>
Dust	< 2 mg/Nm <sup>3</sup>	10 mg/Nm <sup>3</sup>	11 mg/Nm <sup>3</sup>
HCl	< 1 mg/Nm <sup>3</sup>	10 mg/Nm <sup>3</sup>	29 mg/Nm <sup>3</sup>
HF	< 0.5 mg/Nm <sup>3</sup>	1 mg/Nm <sup>3</sup>	n.a
TOC	< 1 mg/Nm <sup>3</sup>	10 mg/Nm <sup>3</sup>	n/a
PCDD/PCDF	< 0.002 ng/Nm <sup>3</sup>	0.1 ng/Nm <sup>3</sup>	0.14 ng/Nm <sup>3</sup>
Mercury, Hg	< 0.0001 mg/Nm <sup>3</sup>	0.05 mg/Nm <sup>3</sup>	0.06 mg/Nm <sup>3</sup>
Cd + TI	< 0.0003 mg/Nm <sup>3</sup>	0.05 mg/Nm <sup>3</sup>	(Cd) 0.02 mg/Nm <sup>3</sup> [216]
Sb + As + Co + Cr + Cu + Mn + Ni + Pb + V	< 0.03 mg/Nm <sup>3</sup>	Total 0.5 mg/Nm <sup>3</sup>	(Pb) 0.2 mg/dscm [217]

Note: dscm = dry standard cubic meter of stack gas

Table 1.14 presents the emission performance of the plant, showing a compliance with European and U.S. EPA standard. As can be seen, all emissions including SO<sub>2</sub>, CO, dust, HCL, HF, total organic carbon, PCDD/PCDF, and heavy metals (mercury, cadmium, titanium, etc.) are much lower than the standards. NO<sub>x</sub> emission of the gasification steam power plant is also lower than the standards, however, its extent can be considered comparably. Therefore, the low emissions of the Valmet gasification steam power plant

are a good example for the existing plants that have a target to achieve a lower emission level by modifying their feedstock type from conventional coal fuel to biomass syngas fuel.

#### **1.6.2.3.3. MSW Gasification and its Pertinent Standards**

Table 1.15 compares the concentrations of the major pollutants emitted by several MSW gasification plants with those of some conventional incineration plants and recalls the EU, Japanese and U.S. EPA standards. The emission levels of the MSW gasification plants comply with the relevant standards and are overall lower than those of the incineration plants, especially for mercury emissions. As described earlier, the heavy metals would be accumulated in the gasifier base and removed through the ash collection system, reducing their presence in the flue-gas stack [30, 34]. In addition, when compared to a landfill scheme featuring gas capture and to incineration, MSW gasification offers better emission control effectiveness. In terms of CO<sub>2</sub> emission, it generates only about 1 kg CO<sub>2</sub>-eq/kWh of generated power, while landfill produces about 2.75 kg CO<sub>2</sub>-eq/kWh and incineration about 1.6 kg CO<sub>2</sub>-eq/kWh [218]. Also, it can produce electricity without releasing greenhouse gas emissions (GHGs) or harmful pollutants, such as methane, dioxins and furans (PCDDs/PCDFs) [21] and can reduce the landfill volume by over 88 percent [219]. Moreover, it releases non-leachable and vitrified slags.

MSW gasification also generates a lower level of criteria pollutants than landfill and incineration. MSW gasification typically generates 31 g of NO<sub>x</sub> and 9 g of SO<sub>2</sub> per ton of waste converted, while landfill releases 68 g of NO<sub>x</sub> and 53 g of SO<sub>2</sub> per ton, and incineration emits more than 192 g and more than 94 g, respectively [218]. Thus, MSW gasification will remarkably both preserve clean air from noxious pollutants and reduce potential health risks of humans.

**Table 1.15. Comparative analyses of emissions performance of MSW gasification and incineration plants [30, 34]**

MSW Gasification plants							MSW Incineration plants					
Company	Nippon Steel	JFE / Thermoselect	Ebara TwinRec	Mitsui R21	Energos	Plasco Energy	WTE A	WTE B	WTE C	European standard	Japanese standard	US EPA standard
Plant location	Kazusa, Japan	Nagasaki, Japan	Kawaguchi, Japan	Toyohashi, Japan	Averoy, Norway	Ottawa, Canada						
Gasifier / combustor type	DD-EAG-HT	DD-OG-HT	ICFB-AG-(LT+HT)	RK-AG-LT	MG-AG-LT	PG-HT						
Waste capacity, tpd	200	300	420	400	100	110						
Power production, MWe	2.3	8.0	5.5	8.7	10.2 (thermal)	n.a						
Emissions, mg/Nm <sup>3</sup> (at 11% O <sub>2</sub> )												
PMs	10.1	< 3.4	< 1	< 0.71	0.24	9.1	0.4	1.8	1.0	10	11	11
HCl	< 8.9	8.3	< 2	39.9	3.61	2.2	3.5	0.5	0.7	10	90	29
NO <sub>x</sub>	22.3	n.a	29	59.1	42	107	80	11	58	200	229	264
SO <sub>x</sub>	< 15.6	n.a	< 2.9	18.5	19.8	19	6.5	7.5	3	50	161	63
Hg	n.a	n.a	< 0.005	n.a	0.0026	0.0001	0.002	7	0.002	0.03	n.a	0.06
CO	n.a	n.a	n.a	n.a	n.a	n.a	15	7	15	50	n.a	45
TOC	n.a	n.a	n.a	n.a	n.a	n.a	0.5	n.a	0.9	10	n.a	n.a
PCDDs/PCDFs, ng/Nm <sup>3</sup> (TEQ)	0.032	0.018	0.000051	0.0032	0.0008	0.006	0.002	0.002	0.0015	0.1	0.1	0.14

Note: DD = Downdraft; EAG = Oxygen enriched-air gasifiers; LT = Low temperature; HT = High temperature; OG = Oxygen; ICFB = Internally circulating fluidized bed; AG = Air gasifier; RK = Rotary kiln; MG = Moving grate; PG = Plasma gasifier; TEQ= Toxic equivalent; TOC = Total organic carbon

#### 1.6.2.4. Wastewater

In the gasification process, wastewater is generally produced from the gas cooler and the wet scrubber, containing soluble fractions such as acetic acid, sulphur, phenols, and other oxygenated organic compounds, and insoluble fractions, such as tars. Wastewater typical production rate is 0.5 kg/Nm<sup>3</sup> treated gas [66]. Since all fractions are mixed in the solution, the waste water treatment system is critical regardless of the disposal rate. A general problem regarding this waste is a low pH and a high salt content, but that can easily be adjusted using neutralization and chemical precipitation [66]. In most cases of commercial plants, a series of treatments is required to anticipate the complex components of the waste water, including: 1) precipitation of sulphur by iron sulphate addition, 2) recovery of sulphur and dust by filtering, 3) disposal of filter cake, 4) stripping off gases dissolved in the water and the major part of hydrocarbons, 4) partial evaporation of water and usage of condensate as scrubber make-up, 5) discharge of evaporator blowdown to conventional bio-treatment [66]. However, instead of using a complex treatment system, recent advances of the syngas cleaning system introduce a more simple system that generates zero-liquid discharge, such as plasma cracking that converts tars into hydrogen and simpler hydrocarbons (ethylene and acetylene) with a substantial reduction of harmful components; using this technique, benzene, toluene, and naphthalene were individually reduced from 12,000, 21,000, and 1000 ppm to 13, 130, and 52 ppm [220].

## 1.7. Conclusions

This chapter focuses on power generation technologies based on biomass and MSW gasification for distributed applications, including their economic and socio-environmental aspects. Recent studies show that power generation derived from biomass and MSW gasification is a promising technology for reducing carbon footprints due to the carbon neutrality of the biomass pathway. Moreover, use of existing commercial power equipment to use syngas does not demand major modifications. For ICEs, the least demanding are NG engines, followed by gasoline and diesel engines, while for MGTs, no modification is required from current technology. For GTs, the modifications are required in the fuel system, compressor, and combustor. Indeed, the contemporary technologies of GTs, gasoline, diesel, and NG ICEs are in a position to accommodate 100% syngas, so that the dissemination of power generation from biomass and MSW gasification technologies is feasible on a world scale. On the other hand, the adaption of biomass and MSW gasification for Stirling engines and ORC generators must be supported by extensive experimental data to accelerate their deployment in the commercial market. FCs offer a promising future for distributed power generation since rigorous developments including capacity enhancement have been made, and hybrid system developments have high electrical efficiency (>60%). However, commercialization of gasification-based power generation technology requires further development to: increase the reliability and efficiency of gasification; reduce syngas contaminants to an acceptable level; increase the conversion efficiency of syngas energy to power, by resorting to an advanced power system, such as FC/GT hybrid units.

Thermal plasma gasification is a promising pathway suitable for exploiting MSW; however, its drawbacks include high CAPEX and energy consumption. Future research on

plasma gasification systems using a lower energy consumption is urgently needed to accelerate MSW gasification technology. Unlike biomass gasification, the economic viability of MSW gasification is enhanced with the tipping fees for its disposal. Gasification of biomass and MSW is expected to bring significant benefits to local communities by creating specific employment streams as well as new economic activities and networks.

From an economic aspect, generating power through gasification of waste is preferable to attain a higher economic viability due to the minimum transportation fees and presence of tipping fees that eventually lower the production cost of electricity. However, the current technology is still evolving to accommodate the complexity of the feedstock, to reduce the power consumption, and to increase the process efficiency. When using biomass, an adequate feedstock supply that can support plant operation is critical to gain economic viability. The use of agricultural residue like the one used in the Muzizi Tea Estate processing utility shows promise. Also, non-edible biomass with a high carbon content and yield such as Miscanthus and switchgrass are also preferable to avoid issues of land and food usage.

Integrating gasifiers with a fuel cell (FC) system or with gas turbine (known as hybrid system) provides a great alternative to enhance system efficiency, compared to a standalone gasifier coupled with an internal combustion engine. The hybrid system can support distributed power generating with load-following capability that can increase access to electricity for local communities.

From a socio-environmental standpoint, gasification of biomass and MSW is expected to bring significant benefits to local communities by creating specific employment streams

as well as new economic activities and networks. Contrary to the conventional incineration and landfilling practices, gasification boasts valuable environmental assets because it releases less GHGs and pollutants. Thus, if the economics of biopower generation through gasification is viable, the technology can be implemented in areas having abundant sources of biomass and wastes, eventually increasing public access to electricity.

## CHAPTER 2

### ENGINE POWER GENERATION AND EMISSION PERFORMANCE OF SYNGAS GENERATED FROM LOW DENSITY BIOMASS

This chapter was published as “N. Indrawan, S. Thapa, P. R. Bhoi, R. L. Huhnke and A. Kumar, Engine power generation and emission performance of syngas generated from low-density biomass, *Energy Conversion and Management*, vol. 148, pp. 593-603, 2017”.

**Abstract:** The power production from renewable sources must increase to meet the growing demand of power across the globe on a sustainable basis. Unlike most of gasification works that use high density biomass (e.g. wood chips) to generate a high quality syngas, here we introduce a novel gasification system that can use underutilized low density biomass resources to produce power and electricity with high efficiency yet minimum set-up requirement and low emissions. Switchgrass, one of locally abundant and low density biomass, was used as the biomass feedstock. A unique pilot-scale patented gasifier with a cyclonic combustion chamber having a capacity of 60 kW was used. A commercial natural gas-based, spark-ignition (SI) engine with capacity of 10 kW was modified to measure and control air-fuel ratio and fed with the syngas produced directly from the gasifier. The engine load was regulated by an electric load bank to evaluate the engine operational characteristics. The natural gas was used as the reference feed to evaluate the engine and emissions performance. Gas composition and flowrate, output power, electrical efficiency, and exhaust emissions such as CO<sub>2</sub>, CO, NO<sub>x</sub>, SO<sub>2</sub>, and hydrocarbons were measured. Net electrical efficiency of 21.3% and specific fuel consumption (SFC) of 1.9 kg/kWh were achieved while producing 5 kW at the maximum load using syngas, while 22.7% of electrical efficiency and 0.3 kg/kWh of SFC were achieved using natural gas at the equivalent load. NO<sub>x</sub> and HC emission produced from the engine was significantly affected by the gas fed and the load applied. CO<sub>2</sub> emission varied moderately yet significantly with the increasing load, while CO and SO<sub>2</sub> emissions did not strongly influenced by the load variation. NO<sub>x</sub> emission was 21.5 ppm that complies with the California emission standard limit (25.9 ppm). The study results showed that with minimum set-up, the downdraft gasification system coupled with

existing commercial natural gas-based spark-ignited (SI) engine can satisfactorily generate sustainable power supply with high efficiency and minimum emissions to support off-grid power application.

**Keywords:** Syngas; Gasification; Switchgrass; Biopower generation; Emissions

## 2.1. Introduction

Electricity, considered one of the most important inventions of all time, is essential for human life and economic development. Globally, one out of five people (about 1.2 billion people) still do not have access to electricity; approximately 2.7 billion people are still dependent on the traditional use of biomass for cooking, which leads to an increase in harmful indoor air pollution and can have negative impacts on human health [221]. Over 95% of the people who lack access to electricity live in predominantly rural areas in sub-Saharan and developing Asiatic countries [221].

Global biopower generation contributed 1.5% of the world's total electricity in 2012. It continuously increased by 100 trillion watt hours (TWh) from 2010-15 to reach over 400 TWh in 2015 [221]. Due to capability gasifiers have to use diverse feedstocks and dioxin and furan free products [21], gasification is considered one of the most promising technologies to produce heat and electricity and is suitable for use at decentralized locations to promote rural socio-economic development.

Commercial internal combustion (IC) engines can be directly run on syngas with minimal modification and emit a considerably low amount of pollutants. Homdoug et al. [88] reported that an 8.2 kW diesel engine with a modified combustion chamber, ignition system, and air-fuel system, produced 3.1 kW with 100% feed syngas with a lower heating value (LHV) of 4.64 MJ/Nm<sup>3</sup> and a specific fuel consumption and engine efficiency of 5.5 kg/kWh and 24%, respectively. With 100% syngas having an LHV of 5.6 MJ/Nm<sup>3</sup>, Sridhar et al. [89] found that a 28 kW and 300 kW diesel engine with a modified combustion chamber and ignition system produced an electrical output power of 17.5 kW and 165 kW; using similar syngas, they also found that a 100 kW modified

natural gas SI engine produced an electrical output power of 55 kW. Shah et al. [87] reported that with 100% feed syngas (LHV of 5.79 MJ/Nm<sup>3</sup>) and the addition of two air venturies in a series at the air-fuel manifold, a 5.5 kW gasoline engine produced the maximum electrical power of 1.39 kW with the overall engine efficiency of 19.3%. While running on 100% syngas with the LHV of 5.6 MJ/Nm<sup>3</sup>, Raman and Ram [64] reported that a 100 kW natural gas, six-cylinder SI engine with a modified fuel intake manifold and a hydraulic governor produced the maximum electrical power of 73 kW with an overall efficiency of 21%. Using peach kernel and without engine modification, Tsiakmakis et al. [86] found that a 4.7 kW single cylinder natural gas SI engine generated the maximum electrical power of 3.68 kW with an engine efficiency of 26.2%. These reports show that with minimal modification, SI engine can be directly fed with 100% syngas for power production with comparable performance but with significant derating.

Although most of the above reports on the performance analysis of SI engine used 100% syngas generated from high density biomass especially from wood chips, only limited studies are available on performance and emission characteristics of biopower generation at pilot-scale using gasification. This study focuses on an off-grid power generation, using switchgrass as one of the most locally abundant and low density biomass feedstock with feeding rate of up to 100 kg/h and air as a gasification medium. Parameters impacting gasifier operation especially engine performance and emission performance are discussed to evaluate feasibility of using this technology for mobile power applications.

## 2.2. Material and Methods

### 2.2.1. Materials

Switchgrass is one of locally abundant and low density biomass feedstock. The proximate (moisture, volatile matter, fixed carbon and ash) and ultimate (C, H, O, N, and S) analyses of switchgrass feedstock (locally abundant biomass feedstock) were analyzed by Hazen Research Inc., Golden, CO, as presented in Table 2.1. Feedstock moisture content was determined prior to each experiment by oven drying samples at 104°C for 24 h. The gas composition of natural gas (reference fuel) and syngas (produced from the gasifier) was measured using gas chromatograph (Agilent, Model 7890a, Agilent Technologies, Santa Clara, CA) using Argon as the carrier gas. The natural gas (lower heating value, LHV, of 37.79 MJ/Nm<sup>3</sup>) mainly contained 86.6% methane (CH<sub>4</sub>), 10.3% ethylene (C<sub>2</sub>H<sub>4</sub>), 1.1% ethane (C<sub>2</sub>H<sub>6</sub>), 0.53% carbon dioxide (CO<sub>2</sub>), and 1.46% nitrogen (N<sub>2</sub>).

**Table 2.1. The properties of switchgrass used in the experiment**

Proximate (wt.%, dry basis)	
Moisture content (wet basis)	7.69
Volatile matter	78.60
Fixed carbon	17.47
Ash	3.93
Ultimate (wt.%, dry basis)	
Carbon, C	49.63
Hydrogen, H	5.72
Oxygen, O	40.37
Nitrogen, N	0.30
Sulphur, S	0.05
Lower heating value, MJ/kg	16.49
Higher heating value, MJ/Kg	17.73
Bulk density (kg/m <sup>3</sup> )	91

### **2.2.2. Gasifier specification**

A unique fixed-bed downdraft gasifier equipped with internal cyclonic combustion chamber with height of 3.2 m, nameplate capacity of 60 kW and biomass rate of 100 kg/hour was used for producing syngas. The gasifier was selected due to its capability to generate syngas with low tar content (0.015 to 0.5 g/Nm<sup>3</sup>) compared to fluidized bed (10 to 40 g/Nm<sup>3</sup>), circulating fluidized bed (5 to 12 g/Nm<sup>3</sup>) and fixed-bed updraft gasifier (30 to 150 g/Nm<sup>3</sup>) [52]. The gasifier is an up-scaled design of 10 kW gasifier with patented design [222] developed over ten years. Detailed description of the gasifier can be found elsewhere [56]. A stirrer was added in the gasifier to uniformly mix biomass, and prevent bridging inside the reactor. A gear motor (Grainger, Roanoke, TX) with 418.9 Nm torque was used to rotate the stirrer rod at 17 rpm. To ensure that ash did not accumulate inside the reactor, an automatic belt conveyor was used to discharge the ash from the bottom of the reactor to an ash drum. The ash conveyor was operated every five minutes. Biomass feed rate was carefully maintained at 85 kg/h to ensure the biomass entering the reactor would not jam the hopper and airlock. The biomass feeding was adjusted by controlling speed of a belt conveyor so that biomass was uniformly fed into the reactor without overloading.

### **2.2.3. Gasification efficiency**

Gasification efficiencies (hot and cold gas efficiencies) are defined as the ratio of the energy in the syngas produced to the energy in the biomass used. The gasification efficiency depends on the properties of biomass used and the gasifier's design and operating conditions [94]. Depending on whether the sensible heat of syngas is considered in the calculation, the gasification efficiency is either hot (HGE) or cold gas

efficiency (CGE). However, cold gas efficiency (CGE) is typically used to describe the gasification performance. Typical CGE obtained from biomass downdraft gasification is in the range of 50% to 80% [94].

#### **2.2.4. Syngas cleaning system**

Tar and other impurities such as particulate matter, ammonia, hydrogen sulfide, hydrogen cyanide, hydrogen chloride, sulfur dioxide, and alkali metals are typically present in the syngas and problematic for power generation [95, 223]. Prior to IC engine application, tar content should not exceed 100 mg/m<sup>3</sup> [65]. Tar measurement protocols used a series of six impingement bottles where the first one served as a moisture collector, allowing syngas flowed through a series of four impinger bottles filled with a solvent, i.e., acetone to dissolve the tars. The last bottle was kept empty to ensure the collection of final condensates. Details of this are described elsewhere [62, 224]. In this study, the syngas cleaning system consisted of a cyclone separator and a gas scrubber. A cyclone separator was directly connected to the gasifier outlet and a gas scrubber was connected to the outlet of cyclone separator. The gas scrubber consisted of ash trap solvent tank (0.19 m<sup>3</sup> vol.) filled with an acetone-water (20:80) solution and two gas scrubbing columns (12-in. diameter columns packed 4 feet deep with stainless steel pall rings of 0.75 in. diameter and 0.75 in. long with a total approximate exchange area of 41.6 m<sup>2</sup>) connected in series of two. The scrubbing columns were sprayed with cold solvent at 0°C from the column top down through the packed bed counter current to the gas flow. Instead of using acetone-water system, a study of using biomass filter is also reported in elsewhere [62].

### 2.2.5. Power generation unit and emissions analysis

The two-cylinder SI engine (Model 040375, Briggs and Stratton Power Products Group LLC, Milwaukee, WI) with maximum capacities of 10 kW and 9 kW on propane and natural gas, respectively, was used. The SI engine has a rated speed of 3600 rpm and the attached generator produced three phase power at 120/240 V at a frequency of 60 Hz (engine specification is provided in Table 2.2).

**Table 2.2. The SI engine and generator specification**

Parameter	Unit	Value
<i>a) Generator Specification</i>		
Manufacturer		Briggs and Stratton
Generator Capacity	kW	9
Rated Maximum Load Current at 240 Volts	Amp	37.5
Rated AC Voltage	Volts	120/240
Phase		Single phase
Rated Frequency	Hertz	60
Generator Breaker	Amp	50
Normal Operating Range	°C	-28.8 to 40
<i>b) Engine Specification</i>		
Displacement	cc	570
Bore	mm	71.9
Stroke	mm	70.1
Oil Capacity	L	1.7
Engine Speed	rpm	3600
Number of Cylinder		2
Cooling System Type		Air Cooling
<i>c) Operating specification</i>		
Rated engine output using natural gas	kW	9
Rated engine output using syngas	kW	5
SFC at peak load using natural gas	kg/kWh	0.3
SFC at peak load using syngas	kg/kWh	1.97
Air fuel ratio at peak load using syngas		1.6

The electric load bank (Avtron, Model K490, Avtron Loadbank, Inc., Cleveland, OH) with voltage and current display was connected to the engine to vary the engine load from 0 to 5 kW. Engine speed (rpm) was monitored using digital laser tachometer (CyberTech, Model 2234A, Litetrek International LLC, Pleasanton, CA).

### **2.2.6. Method of operating the engine on syngas and natural gas**

The gasifier operation started by feeding the switchgrass at a rate of 85 kg/h. The air was accordingly injected using an equivalent ratio (ER) of 0.25. Propane was used to start the gasification process. A gasifier valve, also known as a firing valve, located in the mid-section of the reactor was used to mix. The gasifier temperature was carefully monitored to ensure that the temperature continued to increase. When the temperature of combustion section of the gasifier reached 100°C, the gasifier valve was then closed. At temperature of about 150°C, the propane injection was also stop to allow the gasification process to continue with only supplied with air and switchgrass. The gasification typically reached equilibrium after 30–40 minutes from the initial start-up. The syngas was then directed to enter the suction line of the engine (considered as time of zero of the entire experiment).

Experimental set-up is shown in Figure 2.1. A divider valve was installed prior to the gas scrubber to clean only a partial stream of syngas that was required for feeding into the engine. Another valve divider was placed after the gas scrubber for purging and controlling the syngas stream. The syngas flowrate was measured by a flow meter (Fox, Model FT2A, Fox Thermal Instrument Inc., Marina, CA) with 4 to 20 mA output channel. A U-tube manometer (McMaster-Carr) was installed in the suction line of the engine to monitor inlet pressure.

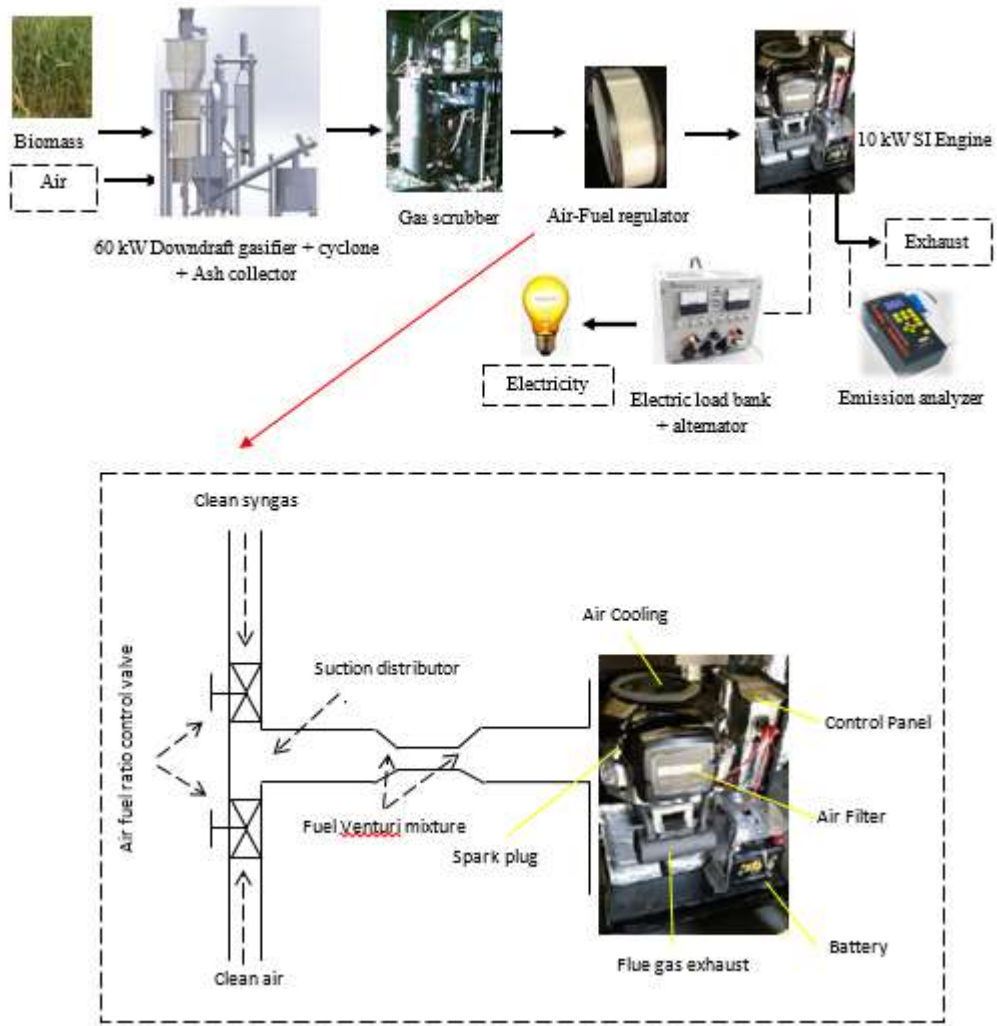


**Figure 2.1. The process diagram of the power generation system with a modified air-fuel regulator coupled with a 60 kW of gasifier**

Composition of syngas, sampled at the engine inlet, was analyzed by a gas chromatograph. The air flow was regulated using a valve placed before the air flowmeter (Fox, Model FT2A, Fox Thermal Instrument Inc., Marina, CA) with 4 to 20 mA of the output channel. Typically, air-fuel ratio (AFR) required for the engine using biomass-derived syngas is different from that required for using natural gas [225]. AFR ranging from 1.2 to 2.8 was recommended for operation of syngas engine to maximize electrical

efficiency [226]. In this study, AFR was modified using a series of pipe in a venturi to form homogenous air-fuel mixture. The air-fuel mixture entering the engine was then regulated by the engine governor. Through preliminary tests, an AFR of 1.6 was found to be optimum for the engine operation. Detailed engine operating condition is presented in Table 2.3.

**Table 2.3. The experimental conditions**

Components	Unit	Value
Gasification equivalent ratio	Mass fraction	0.25
Feedstock type	-	Switchgrass
Feedstock rate	kg/h	85 ± 1%
Engine capacity	kW	10
Load variation	kW	0 – 5
Air flow	m <sup>3</sup> /h	23 ± 5%
Ambient temperature	°C	28 ± 0.5
Engine speed	rpm	3,250 – 3,600
Air-fuel ratio		1.2 – 1.6
Energy content of syngas, LHV	MJ/m <sup>3</sup>	6.47 ± 0.7
Syngas flowrate at maximum load	m <sup>3</sup> /h	14.1 ± 5%
Exhaust gas flow	m <sup>3</sup> /h	26.1 ± 5%

For obtaining engine power and emission performance using natural gas fuel, natural gas was directly connected to the engine using a line separate from the syngas line (Figure 2.1). Natural gas flow rate was measured using a flow meter (Sierra, Model QuadraTherm 640i, Sierra Instruments, Monterey, CA) with 4 to 20 mA of the output channel. Typically, air-fuel ratio (AFR) required for using natural gas in engine ranges

from 17 to 20, depending on its heating value. Similar to syngas operation, the electric load bank was used to vary the load from 0 to 5 kW for natural gas engine operation.

**2.2.7. Power performance and emission analyses**

The electrical efficiency (Eq. 1), a key indicator of power generation performance, is defined as the ratio of the electrical power output of the generator and the energy input, which is quantified as the product of the flow rate and the lower heating value (LHV) of the syngas.

$$\text{Electrical efficiency} = \text{electrical power output} / (\text{LHV} \times Q_m) \dots\dots\dots [2.1]$$

Where LHV is the lower heating value of syngas (MJ/Nm<sup>3</sup>) and Q<sub>m</sub> is the flow rate of air-fuel mixture (m<sup>3</sup>/h). Specific fuel consumption (SFC), another parameter to evaluate engine performance, was calculated as a ratio of fuel consumption (kg/h) and power produced (kW) as shown below.

$$\text{SFC} = Q / P \dots\dots\dots [2.2]$$

Where Q is the fuel consumption (kg/h) and P is the total power generated (kW).

The emission characteristics of the SI engine were monitored by using an integrated portable emissions analyzer (ENERAC Model 700, Holbrook, NY). The emission analyzer installed at the engine exhaust measured the levels of carbon monoxide (CO), carbon dioxide (CO<sub>2</sub>), Nitrogen oxides (NO<sub>x</sub>), Hydrocarbon (HC), and Sulphur dioxide (SO<sub>2</sub>). The exhaust temperature was measured to ensure consistency of operational condition, while the syngas diverted to flare stack was burned to monitor the characteristics of syngas flame.

**2.2.8. Statistical analysis**

ANOVA procedure was conducted using statistical analysis software [227] to analyze significance of models, and the main and interaction effects of load applied and gaseous

fuel type (syngas and natural gas) on the engine emission characteristics. Level of significance was selected at 0.05 ( $\alpha = 0.05$ ). Experiment was conducted using a full factorial design with two type of gaseous fuel (syngas and natural gas) and five loads (1, 2, 3, 4 and 5 kW). All experiments were replicated. The experimental design was completed using Randomized Complete Block Design (RCBD) with gas type as block and load as treatment.

## **2.3. Results and discussion**

### **2.3.1. Gasification operation and condition**

The gasification operation affects syngas quality that directly influences performance of the power generation system. Major operational parameters of the gasifier include equivalence ratio (ER), gasifier temperature, biomass feed rate, and ash removal rate. CGE is a key indicator of gasifier performance, while syngas quality and energy content are main parameters impacting the biopower generation. All gasification runs were made at ER of 0.2 as 0.2 to 0.4 ER is typical for air-blown gasifiers. At the ER of 0.20 (air flow of approximately 48.5 SCFM), the combustion zone of the gasifier reached reactor temperature of 800-900°C with syngas LHV of 6-7 MJ/Nm<sup>3</sup> and CGE of 68%. Typically, ER higher than optimum results in high nitrogen content and, in turn, low energy content of the syngas [64], while conversely ER lower than optimum might result in syngas with high energy content but low yield resulting in low gasification efficiency. Also, reactor temperature of 800-900°C was suitable for typical 310 stainless steel (SS) materials that was used to make the gasifier reactor because 310 SS is rated for up to 1,000°C [228]. A gasifier reactor temperature higher than 900°C can potentially further increase hydrogen

content, and consequently increase the syngas energy content and efficiency of engine [229] and potentially inhibit combustion knock [230]. But, as the inside wall of the gasifier (used in this study) did not contain any refractory lining, we limited the gasifier temperature to prevent damage to the SS materials. Temperature of the gasifier outer wall was in the range of 35 to 40°C, suitable for access. The wall temperature can further be reduced by using a lining inside the reactor. Biomass was fed using conveyor belt and passed through airlock to prevent backflow of syngas. Solid particulates (ash and char) produced from the gasifier were collected from the gasifier bottom (3.3 wt.% of biomass) and cyclone separator (0.2 wt.% of biomass). Biomass conveyor, feeding, ash removal system and cyclone separator performed satisfactorily and did not show any technical issues during their operation and maintenance.

### **2.3.2. Syngas quality**

The syngas flame appearance is considered an indicator of syngas quality. During the operation, syngas flame was red with misty appearance due to unburned gases at the beginning but gradually changed to uniform yellow reddish color at the steady state condition, as exhibited in Figure 2.2. At the steady state condition, the lower heating value (LHV) of syngas was 6.47 MJ/Nm<sup>3</sup> with H<sub>2</sub>, CO, CH<sub>4</sub>, C<sub>2</sub>H<sub>4</sub>, and C<sub>2</sub>H<sub>6</sub> of 11.4 ± 1.9%, 21.0 ± 2.2%, 5.5 ± 1.1%, 0.15 ± 0.1%, and 1.33 ± 0.3% v/v, respectively. CO<sub>2</sub> and N<sub>2</sub> were 18.6 ± 1.7% and 42.6 ± 5.5% v/v, respectively. The heating value of the syngas was about six times lower than that of natural gas (37.79 MJ/Nm<sup>3</sup>), but was consistent with syngas LHV of 4 to 6 MJ/m<sup>3</sup> reported when air was used as the gasification medium [64, 86, 149]. The syngas heating value (6.47 MJ/Nm<sup>3</sup>) obtained in this study (single-state gasification) was also comparable to that (5.2 to 7 MJ/Nm<sup>3</sup>) obtained using circulating fluidized bed

[52] and to that (5.5 to 6.6 MJ/Nm<sup>3</sup>) using multistage gasification using air as gasification medium [57]. However, a high LHV of 15.69 MJ/Nm<sup>3</sup> can be achieved using steam as the gasification medium [73] as steam does not dilute the syngas with nitrogen as air does [64, 86, 88]. In addition, steam promotes hydrogen-producing reactions, such as water gas and water gas shift reaction [37]. The higher the heating value of syngas the better the combustion, flame quality and performance of the power generation it provides because of more combustible compounds in the syngas.

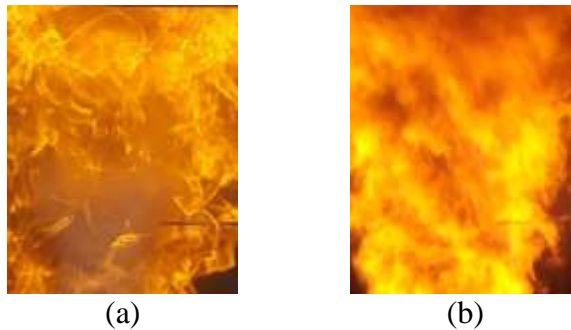


**Figure 2.2. Flame characteristics of syngas observed at flare stack at (a) initial stage and (b) steady-state condition**

With regard to syngas composition, carbon dioxide in the syngas (18.6% v/v) was within the typical range (5 to 20% v/v) produced from biomass gasification with air as the gasification medium [57, 92]. The presence of carbon dioxide is thought to reduce knocking tendency of the engine [94]. Moreover, methane (5.5% v/v) in the syngas was also within the typical range (1.0 to 10% v/v). The presence of methane is thought to support the stability of the engine [86, 87]. Syngas hydrogen (11.4% v/v obtained in this study) has been attributed to increase in flame speed, temperature of the combustion chamber, and efficiency of the engine [231, 232]. Hydrogen concentration in the syngas

can further be increased by reforming the syngas or using steam/oxygen as the gasification medium [52]. The syngas density was calculated using percent composition of individual gases in the syngas and their densities obtained from physical hydrocarbon database of National Institute of Standards and Technology (NIST) [233].

A gas scrubber using acetone-water satisfactorily removed tar. In this study, the tar content reduced from 27 g/Nm<sup>3</sup> at the inlet of gas scrubber to lower than 100 mg/Nm<sup>3</sup> at the outlet of gas scrubber. Tar content of up to 100 mg/Nm<sup>3</sup> in syngas is acceptable for engine application [65]. Other potential impurities in the syngas such as particulate matter, ammonia, hydrogen sulfide, hydrogen cyanide, hydrogen chloride, sulfur dioxide from syngas, and alkali metals [95] were found to be minimum as inside of the syngas pipeline from the outlet of gas scrubber was found clean and free of soot and tars during inspection after the experiment. The syngas temperature at the outlet of gas scrubber during 2 h run was consistently in the range of 25 to 28°C, which is appropriate for injecting into engines, such as IC engine and gas turbine [67].

### **2.3.3. The characteristics of power generation**

As the energy content of syngas (LHV of 6.47 MJ/m<sup>3</sup>) was approximately six times lower than that of natural gas (37.79 MJ/Nm<sup>3</sup>), use of syngas in the engine leads to changes in engine operation and emission characteristics as presented below.

#### **2.3.3.1. Effect on engine performance and operation**

The engine load and AFR significantly influenced the engine speed and power output of the engine (as shown in Figure 2.3). Compared to natural gas, syngas has low heating value, hence, at a specific engine speed, the brake torque and power produced from syngas was lower than that from natural gas [91]. As seen in the figure, engine speed on syngas

fuel dropped at a faster rate reaching a peak at 5 kW. Nevertheless, it should be noted that having an appropriate mixture of air-fuel is critical to boost the engine speed in order to achieve maximum efficiency of the engine and power generation. In addition, the combustion speed of syngas and air mixture is usually low as compared to that of natural gas and air mixture; this consequently reduces the efficiency of the engine.

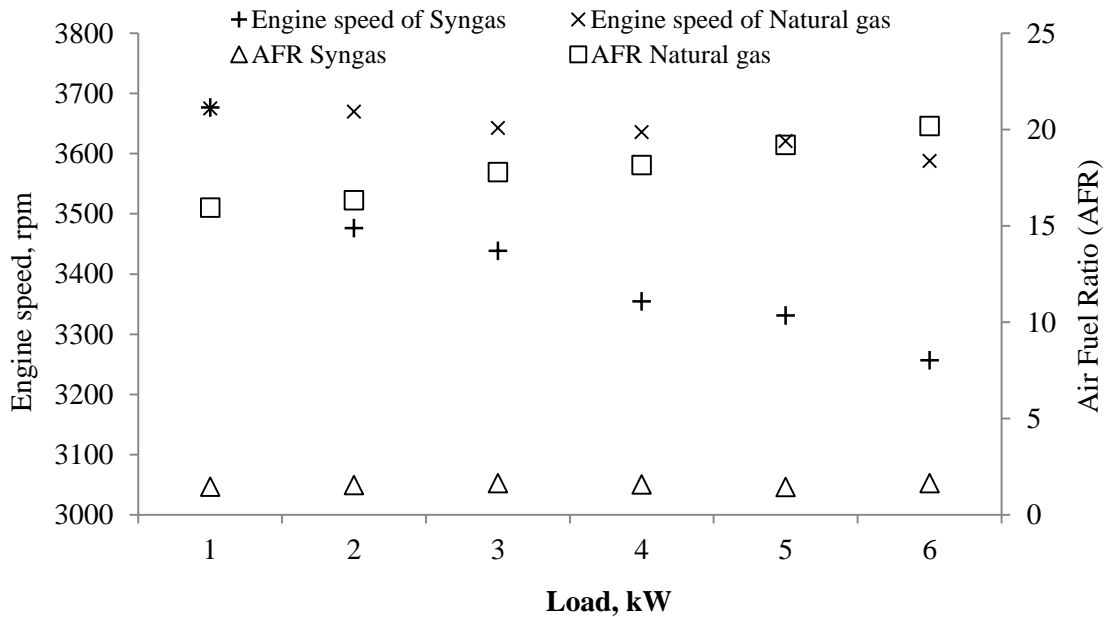


**Figure 2.3. The engine speed and AFR with varying load for engine using syngas and natural gas (note that load on natural gas fuel continued to increase until 9 kW)**

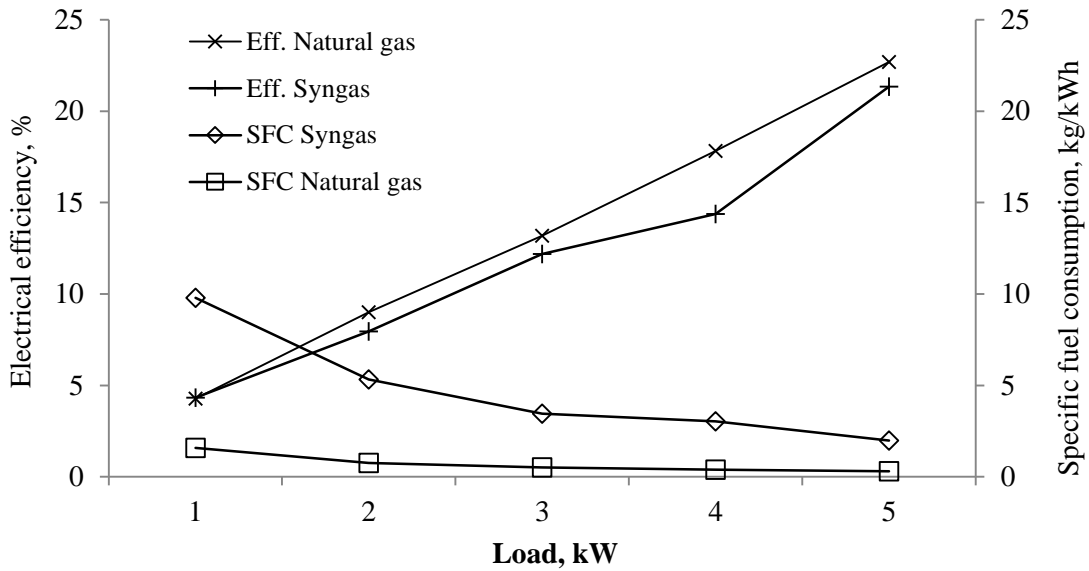


**Figure 2.4. The electrical efficiency and specific fuel consumption of engine run syngas and natural gas**

AFR of 1.6 resulted in a stable operation without any appearance in knock and voltage flickering. Generally, an AFR below stoichiometric AFR, commonly known as rich gas, results in an incomplete combustion, whereas an AFR above stoichiometric AFR, known as lean gas, results in a lower combustion temperature. The lean gas mixture lead to a decrease in combustion efficiency but offers improvements in the thermodynamics [195] and environmental benefits such as low NO<sub>x</sub> emission [234]. The venturi air-fuel intake directly impacted the engine's operation as it created a homogenous mixture of air and syngas. Using two venturies in series can further increase the homogeneity of air-fuel ratio; however, single venturi arrangement used in this study was sufficient for the engine operation.

The electrical efficiency using natural gas and syngas fuels showed similar increasing trend with increasing load, as shown in Figure 2.4. The efficiency using syngas was lower

than that using natural gas at all load conditions. The efficiency of 21.3% (similar to previously reported efficiency of 21% by [64]) was recorded when the engine was run on syngas at the maximum load of 5 kW with the syngas flow rate of approximately 14 m<sup>3</sup>/h. In comparison, at the same load, natural gas achieved efficiency of 22.7% with the flow rate of 2.1 m<sup>3</sup>/h. The low energy content of the syngas was responsible for the low efficiency of engine using syngas.

The lower the SFC of the engine, the higher the efficiency of the power generation system. The lowest specific fuel consumption rate for the engine using syngas and natural gas was 1.9 kg/kWh and 0.3 kg/kWh, respectively, at full load. Additionally, the lowest specific fuel consumption achieved using syngas was remarkably lower than that reported earlier (~3.0 to 5.5 kg/kWh) [64, 235-237]. A detail characteristic of power generation including a comparative analysis with previous works has been provided earlier in the previous chapter (Table 1.5).

### **2.3.3.2. Power de-rating**

A power de-rating of approximate 28% was observed with engine using syngas as compared to natural gas. The engine generated the maximum load of 5 kW using syngas, whereas the engine produced the maximum load of 7 kW using natural gas. The observed power de-rating was in agreement with typical power loss, reported from 20% to 35% [94, 95] and was much lower than a recent study, which is reported as 55% [77].

To minimize power de-rating of the engine, it is essential to have an appropriate air–fuel mixture. The appropriate air–fuel mixture to a cylinder is determined by the cylinder’s displaced volume, pressure, and temperature condition and by the pressure and temperature of the gas–air mixture. Another option to minimize power de-rating is to

modify the carburetor to increase the mixing performance [89]. In this study, the original carburetor from the engine manufacturer was reliable for the syngas operation. The only modification made was to extend the outlet of the carburetor to enable installation of the venturi air–fuel arrangement. Power de-rating can also be minimized by increasing the compression ratio. Normally, the compression ratio of a syngas based commercial engine is from 6.0 to 10, while the compression ratio of a natural gas based engine can be as high as 17 [88, 95]. However, a very high compression ratio creates other problems such as difficulty in starting, vibration, wear and tear of piston and reduction in the life of the engine [88, 95].

Power de-rating can also be minimized with high hydrogen concentration because hydrogen has lower ignition energy and faster flame speed. However, hydrogen can increase the maximum pressure inside cylinder, resulting in high peak pressure close to top dead center (TDC) at the combustion chamber [229, 231]. Additionally, the increasing temperature in the combustion chamber due to hydrogen concentration will increase emissions [231].

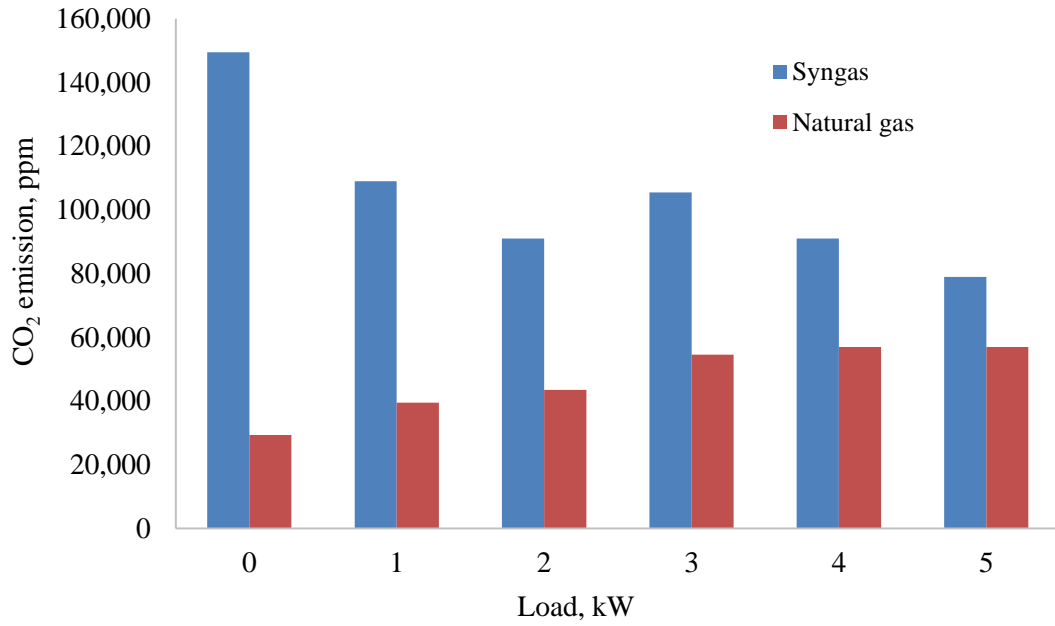
#### **2.3.4. Emissions characteristics**

Whether biopower generation is considered carbon neutral is still under debate [238] but in most cases, electricity power generation derived from biomass cuts GHG emissions (mostly in the form of CO<sub>2</sub>) when compared with that derived from fossil fuels [147]. It is agreed that carbon released during bioenergy production comes from a feedstock that removed the carbon from the atmosphere while the feedstock was growing [238].

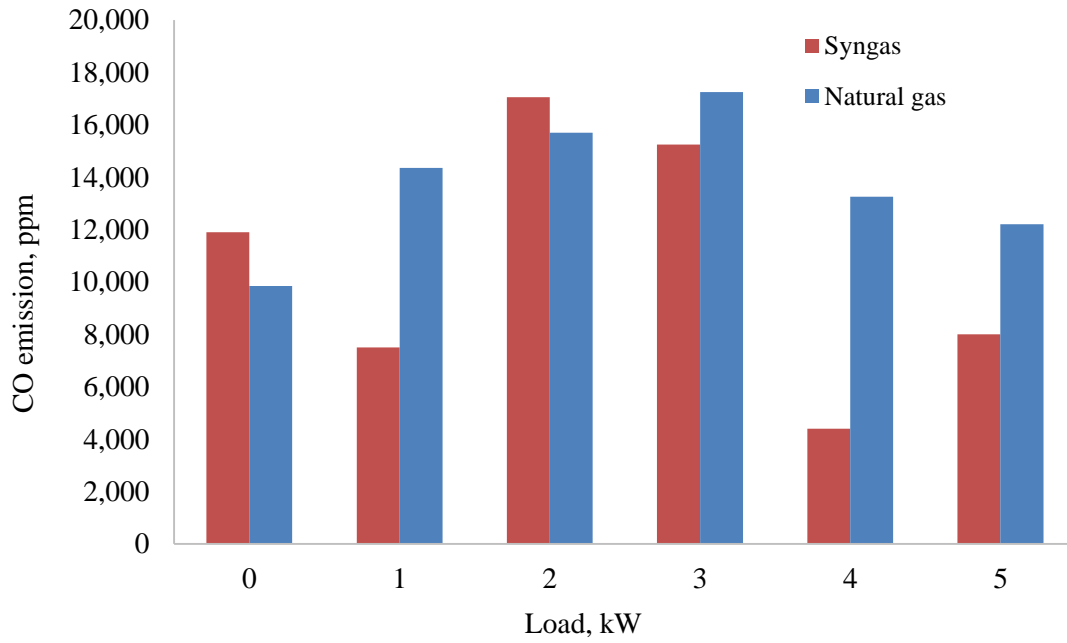
The emissions performance results (CO<sub>2</sub>, CO, SO<sub>2</sub>, NO<sub>x</sub>, and HC) of the power generation from syngas and natural gas with varying load are presented in Figure 2.5.

Statistical correlation between the load and the emissions produced is summarized in Table

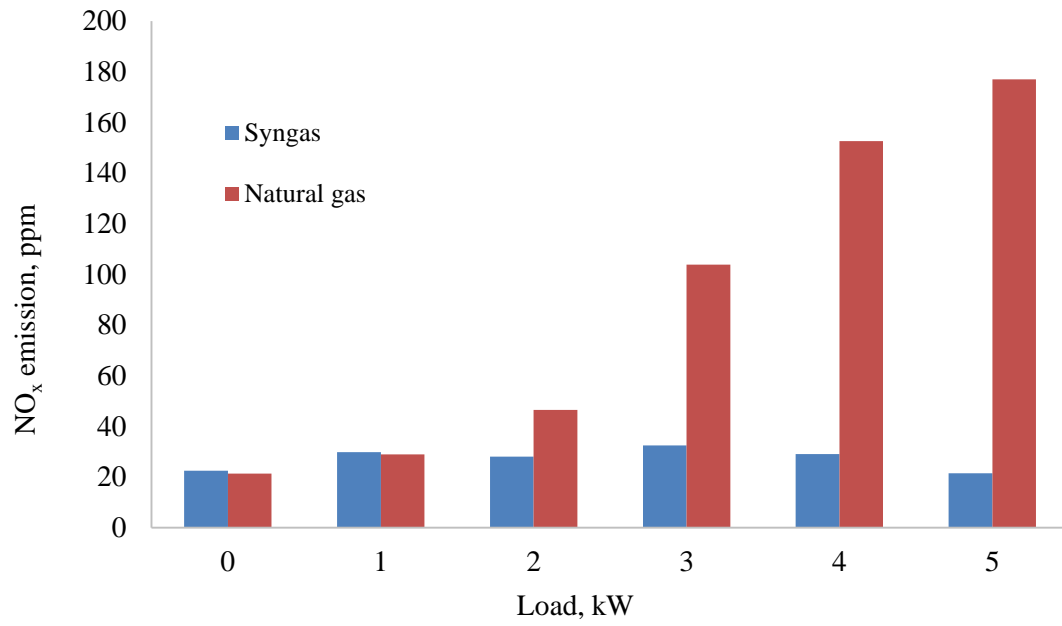
2.4.



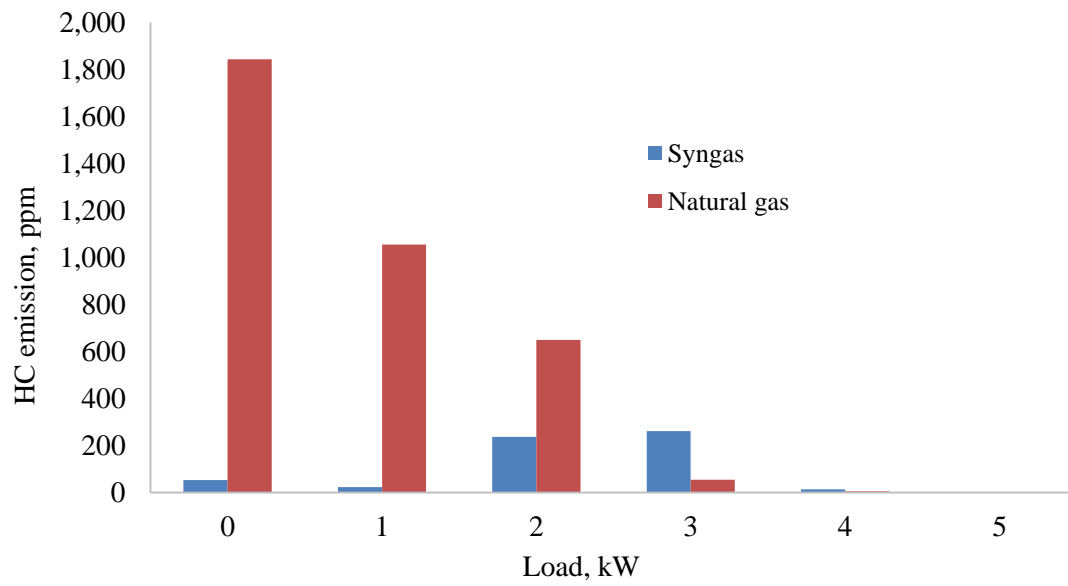
(a)



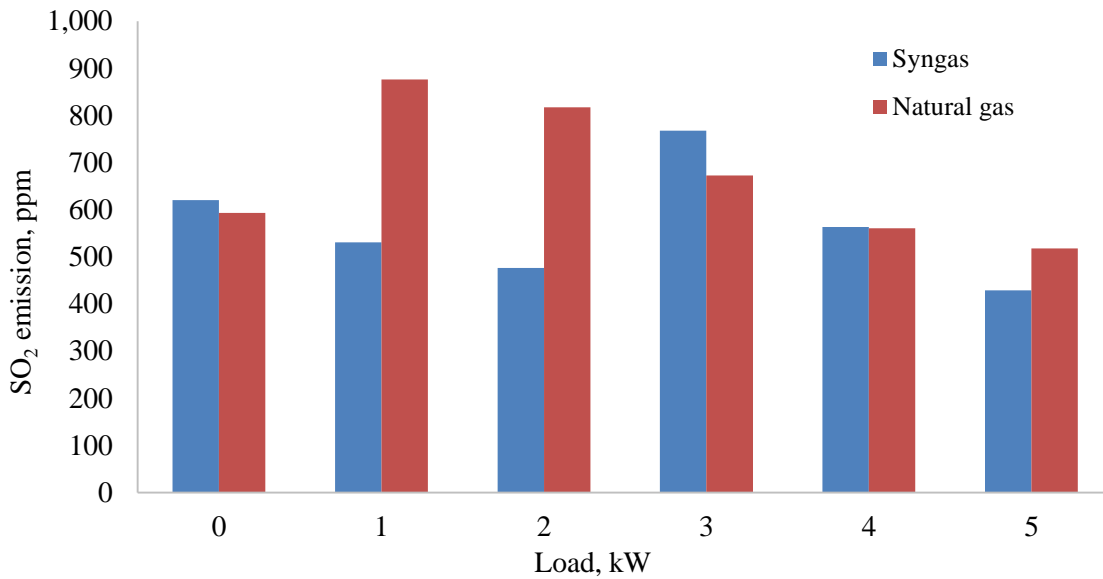
(b)



(c)



(d)



(e)

**Figure 2.5. Emissions levels (ppm) of the engine operated on syngas and natural gas at varying load (kW): (a) CO<sub>2</sub>, (b) CO, (c) NO<sub>x</sub>, (d) HC, and (e) SO<sub>2</sub>**

**Table 2.4. P-values of interaction between the load increment and the emission level**

Emission type P-value	CO <sub>2</sub>	CO	NO <sub>x</sub>	HC	SO <sub>2</sub>
R-Square Model	0.8110	0.4797	0.9216	0.9617	0.7031
Pr > F (Load)	0.8058	0.3686	0.0025	<.0001	0.1742
Pr > F (Gas)	0.0002	0.2402	<.0001	<.0001	0.0604
Pr > F (Load*Gas)	0.1663	0.7297	0.0025	<.0001	0.0988

#### 2.3.4.1. CO<sub>2</sub> emission

As shown in Figure 2.5a, the engine running on syngas shows a decreasing trend of CO<sub>2</sub> emission with increasing load, whereas, the engine running on natural gas shows an increasing trend of CO<sub>2</sub> emission with increasing load. The CO<sub>2</sub> emission using syngas decreased by 50% (149,500 ppm at the initial load to 79,000 ppm at the maximum load). While the CO<sub>2</sub> emission using natural gas, increased from 29,333 ppm at no load to 57,000

ppm at 5 kW. With the increasing load, a reduction of CO<sub>2</sub> emission from the engine using syngas might be due to a more stable operation and the presence of hydrogen fraction in the syngas, as hydrogen combustion creates water instead of CO<sub>2</sub>. The CO<sub>2</sub> emission from the engine using natural gas showed a linear relationship with the load. As the load increased, the CO<sub>2</sub> emission dropped substantially. The lower energy content of the syngas (~6.47 MJ/Nm<sup>3</sup>) compared to that of natural gas (~37.79 MJ/Nm<sup>3</sup>) could be the reason for this occurrence. CO<sub>2</sub> emission obviously contributes to the long-term environmental damage caused by the greenhouse gas effect [239].

#### **2.3.4.2. CO emission**

Similar to CO<sub>2</sub> emission, with the increasing load, the engine exhibited a decreasing trend of CO emission: 4,400-17,050 ppm when running on syngas, and 9,850-17,250 ppm when running on natural gas. The lowest and highest CO emission from syngas were 4,400 ppm at 80% load (4 kW) and 17,050 ppm at middle load (2 kW), respectively, as shown in Figure 2.5b. The decreasing trend of CO emission with increasing load can be attributed to more complete combustion and leaner fuel mixture. The substantial low concentration of CO emission using syngas asserts a decrease in the risk of suffocation caused by the strong adherence of CO to hemoglobin [239].

#### **2.3.4.3. NO<sub>x</sub> emission**

Figure 2.5c shows the profile of NO<sub>x</sub> emission when the engine ran on syngas and natural gas fuels. At high loads ( $\geq 2$  kW), engine NO<sub>x</sub> emission using syngas fuel was significantly lower ( $p < 0.001$ ) than that using natural gas fuel. The lowest NO<sub>x</sub> emission is below the limit set by California's emission standard of 25.9 ppm [240]. Moreover, it was noted that the variation of load significantly impacted the NO<sub>x</sub> emission. The load, the

type of gaseous fuel, and the interaction between those parameters presented significant correlation to the emission levels of NO<sub>x</sub>. The lower NO<sub>x</sub> emission from syngas (as compared to natural gas) can be attributed to its lower flame temperature [229], resulting in lower pressure and temperature in the engine combustion chamber, which consequently reduces NO<sub>x</sub> formation [85, 234]. This result emphasizes that using syngas as engine fuel provides substantial environmental returns because NO<sub>x</sub> causes lung irritation, impairment of functions of the lungs, tissue damage, and harming of mucous membranes [239].

#### **2.3.4.4. Hydrocarbon emission**

As presented in Figure 2.5d, engine hydrocarbon (HC) emission using syngas (0 to 262 ppm) was consistently lower at all load variables compared to that using natural gas (1 to 1,843 ppm). The low methane and high hydrogen concentrations of syngas might be the reason for its low HC emission as compared to natural gas. Hydrogen in syngas has shown to increase the temperature in combustion chamber, which decreases HC emission [231]. The lowest HC emission (0 ppm) was also noted at the full load of 5 kW and the HC emission increased consistently (R-square of 0.96) with decrease in engine load. The increase in HC emission with decrease in load can be attributed to incomplete combustion and efficiency loss at the low engine load [88]. The load, the type of gaseous fuel, and the interaction between these parameters significantly affected HC emission level ( $p < 0.05$ ). Therefore, utilization of syngas for power production can substantially decrease the risks of irritation of the eye, nose and throat to human [241] and the inhibition of plant growth due to low HC emission [242].

#### **2.3.4.5. SO<sub>2</sub> emission**

Typically, SO<sub>2</sub> emission from an internal combustion engine is much more affected by the characteristics of the fuel, than the engine [243]. The engine operated on syngas produced less SO<sub>2</sub> emission at almost all load conditions. As depicted in Figure 2.5e, the engine run on syngas produced SO<sub>2</sub> emission of 429-768 ppm, compared to the engine operated on natural gas that generated SO<sub>2</sub> emission of 518-876 ppm. Statistically, the trend of SO<sub>2</sub> emission was similar to that of CO emission; no factor was significantly affected emission level at the degree of error ( $\alpha$ ) of 0.05 (Table 2.4). The low sulfur concentration in the syngas appeared to be the cause for generating low SO<sub>2</sub> emission as compared to natural gas. A low of SO<sub>2</sub> emission formed from biopower generation might lead to a decrease in the concentration of sulfuric acid, a strong contributor of acid rain and respiratory diseases, in the atmosphere [239, 242].

#### **2.4. Conclusions**

An off-grid small scale power generation was demonstrated using a 60-kW downdraft gasification system with a cyclonic combustion chamber integrated with a 10 kW SI engine running on 100% syngas. The main findings of the study can be summarized as following:

- The biomass gasifier, operated at ER of 0.20, led to combustion zone temperature of 800 to 900°C. The produced syngas (LHV of 6.47 MJ/Nm<sup>3</sup>) contained H<sub>2</sub>, CO, CH<sub>4</sub>, C<sub>2</sub>H<sub>4</sub>, and C<sub>2</sub>H<sub>6</sub> at levels of  $11.4 \pm 1.9\%$ ,  $21.0 \pm 2.2\%$ ,  $5.5 \pm 1.1\%$ ,  $0.15 \pm 0.1\%$ , and  $1.33 \pm 0.3\%$  v/v, respectively.

- Operation of the engine running on 100% syngas directly fed from the gasifier was consistent, stable and generated maximum power of 5 kW whereas the engine running on natural gas generated maximum power of 9 kW. The overall efficiency of the power generation was 21.3% using syngas fuel and 22.7 % using natural gas fuel at 5 kW.
- The CO<sub>2</sub> emission from syngas fuel decreased with increase in load, generating about 149,000 ppm at the initial load of 0 kW to 7,900 ppm at the maximum load of 5 kW.
- At all load, the CO emissions from syngas fuel (4,400-17,050 ppm) was lower than those from natural gas fuel (9,850-17,250 ppm).
- The NO<sub>x</sub> emissions generated from syngas fuel (21.5-32.5 ppm) was significantly lower than those from natural gas fuel (21.3-177 ppm), with the lowest of 21.5 ppm at full load (5 kW) from syngas fuel. California's NO<sub>x</sub> emission standard of 25.9 ppm was satisfied using syngas fuel at full load.
- The HC emissions from syngas fuel (0-262 ppm with 0 ppm at the maximum load) was lower than those using natural gas fuel (1-1,843 ppm).
- The SO<sub>2</sub> emissions from syngas fuel (429-768 ppm) was consistently (but not significantly) lower than those from natural gas fuel (518-876 ppm).

The stable and considerably high efficient engine operation as well as low harmful emissions from syngas fuel derived from biomass gasification show potential to use underutilized resources (biomass and wastes) for generating off-grid power environmental friendly and sustainably. With minimum engine modification, commercial natural gas engine can be coupled to feed syngas directly from gasifier. The off-grid

power generation system is a viable solution for accelerating access to electricity in locations that are beyond the reach of the current electrical grid system.

## CHAPTER 3

### POWER GENERATION FROM CO-GASIFICATION OF MUNICIPAL SOLID WASTES AND BIOMASS: ELECTRICITY GENERATION AND EMISSION PERFORMANCE

This chapter was published as:

“N. Indrawan, S. Thapa, P. R. Bhoi, R. L. Huhnke and A. Kumar, Electricity power generation from co-gasification of municipal solid wastes and biomass: Generation and emission performance, *Energy*, vol. 162, pp. 764-775, 2018”.

**Abstract:** Global generation of municipal solid waste (MSW) is predicted to reach over 2.2 billion tons/year in 2025. Landfilling and incineration, the two most common conventional techniques for MSW processing, negatively impact public health. This study developed and demonstrated electricity generation by co-gasification of two underutilized resources: MSW and agricultural biomass. A patented design of 60-kW downdraft gasifier and an internal combustion engine with 10 kW generator were used to generate electricity from co-gasification of various ratios of MSW and biomass. The maximum heating values (LHV) of syngas obtained at MSW ratio of 0, 20, and 40 wt.% were 6.91, 7.74, and 6.78 MJ/Nm<sup>3</sup>, respectively. At all MSW to biomass ratios, the maximum electric load generated was 5 kW, with electrical efficiencies of 22, 20, and 19.5% at MSW ratios of 0, 20, and 40 wt.%, respectively. The engine CO, NO<sub>x</sub>, SO<sub>2</sub>, and CO<sub>2</sub> emission decreased with increasing load, while HC emission increased with increasing load. CO, NO<sub>x</sub>, and CO<sub>2</sub> emissions decreased, while HC and SO<sub>2</sub> emissions increased with increase in MSW ratio. Thus, the co-gasification system provides a basis for future development of small-scale power generation to utilize local wastes.

**Keywords:** Co-gasification; MSW; Power Generation; Engine Emissions; Switchgrass; Waste to Energy

### 3.1. Introduction

The global municipal solid waste (MSW) generation is predicted to reach over 2.2 billion tons (1.42 kg per person per day) in 2025, from 1.3 billion tons (1.2 kg per person per day) in 2012, and a major component of the MSW will continue to be organic matter [12]. In the U.S., total MSW generation in 2014 reached 258.5 million tons, of which 82.2% consisted of organic materials including paper and paperboard, yard trimming, food, plastic, rubber, leather, textiles, and wood [244]. In the U.S., landfilling is the most common technique to treat MSW, accounting for 52.6% of total MSW generated, followed by recycling (25.7%), combustion with energy recovery (12.8%), and composting (8.9%) [244]. Unfortunately, landfills have the potential of contaminating the soil and groundwater with leachate pollutions as a result of degradation of organic matters through a variety of biological and abiotic redox processes, including dissolution/precipitation of minerals, complex formation, ion exchange and sorption [245]. Landfills can also pollute air due to emission of volatile organic compounds (VOC) including dimethyl disulfide, toluene, and benzene [246]. Whereas, MSW incineration (combustion) can generate polychlorinated dibenzo-p-dioxins (dioxins/PCDDs) and dibenzofurans (furans/PCDFs), which cause chloracne, liver dysfunction, and cancer [247]. One of the alternative techniques to recover energy and byproducts from MSW with minimum environmental issues is gasification.

Commercial gasification of MSW has recently been demonstrated. One of the first commercial plants, the first using plasma gasification technology, was EcoValley WTE facility, located in Utashinai, Japan. During 2003 to 2013, the plant treated a 50/50 mix of MSW and auto shredder residue (ASR) with a total capacity of 165 metric tons per day

(tpd) without having major technical issues and supplied 1.5 MW electricity to the grid [177]. However, due to limited availability of MSW and the cost associated with plasma technology, the plant only ran at half capacity, resulting in an economic loss and a discontinued operation in 2013. Similarly, Air Products constructed a MSW gasification-based power plant, located in Teesside, Northeast England, known as Tees Valley project. The project, claimed as the largest MSW plasma gasification power plant, was initially designed to utilize MSW as the feedstock of 1,000 tpd with total electricity generation of 100 MW [47]. However, due to technical difficulties, the project was suspended in 2016 [49, 248]. A similar plant of plasma gasification treating solid waste materials with a capacity of 22 tpd was constructed in Mihama Mihata, Japan, in 2002. The plant generates syngas that is further converted to heat to dry the sewage sludge prior to gasification [177]. Another plant treating biomedical wastes with a capacity of 78 tpd was constructed in Pune, India [47]. The plant has been operating since 2009, processing more than 600 types of waste materials [248, 249]. Several other major MSW gasification plants for power production throughout the world are currently in operation or under construction/commissioning.

Experimental investigation of the performances of co-gasification of MSW and biomass are very limited in literature [41, 42]; most co-gasification studies relied on numerical simulations [250-253]. Robinson et al. (2017) [42] investigated the co-gasification of woody biomass and refused derived fuel (RDF) in a bubbling fluidized bed gasification using air as gasification medium at equivalence ratio of 0.29-0.31. The results showed that at gasification temperature of 725-875°C, the gasification efficiencies ranged from 48 to 58% and gas lower heating values (LHV) ranged from 4.9 to 5.7

MJ/Nm<sup>3</sup>. Gasification containing RDF materials generated a higher fraction of syngas heavy hydrocarbons (C<sub>2</sub>-C<sub>3</sub>) than that containing biomass materials. However, at 875°C, gasification mixture containing RDF resulted in an agglomeration of bed material preventing steady-state operation of gasifier. Similarly, Ong et al. (2015) [41] investigated the co-gasification of woody biomass and sewage sludge in a downdraft gasifier. They found that the co-gasification resulted in a stable operation with a gas LHV of 4.5 MJ/Nm<sup>3</sup> at 20 wt.% sewage sludge. However, further increase of sewage sludge content to 33 wt.% led to blockage of gasifier due to ash agglomeration; sewage sludge contained ash up to 29.7 wt.%.

Waste to Energy (WtE) facilities typically use incineration to treat MSW as incineration is technically less-complex and has been widely known for years. However, the incineration plants must employ a complex control strategy, namely the Maximum Allowable Control Technology (MACT), to keep the emissions below the limits [34]. MACT generally consists of dry scrubber, fabric filter baghouses, activated carbon injection, selective non-catalytic reduction of NO<sub>x</sub>, and other measures [34]. Using MACT, levels of Hg, Cd, Pb, polychlorinated dibenzo-p-dioxins (dioxins/PCDDs)/dibenzofurans (furans/PCDFs), particulate matters, NO<sub>x</sub>, and SO<sub>2</sub> from US incineration facilities (88 surveyed by the EPA) has reduced on average by over 96% (from 4400 to 15 tons/year (tpy)), 96% (from 9.6 to 0.4 tpy), 97% (170 to 5.5 tpy), 99% (from 4400 to 15 tpy), 96% (18600 to 780 tpy), 24% (64900 to 49500 tpy), and 88% (38300 to 4600 tpy), respectively during 1990-2005 [214]. The US EPA standard for these emissions are 0.06 mg/Nm<sup>3</sup>, 0.02 mg/Nm<sup>3</sup>, 0.2 mg/Nm<sup>3</sup>, 0.14 ng/Nm<sup>3</sup>, 11 mg/Nm<sup>3</sup>, 264 ppm, and 63 ppm, respectively [34]. In addition, about 87 incineration facilities

operating across 22 states, treating over 29.7 million tons of MSW, and generating electricity of 2,547 MW in 2014, released 1% of the U.S. emissions of dioxin and mercury [34].

MSW gasification, in comparison, offers several advantages in term of low emissions, such as low emission levels of PCDDs and PCDFs due to the limited atmosphere and less complex gas cleaning system required [30, 208]. Arena et al. [30] and Tanigaki et al. [173] found that the emission levels of PCDDs/PCDFs of a MSW gasification plant were generally lower than  $0.032 \text{ mg/Nm}^3$ , which is below the  $0.1 \text{ mg/Nm}^3$  limit of European and Japanese standard [30, 34]. Moreover, heavy metals and other contaminants in gasification are mostly transformed into non-hazardous vitrified slags (e.g.,  $\text{SiO}_2$ ,  $\text{CaO}$ , and  $\text{Al}_2\text{O}_3$ ) that are generally inert and do not contaminate the soil [208], thus, reducing the total emissions in the flue gas [30]. The potential environmental characteristics described above related to MSW gasification are based on advanced plasma gasification technology, which is still evolving. This technology requires high power consumption to generate plasma at high temperature ( $>5,000^\circ\text{C}$ ) [177], which leads to technical difficulties, complex construction and ultimately high capital cost [50].

Small-scale gasification that utilize locally generated resources, such as biomass and MSW, has potential to address the high capital costs and complex construction experienced in large high-temperature plasma technologies, support off-grid power generation and minimize environmental impacts. The total electric capacity of off-grid generation (with generator's size  $< 1 \text{ MW}$ ) in the U.S. reached 5,407 MW in 2015 [13]. For off-grid power production, internal combustion (IC) engine is one of the most prevalent technologies. The recent advancement of IC engines can reach efficiency up to

41% [16] and use of syngas in IC engine can drastically reduce emissions (mainly SO<sub>2</sub> and NO<sub>x</sub>) [18].

To address the aforementioned issues of increasing global MSW generation, minimizing negative environmental impacts of MSW disposals due to landfill and direct combustion (incineration), and supporting distributed power generation, experimental investigation on power generation from co-gasification of biomass and MSW is critical and, yet, is still limited in literature [29, 57, 64, 86, 94, 101]. The currently available literature have focus mostly on power generation from only biomass [29, 57, 64, 86, 94, 101]. MSW gasification studies have mostly relied on model development [253, 254]. Few studies are reported on co-gasification of biomass and MSW [41, 42], but power generation from the syngas generated were not investigated. This paper for the first time presents the performance of power generation from co-gasification of switchgrass, a perennial grass in Oklahoma, USA, and MSW using a 60-kW scale-up unit of a patented unique downdraft gasifier [222], previously reported in Refs. [29, 255]. The gasifier system is connected with an IC engine and intended to support for a distributed power application. Our specific objectives were to study effects of MSW to biomass feed ratios on power generation and emission performance of engine fed with the syngas generated.

## **3.2. Materials and method**

### **3.2.1. Materials**

A mixture of pelletized MSW and chopped switchgrass (SG) was used for co-gasification. Pelletized MSW was obtained from Wastaway® LLC., Morrison, TN, consisting of a general composition of food (14.6%), paper (27%), yard trimmings

(13.5%), plastics (12.8%), metals (9.1%), rubber, leather and textiles (9%), wood (6.2%), and others (7.8%). This composition was similar to what has been reported as typical MSW composition in the USA [172]. SG (*Panicum virgatum L.*) was selected as the biomass, a locally abundant feedstock. The proximate (moisture, volatile matter, fixed carbon and ash) and ultimate (C, H, O, N, and S) analyses of MSW and SG were analyzed by Hazen Research Inc., Golden, CO, as shown in Table 3.1.

**Table 3.1. The proximate and ultimate analyses of MSW and SG**

Biomass type / References	MSW	SG
Moisture content, %, wet basis	3.8	7.7
Proximate, wt.%, dry basis		
Volatile matter	77.54	78.60
Fixed carbon	8.72	17.47
Ash	13.74	3.93
Ultimate, wt.%, dry basis		
Carbon, C	50.71	49.63
Hydrogen, H	6.13	5.72
Oxygen, O	29.14	40.37
Nitrogen, N	0.14	0.30
Sulphur, S	0.14	0.05
Lower heating value, MJ/kg	19.19	16.49
Higher heating value, MJ/kg	20.20	17.73
Bulk density, kg/m <sup>3</sup>	1,095	91

MSW and SG were manually mixed based on mass percentage to feed into the gasifier. Feedstock moisture content was determined, prior to each experiment, by oven drying samples at 104°C for 24 h. The syngas produced from the gasifier was measured using gas chromatograph (Agilent, Model 7890a, Agilent Technologies, Santa Clara, CA).

### 3.2.2. Gasifier description

Biomass feeding unit consists of a belt conveyor and air lock valve. The downdraft gasifier is equipped with internal cyclonic combustion chamber with height of 3.2 m, has nameplate capacity of 60 kW, and uses a feeding rate of 100 kg/h. The gasifier is a scaled-up unit of a patented design [222], which was developed in 2009, with capacity of 10 kg/h. The gasifier consists of a biomass section at the top, pyrolysis and tar cracking zone in the middle and char gasification section at the bottom. This downdraft design was selected due to its proven capability to generate syngas with low tar content (less than 0.5 g/Nm<sup>3</sup>) compared to fluidized bed (up to 40 g/Nm<sup>3</sup>), circulating fluidized bed (up to 12 g/Nm<sup>3</sup>) and fixed-bed updraft gasifier (up to 150 g/Nm<sup>3</sup>) [52]. The construction details of the scaled-up gasifier are given in Ref. [56].

The gasifier is equipped with an internal separate combustion section where turbulent, swirling high-temperature combustion flows are generated. The gasification reactor, gas pipes, and cyclone separator are insulated with a 25-mm thick ceramic wool blanket, which is covered by aluminum sheeting. Type-K thermocouples are used for temperature measurements. An air compressor (Sullair, Model 2209AC, Sullair LLC., Michigan City, IN) supplies air, and a flow meter (Fox, Model FT2A, Fox Thermal Instrument Inc., Marina, CA) measures input air flow rate. A stirrer in the gasifier uniformly mixes biomass, preventing bridging inside the reactor. To ensure that ash did not accumulate inside the reactor, a rotating 2-armed ash scrapper is used to unload ash from the reactor and an inclined ash screw conveyor equipped with an electric motor (Dayton, Model 2MXT4A, Dayton Electric Mfg. Co., Lake Forest, IL) is used to transport the ash into the ash drum. MSW/SG feed rate was maintained at 90-100 kg/h.

### **3.2.3. Syngas cleaning system**

Syngas cleaning system plays a critical role for successful operation in power generation [95, 223]. Tar and other impurities such as particulate matter, ammonia, hydrogen sulfide, hydrogen cyanide, hydrogen chloride, sulfur dioxide, and alkali metals must be removed. To achieve sustainable operation of an IC engine, tar content of syngas must be limited to 100 mg/m<sup>3</sup> [65]. In our study, syngas was cleaned using a cyclone separator and a wet gas scrubbing system containing acetone-water mixture. Details of this system are available elsewhere [29].

### **3.2.4. Gasifier operation**

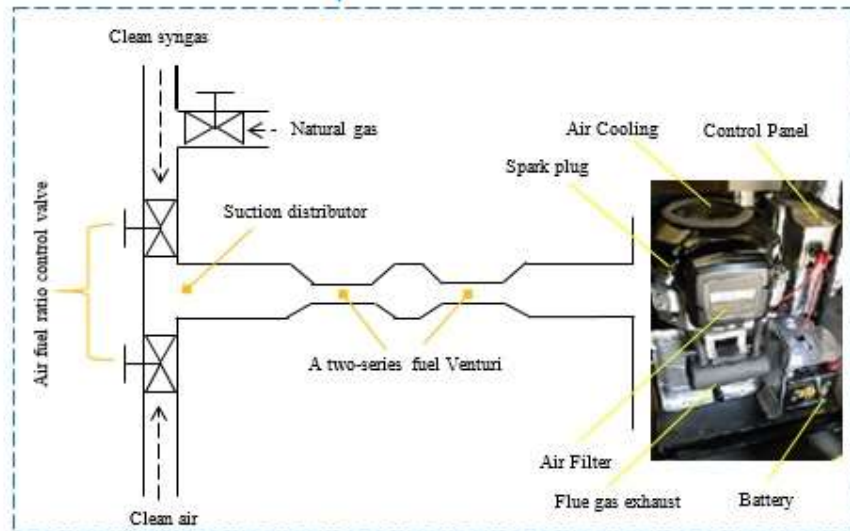
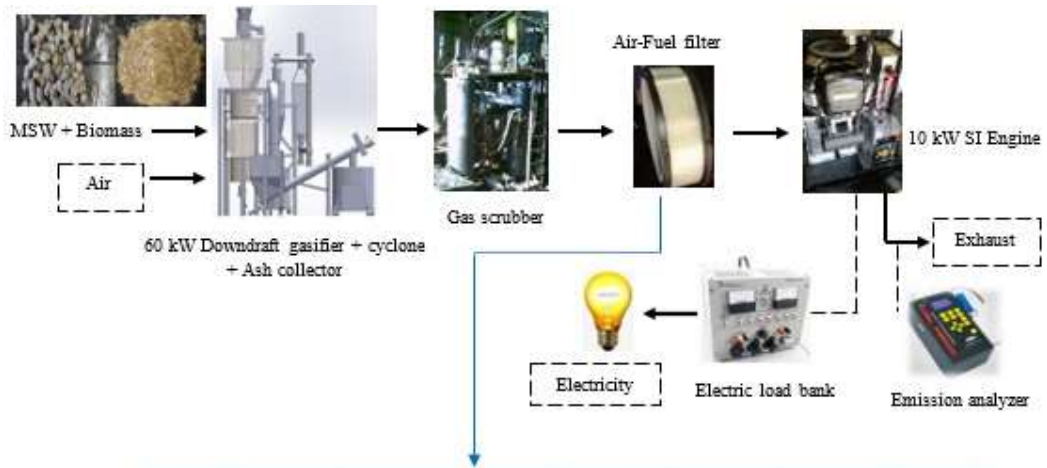
Gasifier start-up began by loading 10 kg of wood charcoal onto the grate. The gasification reactor was then filled with a predetermined MSW/SG mixture. MSW and SG were fed into the gasifier using a belt conveyor and passed through an airlock to prevent backflow of syngas. After the gasifier reached equilibrium, the feeding rate was maintained at approximately 95 kg/h. Each test runs lasted 2-3 hours. For initial firing and preheating, propane was supplied at the top of the pyrolysis and tar cracking (PTC) section, while regulating initial air flow at about half of the desired value or equivalence ratio (ER). The ER was determined as the ratio of the air flow input to the theoretical stoichiometric air required for complete combustion of biomass [174]; in this study, the ER of 0.2 was used based on the previous study [29]. The propane supply was discontinued when the reactor temperature in the annular space of the PTC reached temperature of approximately 100°C. As the reactor temperature reached 600°C and the reactor temperature profile stabilized, the air flow with the specified ER was held constant. The mixture of MSW and SG were then continuously fed into the reactor at

constant feeding rate between 90 and 100 kg/h. The profiles of input air flow rate, pressure drop across the gasification reactor, flame characteristics, reactor temperatures, and syngas temperatures at the exit of the cyclone were closely monitored.

Syngas was sampled between the outlet of the cyclone separator and the flue gas or flame stack. A stream of syngas was passed into the gas scrubber using a divider while the remaining syngas was burned through a diffuser burner. A homogenous flame was an indication of high quality syngas, as reported earlier [29]. A divider valve was connected at the outlet of the gas scrubber for purging the pipelines and controlling the engine operation. Syngas flowrate entering the engine was measured by a flow meter (Fox, Model FT2A, Fox Thermal Instrument Inc., Marina, CA). Syngas pressure at the engine inlet was measured using a U-tube manometer (McMaster-Carr) installed at the suction line of the engine. Air flow into the engine was controlled using a ball valve, which was located ahead of the air flowmeter (Fox, Model FT2A, Fox Thermal Instrument Inc., Marina, CA). Additionally, to obtain better homogenous mixing between syngas and air, a series of two venturi pipes was used. The gasification system and experimental set-up including a modified air-fuel regulation are shown in Figure 3.1. Biomass feeding process involves a belt conveyor (Bunting Magnetics Co., Newton, KS) and air lock valve (Prater Industries Inc., Bolingbrook, IL) (Figure 3.1a). The air-fuel mixture entering the engine was regulated by the engine governor. Through preliminary tests and by regulating the flowrates of air and syngas (after the cleaning system) through the air-fuel regulation (Figure 3.1b), an air fuel-air ratio (AFR) of 0.8-1.0 was found to be satisfactory for the engine operation.



(a)



(b)

**Figure 3.1. (a) Gasification system with total capacity of 60 kW and (b) detail experimental set-up with a modified air-fuel regulation**

### 3.2.5. Power generation unit and emissions analysis

Electric power was generated using a two-cylinder spark-ignited (SI) engine (Model 040375, Briggs and Stratton Power Products Group LLC, Milwaukee, WI) with generator of maximum rated capacities of 10 kW and 9 kW using propane and natural gas, respectively. The SI engine had a rated speed of 3600 rpm, while the attached generator produced three phase power at 120/240 V at a frequency of 60 Hz. The electric load bank (Avtron, Model K490, Avtron Loadbank, Inc., Cleveland, OH) with voltage and current display was connected to the generator to vary the engine loading. Engine speed (rpm) was monitored using digital laser tachometer (CyberTech, Model 2234A, Litetrek International LLC, Pleasanton, CA). Major operating conditions of gasifier and engine are presented in Table 3.2.

**Table 3.2. The experimental conditions**

Components	Unit	Value
Gasification equivalence ratio	Mass fraction	0.20
Feedstock type	-	MSW & SG at various MSW ratio (0, 20, 40, and 60 wt.%)
Feedstock rate	kg/h	95 ± 1
Engine capacity	kW	10 (with propane), 9 (with natural gas)
Air flow of gasifier operation	m <sup>3</sup> /h	100 ± 2%
Ambient temperature	°C	27 ± 0.5
Total syngas flow rate	m <sup>3</sup> /h	155 ± 10
Energy content of syngas, LHV	MJ/m <sup>3</sup>	6.73 to 7.74
Input syngas flowrate into engine	m <sup>3</sup> /h	12.1 – 18.2
Engine load variation	kW	0 – 5 (stable), 7 (max.)
Air-fuel ratio		0.7 – 1.0
Engine speed	rpm	1,886 – 3,556

Electrical power generation efficiency was calculated using Eq. 3.1, where LHV is the lower heating value of syngas (MJ/m<sup>3</sup>) and Q<sub>m</sub> is the flow rate of air-fuel mixture (m<sup>3</sup>/h). An example of calculation for electrical efficiency is provided in Appendix 1. Specific fuel consumption (SFC) was measured using ratio of fuel consumption (kg/h) and power produced (kW), as given in Eq. 3.2, where Q is the fuel consumption (kg/h) and P is the total power generated (kW).

$$\text{Electrical efficiency} = \text{electrical power output} / (\text{LHV} \times Q_m) \dots\dots\dots [3.1]$$

$$\text{SFC} = Q / P \dots\dots\dots [3.2]$$

An integrated portable emissions analyzer (ENERAC Model 700, Holbrook, NY) was used to measure the engine emission (CO, CO<sub>2</sub>, NO<sub>x</sub>, hydrocarbon (HC), and SO<sub>2</sub>) at the engine exhaust. The exhaust temperature was also recorded to ensure consistency of operational condition.

**3.2.6. Statistical analysis**

A statistical analysis software (SAS 2015, Cary, NC) was used to analyze effects of load and type of gaseous fuels (syngas generated at various MSW ratios) on the engine performance and emission characteristics. A full factorial design with three types of gaseous fuels (syngas generated from MSW ratio of 0, 20, and 40 wt.%) and five loads (1, 2, 3, 4 and 5 kW) were used. All experiments were replicated. Randomized Complete Block Design (RCBD) and General Linear Method (GLM) procedure (with the significance level = 0.05) were used to analyze the interactions between factors.

### 3.3. Results and discussion

#### 3.3.1. Gasifier performance

Gasifier operation affects power generation because it directly impacts syngas yield and quality, that the power generation depends on. MSW, which has a broad spectrum of characteristics and compositions, further add influence on power generation. No major operational issues were observed during the gasifier run. The equivalence ratio (ER), reactor temperature, biomass feed rate, and ash removal rate are factors that directly influence syngas quality and energy content, impacting the performance of power generation. The combustion zone of the gasifier reached a stable reactor temperature of 700-950°C with syngas LHV of around 6.7-7.7 MJ/Nm<sup>3</sup>. The temperature observed was in the typical range reported for air gasification (550-1,000°C) [30, 41, 42] and is mainly affected by the ER. A stable operating temperature is essential to maintain the water gas reaction from process kinetic perturbations. An increase of air flow rate promotes the exothermic combustion reactions, releases more energy, generates a high temperature in tar cracking section, and produces more carbon monoxide in the syngas due to the enhanced Boudouard, water-gas shift, and steam reforming reaction (at temp. >700°C) [41, 256]. However, with addition of air, syngas with also get diluted with N<sub>2</sub>, thus lowering LHV of the syngas. Meanwhile, a decrease of air flow rate results in decrease of the syngas yield, increase of syngas LHV but can also result in incomplete gasification and increase of syngas tars [256].

The cold gas efficiencies (CGE) at MSW ratio of 0, 20, and 40 wt.% were 62, 54 and 49%, respectively. The CGEs obtained using MSW feedstock (MSW ratio of 20 and 40 wt.%) were in agreement with a previous study [42], while the CGE value for MSW ratio

of 0 wt.% (pure SG biomass) is comparable with another report [29]. Due to the high ash content of MSW, ash accumulation in the ash drum (up to 29 wt.% to the total feedstock at gasification of MSW 40 wt.%) was high, consequently lowering the syngas yield from the gasifier. Therefore, the run with a higher fraction of MSW (60 wt.%) was not successful. Agglomeration of the bed material in the combustion zone was also observed at MSW ratio of 60%, preventing the steady state operation and blocking the syngas flow for further use of the power generation. The phenomena was also observed in previous studies at a lower fraction of MSW [41, 42]. Solid particulates (ash and char) of about 21, 23, and 29 wt.% of total feedstock were collected in the ash drum at MSW ratio 0, 20, and 40 wt.%, respectively, while on average less than 2.5 wt.% was collected in the cyclone separator.

### **3.3.2. Syngas quality**

Syngas heating value directly affects power generation performance. At the steady state condition, with MSW ratio of 0, 20, and 40 wt.%, the maximum heating value (LHV) of syngas were 6.91, 7.74, and 6.78 MJ/Nm<sup>3</sup>, respectively. Major syngas compositions were as high as 10% H<sub>2</sub> and 15% CO, with details provided in Figure 3.2. The syngas generated from co-gasification of MSW ratio of 20 wt.% yielded the highest heating value, followed by MSW ratio of 0% wt. The high heating value of MSW ratio of 20 wt.% was the result of the presence of a high fraction of hydrocarbon in the syngas. Although MSW has a higher heating value (19.19 MJ/kg) than SG (17.73 MJ/kg), its presence inhibited the syngas generation in the gasifier due its high ash content that consequently lowered the organic content, resulting in a lower efficiency of gasification.

Although the heating value of the syngas was about six times lower than that of natural gas (37.8 MJ/Nm<sup>3</sup>), the syngas LHV was in agreement with other studies [52, 57, 64, 86].

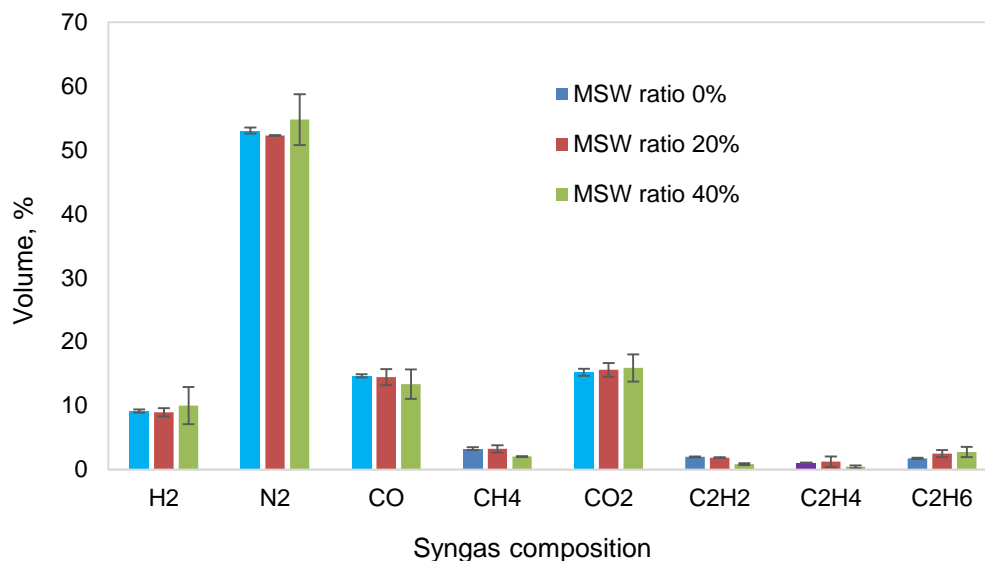


**Figure 3.2. Gas composition of syngas generated at various MSW ratio (0, 20, and 40 wt.%) at maximum load (5 kW)**

Carbon dioxide (13-14.5 vol.%) in the syngas generated was within the typical range (5-20 vol.%) produced from biomass gasification using air as the gasification medium [57]. The presence of carbon dioxide potentially reduces the knocking tendency of the engine [94]. Methane (2-4 vol.%) was also within the typical range (1.0-10 vol.%) and its presence is considered a support for stable operation of the engine [86, 87]. High syngas hydrogen (9-10 vol.%) obtained leads to the increase of flame speed, combustion chamber temperature, and engine efficiency [231].

In this study, a gas scrubber using acetone-water satisfactorily removed tar. Tar content was reduced from 27 g/Nm<sup>3</sup> at the inlet of the gas scrubber to less than 100 mg/Nm<sup>3</sup> at the outlet. A tar content of up to 100 mg/Nm<sup>3</sup> in syngas is satisfactory for engine application [65]. Other potential impurities in the syngas, such as particulate

matter [95] were found to be minimal as inside syngas pipeline from the outlet of the gas scrubber was clean and free of soot and tars. The syngas temperature at the outlet of the gas scrubber during 2-3 hour run was consistently in the range of 25-28°C, which is generally appropriate for injection into engines [67]. However, MSW constituents, such as chlorinated plastics, can potentially lead to harmful pollutants (such as PCDD/PCDF) under an oxygen-rich environment (such as incineration process) [199]. Gasification that provides a starving oxygen environment restricts the generation of those pollutants in the flue stack.

### **3.3.3. The characteristics of power generation**

Given the syngas energy content was approximately six times lower than that of natural gas the engine, which was designed for natural gas operation, required syngas injection at higher flowrate (11.7-18.0 m<sup>3</sup>/h of syngas) compared to 2.1-2.4 m<sup>3</sup>/h of natural gas. At the maximum load (5 kW), syngas flowrate was lower (7.1 m<sup>3</sup>/h) at MSW ratio of 0% compared to that at MSW ratio of 20 (7.3 m<sup>3</sup>/h) and MSW ratio of 40 wt.% (8.9 m<sup>3</sup>/h). It should be noted that the syngas used for engine operation (11.7-18.0 m<sup>3</sup>/h) was only about one tenth of the total syngas generated from the gasifier (140-170 m<sup>3</sup>/h) because the engine capacity was only 10 kW.

#### **3.3.3.1. Effect on engine performance and operation**

Engine speed decreased with increasing loads, as shown in Figure 3.3. The engine speed decreased from 3,478-3,556 rpm at baseload condition (0 kW) to 1,845-1,886 rpm at maximum load (5 kW). However, these engine speeds were higher than those (3,256-3,476 rpm) when the engine was fed with syngas from SG biomass at the peak load. The change in engine speed might be due to the modification of the air-fuel intake regulation

that was completed before using syngas from co-gasification of MSW and biomass was fed into the engine. The modification allowed more homogenous mixture of air and syngas. The electric load bank used also helped stabilize the engine operation, while in practical situation, besides syngas composition, the engine performance is highly impacted by the fluctuation in load on the electric grid [257].

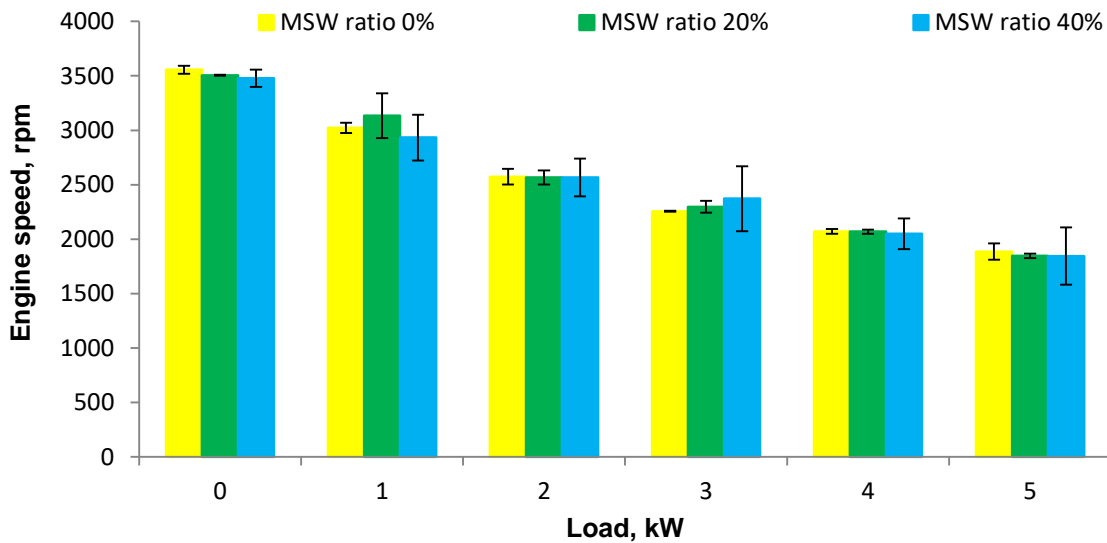


**Figure 3.3. Speed of engine running on syngas generated at various MSW ratio (0, 20, and 40 wt.%)**

Engine AFR ranged from 0.7 to 1.0 while running on syngas, indicating the engine operated at almost stoichiometric air/fuel ratio with rich mixture [258, 259]. With the specified AFR, engine operation was stable without any observation of knock and voltage fluctuation. These AFRs were lower than those reported earlier [29] when the engine ran on syngas generated from pure SG (AFR of 1.5 to 1.6). The low AFR might be due to the more homogenous mixture of air and syngas achieved because of the two venturies arrangement at the engine suction (Figure 3.1b), compared to a single venturi used as

earlier [29]. Generally, rich gas operation (AFR below stoichiometric AFR) results in an incomplete combustion, but more tolerant at broad fuel ranges and ambient conditions and have better transient load capability [259]; whereas, lean gas operation (AFR above stoichiometric AFR) produces a lower combustion temperature and decreases combustion efficiency but generates low NO<sub>x</sub> emission [234]. In comparison, the AFR of natural gas varied from 15.9 to 20.2, while AFR of syngas varied from 0.7 to 1.0, as shown in Figure 3.4. Statistically, for engine operation, operating parameters including the load variation, the types of gaseous fuels, and the interaction between the load and the types of gaseous fuels did not significantly impact the AFR ( $p > 0.05$ ).

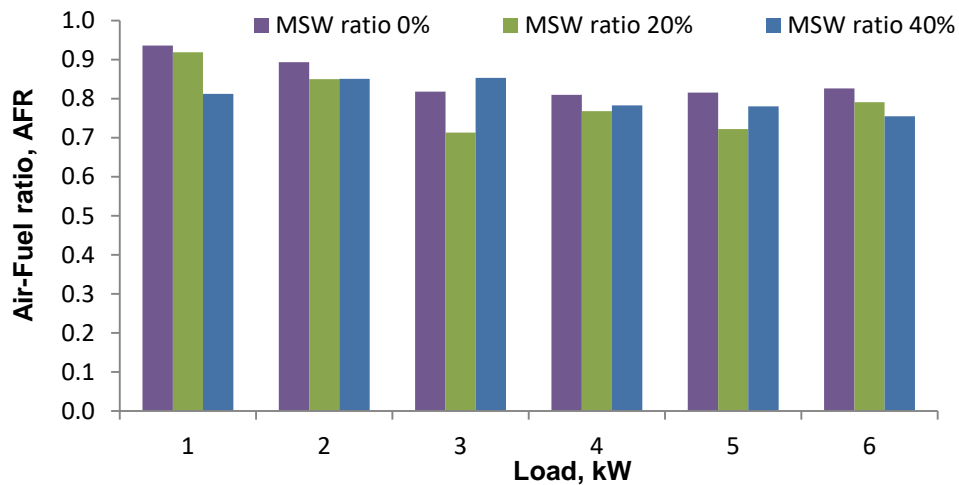


**Figure 3.4. Air fuel ratio (AFR) of engine running on syngas generated at various MSW ratio (0, 20, and 40 wt.%)**

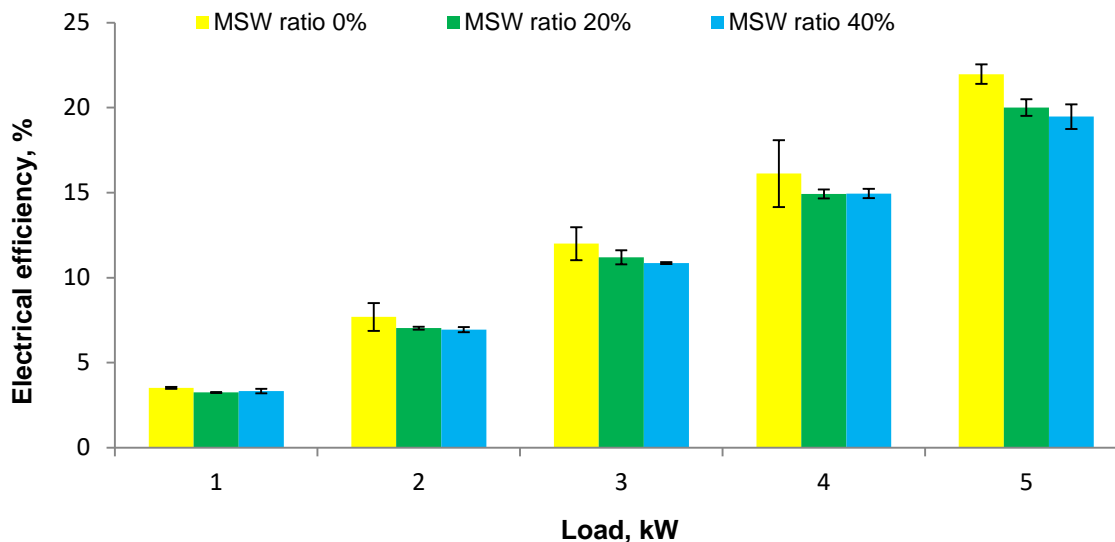


**Figure 3.5. Electrical efficiencies of engine running on syngas generated at various MSW ratio (0, 20, and 40 wt.%)**

Type of gaseous fuel (syngas generated from MSW ratio of 0, 20, and 40 wt.%) and loads had significant effects on electrical efficiency. However, the interaction between fuel types and load variation was not significant ( $P$  value = 0.5982). The electrical efficiency increased with increasing loads (Figure 3.5). At the maximum load (5 kW), electrical efficiencies of 22, 20, and 19.5% (SFCs of  $3.0 \pm 0.3$ ,  $3.1 \pm 0.2$ , and  $3.5 \pm 1.7$  kg/kWh) were achieved when the engine operated on MSW ratio of 0, 20, and 40%, respectively. The electrical efficiencies obtained in this study are in agreement with previous available reports: 19% [87], 21.3% [29] (as electrical efficiency), and 21% [88], 24.7-27.6% [89], 21% [64], 28% [57], 26.2% [86], and 25.6% [101] (as engine efficiency). The efficiency at MSW ratio of 0% was also consistent with that reported earlier [29]. At the same load (5 kW), natural gas achieved efficiency of 22.7% (SFC of 0.3 kg/kWh) [29], which was higher than the efficiency achieved using syngas. The low energy content of the syngas was mainly responsible for low engine electrical efficiency.

Overall, the electrical efficiencies reported in this study of 19.5-22% were equivalent to SFCs of 3.0-3.5 kg/kWh and were in agreement with those previously reported [64, 87-89]. Deploying exhaust gas recirculation (EGR) can further improve efficiency; with the recirculation of 45%, the engine efficiency can potentially increase from 26% to 40% [83].

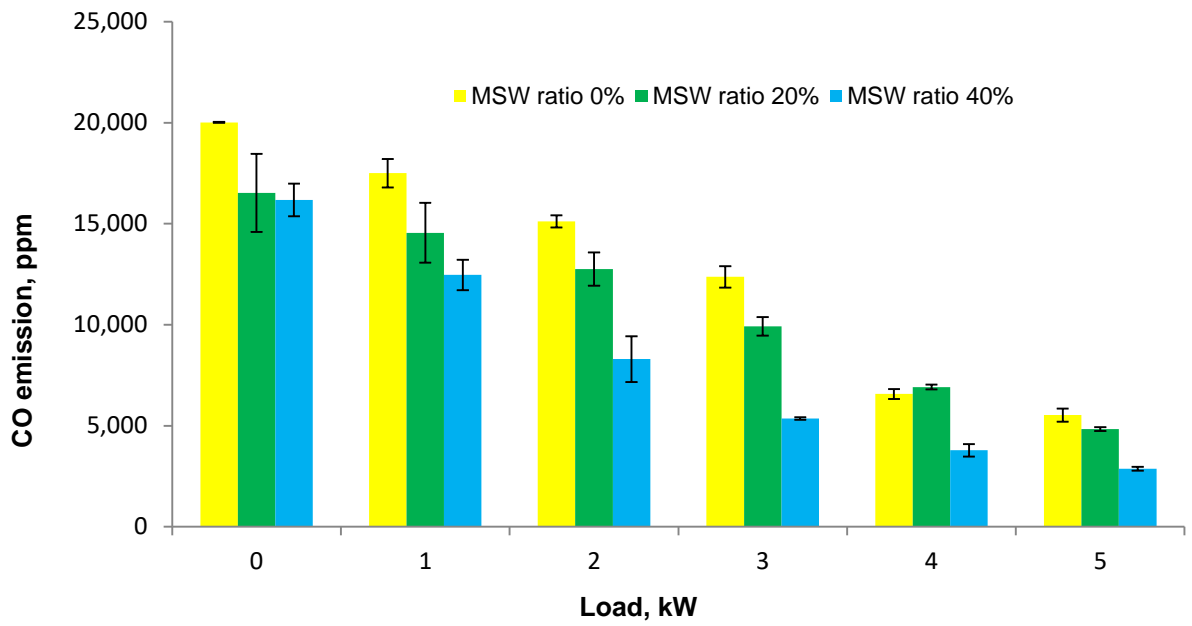
### **3.3.3.2. Power de-rating**

Power de-rating of about 28% was observed when the engine ran on syngas as compared to natural gas operation. The engine achieved a maximum load of 5 kW on syngas; whereas, a maximum load of 7 kW was measured on natural gas. The observed power de-rating was in agreement with typical power losses reported from earlier studies [94, 95].

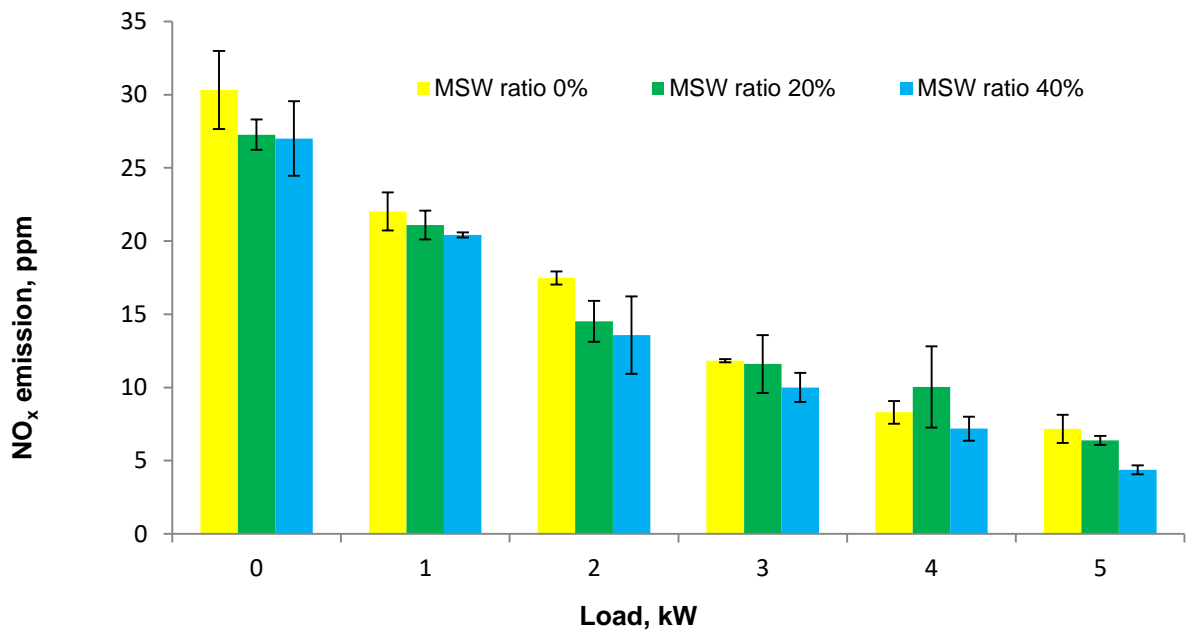
With 100% syngas, most previous studies used downdraft gasifiers with size ranging from 5 to 100 kg/h, resulting in an output power in the range of 3-60 kW and engine efficiencies of about 19-27%. To achieve a stable operation of the engine, most modifications conducted were in the air-syngas intake system. This study not only confirms the previous results but also gives valuable information where MSW can be used as the gasifier feedstock for electricity production with a comparably high-efficiency.

### **3.3.4. Emissions characteristics**

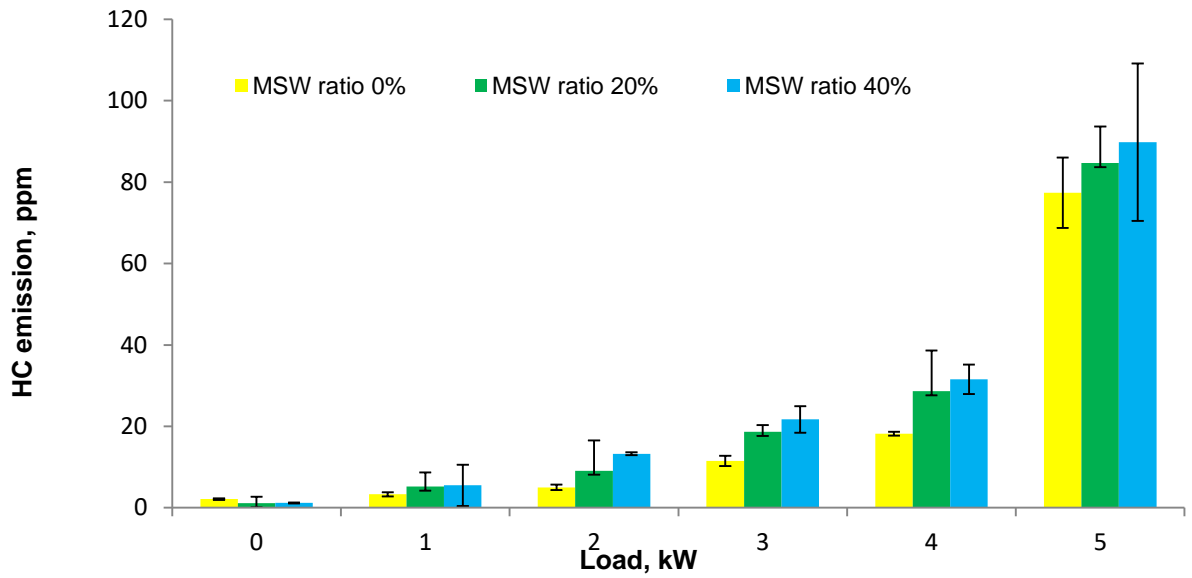
Emission performance results (CO<sub>2</sub>, CO, SO<sub>2</sub>, NO<sub>x</sub>, and HC) of the power generation from syngas with varying MSW ratios are presented in Figure 3.6 (a) to (e). Overall, MSW ratio significantly affected all engine emissions (CO, SO<sub>2</sub>, NO<sub>x</sub>, and HC) except CO<sub>2</sub>.



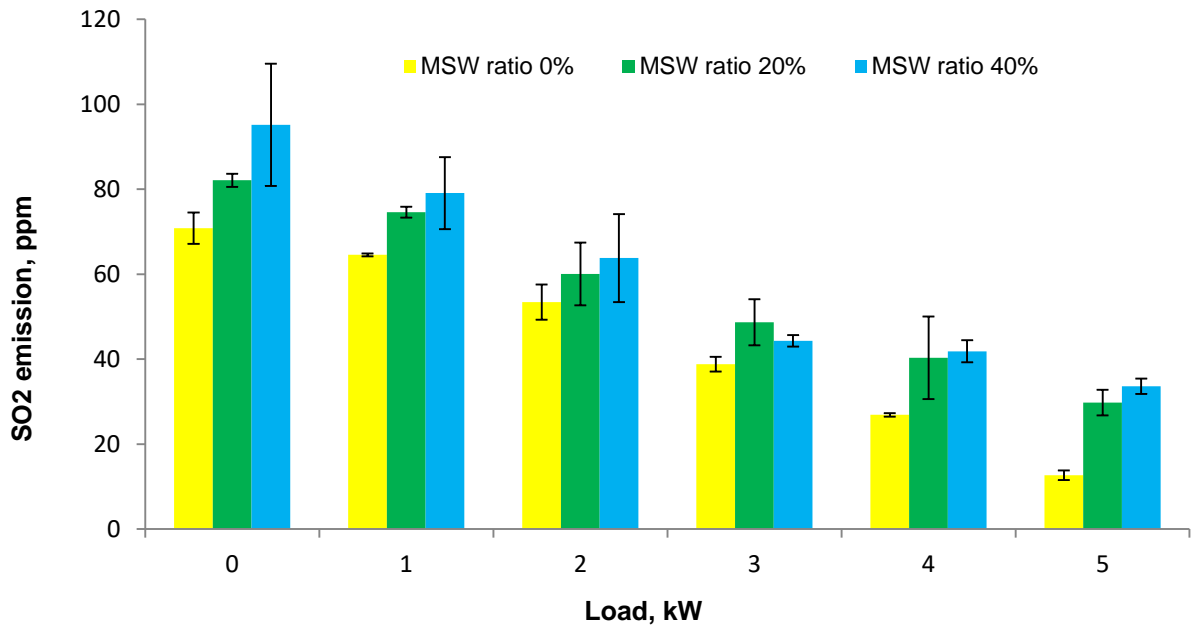
(a)



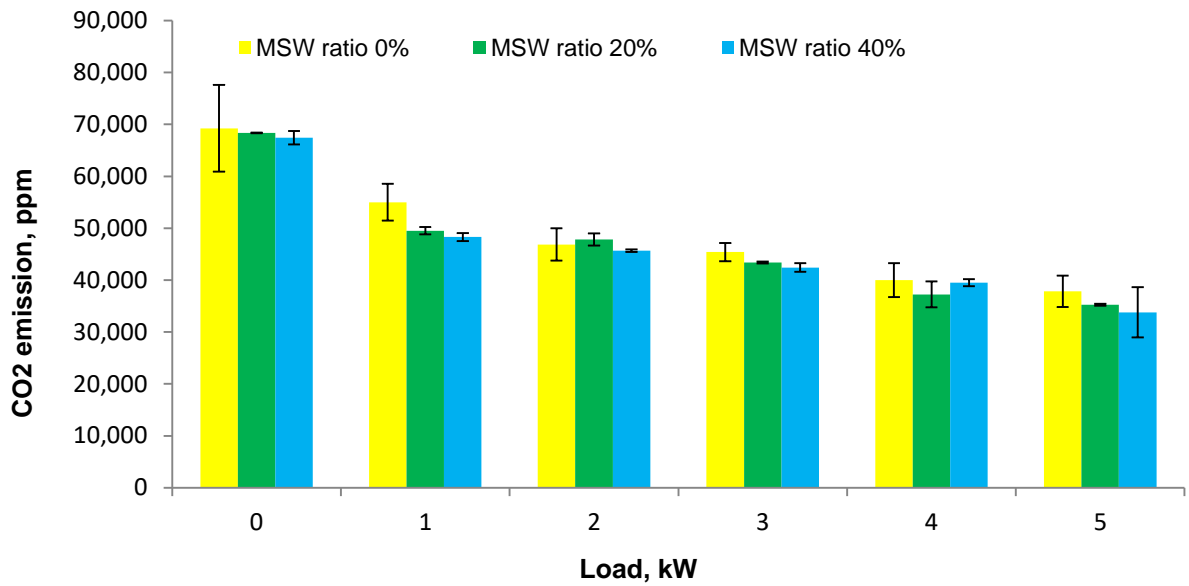
(b)



(c)



(d)



(e)

**Figure 3.6. Emission profile (variation with change in load applied) of (a) CO, (b) NO<sub>x</sub>, (c) HC, (d) SO<sub>2</sub>, and (e) CO<sub>2</sub> of engine running on syngas generated at various MSW ratio (0, 20, and 40 wt.%)**

#### 3.3.4.1. CO emission

CO is typically one of the main combustible compounds in the syngas [52, 95]. Gaseous fuel type (at different MSW ratio) and engine load had significant effects on CO emission. The CO emission decreased with an increasing load and also decreased with increase in MSW ratio (Figure 3.6a). The lowest CO emission (2,867 ppm) was generated when the engine ran on syngas generated at the highest MSW ratio of 40 wt.% at the maximum load (5 kW), while the highest CO emission (5,525 ppm) was generated when the engine ran on pure SG syngas (MSW ratio of 0%) and base load. Decrease in CO emission with increasing MSW ratio can be attributed to unburnt CO of the syngas generated because engine ran on rich-fuel environment; CO concentration of syngas decreased with increase in MSW ratio resulting in decrease of CO emission (Figure 3.2).

Similar decrease in CO emission with increase in load observed by Arroyo et al. [229], who attributed this observation to decrease in engine rpm. Compared to an earlier report [29], this study resulted in lower emissions of CO (indication of more complete combustion) probably due to a better mixing of syngas-air in the gas intake manifold.

**3.3.4.2. NO<sub>x</sub> emission**

NO<sub>x</sub> formation is a function of combustion pressure and flame temperature; and high oxygen concentration in fuel mixture increases NO<sub>x</sub> emission [85, 229]. NO<sub>x</sub> emission was significantly affected by the load variation and type of gaseous fuel (at different MSW ratio). The engine NO<sub>x</sub> emissions decreased with increasing loads (in agreement with literature [229]), and also decreased with increasing MSW ratio (Figure 3.6b). The lowest NO<sub>x</sub> emission was generated when the engine ran on MSW ratio of 40 wt.% (4.4 ppm) at the maximum load (5 kW), while the highest NO<sub>x</sub> emission (30.3 ppm) was generated when the engine operated on pure SG syngas (MSW ratio of 0 wt.%) at base load (0 kW). The maximum NO<sub>x</sub> generated (4.4 ppm) was still lower than the air emissions limit of Federal and California standards (25.9 ppm) [240]. At maximum load (5 kW), the engine running on pure SG syngas (MSW ratio of 0%) generated a higher combustion temperature, which was indicated by the higher exhaust gas temperature (EGT) of 234°C, as compared to exhaust temperature of 210°C at 40 wt.% MSW (Figure 3.7). A higher combustion temperature leads to an increase in combustion pressure that results in more NO<sub>x</sub> generation, following the Zeldovich mechanism as below [260]:



The first step is rate limiting and requires high temperature to proceed due to its high energy activation (314 kJ/mol). Since the syngas has low energy content (6.7-7.7 MJ/Nm<sup>3</sup>), its combustion always occurs at lower temperature and pressure as compared to natural gas (LHV ± 37 MJ/Nm<sup>3</sup>), restricting the generation of NO<sub>x</sub> emission. In addition, the engine operation occurred in rich gas environment that further limit the presence of oxygen.

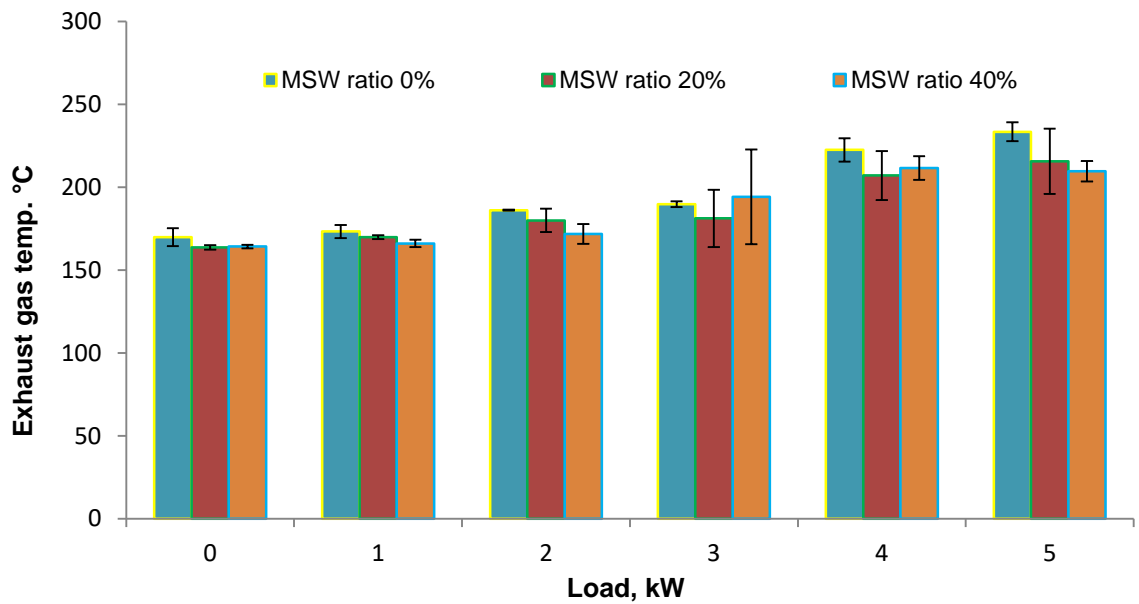


**Figure 3.7. Exhaust gas temperature (EGT) with variable load**

In comparison to natural gas operation, the engine NO<sub>x</sub> emissions using MSW syngas and pure SG syngas were lower (4.4-30.3 ppm) than those using natural gas (21.3-177 ppm) [29]. The result was also in agreement with a previous study (40-100 ppm) [90]. The low NO<sub>x</sub> emission might be caused by the low flame temperature of syngas [229] that results in low pressure and temperature in the engine combustion chamber, consequently reducing the engine speed and NO<sub>x</sub> formation [85, 229]. This result

emphasizes that using syngas in IC engines has an environmental benefit over natural gas.

#### **3.3.4.3. Hydrocarbon (HC) emission**

Part of the unburned syngas HC is released as HC emissions from the combustion chamber of the engine. Both load variation and type of gaseous fuel significantly affected engine HC emissions. Engine HC emissions increased with increasing load (Figure 3.6c) and increasing MSW ratio. With increase in load, combustion of syngas hydrocarbons is more incomplete contributing to the increase in HC emissions [29]. The increase in HC emission with increase in MSW ratio can be attributed to the increase syngas HC concentration (Figure 3.2), part of which remained unburnt. However, HC emissions from syngas (up to 90 ppm) were much lower than those from natural gas (up to 1,843 ppm), and in agreement with previous report of up to 262 ppm [29], 3.5-10 ppm [88], 0-20 ppm [91], and 20-50 ppm [90]. In addition, fraction of hydrocarbons in the syngas generated from co-gasification of MSW and biomass was higher (4.02 vol.%) than that in syngas generated from SG (1.48 vol.%). Thus, HC may have derived from hydrocarbon components of MSW (i.e. plastics, rubber).

#### **3.3.4.4. SO<sub>2</sub> emission**

Syngas sulfur compounds, in the form of hydrogen sulfide, carbonyl sulfide, mercaptans, dimethyl sulfide, and carbon disulfide [18], must be reduced to certain levels before its use for electricity generation. Gas turbines commonly limits these to 20 ppm [61], while fuel cells limit to 5-10 ppm [63, 68]. However, the IC engines is not limited by sulfur compounds for its operation but produce SO<sub>2</sub> emission due to the combustion of sulfur compounds. Typically, the characteristics of the fuel has more of an impact on the

engine SO<sub>2</sub> emission than the engine design [243]. Statistically, SO<sub>2</sub> emission was significantly affected by the load and the types of gaseous fuel (at various MSW ratio) in this study. The engine SO<sub>2</sub> emission decreased with increase in load, and increased with increase in MSW ratio (Figure 3.6d). A decrease in SO<sub>2</sub> emission at a higher load was perhaps due to the incomplete combustion at the higher load that resulted in converting most of the sulfur content of the syngas into H<sub>2</sub>S instead of SO<sub>2</sub> [261]. The increase in SO<sub>2</sub> emission with increase in MSW ratio can be attributed to the high sulfur content of MSW (0.14 wt.%) as compared to that of biomass SG (0.05 wt.%).

#### **3.3.4.5. CO<sub>2</sub> emission**

CO<sub>2</sub> emission was significantly affected by the load variation but not by the type of gaseous fuel. CO<sub>2</sub> emissions decreased consistently with increasing loads (Figure 3.6e). CO<sub>2</sub> emission depends on combustion of the syngas CO and hydrocarbons, as well as original CO<sub>2</sub> available in the syngas. The CO<sub>2</sub> emissions (up to 68,367 ppm) were in agreement with the earlier results (up to 75,000 ppm) of engine running on pure SG syngas [29], but lower than emission obtained from another study (up to 190,000 ppm) at an equivalent load (4.6 kW) [243]. A relatively low level of CO<sub>2</sub> emission obtained in this study might be due to a lower concentration of syngas CO<sub>2</sub> in this study ( $\pm 15$  vol.%).

### **3.4. Conclusions**

An off-grid small-scale power generation unit was demonstrated using a 60-kW downdraft gasification system integrated with an SI engine running on 100% syngas. The syngas was generated from co-gasification of municipal solid waste (MSW) and switchgrass (SG) with MSW ratios of 0, 20, and 40 wt.%. With limited air (ER of 0.20),

gasifier performance with combustion zone temperature (700-950°C) was stable and produced syngas with maximum LHV of 6.91, 7.74, and 6.78 MJ/Nm<sup>3</sup> at MSW ratio of 0, 20, and 40 wt.%, respectively. The major combustible components of syngas were H<sub>2</sub> (9-10 vol.%) and CO (13-15 vol.%).

With a modification of gas intake, an AFR of 0.7-1.0 was found to be effective to run the engine using syngas generated from co-gasification. The engine (rated at 10 kW) running on syngas reached the maximum load of 5 kW. The overall electrical efficiencies of the power generation system were 22, 20, and 19.5% at MSW ratios of 0, 20, and 40 wt.%, respectively. At the maximum load, the engine operated on syngas resulted in SFC of  $3.0 \pm 0.28$ ,  $3.1 \pm 0.15$ , and  $3.5 \pm 1.66$  kg/kWh, for MSW ratios of 0, 20, and 40 wt.%, respectively.

The engine CO, NO<sub>x</sub>, SO<sub>2</sub> and CO<sub>2</sub> emission decreased with increasing load, while HC emission increased with increasing load. CO, NO<sub>x</sub>, and CO<sub>2</sub> emissions decreased, while HC and SO<sub>2</sub> emissions increased with increasing MSW ratio. At MSW ratios of 0, 20, and 40 wt.%, the CO emissions decreased from 20,017, 16,533, and 16,175 ppm, respectively, at the initial load to 5,525, 4,833, and 2,867 ppm, respectively, at the maximum load, respectively. At the initial load, the engine NO<sub>x</sub> emission was 30.3, 27.3, and 27 ppm at MSW ratio of 0, 20, and 40 wt.%, respectively. At the maximum load, NO<sub>x</sub> emission was 7.2, 6.4, and 4.4 ppm at MSW ratio 0, 20, and 40 wt.%, respectively. HC emission, in contrast with the other major emissions, increased with increasing load; the highest HC emission (89.8 ppm) was generated at the maximum load at MSW 40 wt.%. The engine operated on MSW syngas produced much higher SO<sub>2</sub> emission than pure SG syngas at all load conditions. CO<sub>2</sub> emission at 0, 20, and 40 wt.% MSW ratio

decreased from 69,250, 68,367, and 67,417 ppm at the initial load to 37,850, 35,250, and 33,785 ppm, respectively at the maximum load. The stable operation, and comparable performance and low engine emissions of the co-gasification and power generation system demonstrates the potential for generating power in a sustainable basis from waste streams.

## CHAPTER 4

# ECONOMICS OF DISTRIBUTED POWER GENERATION VIA GASIFICATION OF BIOMASS AND MUNICIPAL SOLID WASTES

**Abstract:** More than 1.2 million people worldwide still lack access to electricity. Distributed power generation has potential to steadily increasing in satisfying the electricity demand and increase access to electricity. Gasification is one of the viable technologies that is suitable for distributed power generation having capability to produce electricity from various carbonaceous feedstocks including coal, biomass and municipal solid waste. This study aims to investigate the economic analysis of power generation through gasification of biomass and municipal solid waste (MSW) using a 60-kW downdraft gasifier with a feed rate of 100 kg/h (2.4 tons/day) and a capability to treat MSW streams at 40 wt.%, developed at Oklahoma State University. Effects of feedstock (biomass) cost (\$/ton), electricity selling price (\$/kWh), feed-in-tariff (\$/kWh), tipping fee (\$/ton), tax rate (%), and the output power (kW) are evaluated using major financial parameters including the net present value (NPV), internal rate of return (IRR), modified internal rate of return (MIRR), simple payback period and discounted payback period. A comparison with a similar gasification power generation technology suitable for distributed power generation is conducted to further investigate the economic performance of the downdraft gasifier.

Results show that the downdraft gasification power system offers a payback period of 7.7 years, generates an IRR, MIRR, and NPV of 10.9%, 7.7%, and \$84,550, respectively. Results from sensitivity analysis indicate that the feed in tariff, has the greatest positive impact on the project's NPV, followed by the electricity selling price, the output power and the tipping fee. In turn, the feedstock cost and the tax rate have a negative impact on the project's NPV. Thus, a 60-kW downdraft gasification system has an economic

potential that is competitive with larger scale downdraft gasification systems in supporting distributed power application.

**Keywords:** Biopower Generation; Gasification; Efficiency; Economics Analysis

#### **4.1. Introduction**

A recent report of the International Energy Agency (IEA) stated that there have been only four periods in the past 40 years that CO<sub>2</sub> emission levels remained flat compared to the previous year – the early 1980s, 1992, 2009, and 2015. Unlike the three previous periods that occurred in a global economic downturn, the last year mentioned came in a period of economic growth [262]. According to Bloomberg New Energy Finance, 2015 was a record year for world clean-energy investment, with renewable energy sources increasing by twice as much global capital as fossils fuels, reaching over \$350 billion [262, 263]. Renewable electricity costs also decreased significantly between 2008 and 2015; the cost of electricity fell 41%, 54%, 64%, 73%, and 94% for wind, rooftop solar photovoltaic (PV), utility scale PV, electric vehicles and LED bulbs – five clean energy technologies considered as having a promising future [264].

At the same time, access to electricity is becoming more critical in modern life and economic development. A recent report of the International Energy Agency (IEA) also presented that even though over 100 million people per year have gained access to electricity since 2012 compared with around 60 million per year from 2000 to 2012, by 2030, around 675 million people (8% of global population) – 90% of them in sub-Saharan Africa – will remain without access to electricity, as shown in Figure 4.1. About 2.3 billion continue to still use biomass, coal, and kerosene for cooking (from 2.8 billion today), remaining vulnerable to harmful indoor air pollution that potentially causes lethal poisoning to humans that is currently linked to 2.8 million premature deaths per year [1].

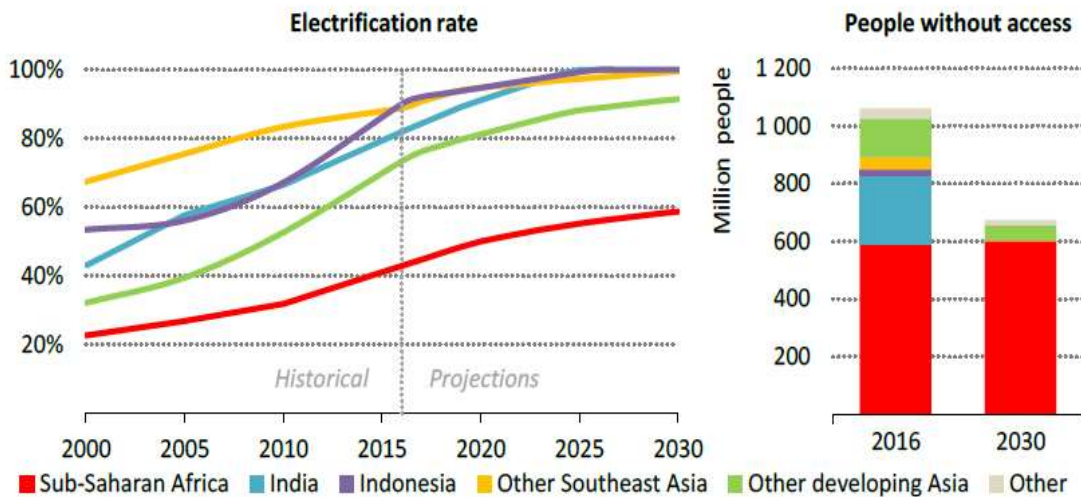


**Figure 4.1. People without access to electricity worldwide: nine of ten people are located in sub-Saharan Africa in 2030 [1]**

One of the clean technologies that can address the aforementioned issues while expanding access to electricity is power generation via gasification of locally available biomass and MSW. Syngas, the main product of gasification, consists mainly of carbon monoxide (CO) and hydrogen (H<sub>2</sub>), and small fractions of methane (CH<sub>4</sub>) and heavier hydrocarbons. Syngas is generated through multiple reactions at a temperature range of 500-1400°C [265]. Through the gasification reactions, the carbon fraction of carbonaceous materials can be converted into syngas with an efficiency of 80-95% [30, 40], while heavier components, including contaminants of the feedstock, can be collected as ash and slag. Thus, gasification is becoming popular as it can utilize any organic feedstocks, such as coal, biomass and municipal solid waste. The purified syngas generated from gasification can directly feed internal combustion engines (ICEs), gas turbines (GTs), or fuel cells (FCs) for supporting distributed power application. Using these power generation technologies, an electrical efficiency of 35-60% can be achieved with a service life of 20 years [24, 29,

266, 267]. A techno-economic comparison of various technologies to generate power from syngas is presented in the previous chapter (Chapter 1, Table 1.9). Among these technologies, integrated gasification combined cycle (IGCC) power plants using coal are the most common [22, 104]. In addition, deploying syngas in fuel cell and gas turbine hybrid power system will achieve the highest efficiency (up to 65%); however, compared to conventional steam and gas turbine plants, current challenges of fuel cells, such as performance degradation and short service life (less than 20 years), complex thermal management and control strategy, and high capital cost, must be addressed [130, 133, 268, 269].

In terms of capacity, power generation systems derived from gasification can be flexible and suitable for distributed power application as the size of the gasifier can range from kW-scale to MW-scale. Current total electric capacity of distributed and dispersed (independently operating) generation (with generator's size < 1 MW) in the U.S. reached 5,407 MW in 2015 and is predicted to still increase in coming years [13], while the global net electricity generation is also projected to increase from 23.4 trillion kilowatt hours (kWh) in 2015 to 34.0 trillion kWh in 2040 [14, 15]. Power generation from biomass (known as biopower generation) emits CO<sub>2</sub> and SO<sub>2</sub> equivalents of 67 and 18 times lower, respectively [147], than that from fuel oil. Due to avoided methane emission, biopower generation can generate negative greenhouse gas emissions (GHGs) in the range of 600-650 g CO<sub>2</sub>-eq/kWh when waste materials are used [270].

Studies on evaluating the economic performance of biopower generation using sensitivity analysis have been reported [271, 272]. Moriarty [271] used sensitivity analysis to investigate biopower generation having capacities of 10 and 20 MW. At a feedstock cost

of \$34/ton, a discount rate of 6-8%, and a projected life of 30 years, the author found positive net present values (NPVs) at breakeven electricity rates of \$141.60 and \$123.12/MWh for the 10 and 20 MW plants, respectively. However, other key financial parameters, such as the internal rate of return (IRR), were not included in the analysis. Nderitu et al. [272] analyzed the feasibility of large scale biopower generation (>50 MW) throughout states in the U.S. using sensitivity analysis at a feedstock price of \$40/ton, a discount rate of 10%, and a life of 20 years. When state-level renewable portfolio standards and incentives (i.e. feed-in tariffs, tax credit, and new federal subsidies) were not applied and selling electricity into the market place was the only source of revenue for the biopower plant, the authors found that the electricity sales need to be (at least) 25% higher than the base case to make the project economically feasible. However, the NPV and PP were not presented. The aforementioned studies were also based on the combustion technology; thus, results obtained from these studies could vary significantly with the gasification technology. In a more recent study, Buchholz et al. [171] reported an economic analysis of a 250 kW downdraft gasifier to replace one of the diesel generators (200 kW in capacity) that supported a tea estate processing utility (as previously discussed in 1.5.1.2). The gasifier used fuelwood (cut 10 x 10 x 10 cm) with a feed rate of 320-400 kg/h. Equipped with ash removal system, a syngas cleaning system, and a 250 kW syngas engine, the gasification system successfully replaced the use of a 200-kW diesel fuel generator. When the internal load was supplied by the gasifier, the gasification power system offered an internal rate of return (IRR) and payback period of 11 percent and 8 years, with the diesel fuel savings of 149,000 liters/year. The electricity production and avoided diesel costs were correspondingly achieved at \$0.18/kWh and \$93,631/year. However, the project NPV and

sensitivity analysis on factors impacting the economic performance of the gasification power system were not presented.

As the economic analysis of syngas generated from gasification of biomass and MSW for distributed power application is still limited in the literature, this paper specifically presents an economic analysis of a 60-kW downdraft gasification power system developed at Oklahoma State University. Financial parameters, including the NPV, IRR, modified internal rate of return (MIRR), simple payback period (PP), and discounted payback period (DPP), with the analyzed period of 20 years, are selected to investigate the economic viability of the project. The sensitivity analysis uses spider diagrams to further investigate the main economic parameters, namely the feedstock cost, electricity selling price, output power, tax rate, tipping fee, and feed-in-tariff (FIT). In the U.S., FIT policies provide a guarantee of payment for power plants using renewable energy sources for typically 15-20 years [273]. Aiming at further evaluating the economic performance, the results are then compared with a similar type of gasifier with a 250-kW size reported by Buchholz et al. [171].

#### **4.2. Economic assets of gasification technologies**

Gasification technologies have recently shown an increasing trend in the global energy economy. Syngas generated from gasifiers is typically used to produce valuable chemical commodities such as methanol (through a catalytic conversion), ammonia (through a “shift reaction” leading to H<sub>2</sub> followed by a Haber process) and synthetic hydrocarbons (through Fischer-Tropsch process) [25]. In 2016, these alternative products

represented huge markets worldwide: 180 million metric tons (MMT) for ammonia, 85 MMT for methanol, and 40 MMT for hydrogen [26].

A major asset of gasification is that syngas can be produced from numerous types of organic feedstock, including coal, biomass, agricultural residues and municipal solid waste (MSW) [5]. With the prospect of increasing natural gas prices, syngas has the potential to take a positive role in future energy economy. As an illustration, in China, and in Indonesia and other Southeast Asian countries, the current prices of natural gas for the industrial market have recently reached \$10-15/MMBtu, with predictions to steadily increase in the coming years [5]. This surge in prices is due to the increased demand for liquefied natural gas (LNG). The LNG chain demands high capital expenditures (CAPEX) and operating expenses (OPEX), especially for the steps of liquefaction and cryogenic overseas transportation, from the producing countries to the receiving/regasification terminals, resulting in high “landed prices” [5]. In comparison, syngas production cost from wood biomass can be in the range of \$0.042/kWh (~\$12.3/MMBtu), while \$0.02/kWh (~\$5.9/MMBtu) from municipal solid waste [153, 155]. In addition, based on the experience with the old town gas – syngas produced from gasification of coal for home lighting – of the 20<sup>th</sup> century, syngas can be stored, transferred, and injected into any existing network of natural gas, using conventional gas handling technologies [274].

### **4.3. Methodology**

The performance of power generation systems developed at Oklahoma State University (OSU) has been reported previously [29, 60]. The major equipment consists of a reactor (a downdraft gasifier), a belt conveyor, a cyclone separator, an ash collecting

system equipped with a screw conveyor, a water-acetone gas cleaning system, and an internal combustion engine (ICE), as shown in the previous chapter (Chapter 3, Figure 3.2).

The economic evaluation uses sensitivity analysis, which investigates the main effects, considered the main economic parameters, including the feedstock (biomass) cost (\$/ton), electricity selling price (\$/kWh), feed-in-tariff (FIT) (\$/kWh), output power (kW), tax rate (%), tipping fee (\$/ton), and the labor cost (\$/ton). The net present value (NPV) and internal rate of return (IRR), two of the most widely used investment analysis and capital budgeting decision tools [275, 276], are used to determine the feasibility of the project, as expressed below.

$$NPV = \sum_{t=0}^n \frac{CF_t}{(1+k)^t} \dots\dots\dots [4.1]$$

$$NPV = \sum_{t=0}^n \frac{CF_t}{(1+IRR)^t} = 0 \dots\dots\dots [4.2]$$

where CF is cash flow; k is the discount rate; t is the corresponding year; n is the total year of the analysis. In addition to NPV and IRR, the payback period (PP), the discounted payback period (DPP), and the modified internal rate of return (MIRR) are calculated to further observe the project's economic performance. The PP, defined as the length of time it takes for the original cost of an investment to be recovered from its expected cash flows, is used to provide an estimation of the length of time required for an investment to recover its initial outlay in terms of profits or savings, while DPP, the next level of PP where the cash flows are discounted before calculating the period of payback, is used to

present more accurate results as it includes the time value of money [275, 276]. MIRR, defined as the discount rate at which the present value of a project's cost is equal to the present value of its terminal value, where the terminal value is found as the sum of the future values of the cash inflows compounded at the required rate of return, is included to reinforce the analysis as it correctly assumes reinvestment at the project's cost of capital and avoids the problem of multiple IRRs. The PP, DPP, and MIRR can be expressed as the following [276]:

$$PP = A + \left(\frac{B}{CF_t}\right) \dots\dots\dots [4.3]$$

$$DPP = \ln\left(\frac{1}{1 - \frac{CF_0 \times k}{CF_t}}\right) : \ln(1 + k) \dots\dots\dots [4.4]$$

$$PV \text{ of cash outflows} = \frac{TV}{(1 + MIRR)^n} \dots\dots\dots [4.5]$$

where *A* is the number of years before full recovery of initial investment; *B* is the amount of initial investment that is unrecovered at the start of the recovery year; *CF<sub>0</sub>* is the initial investment; *TV* is the terminal investment.

#### 4.3.1. Gasifier characteristics

A 60-kW downdraft gasifier is used in the current study since it has several advantages over other types of gasifiers. The gasifier can generate syngas that has low tars (< 3 mg/Nm<sup>3</sup>) and high calorific value (4-6 MJ/Nm<sup>3</sup>), thus providing a high cold gas efficiency (CGE) (85-90%) [37]. Moreover, the gasifier is easy to set-up and control during operation and capable of treating various feedstocks (including MSW) with stable performance [60]. Due to the unique design of the reactor, the gasifier is generally only suitable for a small to medium power scale (up to 10 tpd ~ 1 MW) [37], as shown in

Figure 4.2; a simplified process diagram describing the process of downdraft gasification for power generation is illustrated in Figure 4.3.

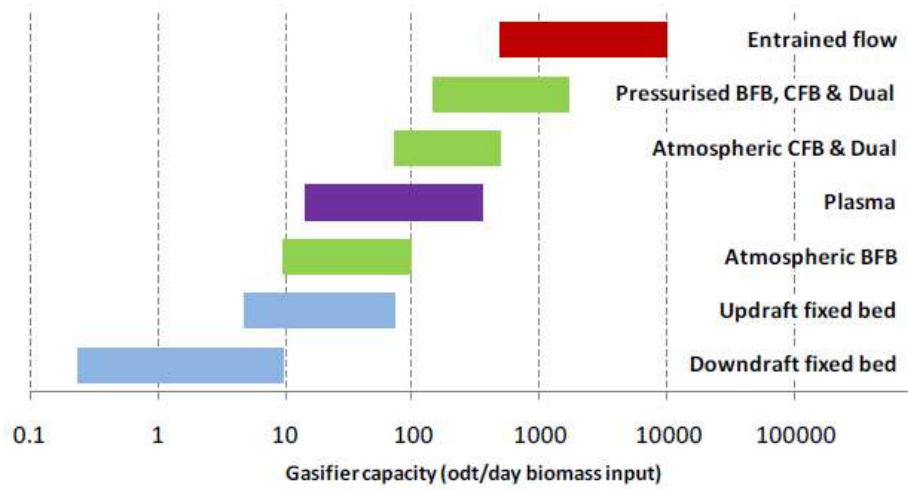


**Figure 4.2. Gasifier technology versus capacity range [51]**

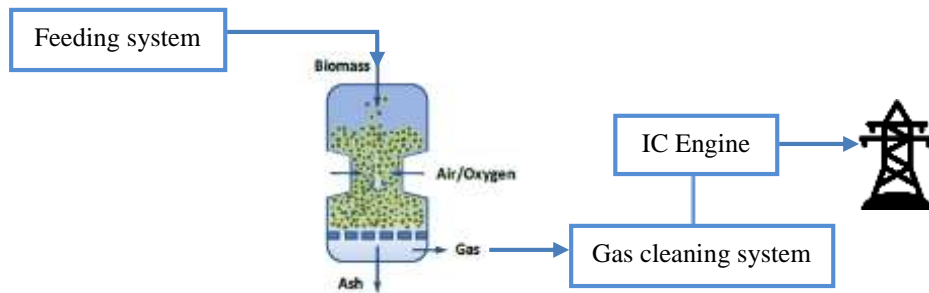


**Figure 4.3. A schematic diagram of power generation derived from downdraft gasifier [51]**

#### 4.3.2. Basic key economic inputs

Basic key economic inputs are the main parameters that directly influence the economic performance of a project. Some inputs can either refer to the practical situation

or the assumptions based on literature. In this study, the key economic inputs include the total capital costs, the total operating and maintenance (O&M) costs, the biomass feedstock cost and the tipping fee, the weighted average cost of capital (WACC), the plant availability, the plant lifetime, the salvage value, the depreciation rate, the electricity price, the FIT, the marginal tax rate, and the contingencies.

**Table 4.1. The equipment and materials of the downdraft gasifier**

Equipment	Cost	Remarks
Reactor, cyclone separator, and control system	\$60,000	
Belt conveyor	\$10,000	Bunting Magnetic Co.
Ash removal system (ash drum, screw conveyor, electric motor)	\$10,000	
Air compressor	\$10,000	Sullair air compressor
Gas scrubbing system (double gas scrubber, pump)	\$4,500	Water-acetone based, mixable with renewable filters [62]
Power generation unit (natural gas ICE)	\$18,000	Briggs and Stratton [272]
Total	\$112,500	

The total capital costs including basic equipment and materials for the 60-kW downdraft gasifier are \$112,500, consisting of the reactor, belt conveyor, ash removal system, syngas cleaning system, and power generation unit, as a detailed breakdown shown in Table 4.1. The total O&M costs (including fixed and variable costs) consist of labor, supporting equipment (i.e. pumps, compressors, and electric motors – commonly known as balance of plant (BOP)) and utilities, and chemicals (as shown in Table 4.2) with major operating costs shown in Figure 4.4. With the total output power of 60 kW (~43,800 kWh/month), the total O&M costs are consequently \$0.196/kWh.

**Table 4.2. The operation and maintenance costs of the 60–kW downdraft gasifier**

Description	Amount, \$/month <sup>1)</sup>	Remarks	Refs.
<b>Operational costs</b>			
<i>Fixed</i>			
Labor	4,640.0	1 operator/shift, with a total of 4 shift. @\$7.25/person/hour	[277]
<i>Variable</i>			
Electricity for BOP			
Air Compressor, 28.4 kW	393.1	4146.4 kWh/month (in average), operating at 20% capacity.	(Sullair, Model 2209AC, Sullair LLC., Michigan City, IN)
Electric heaters, 5 pcs @360W	120.9	1314 kWh/month (average energy consumption)	
Chiller, 1.5 hp	75.1	(815.8 kWh/month (average energy consumption)	(Schreiber, Model 300 AC, Engineering Corporation, Cerritos, CA)
Water pump, 0.5 hp	25.0	543.9 kWh/month (average energy consumption)	
Belt conveyor, 1 hp	50.0	543.9 kWh/month (average energy consumption)	(Bunting Magnetics Co., Newton, KS)
Air log motor, 1 hp	50.0	543.9 kWh/month (average energy consumption)	(Grainger, Roanoke, TX)
Ash scrapper, 1 hp	50.0	543.9 kWh/month (average energy consumption)	(Grainger, Roanoke, TX)
Ash conveyor, 1 hp	50.0	543.9 kWh/month (average energy consumption)	(Dayton, Model 2MXT4A, Dayton Electric Mfg. Co., Lake Forest, IL)
Syngas cleaning system (i.e. acetone)	2,142.0	5 gal/day is used, with a retail price of \$14.28/gal	Water-acetone based, mixable with renewable filters [62]
Disposal cost of liquid waste (i.e. acetone)	225.3	5 gal/day is used, with a disposal cost of	Hazardous Materials

Description	Amount, \$/month <sup>1)</sup>	Remarks	Refs.
		\$0.23/lb and density 784 kg/m <sup>3</sup>	Management Facility, Boulder County [278]
Propane gas	16.2	4.7 gal cylinder with a retail price of \$3.44/gal	
<b>Maintenance costs</b>			
<i>Fixed</i>			
Tools	25.0		
Sealant and insulations	20.0		
Air lock fins, 8pcs	200.0		
Spare electric motor	17.0		
<i>Variable</i>			
Charcoal	480.0	2 packages/day with a retail price of \$8/package	
<b>Total O&amp;M costs, \$/month</b>	<b>8579.8</b>		

Note: <sup>1)</sup> Calculated using electricity rate of \$9.48/kWh

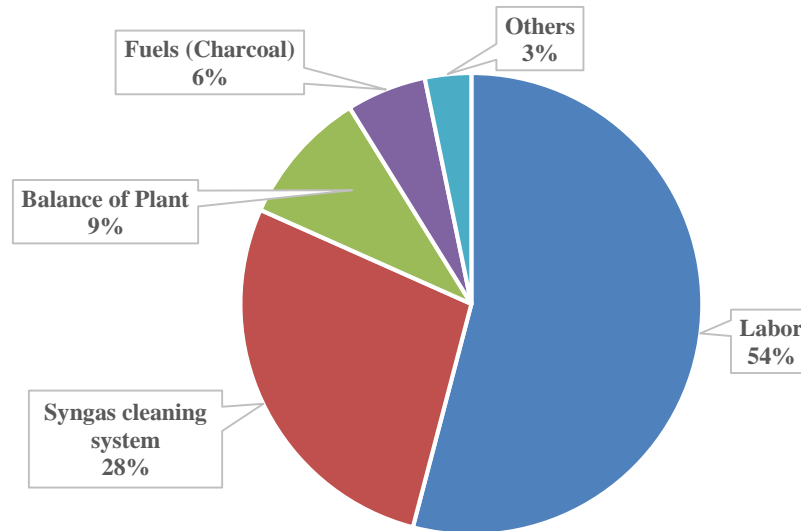


**Figure 4.4. Major operating costs of the downdraft gasification power system at OSU**

Labor cost, representing 54% of total operating cost, is critical because it directly affects the total O&M cost of the power generation system, as shown in Figure 4.4. A

labor cost of \$7.45/h is considered as current minimum wage in the state of Oklahoma in 2018 [277]. Syngas cleaning system, the second largest contributor of total operating cost, still uses water-acetone solution as a commercially proven method to remove syngas tar and other contaminant. An additional cost to dispose the solution is required to maintain the removal efficiency; here it is assumed to be \$0.23/lb., following a typical disposal rate of hazardous waste in a neighboring area [278].

Biomass feedstock is one of the major factors that greatly impacts the economics of power generation. Biomass feedstock cost, including production, harvesting, and delivery, is assumed to be \$20/ton as it comes from local agricultural sources, which are close to the plant thus delivery cost can be neglected. In the U.S, the current cost generally ranges from \$40 to \$80/ton [279], which is contributed by harvesting, storing, and transporting; with preprocessing, the cost will increase to be about \$83-150/ton [280]. In the state of Oklahoma, a higher economic value can be achieved by using non-edible feedstocks such as switchgrass and eastern red cedar because these feedstocks are wildly present and some of these are parasitic plants [56]. Moreover, the downdraft gasifier has a feeding rate of 2.5 tpd and successfully ran in processing MSW at 40% wt.% with biomass (e.g. switchgrass) without operational issues [60]. This becomes a prominent advantage for the project in gaining a greater economic return because of potential tipping fees of MSW disposal. A tipping fee of \$55.11/ton was used as referred to in 2017-data [178]. In addition, the downdraft gasification system uses air as the gasification medium because it offers a simple operation, low operational cost [182], and generates a high btu syngas, 4-7 MJ/Nm<sup>3</sup> [29, 37].

Total direct costs typically include the capital cost, general contractor and subcontractor, materials, and labor [149]. Based on the construction activities during 2015-2016, the general contractor and subcontractor costs of downdraft gasifiers were considered to be nearly 30% of the total capital cost; a range of 45-53% was commonly used in commercial projects [149].

The weighted average cost of capital (WACC) is a reliable tool that a company uses to evaluate the economic value of a project, as it includes all capital sources, including common stock, preferred stock, bonds, and any other long term debt [281]. In this study, a WACC of 5.9% is adopted from the Bloomberg database as an average value of WACCs taken from four public companies which develop a small to medium scale biofuel production – Aventine Renewable Energy (6.1%), GEVO (4.4%), Renewable Energy Group (6.5%), and Verenium (6.4%) [282].

**Table 4.3. The depreciation with the 50% first-year bonus depreciation**

<b>DEPRECIATION DETAILS</b>					
MACRS table:	Normal Table	Normal Table x 50%	Year 1 additional 50%	Total (modified table)	Tax Depreciation
1	14.29%	7.15%	50.00%	57.15%	-82,860
2	24.49%	12.25%		12.25%	-17,755
3	17.49%	8.75%		8.75%	-12,680
4	12.49%	6.25%		6.25%	-9,055
5	8.93%	4.47%		4.47%	-6,474
6	8.92%	4.46%		4.46%	-6,467
7	8.93%	4.47%		4.47%	-6,474
8	4.46%	2.23%		2.23%	-3,234

The availability of power generation is targeted to reach 90% due to disturbances during operation, even though the availability of the biomass gasification power plant

could reach 99% in practical operation [35]. The life of the facilities and the salvage value is assumed 20 years and 15%, respectively.

Since biopower uses combined heat and power from renewable energy sources, and to account for the cost of wearing down the equipment over a 20-year period, a 50% first-year bonus depreciation provided by the federal Modified Accelerated Cost-Recovery System (MACRS) is used to increase the economics of the project [283, 284], as shown in detail in Table 4.3.

**Table 4.4. Basic key economic inputs**

<b>No.</b>	<b>Parameters</b>	<b>Downdraft</b>
A	Feed rate / Capacity, tpd	2.4
B	Total output power, kW	60
C	Availability, %	90
D	Feedstock cost, \$/ton	20 / -10 <sup>b</sup>
E	Total capital cost <sup>a</sup>	\$112,500
F	General contractor and labor	\$30,000
G	Sub-contractor material & labor	\$2,500
H	Total direct cost	\$145,000
I	Indirect cost, %	25
J	Total Indirect cost	\$36,250
K	Total direct and indirect cost	\$181,250
L	Contingency, %	15
M	Contingency	\$27,188
N	Start-up and training, %	2
O	Start-up and training	\$2,900
P	Total project investment	\$211,338
Q	WACC, %	5.9
R	Total O&M costs, \$/kWh	0.196
S	Lifetime, years	20
T	Salvage value, %	15
U	Depreciation rate, %	See Table 4.4
V	Electricity price, \$/kWh	0.0948
W	FIT, \$/kWh	0.15
X	Marginal tax rate, %	30

Note: <sup>a</sup> Capital cost includes equipment and materials, <sup>b</sup> The downdraft gasifier was designed to treat MSW 40 wt.% (maximum ratio) [60], with the feedstock costs of biomass and MSW, \$20/ton and -\$55.11/ton, respectively

A local electricity price of \$0.0948 cent/kWh is used as referred to current local electricity price (all sectors) in the state of Oklahoma in 2017 [285], while a FIT of \$0.15/kWh is used referring to the normal scheme of financial support for biogas and biomass based power generation [286]. A marginal tax rate of 30% is used and the contingencies, which include contractor overhead costs, fees, profit, and construction, are assumed 15% as referred to earlier [149].

However, it should be noted since assumptions used in the study refer to local economics and technological advances, the economic results presented in the next sections may vary from one region to another. The basic key economic inputs and assumptions used in the present study are summarized in Table 4.4.

#### **4.4. Results and discussion**

The economic evaluation of power generation via gasification of biomass and MSW using the downdraft gasification system is analyzed using sensitivity analysis. The main factors considered affecting the project economics, including the feedstock cost (\$/ton), electricity selling price (\$/kWh), FIT (\$/kWh), tipping fee (\$/ton), tax rate (%), and the output power (kW), are evaluated in detail. The results are then compared to a 250-kW downdraft gasification power generation system as reported by Buchholz [171]. The main findings are presented in detail in the following sections.

#### **4.4.1. Downdraft gasification power system**

The downdraft gasification system has the capability to treat biomass and MSW (at maximum 40 wt.%) for electricity production, as reported in detail earlier [60]. The technology provides a positive NPV of \$84,550 and a PP and DPP of 7.7 and 11.0 years, and generates an IRR and MIRR of 10.9% and 7.7%, respectively. These results show that the downdraft gasification power system is economically viable as it results in a positive NPV and the IRR generated is higher than the considered WACC (5.9%).

Figure 4.5 shows the sensitivity analysis of the downdraft gasification power system, using the feedstock (biomass) cost, electricity selling price, FIT, tipping fee, tax rate, and the output power. Among these parameters, the FIT shows the greatest impact, followed by the electricity selling price, the output power, and the tipping fee. In contrast, the labor cost substantially affects the project's NPV. An increase labor cost by 15% will decrease the project's NPV by nearly 72% (\$60,845). In addition, the feedstock (biomass) cost and the tax rate also demonstrate a negative impact to the project's NPV in a similar magnitude. The presence of the MSW negates the sensitivity of biomass feedstock. If the feedstock only depends on biomass, a slight change of the feedstock cost at local market will greatly impact the project viability, which will eventually prolong the payback period, thanks to gasifier capability of treating the MSW feedstock. The tax rate also negatively impacts on the project's NPV at similar magnitude with the biomass feedstock cost.

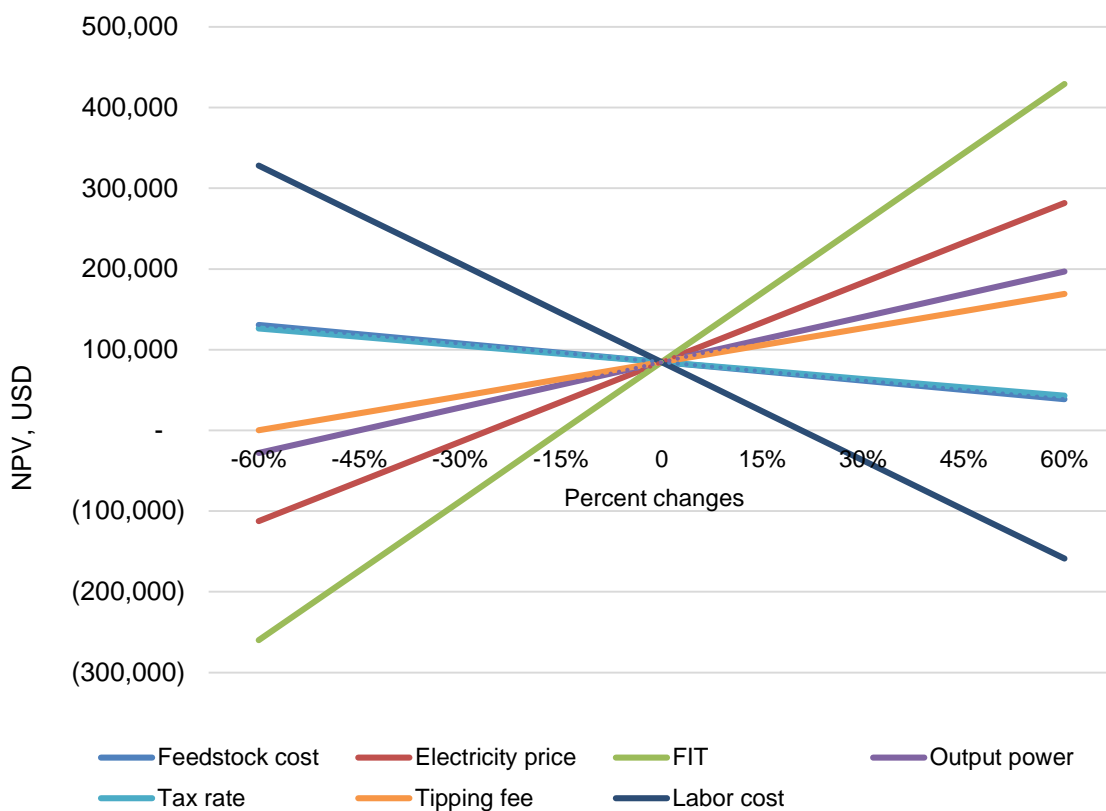


**Figure 4.5. The major factors impacting on the project's NPV of the downdraft gasification power system with MSW 40 wt.%**

As can be seen, the presence of FIT greatly increases the project's viability. An increase or a decrease of the FIT by 30% will consequently raise or drop the project's NPV by 204% (\$172,307). Therefore, FIT policies can benefit ratepayers, renewable energy (RE) developers, and society at large. However, some drawbacks have been reported regarding the FITs, such as they do not directly address the high initial cost of RE development [286]. The FIT payments can essentially be constructed by three mechanisms: based on the actual price of levelized cost of electricity generation, based on

the utility avoided cost, and based on a fixed price incentive; thus, its magnitude may vary from one region to another [286].

The electricity selling price also greatly affects the project's economics. An increase or a decrease of the electricity price by 30% will raise or shrink the project's NPV by 117% (\$98,589). Similar to FITs, the electricity price varies from one region to another, depending on local electricity supply and demand. As an illustration, from January 2011 to April 2018, an average retail price of electricity across states in the U.S. varied from \$0.0948/kWh to \$0.1103/kWh [285].

The output power also has a significant impact on the project's NPV. A fluctuation of \$56,187 (~66.5%) on the NPV was observed when the output power changes by 30%. A greater output power can only be achieved when the feeding rate and the reactor capacity are modified. However, it will also increase the capacity of the syngas cleaning system, as the second largest cost component after the capital cost and the labors (Table 4.3). An augmentation of the output power can only be reached by a hybrid power generating system, such as a solid oxide fuel cell and gas turbine (SOFC/GT) hybrid power system because a higher content of hydrogen can be generated by cracking syngas tars using syngas reforming or high-temperature gasification technology.

In addition, the tipping fees positively contribute to an increased project's NPV. An increasing of the tipping fee at 30% directly improves the project's NPV by nearly \$42,204 (~50%). In the near future, this prospect will be easier to achieve; an increase of tipping fees from \$51.82/ton in 2017 to \$55.11/ton in 2018 at a national level was recently observed [178].

Among major evaluated parameters, output power is the only one related to the system performance. An operational disturbance could lower the power production into some extents. In the current study, a reduced output power by 15% (51 kW) and 30% (42 kW) is considered. As shown in Figure 4.6, an increase of output power from 42 kW to 60 kW directly reduces the PP from 9.8 years to 7.7 years, with an increase of IRR from 7.7% to 10.9%. The project's NPV also increases from \$28,363 to \$84,550. In turn, when the output power can only be generated at 51 kW, compared to maximum rating of generation, the project's PP will consequently increase from 7.7 years to be 8.7 years, while the IRR will decrease from 10.9% to be 9.3%.

The changes of output power are a direct function of the operational performance of the power generation system, including potential operational disturbances (i.e. reactor leak, electric motor failures, etc.) that can restrict the output power to achieve its maximum rating. Thus, for a further illustration, Table 4.5 presents three scenarios that can occur in the power generation system in term of operational availability; operational challenges and disturbances may cause the plant can only operate at availability of 60% (where the project still generates a marginal positive NPV with  $IRR=WACC$ , considered worse scenario) and 75% (where the project generates a positive NPV with  $IRR > WACC$  (5.9%), considered medium scenario) from its operational targeted availability of 90% (best scenario) throughout the year. The availability of the plant for distributed power plant is not as critical as the one connected to the grid as the power plant only affects the local electricity network.

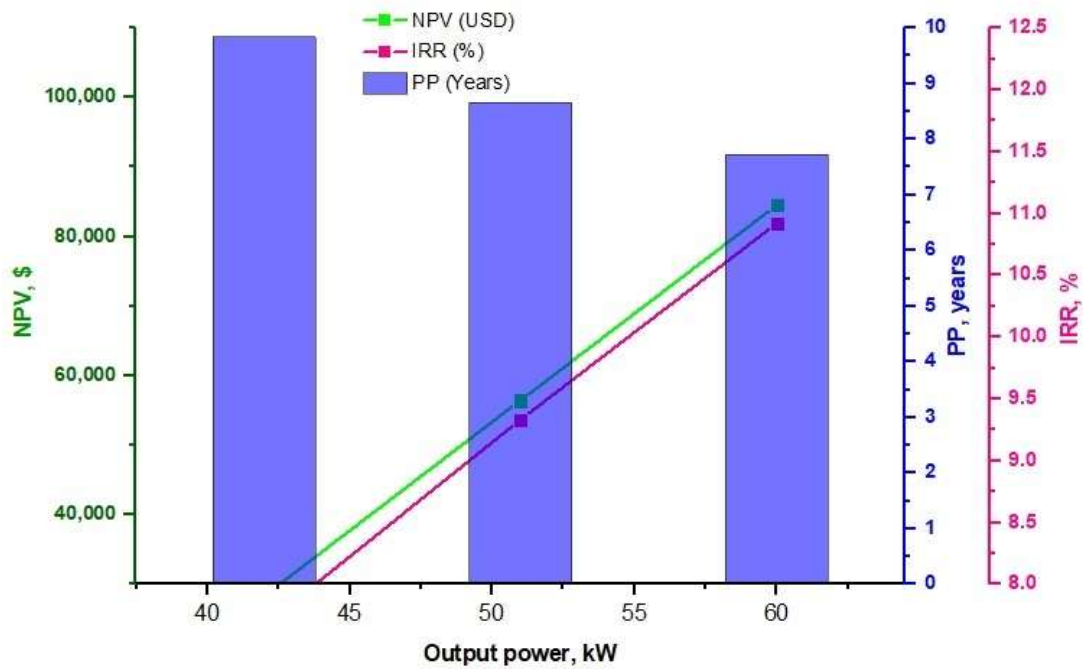


**Figure 4.6. The impact of output power on the NPV, IRR, and PP of the downdraft gasification power plant**

**Table 4.5. The worse, baseline and best scenario that can occur during operation**

Parameter	Worse Scenario	Medium Scenario	Best Scenario
Plant availability, %	60	75	90
PP, years	11.4	9.2	7.7
DPP, years	18.1	13.8	11.0
NPV, \$	753.9	42,652	84,550
IRR, %	6.0	8.5	10.9
MIRR, %	5.9	6.9	7.7

#### 4.4.2. Comparison to other downdraft gasification power plant

The economics of power generation using the 60-kW downdraft gasification technology developed at OSU are compared with a 250-kW downdraft gasification technology as reported by Buchholz [171]. The gasification power plant was constructed

to support the Muzizi Tea Estate processing utility in Uganda. A detailed description of the plant can be found in Chapter 1 (sub-section 1.5.1.2).

**Table 4.6. The comparison of economics performance between two gasification power plants**

No.	Parameters	OSU	Muzizi Plant
A	Capacity, kW	60	250
B	Feedstock	MSW 40 wt.% and Switchgrass	Woodchips
C	Capital costs, \$	112,500	442,198
D	PP, years	7.7	8.0
E	DPP, years	11.0	n.a
F	IRR, %	10.9	11.0
G	MIRR, %	7.7	n.a
H	NPV, \$	84,550	n.a
I	Labor costs, \$/year	55,680 (four persons)	17,497 (six persons)
J	Electricity production costs, \$/kWh	0.18	0.18

Table 4.6 presents the comparison of the major economic parameters between the two gasification technologies that can be used for distributed power application. As shown, the downdraft gasification power generation developed at OSU has a smaller scale compared to the Muzizi plant, it performed better economically, with a shorter PP, a comparable IRR, and a lower production costs. Moreover, the calculation made is based on the local condition that one of the major cost components impacting the total O&M is the labor (as shown in Figure 4.4). When the technology is applied in other regions having a lower labor rate, the economic viability of the system will consequently be higher. It should be noted that the calculations above have already included the costs

associated with the feedstock handling. Therefore, compared to OSU's gasification system, the gasification power plant in the Muzizi even using a higher number of workers, still performed a lower rate of total labor.

Aside from labor costs, the syngas cleaning system can be improved using a more advanced technology that is free-chemical (i.e. acetone) use with a low energy consumption, such as advanced hot filtration system. In practical application, replacing acetone during operation is a big challenge, especially for an application in the rural regions. Thus, a replacement of the current syngas cleaning system with other possible technologies can potentially reduce the O&M cost as well as increase the operational ease.

#### **4.5. Conclusions**

The economic evaluation of power generation via gasification of biomass and MSW was performed using sensitivity analysis. The economics of a downdraft gasification power system with a feed rate of 2.5 tpd and an output power of 60 kW was analyzed for supporting distributed power application.

The results show that among seven major economic parameters being evaluated (i.e. the feedstock (biomass) cost, electricity selling price, feed-in-tariff (FIT), output power, tax rate, tipping fee, and the labor cost), the FIT results in the greatest impact on the project's NPV, followed by the electricity selling price, the output power and the tipping fee, while the labor and feedstock cost and the tax rate generate a negative impact for the power generation.

The downdraft gasification power system offers a payback period of 7.7 years, while an IRR, MIRR, and NPV of 10.9%, 7.7%, and \$84,550 are achieved. In comparison with a 250-kW downdraft gasification power plant, the downdraft gasifier developed at OSU performed a shorter payback period and a higher IRR. However, the economic results may vary significantly depending on the assumptions made regarding local economics and technological advances. The results show that a 60-kW downdraft gasification system has an economic potential that is competitive with a larger scale downdraft gasification system in supporting distributed power application.

## CHAPTER 5

# MODELLING LOW-TEMPERATURE PLASMA GASIFICATION OF MUNICIPAL SOLID WASTE

**Abstract:** Biopower generation represents nearly 9.5% of global electricity production from renewable energy sources. Plasma gasification has been gaining attention as an environmentally-friendly solution for electricity generation from biomass and wastes. However, the intensive energy and temperature required for this system has become a bottleneck for its commercial application. In this study, a model of low-temperature plasma gasification is investigated to convert municipal solid waste (MSW) into syngas. The low-temperature plasma model was employed at a temperature of 1,500, 2,000, and 2,500°C to assess effects on syngas composition and system performance with air as plasma gas at atmospheric condition. At plasma temperatures of 1,500, 2,000, and 2,500°C, the model generated syngas lower heating values (LHVs) of 5.41, 6.02, and 6.45 MJ/Nm<sup>3</sup>, respectively, with energy inputs of 2,358, 2,775, and 3,245 kW, respectively, and plasma gasification efficiencies of 49.6, 49.2, and 48.9%, respectively. In comparison to conventional non-plasma air gasification of MSW, the syngas generated from low-temperature plasma gasification demonstrated considerably higher concentrations of hydrogen and carbon monoxide, resulting in a higher energy density of the syngas.

**Keywords:** Syngas; Gasification; Low-Temperature Plasma; Efficiency; MSW

## 5.1. Introduction

Biopower generation reached 570 trillion Watt-hours (TWh) and represented nearly 9.5% of global electricity production from renewable energy sources in 2016 [1]. This growth trend is predicted to continue in the near future due to high demand of electricity and heat in developing countries such as China and India. Studies on biopower generation at small and large scales have been reported earlier [144]. Gasification, in particular, is a strong candidate for biopower generation because it can use diverse types of feedstocks, including coal, biomass and municipal solid waste (MSW). In contrast to incineration, a common technique to use MSW at commercial scale, gasification generates less hazardous pollutants, including heavy metals, polychlorinated dibenzo-p-dioxins (PCDDs) and polychlorinated dibenzo-p-furans (PCDFs) [21, 34].

Unlike conventional biomass gasification, which occurs at 500-1,400°C and has been well known since the World War II (1943) when about 700,000 of cars, trucks, and buses in Europe were powered by wood-gas generators [11, 287], gasification of MSW is relatively new and generally uses thermal plasma technology with high temperature ranges, exceeding 5,000°C [288]. Due to the extreme high temperature environment, plasma minimizes tar formation by converting it into inert slag, and breaks down char and dioxin [36]. However, drawbacks include high energy use for generating plasma and operational challenges, perhaps, due to the extreme temperature that eventually impact the capital cost and project viability [49, 289]. A total capital cost of \$13,000/kW has been estimated for this technology at 100 MW scale [50], creating challenges for commercial adoption [49]. The plasma torch also needs to be replaced regularly since the generated plasma erodes the electrodes during its operation [290].

Previous studies focusing on plasma gasification of MSW are still limited in literature. Mountouris et al. [36] investigated solid waste plasma gasification using an equilibrium technique (using MathCad) and found that with the increased plasma temperature from 1,073 K to 1,473 K, the total concentration of H<sub>2</sub> and CO increases from 45-47% to 48-50%. They found that the moisture content must be kept below 15% to maintain the plasma temperature of 1,273 K with no electricity utilization (i.e. plasma generation was not utilized). Minutillo et al. [291] developed a thermochemical model to analyze an integrated plasma gasification combined cycle (IPGCC) power plant. They used a refuse derived fuel (RDF) as the gasifier feedstock with a lower heating value (LHV) of 16.7 MJ/kg that resulted in a syngas with 9 MJ/kg LHV and 69.1% gasification efficiency. The authors found that system efficiency of IPGCC plant (31%) can reach higher than that of conventional waste incineration using steam cycle (20%). Janajreh et al. [292] investigated a plasma gasification model to convert eight feedstocks (low rank coal, used tire, MSW, low ash algae, woods, pine needles and plywood) having different position in Van Krevelen diagram. The authors found a gasification efficiency of about 42% at 4,000°C and an atmospheric pressure. Galeno et al. [267] investigated an integrated plasma gasification and solid oxide fuel cell (IPGC) power generating system using refuse derived fuel (RDF) as the gasifier feedstock. They found that an IPGC plant can offer an efficiency of 32.7% with a net power of 87 kW from the feedstock flow rate of 0.02 kg/s (~72 kg/h).

All plasma models presented above are based on the principle of a thermal plasma gasification system operating at high temperature (>4,000°C) except the one reported by Mountouris et al.; at the best of our knowledge, none of the studies presented used low-

temperature plasma gasification systems. The specific objective of this study is to investigate the performance of a low-temperature plasma gasification of MSW operating below 2,500°C at an atmospheric pressure. The outcome of this study is expected to provide guidance on the application of low-temperature plasma gasification for producing high quality syngas with low energy consumption.

## **5.2. Material and Methods**

The feedstock used in this study was MSW, with proximate and ultimate analysis and particle size distribution, as shown in the previous chapter (Chapter 3, Table 3.1) and previous report [60].

The components associated with metals in MSW should be removed before gasification, because these components will stay in the base of gasifier and will be discharged in the ash removal system. Only organic compounds can be converted into syngas through many reactions listed in the previous chapter (Chapter 1, Table 1.2), while metal components are directly discharged through ash removal system. In plasma gasification, reactions 7, 8, 9, 11, and 15 are generally used [36].

### **5.2.1. Plasma gasification model**

In plasma generation, higher current densities are generally associated with lower voltages, as displayed in Figure 5.1 [293]. Based on this voltage-current relationship, three major plasma discharge types can be observed are dark, glow, and arc plasma. The thermal plasma in the arc discharge regime is the main focus of this study. The arc discharge regime consists of three regions: glow to arc transition, non-thermal arc, and thermal arc. Typically, the glow to arc transition occurs in the current range of 1 to 10 A;

while a low temperature plasma occurs beyond the non-thermal plasma generation in the arc discharge region at current level of about 100 Amps [293].

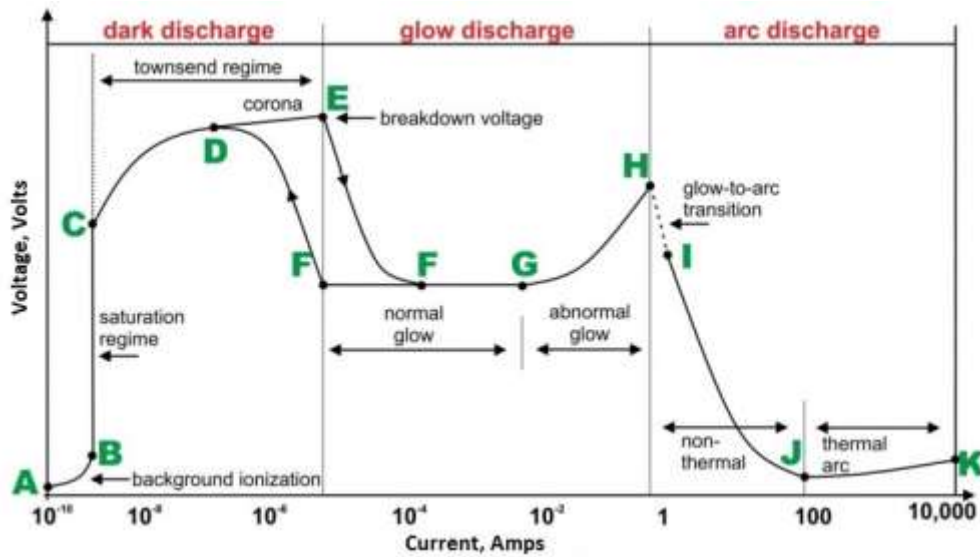


**Figure 5.1. Types of plasma discharge based on voltage and current density [293]**

**Table 5.1. Main blocks description in AspenPlus™ plasma gasification model**

Block Name	Block Yield	Description
Decomp	RYield	Non-stoichiometric reactor based on known yield distribution
HTR / LTR	RGibbs	Rigorous reactor and multiphase equilibrium based on Gibbs free energy minimization
HEX-1 / HEX-2	Heater	Heat Exchanger
SEP	Separator	Separator unit
DC-Arc	Heater	Heat exchanger
Mix	Mixer	Stream mixer

The plasma gasification process was modelled using AspenPlus™. Table 5.1 describes the main blocks to model the plasma reactor, while Figure 5.2 shows the

flowsheet of the model. Similar main blocks and flowsheet have been used in previous studies on gasification [267, 291, 292].

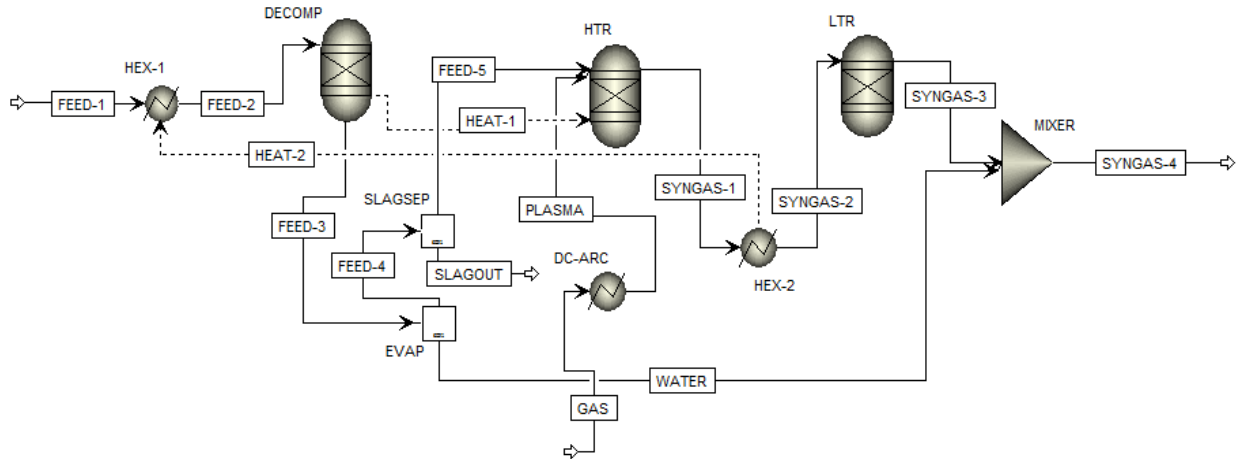


**Figure 5.2. Process diagram of MSW plasma gasification**

The feedstock input stream (FEED-1) was a non-conventional solid stream. The properties of this stream were determined based on the ultimate and proximate analysis of the feedstock as listed in Table 3.1, using the HCOALGEN enthalpy model and the DCOALIGT density model in AspenPlus<sup>TM</sup>. FEED-1 stream entered into the reactor after absorbing heat (HEAT-2) from the syngas that exited from the high temperature plasma zone through the heat exchanger 2 (HEX-2).

For the decomposition of materials inside the plasma reactor, a unit of decomposition using a RYield reactor (DECOMP) was set-up to model the condition. The reactor yield was specified according to the proximate and ultimate analysis where the organic fraction of MSW was decomposed into its constituent element. The heat (HEAT-1) for breaking down MSW was supplied by the high temperature reactor (HTR). Two reactors, the high temperature reactor (HTR) and low temperature reactor (LTR) were used to allow a complete conversion of the feedstock into syngas inside the plasma reactor. For a given

set of possible syngas composition, both reactors were used to determine the equilibrium composition using direct minimization of the Gibbs free energy. The HTR operated at 1,500-2,500°C and simulated main zone of the plasma reactor. The LTR operated at an average temperature of 600-800°C where conventional gasification typically occurs, converting the organic fraction into syngas. The temperature range of 1,500-2,500°C was selected to reduce the energy requirement for generating plasma gas, but still ensuring that the chemical reactions attains equilibrium inside the plasma reactor because an equilibrium typically occurs when the gasification temperature exceeds 800°C [294, 295]. Moreover, the minimum temperature used in this study (1,500°C) is higher than the minimum temperature (1,273 K) required to destruct dioxins [36]. The three main independent equilibrium reactions of plasma gasification refer to the reactions of 7, 8 and 9 (Table 2) [36], with the equilibrium constants expressed as:

$$K_1 = \frac{[CO].[H_2]^3}{[CH_4].[H_2O]} \dots\dots\dots [5.1]$$

$$K_2 = \frac{[CO_2].[H_2]}{[CO].[H_2O]} \dots\dots\dots [5.2]$$

$$K_3 = \frac{[CO].[H_2]}{[H_2O]} \dots\dots\dots [5.3]$$

And the equilibrium constant (K) is a function of temperature  $T$  and is formulated as

$$\ln K = \frac{-\Delta G^0}{RT^2}.$$

According to the main reaction (Chapter 1, Table 1.2), the enthalpy balance

equation includes the amount of electricity used in the plasma reactor and can be written

as:

$$H_{f,waste}^0 + wH_{f,H_2O(l)}^0 + mH_{f,O_2}^0 + 3.76mH_{f,N_2}^0 + E_{electricity} = n_1H_{f,H_2}^0 + n_2H_{f,CO}^0 + n_3H_{f,CO_2}^0 + n_4H_{f,H_2O(g)}^0 + n_5H_{f,CH_4}^0 + n_6H_{f,N_2}^0 + n_7H_{f,C}^0 +$$

$$\int_{T_1}^{T_2} (n_1 C_{p,H_2} + n_2 C_{p,CO} + n_3 C_{p,CO_2} + n_4 C_{p,H_2O} + n_5 C_{p,CH_4} + n_6 C_{p,N_2} + n_7 C_{p,C}) dT \dots\dots\dots [5.4]$$

where  $H_{f,waste}^0$  is the heat of formation of MSW,  $H_{f,H_2O(l)}^0$  is the heat of formation of liquid water,  $H_{f,H_2O(g)}^0$  is the heat of formation of water vapor,  $H_{f,H_2}^0$ ,  $H_{f,CO}^0$ ,  $H_{f,CO_2}^0$ , and  $H_{f,CH_4}^0$  are the heats of formation of gaseous products,  $H_{f,C}^0$  is the heat of formation of solid carbon,  $C_{p,H_2}$ ,  $C_{p,CO}$ ,  $C_{p,CO_2}$ ,  $C_{p,H_2O}$ ,  $C_{p,CH_4}$ ,  $C_{p,N_2}$  are the specific heats of gaseous products and  $C_{p,C}$  is the specific heat of solid carbon (soot),  $T_2$  is the gasification targeted temperature (K),  $T_1$  is the ambient temperature (298 K), and  $E_{electricity}$  is the energy required for the gasification reactions but not for the vitrification of inorganic fractions of MSW [36]. In addition, the typical time required to reach the equilibrium of the reactions is less than 3s at 1,200°C [296]; a significant increase of gas yield is noted in that time range due to the decomposition of tar [297].

A plasma torch was represented using a heat exchanger block (DC-ARC) that heated the GAS stream up to a temperature of 1,500-2,500°C, at which heat was supplied to generate plasma gas. The GAS stream can potentially be helium, oxygen or other, but air was selected because due to its low cost and abundantly availability. The energy consumption of the plasma torch is obtained by energy transferred from the GAS stream to the heat exchanger.

Two heat exchangers were used to model the solid and gas materials inside the reactor. HEX-1 is used to model the solid waste (MSW), while HEX-2 is used to model the syngas. The heat integration was used to connect the two heat exchangers where the heat input (HEAT-2) was taken from the HTR reactor. After contacting with the hot

syngas (through HEAT-1), the water content of MSW evaporates and leaves the DECOMP reactor together with the syngas. A separation unit (SEP) was used to remove most water and solid materials (including slag) from the plasma reactor gasification model. The output of the HTR reactor (syngas 1), containing liquid slag and syngas, was cooled through a heat exchanger (HEX-2), and then fed into LTR reactor (producing syngas 2) where the conventional gasification occurred at a temperature of 800°C. The output of the LTR reactor (syngas 3) was mixed with the evaporated water in a mixer (MIX) before it exited as the stream of final product (syngas 4).

### **5.2.2. Model comparison**

The model was then compared with previous modeling analysis with a similar range of plasma temperature using equilibrium techniques and solid waste materials as the gasifier's feedstock, as reported by Mountouris et al. [36] and Benilov and Naidis [298]. Mountouris et al. [36] developed the plasma gasification model using MathCad based on equilibrium technique at temperature of 1073-1473 K. Similarly, Benilov and Naidis [298] investigated the plasma gasification using CHEMKIN-II based on reaction kinetics.

In order to further validate the low-temperature plasma gasification model, results are compared to experimental data generated from high-temperature air gasification. The experimental set-up and system operation has been explained in detail in previous reports [29, 56, 60, 299]. MSW in pelletized form with properties presented in Table 3.1 (Chapter 3) was fed into the downdraft gasifier with a feeding rate of 72 kg/h and an equivalence ratio (ER) (a ratio between actual flow rate of air to the stoichiometric flow rate of air required for a complete combustion of the MSW) of 0.25. The compressed air was used and air flow was adjusted by an air valve to control the ER and reactor

temperature. Syngas generated from MSW gasification was analyzed by a Gas Chromatograph (Agilent, Model 7890a, Agilent Technologies, Santa Clara, CA). Syngas compositions and operating parameters were captured before ash agglomeration occurred in the reactor, as similar to what has been reported earlier by Indrawan et al. [60] and Bhoi et al. [299] using a mixture of switchgrass and MSW (up to 60 wt.%).

### **5.2.3. System performance**

System performance analysis included comparison results (such energy consumption, syngas composition and gasification efficiency) obtained from low-temperature plasma gasification model and high-temperature air gasification. The equilibrium model described in the previous section (Section 5.2.1) is used to analyze the performance of low-temperature plasma gasification. The mass ratios of plasma gas (GAS) to MSW were 0.78, 1.1, 1.2, and 1.4, corresponding to four different temperatures (4,000, 2,500, 2,000, and 1,500°C, respectively). The temperature of 4,000°C was selected to compare with not only the models of low-temperature operating ranges (< 2,500°C), but also the performance of typical MSW gasification available in literature and commercial application [153]. Air was used as the gasification medium because it is readily available and requires a low energy input to reach high temperatures due to its low specific heat [292].

The efficiency of this system was evaluated at three different temperatures (1,500, 2,000, and 2,500°C). These efficiencies were then compared with the efficiency of conventional plasma gasification, which operates at 4,000°C using air at atmospheric conditions. The plasma gasification efficiency ( $\eta_{CGE}$ ) of the system is calculated as:

$$\eta_{PGE} = \frac{(m_{syngas} \times LHV_{syngas})}{(m_{feed} \times LHV_{feed}) + (\frac{W_{torch}}{\eta_{torch} \times \eta_{electric}})} \dots\dots\dots [5.5]$$

where  $m_{syngas}$  and  $m_{feed}$  are mass flow rates of the syngas and feedstock (MSW), respectively (kg/s).  $LHV_{syngas}$  and  $LHV_{feed}$  are the lower heating values of the syngas and feedstock, respectively (MJ/Nm<sup>3</sup>).  $W_{torch}$  is the electric power consumption of the plasma torch (MJ/s), and  $\eta_{torch}$  is the plasma torch efficiency, which is considered 86% as a general torch efficiency [177], while,  $\eta_{electric}$  is the electrical efficiency of coal power plant, which is considered 30% in this study; typical efficiency of coal power plants range 30-35% [300].

In order to eliminate slag build-up and refractory issues downstream of the gasifier, the syngas temperature existing in the gasification reactor must be kept in the range of 600-800°C while maintaining particulates in the form of ash [177].

#### 5.2.4. Sensitivity analysis

In order to further optimize the low-temperature plasma gasification process, a sensitivity analysis, generated from the AspenPlus<sup>TM</sup> model was conducted based on the plasma gas flow-rate input variable as the plasma generation was considered the most energy consuming contributor of the system. The operating temperature of the LTR was fixed at 800°C, which is the required input temperature for further use of the syngas, such as the one using a solid oxide fuel cell (SOFC) for electricity generation [267].

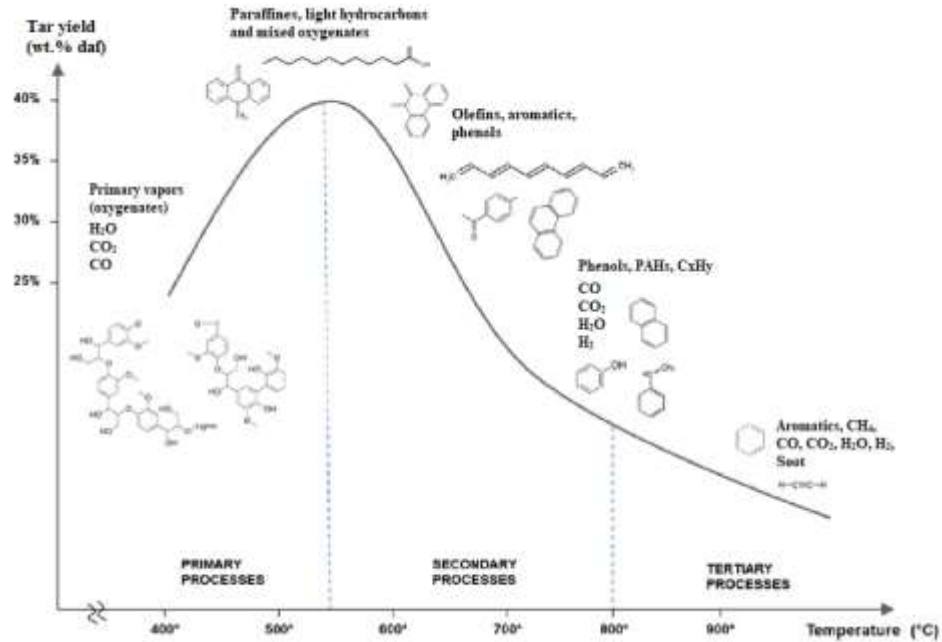


**Figure 5.3. Tar yields in generic gasification process at different temperatures [220]**

Plasma temperature was kept above 1,500°C to avoid tar formation. Previous studies found that tar generally cracks completely above 1,200°C, following the profile shown in Figure 5.3 [220, 301, 302].

### 5.3. Results and Discussion

#### 5.3.1. Model comparison

Compared to previous studies using equilibrium techniques, the model presents a reasonable agreement with Moutoris et al. [36], where the CO and H<sub>2</sub> were dominantly generated at 1,200°C with an Oxygen/Carbon (O/C) ratio of 0.3, as shown in Table 5.2. Additionally, the model also generates a higher fraction of CO and H<sub>2</sub> (22% and 24.4%, respectively) compared to Benilov & Naidis [298] (13.5-14.5% and 9-10%, respectively)

at around 1,500°C. The discrepancy occurs most likely because of the difference of either feedstock characteristics or moisture content that is not mentioned in their study [298].

**Table 5.2. The model comparison with previous studies using equilibrium techniques**

Models	Plasma Temp., °C	Syngas composition, %v/v					O/C ratio	Moisture, %
		CO	H <sub>2</sub>	CH <sub>4</sub>	CO <sub>2</sub>	N <sub>2</sub>		
Mountoris et. al. [294]	1,200	22–23	27–28	<1.0	4–6	31–32	0.30	30%
Benilov and Naidis [303]	1,527	13.5–14.5	9–10	<0.5	4	N/A	1.80	N/A
Present study	1,500	22	24.4	<0.1	9	35.4	0.38	3.8
	2,000	24.5	27.2	<0.1	8.1	32	0.33	3.8
	2,500	26.3	29.1	<0.1	7.5	29.6	0.30	3.8

Owing to the higher gasification temperatures (1,500, 2000, and 2,500°C), the presented model results in higher syngas LHV<sub>s</sub> (5.41, 6.02, and 6.45 MJ/Nm<sup>3</sup>) than the experimental data (5.12 MJ/Nm<sup>3</sup>) at gasification temperature 1,000°C. The high temperature of the gasifier allows tar decomposition into more combustible products including CO and H<sub>2</sub>; total syngas concentrations of CO and H<sub>2</sub> in the presented model are 55.4%, 51.4% and 46.4% at 2,500, 2,000 and 1,500°C, respectively, while 19.1% was obtained from the experiment. A detailed comparison of individual main syngas composition is presented in Table 5.3 that will be discussed later.

### 5.3.2. The energy consumption

The low-temperature plasma gasification presents a significant decrease in energy consumption compared to conventional plasma gasification, as shown in Figure 5.4. The energy consumption of the plasma torch is decreased from 3,816 kW at the conventional

plasma gasification temperature (4,000°C) to 3,157 kW, 2,775 kW, and 2,358 kW (at 2,500, 2000, and 1,500°C, respectively).

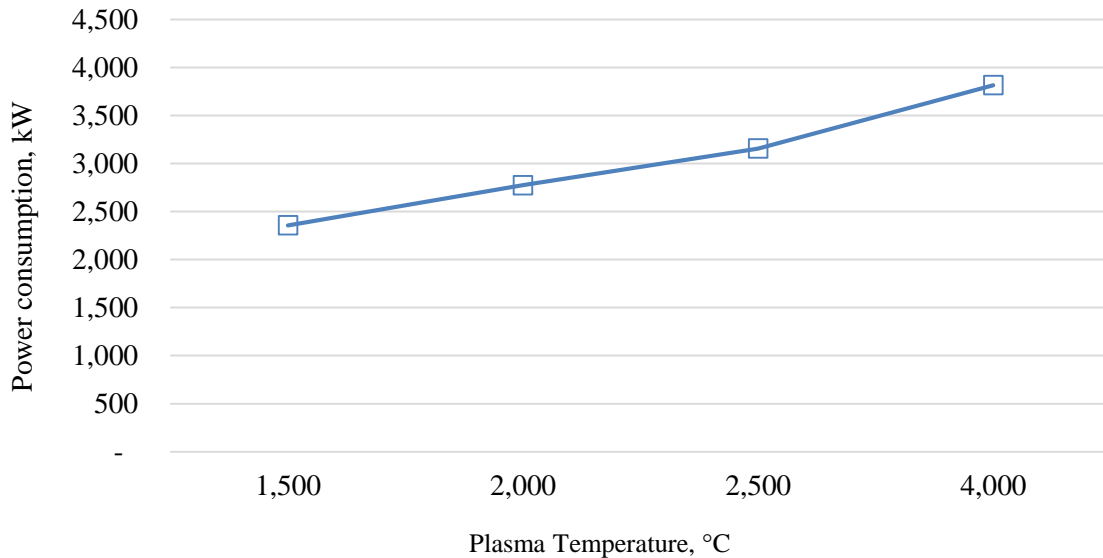


**Figure 5.4. Effect of plasma temperature on energy consumption for generating plasma gas**

This reduced energy consumption consequently increases the efficiency of plasma gasification and potentially reduces system capital cost. Current capital cost of MSW gasification systems for electricity generation operating at 5,000°C is still high, reaching \$13,000 per kW [50].

### 5.3.3. Gasification efficiency

The low-temperature plasma gasification has the potential for a higher efficiency due to lower energy loads, as depicted in Figure 5.5. Compared to conventional plasma gasification operating at 4,000°C, the plasma gasification efficiency (PGE) only slightly increases from 48.8% (at 4,000°C) to 48.9%, 49.2%, and 49.6% (at plasma temperature of 2,500, 2,000, and 1,500°C, respectively), due to the plasma energy requirement.

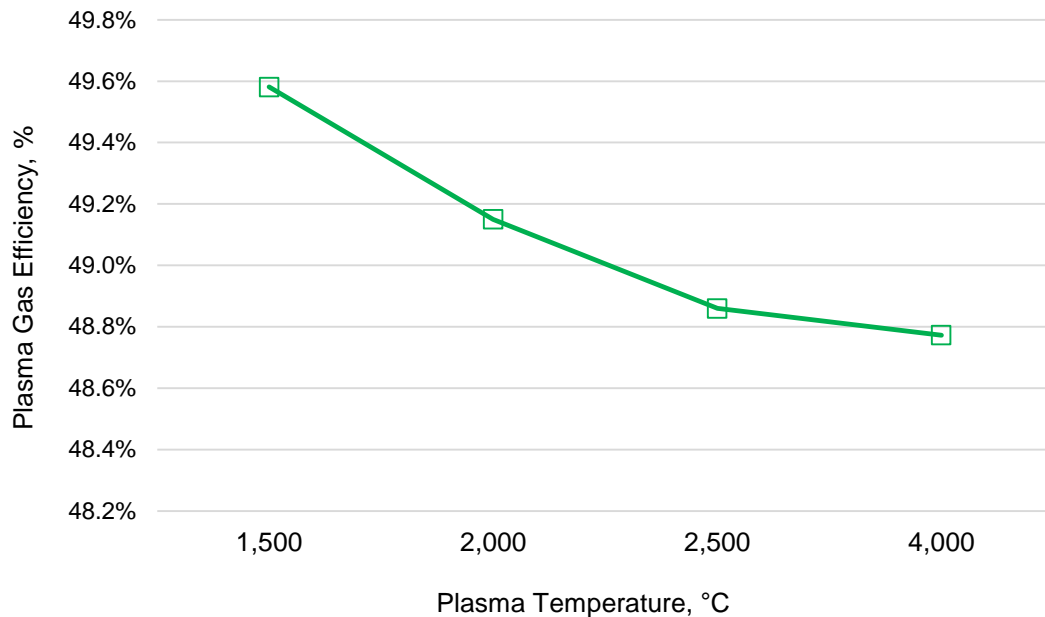


**Figure 5.5. Effect of plasma temperature on plasma gasification efficiency (PGE)**

In a lower plasma temperature, the energy consumption to generate the plasma decreases, however, the reduction is penalized with the decrease in syngas heating values. At a plasma temperature of 4,000°C, the PGE (48.8%) is lower than (63.6%) [291], but higher than (43.3%) [292]. For further application of power generation, to enhance the efficiency of gasification system, incorporating the plasma gasifier with the fuel cell technology will increase the electrical plant efficiency from 31% to approximately 33% [267].

#### **5.3.4. Effect on syngas characteristics**

The syngas obtained by the model mainly consists of H<sub>2</sub>, CO, and inert gases (N<sub>2</sub> and CO<sub>2</sub>). The variation of plasma temperature impacts syngas composition, as presented in Figure 5.6. The concentration of H<sub>2</sub> in syngas decreases with reduced plasma temperature, from 33.8% at 4,000°C to 24.4% at 1,500°C, while, the concentration of CO decreases from 30.9% at 4,000°C to 22.0% at 1,500°C. Therefore, lowering the

temperature of plasma gasification has a high impact on the fuel content of the syngas. The results align with Mountoris et al. [36] where total concentration of CO and H<sub>2</sub> increases at higher temperatures. A high concentration of H<sub>2</sub> in the syngas is preferred because it lowers other hydrocarbon components (i.e. CO, CH<sub>4</sub>, C<sub>2</sub>H<sub>2</sub>, C<sub>2</sub>H<sub>4</sub>, C<sub>2</sub>H<sub>6</sub>), consequently reducing potential of carbon deposition for further application of fuel cells [267, 304].

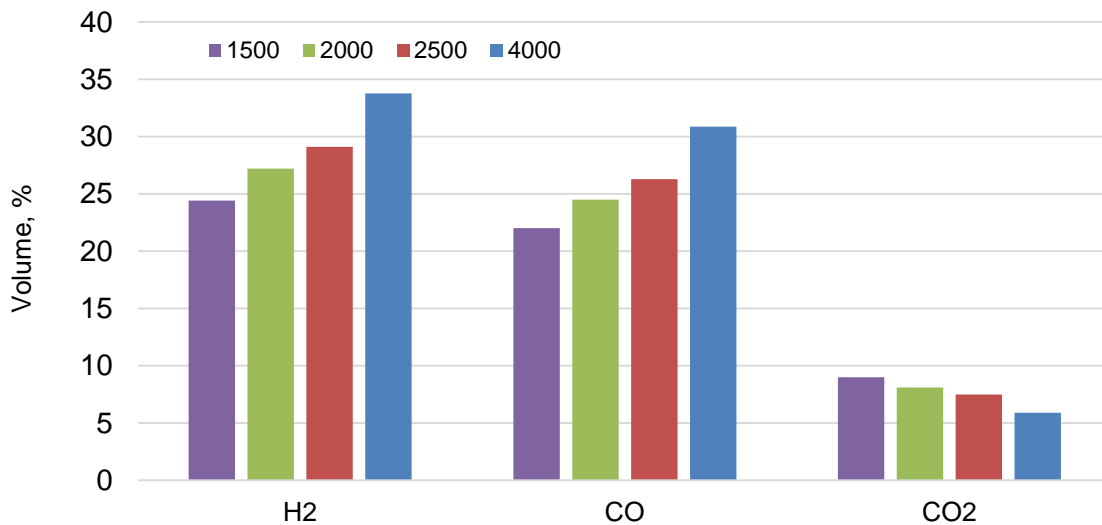


**Figure 5.6. Syngas composition on different plasma temperatures**

Syngas heating values, expressed in terms of lower heating value (LHV) and higher heating value (HHV), are also affected by temperature, as shown in Figure 5.7. A decrease of plasma temperature slightly decreases syngas heating value, from 7.56 MJ/Nm<sup>3</sup> at 4,000°C to 5.41 MJ/Nm<sup>3</sup> at 1,500°C. The decrease of syngas heating value is likely due to the change in syngas composition, mainly a decrease of H<sub>2</sub> and CO content. However, a slight reduction in syngas heating value at lower temperature will likely be offset by the benefits of higher efficiency of plasma gasification due to lower energy

consumption of the plasma torch, which could lead to a reduction in capital cost of the system.

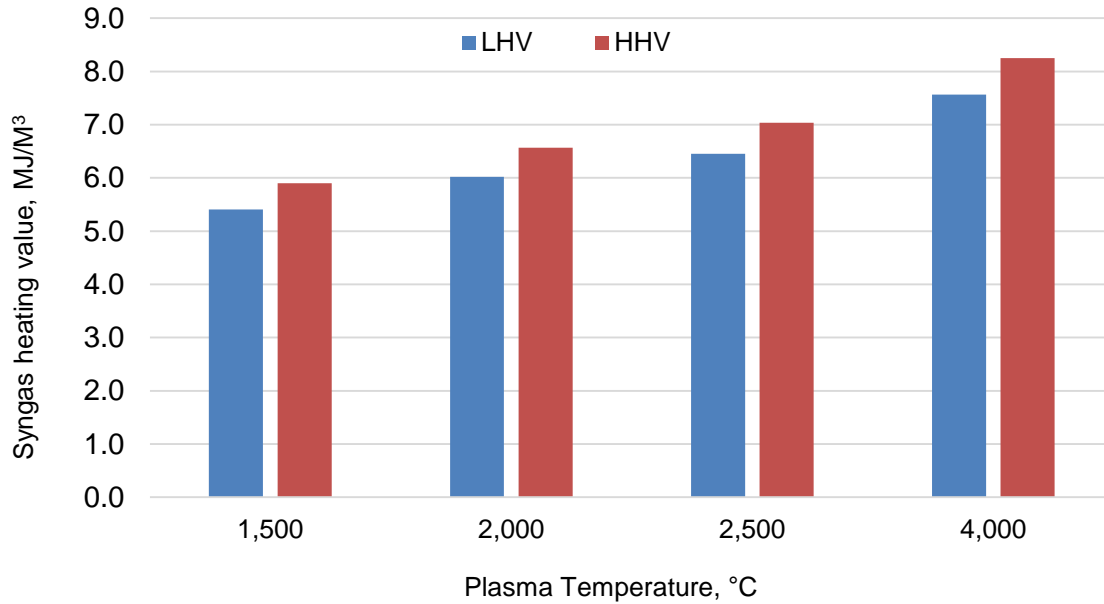


**Figure 5.7. Effect of plasma temperature on syngas heating values**

### 5.3.5. System performance

Table 5.3 presents the performance comparison of the low temperature plasma gasification generated from the model and conventional high-temperature air gasification generated from experimental. An energy consumption of 2,358 kW at 1,500°C is considered as the lowest compared to other low-temperature variations (2,000, 2,500 and 4,000°C). This energy consumption can be offset by a syngas LHV of 5.41 MJ/Nm<sup>3</sup>, which is mainly contributed by H<sub>2</sub> and CO. High-temperature air gasification requires zero energy consumption for plasma generation, however, its syngas LHV of 5.12 MJ/Nm<sup>3</sup> is mainly contributed by a heavy fraction of hydrocarbons (mainly C<sub>2</sub>H<sub>4</sub>); a syngas containing heavy hydrocarbons is not preferred for further use (i.e. power generation using internal combustion engine and fuel cell) as the heavy hydrocarbons

cannot be burned spontaneously in the internal combustion engine and can cause carbon deposition and reduce the lifetime of the fuel cell.

**Table 5.3. Performance of the plasma gasification and conventional air gasification of MSW**

Parameters	Model at varying temperatures				Conventional
	4,000°C	2,500°C	2,000°C	1,500°C	1,000°C
Feedstock flow (MSW), kg/s	1	1	1	1	0.02
Plasma gas flow, kg/s	0.78	1.1	1.2	1.4	0.0
Energy consumption (torch), kW	3,816	3,157	2,775	2,358	0.0
Gasification efficiency, %	48.7	48.9	49.2	49.6	63.8
Syngas outlet temp., °C	800	800	800	800	425
Syngas composition, % mole					
H <sub>2</sub>	33.8	29.1	27.2	24.4	8.5
N <sub>2</sub>	23.5	29.6	32.0	35.4	55.0
O <sub>2</sub>	0.0	0.0	0.0	0.0	0.0
CO	30.9	26.3	24.5	22.0	10.6
CH <sub>4</sub>	0.1	0.0	0.0	0.0	2.9
CO <sub>2</sub>	5.9	7.5	8.1	9.0	20.0
C <sub>2</sub> H <sub>2</sub>	0.0	0.0	0.0	0.0	0.3
C <sub>2</sub> H <sub>4</sub>	0.0	0.0	0.0	0.0	2.3
C <sub>2</sub> H <sub>6</sub>	0.0	0.0	0.0	0.0	0.5
NH <sub>3</sub>	36 ppm	32 ppm	30 ppm	27 ppm	0.0
HCN	1 ppm	596 ppb	479 ppb	346 ppb	0.0
H <sub>2</sub> O	5.9	7.5	8.2	9.1	0.0
Total	100.0	100.0	100.0	100.0	100.0
LHV, MJ/Nm <sup>3</sup>	7.56	6.45	6.02	5.41	5.12
HHV, MJ/Nm <sup>3</sup>	8.52	7.03	6.57	5.90	5.52

A higher concentration of H<sub>2</sub> and CO is observed at a higher temperature of plasma gasification as a result of partial decomposition of heavy hydrocarbon components (C<sub>3</sub>-

C<sub>4</sub>) of the syngas, consequently increasing the syngas heating values, as described earlier. At plasma temperature of 1,500°C, a total concentration of H<sub>2</sub> and CO of 46.4% is achieved and comparable with that obtained by Mountouris et al. (45-50%) [36]. Although the total concentration of H<sub>2</sub> and CO at 1,500°C (46.4%) is lower than that obtained from plasma temperature of 4,000°C (64.7%), 2,500°C (55.4%), and 2,000°C (51.7%), the total concentration of H<sub>2</sub> and CO at 1,500°C is still higher than that obtained from a high-temperature gasification (19.1%).

Gasification efficiencies resulted from the low-temperature plasma models are in the range of 48.7-49.6%, lower compared to the hot-temperature air gasification (~63.8%). This is primarily caused by the energy consumption of the heat exchanger to increase the air from atmospheric temperature to temperature required for plasma generation. A high energy consumption is generally a major drawback of commercial plasma gasification, especially thermal plasma generation that consumes a current level of more than 10,000 amps (Figure 5.1).

### **5.3.6. Sensitivity analysis**

A sensitivity analysis of the plasma gas flow-rate generated from the AspenPlus<sup>TM</sup> model shows that syngas composition (and consequently syngas heating value) are strongly dependent on the flow-rate of plasma gas. As illustrated in Figure 5.8, a higher mass flow-rate of plasma gas considerably reduces the concentration of H<sub>2</sub> and CO fuels in syngas. The concentration of H<sub>2</sub> drops significantly from 24.3% at 1.4 kg/s to 18.4% at 2.3 kg/s. Similarly, the concentration of CO decreases from 21.9% at 1.4 kg/s to 16.3% at 2.3 kg/s. This dramatic trend is explained by looking at reactions of 1 to 6 in Table 1.2 (Chapter 1), which are responsible for the formation of H<sub>2</sub> and CO. To increase the H<sub>2</sub>

concentration and syngas heating value of the syngas, perhaps using steam/oxygen as gasification medium is an alternative as steam does not contain nitrogen that can dilute the syngas [52].

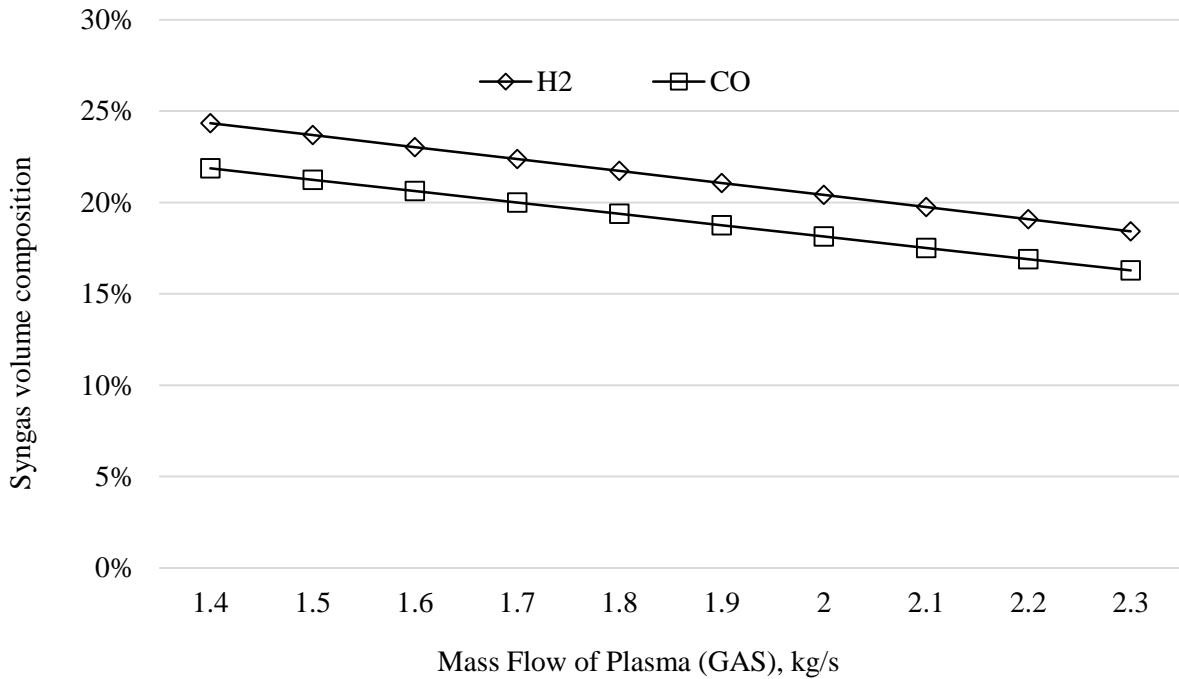


**Figure 5.8. The effect of mass flow of plasma gas on syngas composition at 1,500°C**

Therefore, using a plasma temperature of 1,500 to 2,500°C resulted in high-quality syngas due to perhaps a higher decomposition and ionization rate of MSW, with minimum energy input ranging from 2,358 to 3,157 kW.

#### 5.4. Conclusions

A model of low-temperature MSW plasma gasification system was analyzed as a lower cost, more environmentally-friendly alternative to current methods for MSW disposal using high-temperature plasma gasification. The model developed in AspenPlus<sup>TM</sup> showed a significantly lower energy input for plasma torch. The energy

consumption of the plasma torch decreased from 3,816 kW at conventional temperature (4,000°C) to 3,157, 2,775, and 2,358 kW at temperatures of 2,500, 2,000, and 1,500°C, respectively. The plasma gasification efficiency (PGE) also increased slightly at lower temperatures (efficiencies of 48.7%, 48.9%, and 49.2% at 2,500, 2,000, and 1,500°C, respectively), compared to 48.8% (at 4,000°C). Decrease in plasma temperature slightly decreased the syngas heating value (from 7.56 MJ/Nm<sup>3</sup> at 4,000°C to 5.41 MJ/Nm<sup>3</sup> at 1,500°C).

A low mass flow-rate of 1.4 kg/s for the plasma gas resulted in optimal performance of LHV 5.41 MJ/Nm<sup>3</sup> and HHV 5.90 MJ/Nm<sup>3</sup> at plasma temperature of 1,500°C. At this temperature, plasma gasification generated a syngas composition mainly consisting of H<sub>2</sub> and CO (with 46.4% in total). High concentration of CO and H<sub>2</sub> is required for power generation using internal combustion engine and fuel cell.

## CHAPTER 6

### PERFORMANCE ANALYSIS OF SOFC/GT HYBRID POWER GENERATION FROM GASIFICATION OF MUNICIPAL SOLID WASTE

**Abstract:** Disposing of municipal solid waste (MSW) has become a critical issue worldwide. Current available technologies to dispose of MSW, including landfills and incineration, have negative impacts such as soil contamination and air pollution. Gasification has the potential to process MSW because it can convert MSW into syngas intermediate that can be converting into chemicals and electricity. For electricity production from syngas, solid oxide fuel cell (SOFC) and gas turbines (GT) are emerging technologies that can drastically increase the conversion efficiency as compared to currently used reciprocal internal combustion engines. This study aims to investigate the performance of advanced SOFC/GT hybrid power generating system using syngas generated from gasification of municipal solid waste and biomass. Effects of syngas composition on system performance and efficiency, including current density, degradation rate, fuel cell solid and gas temperature, gas composition, activation loss, ohmic loss, and Nernst potential, were investigated. The system electrical efficiency reached 49.5%, thus, the SOFC/GT hybrid power generation brings a potential breakthrough solution to increase efficiency of power generation from MSW and biomass.

**Keywords:** Syngas; Gasification; SOFC/GT Hybrid Power; MSW

## 6.1. Introduction

Municipal solid waste (MSW) generation is a critical issue. Global MSW generation has sharply increased from 1.3 billion tons in 2012 to an estimated of 2.2 billion tons in 2025 [12] due to increased world population from 7.4 billion people today to more than 8.1 billion people in 2025 [305]. Technologies capable of processing MSW has become more urgent because current practices, including landfill and incineration, have created negative impacts on environment and human health. Landfills can contaminate the soil and groundwater with leachate pollutions as a result of degradation of organic matters [245], and pollute air due to emissions of volatile organic compounds (VOC) including dimethyl disulfide, toluene, and benzene [246]. MSW incineration potentially generates polychlorinated dibenzo-p-dioxins (dioxins/PCDDs) and dibenzofurans (furans/PCDFs), which cause chloracne, liver dysfunction, and cancer [247].

MSW gasification has been considered as a promising solution to reduce global waste disposal while providing alternative energy and power through power generation. For most half of global, MSW is composed of organic waste and paper (~63%) (Chapter 1, Figure 1.12) that can be converted into syngas, which can further be transformed into methanol, ammonia, and hydrogen. These alternative products represent huge markets of syngas worldwide: 180 million metric tons (MMT) for ammonia, 85 MMT for methanol, and 40 MMT for hydrogen in 2016 [43]. In the U.S., recently, the concern of waste disposal has been gaining more attention because of a significant increase of tipping fees from \$51.82/ton in 2017 to \$55.11/ton in 2018 (~\$3.29/ton or ~6.3% increment as average increase) at a national level [178]. This increment surpasses the previous national records (as average increase per year): \$3.15/ton within 1985-1990, \$0.77/ton within

1995-2004, and \$0.83/ton within 2003-2014 [306]. By combining these two facts – the potential of a syngas market and an increased waste disposal - MSW gasification will provide a significant role in future industrial markets, including chemical and electricity production, yet reduces environmental impacts from landfills and incineration technologies.

In contrast to conventional biomass gasification, which occurs at 500°C to 1,400°C [287], gasification of MSW typically uses thermal plasma technology that deploys high temperature ranges, exceeding 5,000°C [307]. Due to extreme temperature environment, plasma minimizes tar formation by converting it into inert slag, and breaks down char and dioxin [294]. However, there are drawbacks associated with a thermal plasma gasification system. The major barrier is the large energy use for generating plasma at high temperature (>5000°C) that reduces the economic viability and increases operational challenges [49, 289]. A total capital cost of \$13,000/kW has been estimated for this technology at the 100 MW scale [308], resulting in a long economic return [49]. The plasma torch also must be replaced regularly since the generated plasma alludes the cathodes during its operation [290].

Power generation through gasification of MSW has the potential of meeting the electricity demand while reducing area footprints due to MSW disposal. Current stages of development for power generation deploying syngas rely on the use of internal combustion engines (ICEs) and gas turbines (GTs). ICEs have several advantages, such as a wide range of capacity and a considerable high efficiency (30-35%); some latest IC engines have even more than 41% efficiency [309]. Even though the efficiency of IC engines will tend to continuously increase in coming years because advances in research

are attempting to solve current limitations such as reducing friction and parasitic loss and improving exhaust heat recuperation performance, IC engines are restricted by their operating envelope due to the Carnot principle. Similarly, GTs are more preferred due to their higher efficiency than IC engines with a typical range of 35-40%; some recent advanced heavy-duty gas turbines in a combined cycle operation can reach efficiency up to 64% [310]. However, aeroderivative GTs are mostly suitable units to support distributed power generation (typically from hundreds kW to 20 MW) with recent types able to reach full power in less than 9 minutes [310]. However, they are still not as flexible as IC engines in terms of sizing; certain limits of operation are required to maintain their efficiency. Thus, a hybrid power generation capable of reaching a high efficiency using various fuels and having a flexibility in capacity and load following is required for future power market needs.

Solid oxide fuel cells (SOFCs) are one of the most promising technologies capable of integrating with gasifiers. The working principles of SOFC are similar to batteries; however, SOFCs can continuously generate electricity as long as fuel and oxidants (i.e. air or oxygen) are constantly supplied to the system. Figure 6.1 illustrates the basic configuration of planar SOFCs [128], which consist of solid structures called anodes, ion conducting electrolytes, and cathodes. On top of that, channels are constructed to deliver fuels and oxidants along the fuel cell length. The anode channels are used for fuel transportation, whereas cathode channels are for oxidant flow [311].

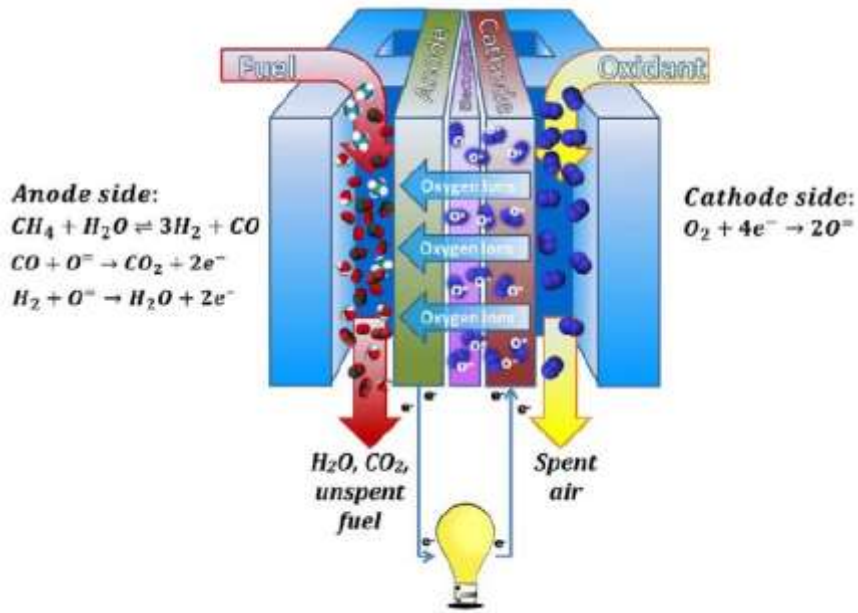


**Figure 6.1. Basic diagram of an SOFC unit**

Studies on SOFC/GT hybrid power generation are limited. Harun et al. [312] investigated the impact of fuel composition on solid oxide fuel cell (SOFC) performance in gas turbine hybrid power generation. Researchers found that a SOFC/GT hybrid system can accommodate the fuel switch from syngas derived coal to humidified methane fuel (methane content 14 vol.%), resulting in an increase of fuel cell thermal effluent by 17% and maximum current density by 15%. The fuel switch ran smoothly without causing the compressor to stall or surge, and without violating SOFC safe operating constraints or otherwise adversely affecting the hardware or functionality of the SOFC/GT system. In another study [130], they found that in an open loop environment control (where the turbine speed is not maintained), the fuel switch from methane lean syngas (CH<sub>4</sub> 0%, CO<sub>2</sub> 12%, CO 28.6%, H<sub>2</sub> 29.1%, H<sub>2</sub>O 27.1%, N<sub>2</sub> 3.2%) to methane rich gases (CH<sub>4</sub> 13.6% and steam 86.4%) resulted in a decrease of turbine speed by about

8% (of 40,500 rpm as actual speed), consequently reducing cathode air mass flow by about 15%. Moreover, fuel cell solid temperature control is critical to avoid excessive temperature gradients; thus, temperature control management through cathode air flow control must be implemented for future SOFC/GT hybrid systems. Buonomano et al. [120] reviewed nearly 300 recent studies on SOFC/GT hybrid systems, including complex IGCC SOFC/GT power plants and Organic Rankine Cycle (ORC) systems. They found that the majority of the studies are based on energy and exergy balance where SOFC/GT hybrid system are fed by methane, which is much cheaper and easier to manage than hydrogen. Also, they found that most SOFC/GT hybrid systems are based on pressurized arrangements; while, in practical plants, atmospheric systems are easier to manage, due to the flexibility to operate GT and SOFC independently.

In addition, studies focusing on MSW gasification are limited. Most studies relied on thermodynamic analysis using high temperature plasma technology. Mountouris et al. [294] investigated solid waste plasma gasification using an equilibrium technique (MathCad) and found that with the plasma temperature variation of 1,073–1,473 K, the total concentration of H<sub>2</sub> and CO increases from 45-47% to 48-50%. They also found that a minimum moisture content of 15% must be kept to maintain the plasma temperature of 1,273 K with no electricity utilization. Minutillo et al. [313] developed a thermochemical model to estimate the performance of an integrated plasma gasification combined cycle (IPGCC) power plant. They used a refuse derived fuel (RDF) as the gasifier feedstock with a LHV of 16.7 MJ/kg, and resulted in a syngas with LHV of 9 MJ/kg and a gasification efficiency of 69.1%. They also found that an IPGCC plant can reach high system efficiency (31%), which is higher than a conventional waste incineration system

(20%). Janajreh et al. [314] investigated a plasma gasification model in converting eight different feedstocks of Van Krevelen diagram including low rank coal, used tire, MSW, low ash algae, woods, pine needles and plywood. They found a plasma gasification efficiency of about 42% at 4,000°C at atmospheric pressure. Galeno et al. [315] investigated an integrated plasma gasification and solid oxide fuel cell (IPGC) system using RDF as the gasifier feedstock. They found that IPGC plant can offer an efficiency of 32.7% with a net power of 87 kW. However, all studies relied on high thermal plasma gasification that is still a challenge to develop in practical situations [49], although a recent plasma gasification technology with a lower energy consumption has evolved in a distributed scale [316].

Motivated by the existing knowledge gap, this work aims to investigate the performance of an advanced SOFC/GT hybrid power generation system using syngas generated from gasification of MSW. The outcomes address current challenges of MSW gasification requiring high energy consumption and support distributed power generation with high efficiency and lower energy consumption.

## **6.2. Materials and Method**

Details of materials have been reported earlier (Chapter 3) [60]. As only organic compounds can be converted into syngas through gasification, therefore the reactions involved in the gasification of biomass were used for the model, following reactions 7, 8, 9, 11, and 15 as shown in Chapter 1, Table 1.2 [294].

The entire experiment consists of two main processes: gasification, and hybrid power generation performance, as shown in Figure 6.2. The gasification was based on

experimental work at the gasification laboratory, Oklahoma State University (OSU), Stillwater, while the hybrid power generation performance was constructed based on a combined hardware and model simulation platform at National Energy Technology Laboratory (NETL), Morgantown, WV.

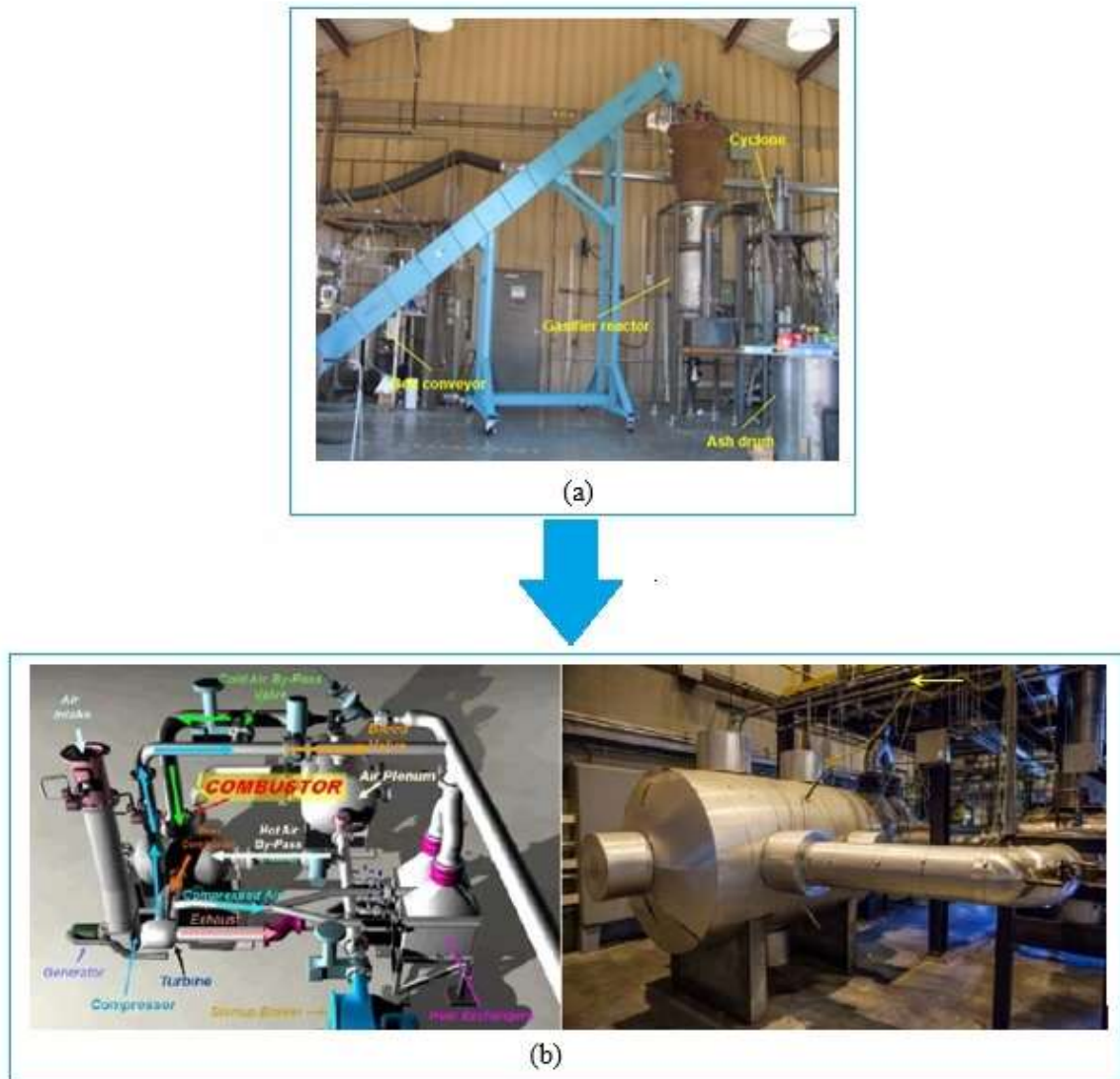


**Figure 6.2. Schematic process of experiment: a) gasification plant at OSU, b) SOFC/GT hybrid power generation system at NETL**

### 6.2.1. Gasification performance

The performance of co-gasification of MSW and biomass has been presented in Chapter 3. A detailed schematic process of the gasification plant is shown in Figure 6.3.

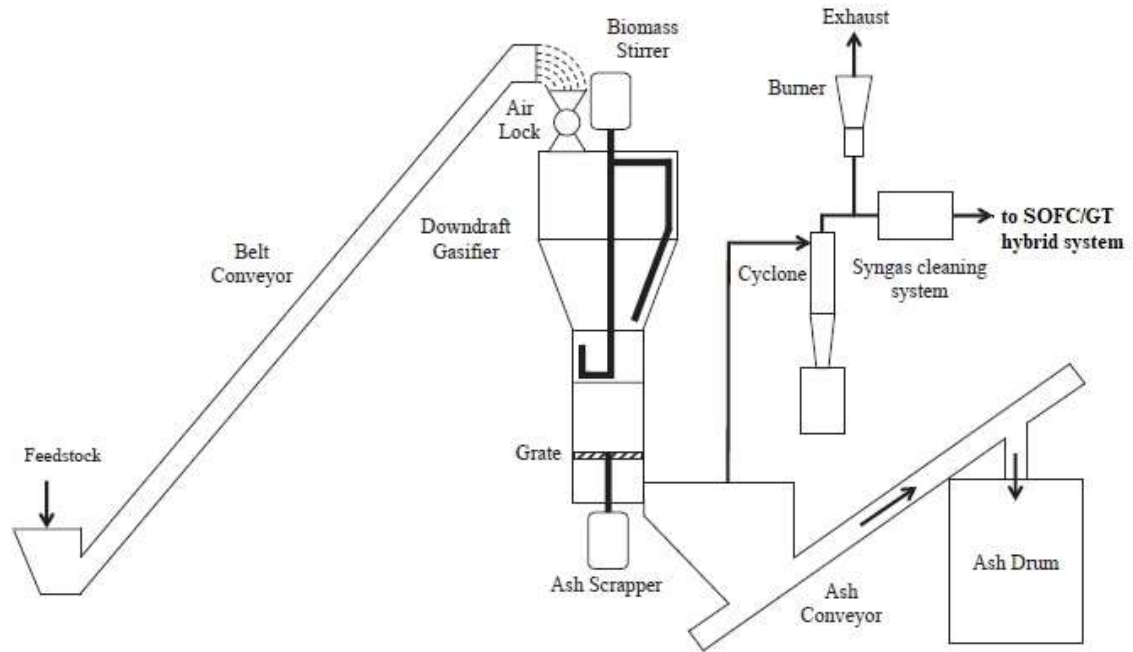


**Figure 6.3. Schematic process of gasification plant, consisting of belt conveyor, air lock, biomass stirrer, downdraft reactor, grate, ash scrapper, ash conveyor, ash drum, and cyclone separator.**

A detailed composition of syngas is presented in Table 6.1. It can be seen that the concentration of  $H_2$ ,  $CO$ , and  $CH_4$  is 25.3% in total, while the concentration of other heavier hydrocarbons (i.e.  $C_2H_2$ ,  $C_2H_4$ ,  $C_2H_6$ ) is about 4.0%.

In order to apply syngas for further use of the fuel cell, a high content of hydrogen is preferred, while heavier hydrocarbons must be minimum to avoid carbon deposition in the fuel cell. A steam to carbon ratio (STCR) of at least 2.0 is used to avoid carbon deposition in the anode of the SOFC [304], following Eq. 6.1 below.

$$STCR = \frac{n_{H_2O}}{n_{CH_4} + n_{CO}} \dots\dots\dots [6.1]$$

**Table 6.1. Major composition of syngas derived from co-gasification of MSW and switchgrass**

Components	Vol. %
H <sub>2</sub>	9.99 ± 2.89
N <sub>2</sub>	54.75 ± 3.98
CO	13.34 ± 2.31
CH <sub>4</sub>	2.01 ± 0.06
CO <sub>2</sub>	15.89 ± 2.13
C <sub>2</sub> H <sub>2</sub>	0.84 ± 0.17
C <sub>2</sub> H <sub>4</sub>	0.43 ± 0.23
C <sub>2</sub> H <sub>6</sub>	2.75 ± 0.79
Lower heating value, MJ/Nm <sup>3</sup>	6.08 ± 0.03

In addition, contaminants of syngas, such as tars, particulates, alkali, and sulfur must substantially be removed to maintain the lifetime of the fuel cell [33, 63, 68].

### 6.2.2. Syngas requirement

Before delivering syngas into the SOFC, it is essential to assure the syngas composition has met several criteria, including a high hydrogen content, free of tars and sufficiently having a certain level of water content, to maintain SOFC’s performance and avoid deposition of the carbon on the anode of the fuel cell. Carbon deposition can cause damage to the structural integrity of the anode as well as reduce the catalytic activity by poisoning the active sites [317]. Thus, steam-to-carbon-ratio (STCR) is the most critical factor [130]; the minimum STCR of 2.0 is required as a typical requirement of the SOFC system [304], allowing water vapor in the syngas able to reform CH<sub>4</sub>, shift CO towards

H<sub>2</sub>, and consequently prevent carbon deposition, as shown in reaction nos. 8-10 and 18 (Chapter 1, Table 1.2). Table 6.2 presents the diluted syngas taken from the dry analysis (Table 6.1) that is further used to investigate the SOFC/GT performance in the hyper facility.

**Table 6.2. Syngas compositions at STRC=2.0 used in the hybrid system**

Syngas Component	Vol. % (after dilution)
H <sub>2</sub>	7.2
N <sub>2</sub>	39.4
CO	9.6
CH <sub>4</sub>	1.4
CO <sub>2</sub>	11.4
C <sub>2</sub> H <sub>2</sub>	0.6
C <sub>2</sub> H <sub>4</sub>	0.3
C <sub>2</sub> H <sub>6</sub>	2.0
H <sub>2</sub> O	28.1

### 6.2.3. SOFC/GT hybrid power generation system

A public testing facility of SOFC/GT (also known as hybrid performance / hyper facility) in the U.S. Department of Energy, National Energy Technology Laboratory (NETL), Morgantown, West Virginia was used to carry out the test on simulating MSW syngas.

#### 6.2.3.1. System description

As shown in a simplified process diagram (Figure 6.4), the hyper project was used to investigate system transient capabilities that are associated with feasible dynamic operating ranges, coupling effects between fuel cell subsystem and recuperated gas turbine cycle, and highly complex dynamic control strategies [131]. The system consists of three major processes: gasification, fuel cell, and gas turbine. The gasification process

uses a virtual gasifier that mainly generates syngas from any organic materials, including coal, biomass, and solid wastes. Since the gasifier relies on the virtual system based on developed models, the gasification system can use any type of gasification system, including fixed-bed, moving bed, entrained, and plasma system. Syngas composition as the main output of the virtual gasifier is then used for the fuel cell.

The fuel cell system is mainly based on a one-dimensional (1D) real-time distributed SOFC model, which was developed based on a planar design, co-flow, and anode-supported fuel cell configuration. The operation of a co-flow SOFC was represented by using a 20 cm x 20 cm electroactive area with respect to space in the direction of fuel and oxidant flow (i.e. down the direction of the flow channel) using a coupled finite volume approach, as its unit cell PEN geometry shown in Figure 6.5a and 1-D model discretization consisting of twenty nodes (only six nodes shown) displayed in Figure 6.5b [318].

A standard material using 441 stainless steel was considered for interconnects, while nickel-doped yttria-stabilized zirconia (Ni-YSZ), YSZ- lanthanum strontium magnetite (LSM), and YSZ were used as anode, cathode, and electrolyte, respectively [130]. This model was developed by considering the occurrence of both steam methane reforming and water-gas shift reactions (reactions no. 7-10, Table 2), in addition to electrochemical oxidation of the hydrogen component [131]. In this configuration both the anodic gas stream (unreacted H<sub>2</sub>O, CO, CO<sub>2</sub>, or other possible mixtures) and the cathodic gas stream (unreacted O<sub>2</sub> + N<sub>2</sub> + H<sub>2</sub>O) leaving the SOFC are directed to the gas turbine combustors to perform a direct combustion (H<sub>2</sub>/O<sub>2</sub> reaction) [128]. A complete interaction cycle

between the fuel cell model and the hardware system can be achieved in real-time as fast as 80 milliseconds.

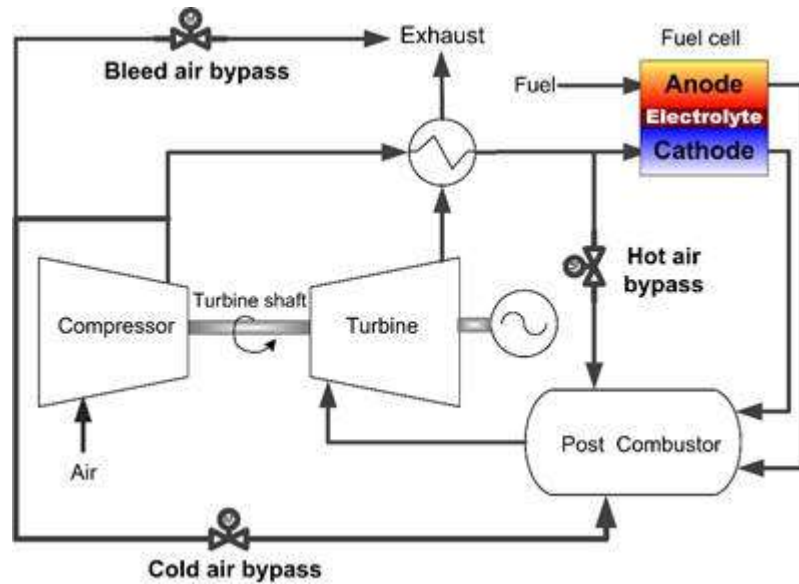
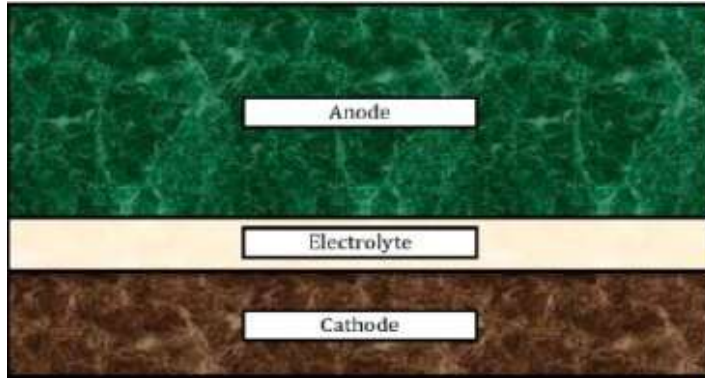
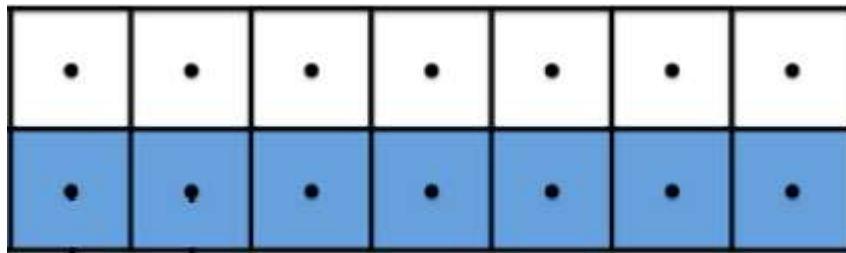


**Figure 6.4. Simplified process diagram of SOFC/GT hybrid power generation system [312]**

The gas turbine having a rotational speed of 40,500 rpm is a 120 kW Garret Series 85 auxiliary power unit (APU) for turbine and compressor systems. Additionally, various sensors and actuators were mounted in the hardware system to measure pressure, mass flow, temperature, and turbine rotational speed; a detailed description regarding these has been reported elsewhere [130]. The experiment used real sensor measurement of cathode inlet conditions in the model of a pressurized SOFC, with a normal rating of the GT operation of 40 kW [130, 131]. Syngas density was calculated using individual syngas composition taken from the National Institute of Standards and Technology (NIST) provided elsewhere [233].



(a)



(b)

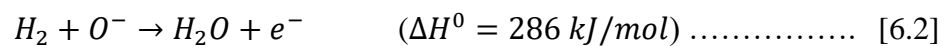
**Figure 6.5. A one-dimensional (1D) real-time distributed SOFC model: a) unit cell PEN geometry, and b) model discretization [318]**

Several major equations, including assumptions considered in the SOFC system, are presented as following:

$$Q = m_2 \cdot \Delta H_2 - m_1 \cdot \Delta H_1 \quad \dots\dots\dots [6.1]$$

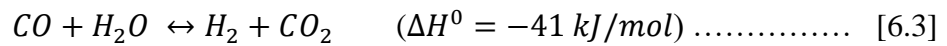
where  $Q$  is the fuel cell model net thermal effluent, while  $\Delta H_1$  and  $\Delta H_2$  were the sensible heats of the cathode feed stream before preheating and the post combustion exhaust after cooling with a reference to standard conditions. Meanwhile,  $m_1$  and  $m_2$  were the mass flow rate of the respective streams.

The hydrogen electrochemical oxidation occurring in the anode is presented as below:



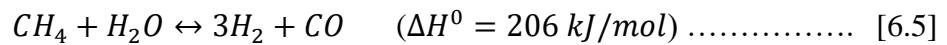
The model assumes hydrogen was the only electrochemically active component for hydrogen oxidation, as expressed in Eq. 6.2, while CO and CH<sub>4</sub> direct electrochemical oxidations are considered negligible as they have slow kinetics, slow mass transfer to the triple-phase boundary (TPB), and less active area available for electrochemical oxidation [130, 131]. Pressure loss across the fuel cell is not considered. The water-gas shift reaction for carbon monoxide and direct internal reforming reaction of methane (reaction no. 8 and 9, Chapter 1, Table 1.2) based on the first-order kinetic are considered following Eqs. 6.3-6.6 [130, 131].

Water-gas shifting:



$$K_{P,WGS} = \frac{P_{H_2} P_{CO_2}}{P_{H_2O} P_{CO}} = \frac{X_{H_2} X_{CO_2}}{X_{H_2O} X_{CO}} = \exp \left[ \frac{4276}{T} - 3.961 \right] \dots\dots\dots [6.4]$$

Steam methane reforming:



$$r_{SMR} = 4274 \frac{\text{mol}}{\text{s.m}^2.\text{bar}} P_{CH_4} \exp \left[ \frac{-82,000 \text{ J/mol}}{R_u T} \right] A_{rx} \dots\dots\dots [6.6]$$

where  $A_{rx}$  is a pre-exponential factor,  $T$  is the fuel cell solid temperature, and  $R_u$  is the ideal gas constant. The model incorporated dynamic calculation for thermal performance (heat generation, solid and gas temperature profiles), electrochemical characterization (Nernst potential, polarization losses, current density, and voltage), anode composition gradients, and associated fuel cell variables (power, fuel cell post combustor thermal effluent, etc.); a detailed description of the model development can be found elsewhere [130, 131, 318]. Table 6.3 summarizes the SOFC/GT parameters and initial operating condition.

**Table 6.3. SOFC/GT parameters and operating condition**

System parameters	Values
Fuel cell load	200 A
Anode recycle	0%
Initial fuel cell temperature	800°C
Total cell area	200 mm x 200 mm
Anode thickness	0.5 mm
Electrolyte thickness	0.008 mm
Cathode thickness	0.05 mm
Oxidant/fuel channel size	2 mm x 2 mm
Stack size	2,000 cell
Total stack mass	2,800 kg
Total stack heat capacity	2,100 kJ/K
<i>Fuel cell cathode inlet condition</i>	
Air mass flowrate	1.03 kg/s
Air temperature	490°C
Air pressure	240 kPag (~2.4 barg)
Air composition	21% O <sub>2</sub> , 79% N <sub>2</sub>
<i>Fuel cell anode inlet condition</i>	
Fuel temperature	800°C
Fuel pressure	512 kPa (~5.12 bar)
<i>Fuel cell initial condition</i>	
Cell voltage	0.77
Fuel utilization	70%
<i>Gas turbine initial conditions</i>	
Turbine load	40 kW
Turbine speed	40,500 rpm

### 6.2.3.2. System performance

The performance of a pressurized SOFC running on MSW/biomass derived syngas with a GT operation (if fully coupled, commonly known as SOFC/GT hybrid power generation) is evaluated in the hyper facility. The performance of the syngas running on the hybrid power system will be investigated based on the controlled load of the fuel cell

(200 A) because the fuel cell load is one of the most critical operating parameters that directly affects the stack power output and the lifetime of the fuel cell. The overall performance of the hybrid power system will be evaluated, including electrical system efficiency and major SOFC/GT operating parameters, such as current density, degradation rate, fuel utilization, fuel cell solid temperature, syngas composition changes within fuel cell nodes (i.e. H<sub>2</sub>, CO, CO<sub>2</sub>, and H<sub>2</sub>O), activation loss, ohmic loss, and Nernst potential.

Overall efficiency of the power generation system can be calculated as following (Eq. 6.7).

$$\eta_e = \frac{(total\ power\ output_{system}(kW))}{\left(m_{syngas} \left(\frac{kg}{h}\right) * LHV_{syngas} \left(\frac{MJ}{kg}\right) x 0.278 \left(\frac{kW}{MJ/h}\right)\right)} \dots\dots\dots [6.7]$$

where  $\eta_e$  is overall electrical system efficiency, while total power output of the system is total power output generated from the SOFC and the GT.  $m_{syngas}$  and  $LHV_{syngas}$  are mass flow rates of the syngas (kg/h), and the lower heating values of the syngas (MJ/kg). In practical application, it can also be expressed as following:

$$\eta_e = \frac{total\ power\ output_{system} (kW)}{\left(m_{syngas} \left(\frac{kg}{h}\right) x LHV_{syngas} \left(\frac{MJ}{m^3}\right) x 0.278 \left(\frac{kW}{MJ/h}\right) / syngas\ density \left(\frac{kg}{m^3}\right)\right)} \dots\dots [6.8]$$

In addition, the Nernst potential and cell voltage for SOFCs are based on expressions shown in Eq. 6.8 and 6.9, as below [268, 304].

$$V_{Nernst} = -\frac{\Delta G_{H_2O}^0}{2F} + \frac{R_u T}{2F} \ln \left[ \frac{P_{H_2} \cdot P_{O_2}^{0.5}}{P_{H_2O}} \right] \dots\dots\dots [6.9]$$

$$V_{cell} = V_{Nernst} - V_{dif} - V_{act} - V_{ohm} \quad \dots\dots\dots [6.10]$$

where  $V_{Nernst}$  is the Nernst potential or open circuit SOFC voltage (V);  $\Delta G_{H_2O}^0$  is the Gibbs free energy change of reaction at the standard state pressure (1 atm) and at temperature T (kJ/mol); F is faraday constant (C/mole);  $R_u$  is the ideal gas constant (J/mol.K);  $P_{H_2}$  is the partial pressure of hydrogen,  $P_{O_2}$  is the partial pressure of the oxygen;  $P_{H_2O}$  is the partial pressure of water;  $V_{cell}$  is cell voltage (V),  $V_{dif}$  is polarization or diffusion SOFC voltage over potential (V),  $V_{act}$  is activation SOFC voltage over potential (V), and  $V_{ohm}$  is Ohmic SOFC voltage over potential (V).

### 6.3. Results and discussion

This section presents the results from the evaluation of SOFC/GT hybrid power generation running on MSW gasification syngas in several focuses, including gasification and SOFC/GT system performance, that are discussed as following:

#### 6.3.1. Gasification performance

The performance of co-gasification of biomass and municipal solid waste has been presented in detail in the previous chapter (Chapter 3). The gasification was performed at various MSW ratios of 0, 20, and 40 wt.%. Neither technical nor operational concerns were found during the operation.

#### 6.3.2. SOFC/GT performance

The operating performance of a SOFC/GT hybrid power generating system is evaluated and presented as the following.

### 6.3.2.1. SOFC/GT operating performance

Among other types of power generation, the SOFC/GT hybrid power generation system has been recognized as one of the most efficient power generations (about 70% electrical efficiency) [23, 71, 72]. Total output stack power of the fuel cell and gas turbine are recorded to be further used to calculate the efficiency of the SOFC/GT system. With a total syngas flowrate and Eq. 6.7, the overall system efficiency can be determined and summarized as the following (Table 6.4).

**Table 6.4. The overall operating performance of SOFC/GT at steady state**

Parameters	Values
<i>Fuel cell</i>	
Total stack power, kW	307.1
Fuel cell load, A	200
Fuel cell utilization, %	70
Fuel cell voltage, V	0.77
Cell average temperature, °C	801.9
Delta solid temperature, °C	102.8
Inlet solid temperature, °C	742.2
Outlet solid temperature, °C	845.1
<i>GT</i>	
Total GT output power, kW	40
<i>Syngas fuel</i>	
Total syngas flow, g/s (kg/h)	321.9 (1,158.8)
Syngas LHV, MJ/Nm <sup>3</sup> (MJ/kg)	5.96 (2.18)
<i>Overall system performance</i>	
Total fuel cell transferred heat, kW	667.1
Electrical efficiency, %	49.5

It should be noted that the data presented above (Table 6.4) were taken once the system achieved a steady-state condition. Regulating the syngas fuel valve and fuel utilization was required to achieve a stable load of the fuel cell (200 A) and the maximum stack output power of the fuel cell, while the output power of the GT (40 kW) was

maintained as the rating output in the hyper facility. As it can be seen, the stack output power was achieved at 307.1 kW, and considering total syngas flow rate of 321.9 g/s and total system output power of 347.1 kW, a system electrical efficiency of 49.5% was generated.

In addition to the system operating performance, other major operating parameters of the SOFC/GT including current density, degradation rate, solid and gas temperature, syngas composition change, activation loss, ohmic loss, and Nernst potential are presented next.

#### **6.3.2.1.1. Current density**

Current density is a critical operating parameter as it directly determines total power generated from the fuel cell [304]. It also closely relates to the solid temperature of the cell. As can be seen in Figure 6.6, current density increases at the beginning of the cells and decreases from the middle (around node 12-13) to the end (node 20). Afterwards, the rate of hydrogen oxidation by electrochemical process is higher than hydrogen generation by water gas, water gas shift, and steam methane reforming reactions (reaction no. 7-10, Table 1.2). H<sub>2</sub> is the only syngas constituent considered to be oxidized in the electrochemical process, while CO and CH<sub>4</sub> direct electrochemical oxidations are considered negligible, as stated earlier [268].

As can be seen, a higher current density region is achieved at the elevated solid temperature segments. A high current density was also generally observed at a relatively high partial pressure of H<sub>2</sub> as well as higher Nernst potential [131]. With a higher load on the fuel cell, the fuel utilization must increase to meet the load demand, which in turn will raise the usage of hydrogen and oxygen producing more current, ultimately increasing the

current density of the fuel cells. An increase of current density commonly results in a decrease of voltage and an increase of power density [311]. However, a constant operating temperature and a stable current density must be maintained; otherwise, thermal gradient as an indicator of thermal stress might occur. Thermal stress can create a long-term voltage degradation and lead to fracture and immediate failure of the fuel cells [319].

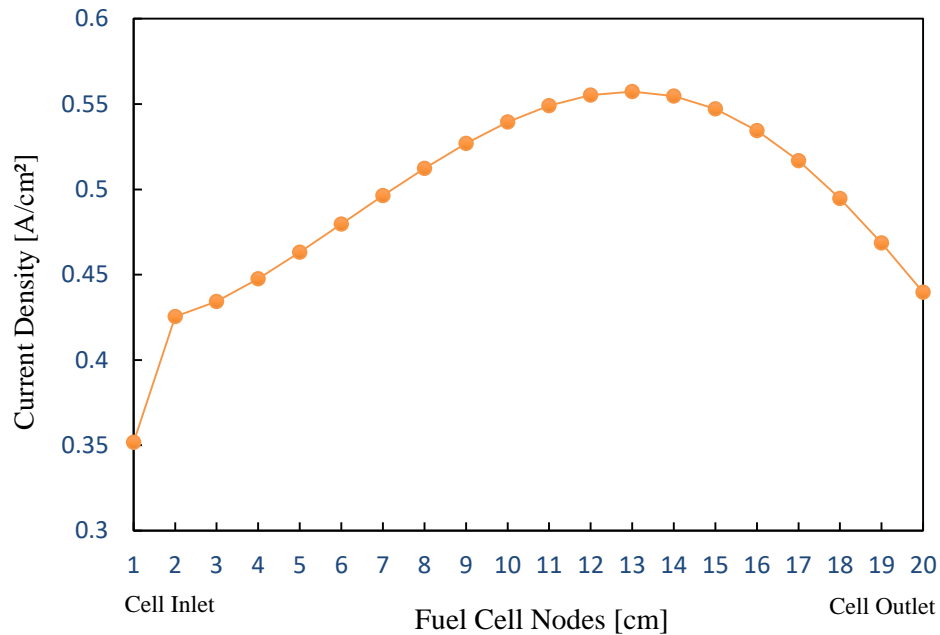


**Figure 6.6. Current density profile across the fuel cells**

### 6.3.2.1.2. Degradation rate

Degradation rate is another critical parameter that must be considered during operation of the fuel cells. It is basically a consequence of the behavior of current density, fuel utilization and temperature [268]. Degradation of the fuel cell will typically increase due to a high load operation, but it can be also be caused by the carbon deposition occurring at high temperatures [320]. Figure 6.7 shows the initial degradation rate at different parts along the fuel. Within cell nodes 1-11, the rate of degradation gradually

increases and reaches the peak at node 12. After that point, the degradation rate decreases till the cell outlet, following the profile of current density. Typically, in a SOFC, maintaining operation at a fixed high temperature is recommended to have the least degradation rate [268, 319].

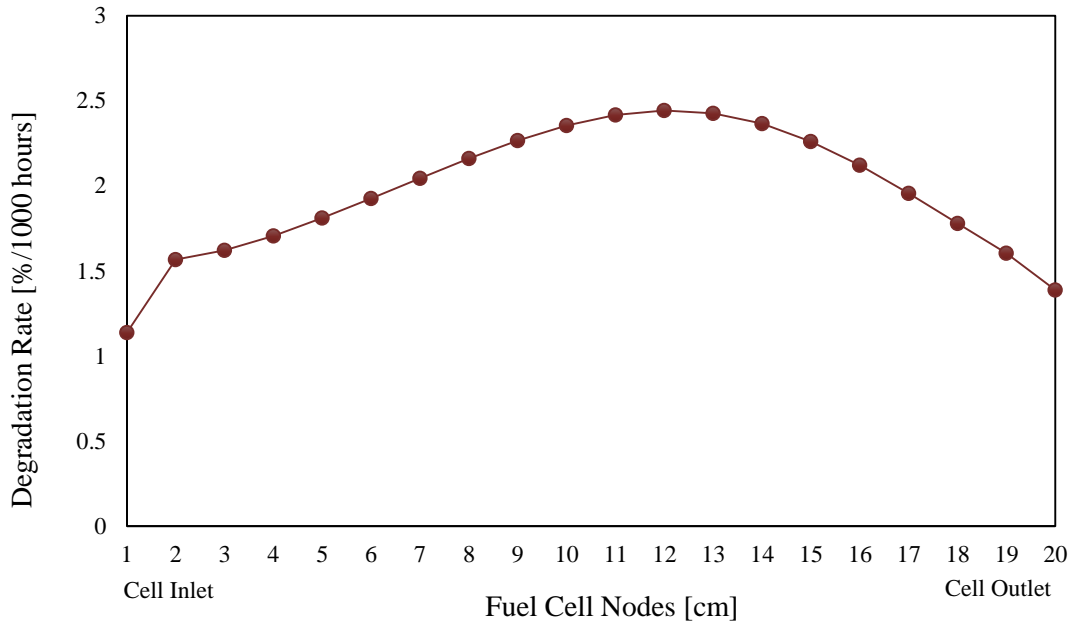


**Figure 6.7. Degradation rate profile across the fuel cells**

### 6.3.2.1.3. Fuel cell solid and gas temperature

Solid fuel cell temperature is another important operating parameter of the fuel cells and directly related to the current density. It also depends on the heat generated by the electrochemical reactions and the transferred heat to the airflow in each node [268]. As it can be seen in Figure 6.8 and 6.9, solid and gas cell temperatures increase along the cell. Solid temperature increases along the cell with a non-linear trend since the reactions are taking place. In addition, the air temperature is increasing as well, reducing the  $\Delta T$  between solid and air and consequently the heat flux from solid to gas. An increased solid

temperature is observed, perhaps due to an increased current density occurring from the initial nodes (node 1) to mid nodes (nodes 12) of the cells (following Figure 6.5). Also, the electrochemical reactions ( $\text{H}_2 + \text{O}^{2-} = \text{H}_2\text{O} + 2\text{e}^-$ ) directly take place and minimize the possible required reactions of producing  $\text{H}_2$  through water gas, water-gas shift and steam methane reactions (reactions no. 7-10, Chapter 1, Table 1.2).

Similarly, fuel cell gas temperature increases along the nodes. The increased temperature is predominantly due to the exothermic reactions (mostly water-gas shift (WGS) reaction) taking place.

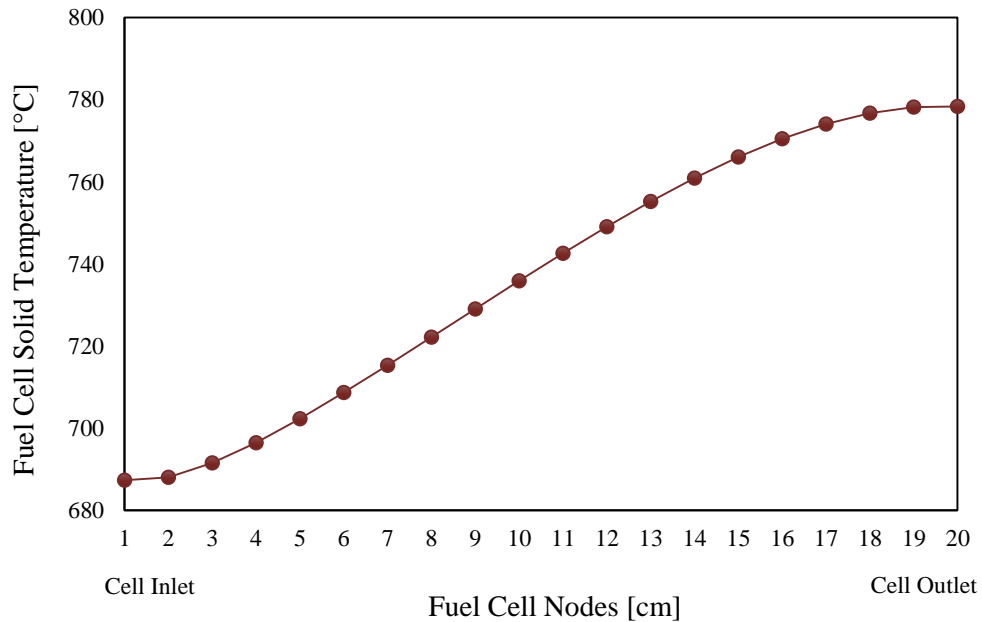


**Figure 6.8. Fuel cell solid temperature across the fuel cells**

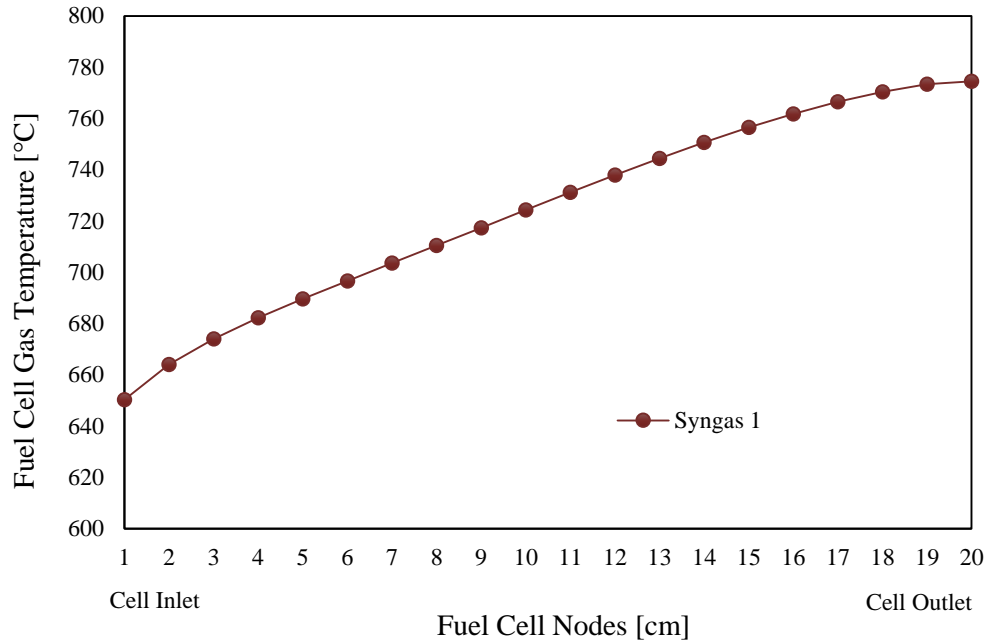


**Figure 6.9. Fuel cell gas temperature across the fuel cells**

#### 6.3.2.1.4. Syngas composition changes

Syngas composition changes within the fuel cells accordingly. In the first part of the cell, where less current is generated, H<sub>2</sub> mole fraction increases along the cell nodes, as shown in Figure 6.10 (node 1-2). Starting from node 2, the generation of H<sub>2</sub> through water gas and water-gas shift (WGS) reactions decreases along the nodes due to H<sub>2</sub> consumption by the electrochemical process ( $\text{H}_2 + \text{O}^{2-} = \text{H}_2\text{O} + 2\text{e}^-$ ). Even if high temperature contributes to shifting the equilibrium of WGS reaction toward the reactant (reaction no. 8, Chapter 1, Table 1.2:  $\text{CO} + \text{H}_2\text{O} = \text{CO}_2 + \text{H}_2$ ), the high consumption of H<sub>2</sub> and consequent formation of water drive the equilibrium to the products' side [268]. Similarly, CO mole fraction substantially decreases in the beginning of the cell due to, perhaps, a spontaneous WGS reaction (Figure 6.11). However, due to sufficient STCR (STRC=2.0), with the presence of water, the generation of CO through reactions of steam

methane reforming, water-gas, and steam reforming (reaction no.7, 9, 10, Chapter 1, Table 1.2) is continuously present to produce CO in the cells. Along the nodes, the generation of CO decreases due to the WGS reaction that converts CO into H<sub>2</sub>.

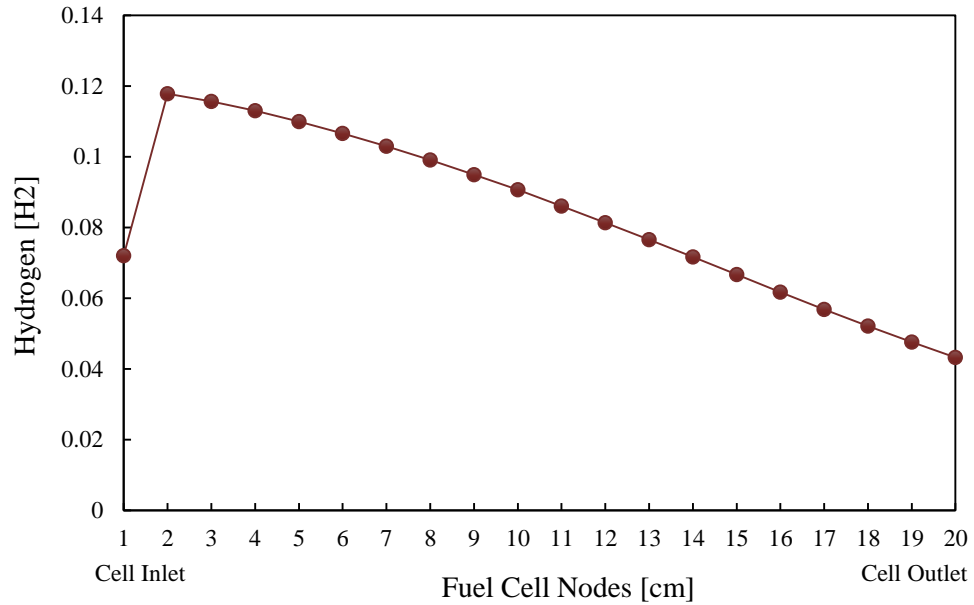


**Figure 6.10. H<sub>2</sub> profile across the fuel cells**

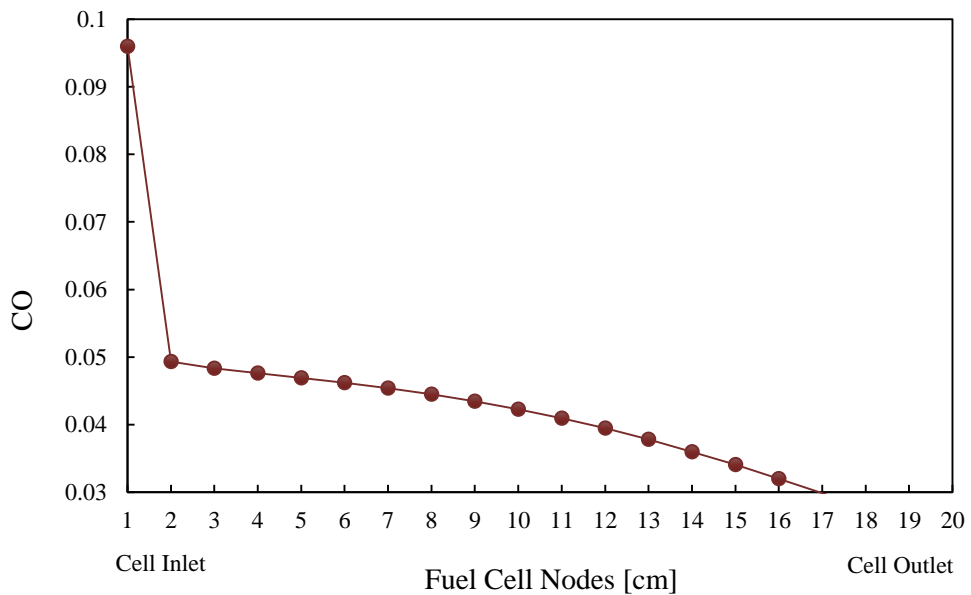


**Figure 6.11. CO profile across the fuel cells**

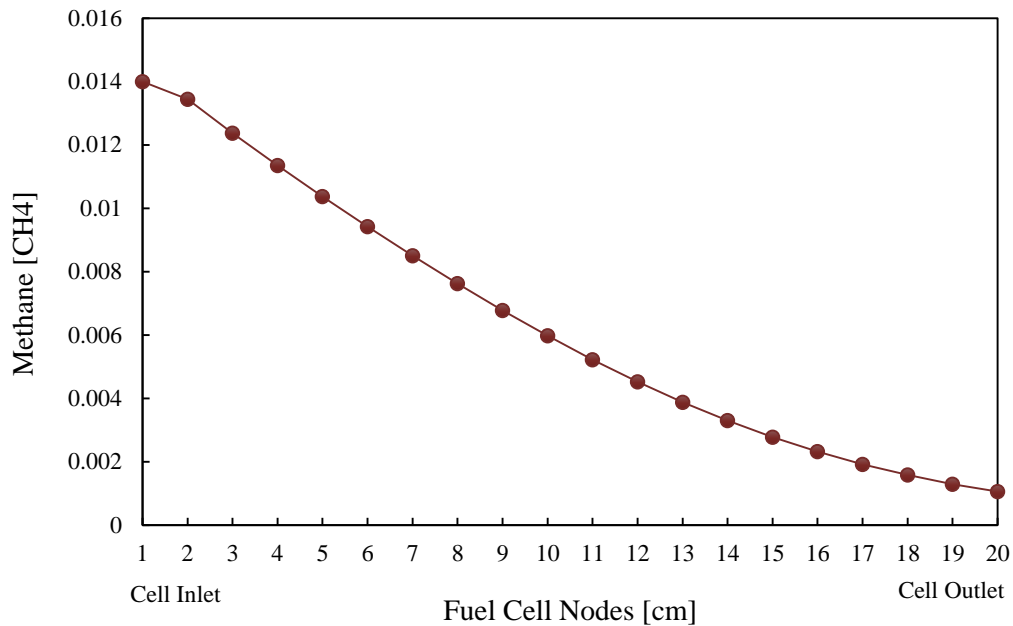


**Figure 6.12. CH<sub>4</sub> profile across the fuel cells**

Methane (CH<sub>4</sub>) is another critical composition in syngas. Especially in fuel cells, without sufficient water (STRC < 2.0), the presence of CH<sub>4</sub> potentially increases the carbon deposition [304, 321]. Figure 6.12 shows that CH<sub>4</sub> concentration decreased along the cells. It mainly reflects the reaction of steam methane reforming that converts CH<sub>4</sub> into CO and H<sub>2</sub> (reaction no. 7, Chapter 1, Table 2), with the presence of water.

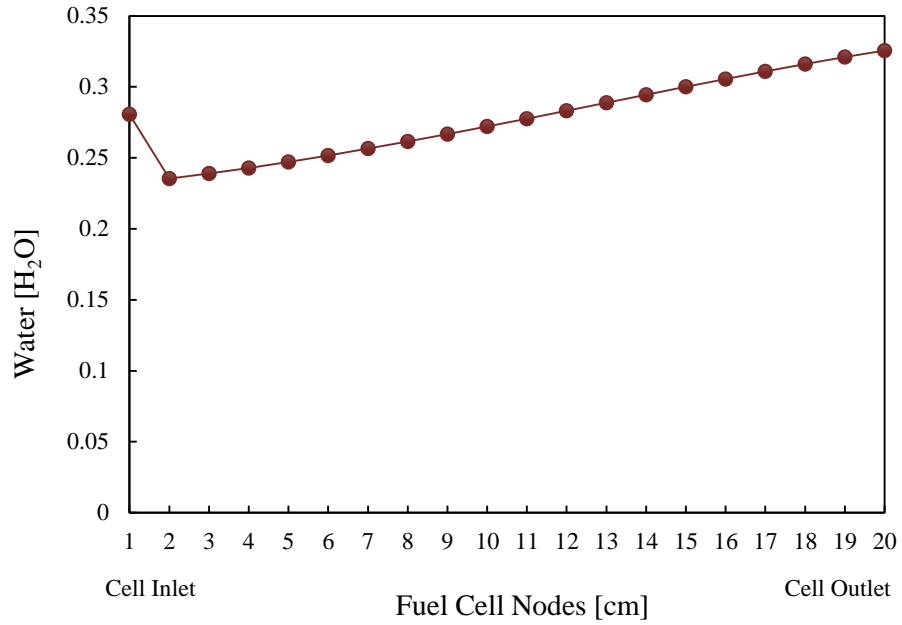


**Figure 6.13. H<sub>2</sub>O profile across the fuel cells**

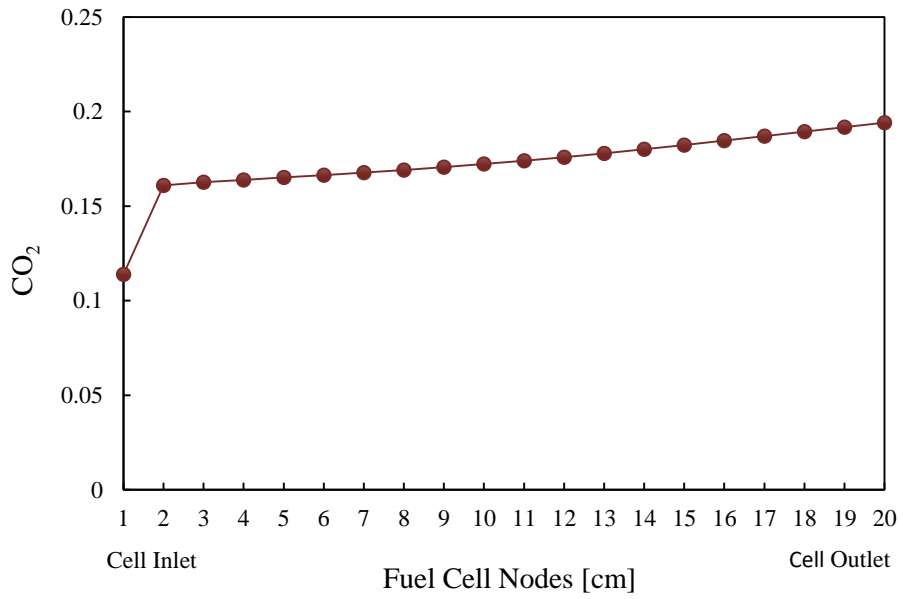


**Figure 6.14. CO<sub>2</sub> profile across the fuel cells**

Water (H<sub>2</sub>O) plays the most critical part in the fuel cells. It essentially shifts the reactions of carbon present in the syngas into CO and H<sub>2</sub> through steam methane reforming and WGS reactions (reaction no. 7 and 8, Chapter 1, Table 1.2). Also, H<sub>2</sub>O is generated by the oxidation of oxygen in the anode; consequently, its mole fraction decreases at the beginning (up to node 2), while its presence then increases till the end of the cell nodes (Figure 6.13). The electrochemical process mainly impacts this profile due to the generation of H<sub>2</sub>O ( $\text{H}_2 + \text{O}^{2-} = \text{H}_2\text{O} + 2\text{e}^-$ ).

Similar to the H<sub>2</sub>O profile, the same happens to CO<sub>2</sub> mole fraction, as a consequence of CO utilization along the cell through water-gas shift reaction. Thus, a high CO content of the syngas directly contributes to the generation of CO<sub>2</sub> through the WGS reaction ( $\text{CO} + \text{H}_2\text{O} = \text{CO}_2 + \text{H}_2$ ); the trend is shown in Figure 6.14.

#### **6.3.2.1.5. Activation loss**

Activation loss can be defined using the Butler-Volmer equation [268] and is generally caused by sluggish electrode kinetics as a result of complex surface electrochemical reaction steps, and relates to an activation energy of each reaction [311]. Activation losses generally follow Arrhenius behavior and can decrease cell voltage; thus, this parameter is essential to consider in fuel cell operation.

As seen in Figure 6.15, activation losses decline along the nodes. Generally, activation losses are affected by the solid and gas temperature (Figures 6.8-9) and decline exponentially with increasing temperature [311].

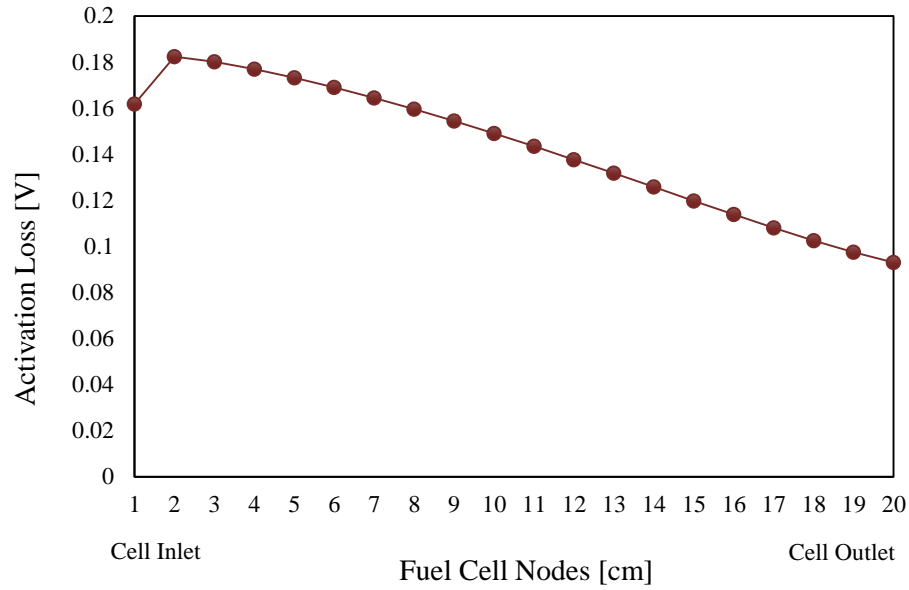


**Figure 6.15. Activation loss profile across the fuel cells**

**6.3.2.1.6. Ohmic loss**

Ohmic losses occur because of resistance to the flow of ions in the electrolyte and resistance to the flow of electrons through the electrode. The dominant ohmic losses through the electrolyte are reduced by decreasing the electrode separation and enhancing the ionic conductivity of the electrolyte [311]. As seen in Figure 6.16, ohmic losses generated in the fuel cell are minimal; commonly in a high temperature fuel cell, such as SOFCs, resistances or ohmic losses are minimal [311].

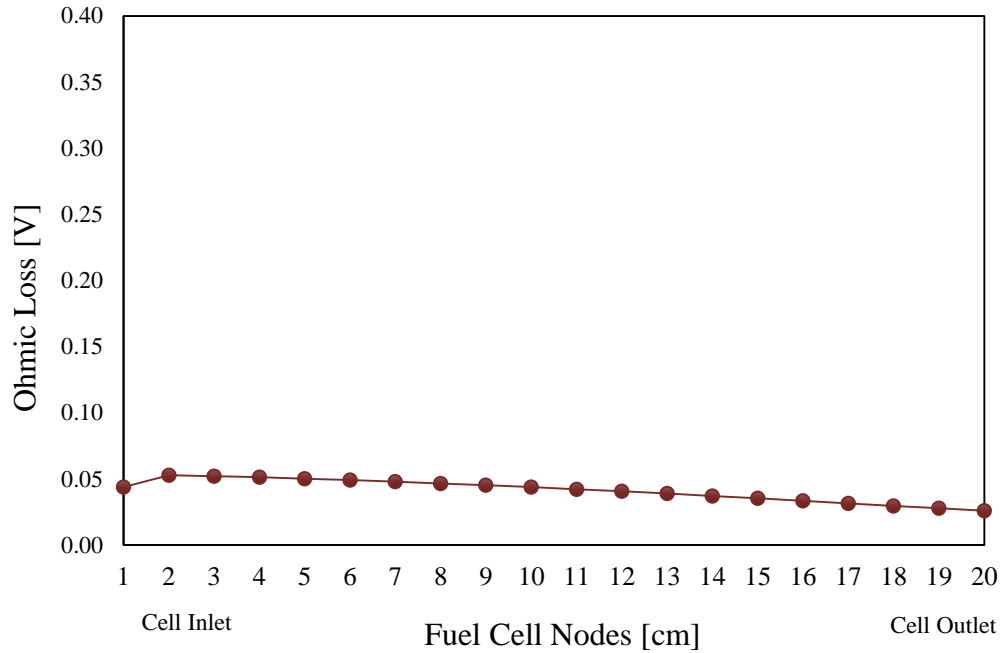


**Figure 6.16. Ohmic loss profile across the fuel cells**

### 6.3.2.1.7. Nernst potential

Nernst potential is an important parameter in fuel cell operation. The Nernst equation provides a relationship between the ideal standard potential ( $E^\circ$ ) for the cell reaction and the ideal equilibrium potential ( $E$ ) at other partial pressures of reactants and products. The ideal standard potential ( $E^\circ$ ) at 298 K as a result of the reaction of  $H_2$  and  $O_2$  is 1.229 V [311]. Nernst potential is calculated according with Eq. 6.9, assuming that hydrogen is the only species that is directly oxidized. The water-gas shift reactions are considered fast enough to be at equilibrium and to negate the effect of direct electrochemical CO oxidation on the cell [269]. Nernst potential is higher for lower temperature and higher  $H_2$  partial pressure. At the beginning of the cell nodes, its profile mainly follows the profile of  $H_2$  content distribution, which is directly proportional to  $H_2$  partial pressure [268]. At the first nodes (node 1-2), as the  $H_2$  content increases (as shown in Figure 6.10),

the partial pressure of  $H_2$  also rises, thus consequently increasing the Nernst potential.

The minimum of Nernst potential is generally observed at the cell outlet as the  $H_2$  content decreases, consequently reducing the  $H_2$  partial pressure [311], as shown in Figure 6.17.

Therefore, syngas containing a higher  $H_2$  content will generate a higher partial pressure across the cells and increase the Nernst potential, leading to an increase of the fuel cell stack power.

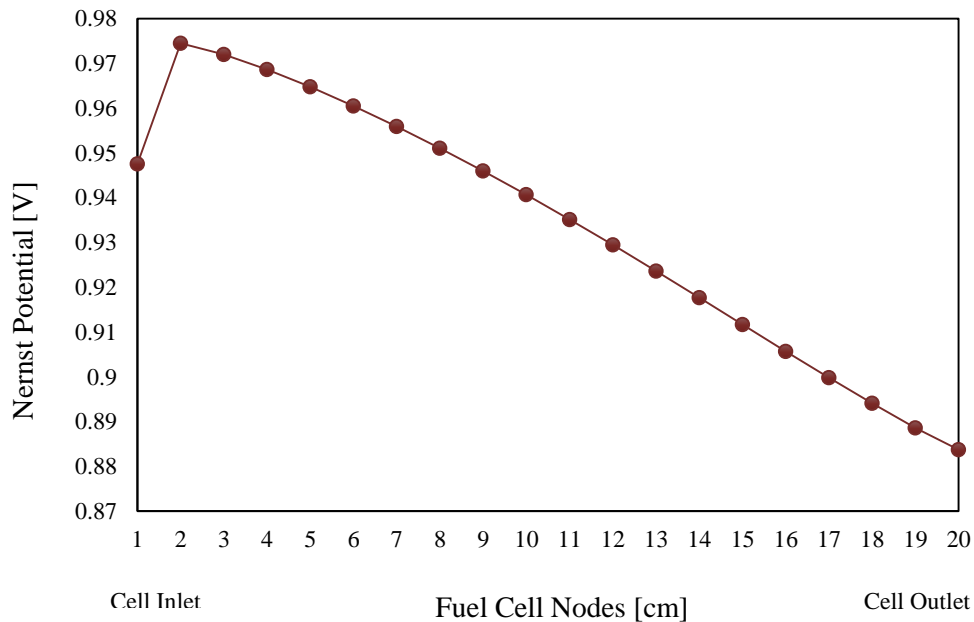


**Figure 6.17. Nernst potential across the fuel cells**

#### 6.4. Conclusions

This study aims to investigate the potential use of municipal solid waste (MSW) syngas generated from a downdraft gasification technology developed at Oklahoma State University for an advanced SOFC/GT hybrid power generating system. The syngas produced from co-gasification of MSW and biomass at 40 wt.% MSW ratio was found to be feasible applied in the SOFC/GT hybrid power generation system. The utilization of

the syngas in SOFC/GT hybrid power generation resulted in a total syngas flow of 321 g/s, a total stack power of 307 kW, and a gas turbine output of 40 kW, consequently generating a system electrical efficiency of 49.5%.

A further analysis of the operating performance of an SOFC/GT hybrid power generating system was investigated. Fuel cell SOFC operating performance parameters including current density, degradation rate, fuel cell solid and gas temperature, composition changes, activation loss, ohmic loss, and Nernst potential, were evaluated at a steady-state condition. No technical challenges were found during the operation. To confirm with these results, a further research is required to create a dynamic performance of SOFC/GT hybrid power generation using syngas generated from MSW gasification. The results support the future potential of MSW processing for a high efficiency power generating system and for reducing environmental footprints, including air pollution and soil contamination, due to combustion technologies and landfill disposals.

## CHAPTER 7

### SUMMARY AND RECOMMENDATIONS FOR FUTURE WORK

## 7.1. Summary

The current study focused on development of advanced power generation from gasification of biomass and municipal solid waste as a promising technology for power generation.

Chapter 1 presents a literature review on latest development of distributed power generation derived from gasification of biomass and municipal solid waste. Many existing commercial power equipment can be run with syngas without major modifications. Among internal combustion engines, the least demanding are natural gas engines, followed by gasoline and diesel engines, while among micro gas turbines, no modification is required from current technology. Among gas turbines, the modifications are required in the fuel system, compressor, and combustor. Stirling engines and Organic Rankine Cycle generators still require extensive research and experimental data for their operation with syngas. Similarly, fuel cells offer a promising future, however, reducing syngas contaminants to an acceptable level and increasing the conversion efficiency of syngas to power, by utilizing an advanced hybrid power system such as FC/GT hybrid units, are challenges.

Compared to biomass gasification, municipal solid waste gasification is more challenging due to variation in feedstock composition. Thermal plasma gasification is considered a promising technology suitable for utilizing municipal solid waste; however, its broad commercialization is hindered due to high CAPEX and energy consumption.

Generating power through waste gasification is more economical due to the minimal transportation needed and revenue of tipping fees. However, the current technology is still evolving to accommodate the complexity of the feedstock, to reduce the power

consumption, and to increase the process efficiency. From a socio-environmental standpoint, gasification of biomass and MSW is expected to bring significant benefits to local communities by creating specific employment streams as well as new economic activities and networks. In addition, contrary to the conventional incineration and landfilling practices, gasification releases less greenhouse gas emissions and pollutants.

In Chapter 2, through experimental tests of small scale power plant consisting of a 60-kW downdraft gasifier incorporated with a 10 kW SI engine running on 100% syngas, it was demonstrated that with little modification of the air intake system of the engine using a single venturi pipe, a consistent and stable operation was achieved at maximum load of 5 kW (with an overall electrical efficiency of 21.3%) and 9 kW (with an overall electrical efficiency of 22.7%) using syngas and natural gas, respectively. The gasifier, operated at equivalence ratio of 0.20, led to combustion zone temperature of 800 to 900°C with syngas LHV of 6.47 MJ/Nm<sup>3</sup> containing H<sub>2</sub>, CO, CH<sub>4</sub>, C<sub>2</sub>H<sub>4</sub>, and C<sub>2</sub>H<sub>6</sub> at levels of 11.4 ± 1.9%, 21.0 ± 2.2%, 5.5 ± 1.1%, 0.15 ± 0.1%, and 1.33 ± 0.3% v/v, respectively. From an environmental standpoint, the engine CO, NO<sub>x</sub>, and HC emissions running on syngas were, in overall, lower than those running on natural gas; the engine CO<sub>2</sub> and SO<sub>2</sub> emissions at the highest load were comparable.

MSW was co-gasified with biomass for producing syngas and generate power in Chapter 3. The gas intake was modified using a two-series venturi pipe. A consistent and stable engine operation was achieved at maximum load of 5 kW at MSW ratio of up to 40 wt.%. Gasifier performance with combustion zone temperature (700-950°C) was stable and produced syngas with maximum LHV of 6.91, 7.74, and 6.78 MJ/Nm<sup>3</sup> at MSW ratio of 0, 20, and 40 wt.%, respectively. The overall electrical efficiencies of 22, 20, and

19.5% were obtained at MSW ratios of 0, 20, and 40 wt.%, respectively. The engine CO, NO<sub>x</sub>, SO<sub>2</sub> and CO<sub>2</sub> emission decreased with the increasing load, while HC emission increased with the increasing load. CO, NO<sub>x</sub>, and CO<sub>2</sub> emissions decreased, while HC and SO<sub>2</sub> emissions increased with increasing MSW ratio.

Chapter 4 discusses economics of a downdraft gasification power generation system with a feed rate of 2.5 tons per day and an output power of 60 kW. The results showed that among seven major economic parameters being evaluated (i.e. the feedstock (biomass) cost, electricity selling price, feed-in-tariff (FIT), output power, tax rate, tipping fee, and the labor cost), the FIT results in the greatest impact on the project's NPV, followed by the electricity selling price, the output power and the tipping fee, while the labor and feedstock cost and the tax rate generate a negative impact for the power generation. The power system offers a payback period (PP) of 7.2 years, while an internal rate of return (IRR), a modified internal rate of return (MIRR), and a net present value (NPV) are achieved at 12.0%, 8.0%, and \$104,242, respectively. In comparison with a 250-kW downdraft gasification power plant, the downdraft gasification power system developed at Oklahoma State University performed better with a shorter PP and a higher IRR. However, these results may vary significantly based on local economic factors and assumptions made.

Chapter 5 presents a modeling of low-temperature plasma gasification system as a potential environmentally-friendly alternative to treat municipal solid waste disposal as compared to conventional plasma gasification. The energy consumption of the plasma torch decreased from 3,816 kW at conventional condition (4000°C) to 3,157, 2,775, and 2,358 kW at temperatures of 2,500, 2000, and 1,500°C, respectively; the plasma

gasification efficiency (PGE) increased with decrease in temperature (48.7%, 48.9%, and 49.2% at 2,500, 2,000, and 1,500°C, respectively). A low mass flow-rate of 1.4 kg/s for the plasma gas resulted in optimal performance: LHV 5.41 MJ/Nm<sup>3</sup> and HHV 5.90 MJ/Nm<sup>3</sup> at plasma temperature of 1,500°C, generating syngas composed mainly of H<sub>2</sub> and CO (with 46.4% in total).

Chapter 6 presents the potential use of syngas generated from co-gasification of MSW and biomass in an advanced solid oxide fuel cell and gas turbine (SOFC/GT) hybrid power generating system. The syngas composition produced from co-gasification of MSW and biomass at 40 wt.% MSW ratio was tested in SOFC/GT hybrid power generation system at National Energy Technology Laboratory (NETL). A total syngas flow of 321 g/s, a total stack power of 307 kW, and a gas turbine output of 40 kW was observed with a system electrical efficiency of 49.5%.

Therefore, an advanced power generation from gasification of biomass and municipal solid waste is a promising option for efficient utilization of wastes, distributed power generation and for supporting economic development in rural regions.

## **7.2. Future work**

Recommendations for future development are:

1. An improved design of the gasifier reactor with a refractory lining

The gasifier reactor used in the current study was not equipped with the refractory lining thus the experiments could only use a low equivalence ratio (~0.2) generating a reactor temperature of 750-900°C considering operational safety and gasifier reactor life. A higher equivalence ratio will lead to a higher reactor temperature (> 1,000°C) that can

improve hydrogen fraction while minimizing tar concentration through decomposition reactions of tars and hydrocarbons following the reactions:  $pC_xH_y \rightarrow qC_nH_m + rH_2$  and  $C_nH_m \rightarrow nC + m/2 H_2$ ).

Moreover, total height of the gasifier reactor can be reduced to fit the entire power system within a trailer size for a mobile unit power generation. Technical aspects should be considered when making adjustment of the reactor height to keep the reactor performance.

## 2. The power generation using a higher engine capacity

The power generating unit used in the current study is a natural gas internal combustion engine having a nameplate capacity of 10 kW. The gasifier as the main equipment of the power plant has a nameplate capacity of 60 kW thus the current engine generator set is much below the size required. Therefore, an experimental investigation using a 60-kW engine capacity is critically essential for further analysis on performance of the power plant and emissions.

## 3. Advanced syngas cleaning system using a non-thermal plasma reformer

The syngas cleaning system is paramount for the power plant system based on gasification technology. For removing syngas tars and contaminants, the current study used water-acetone solution, which is high-cost and potentially impractical for application in rural areas because the solution must be replaced after several hours of operation. Therefore, an advanced syngas cleaning system is extremely required to increase the feasibility of the power plant using syngas derived from gasification technology. One of the promising technologies to reduce syngas tars and increase hydrogen concentration of the syngas is a non-thermal surface dielectric barrier discharge

(SDBD) plasma reformer. The technology is current under development through a collaborative project of Oklahoma State University and University of California-Merced.

4. Further operational exploration of advanced solid oxide fuel cell and gas turbine (SOFC/GT) hybrid power generation system using syngas generated from municipal solid waste gasification

Deploying syngas in a SOFC/GT hybrid power generation system can lead to one of the highest possible efficiencies of a power generation system (up to 70%). However, numerous intensive research must be conducted to overcome current operational issues of the hybrid power generation system. The short fuel cell lifespan, highly sensitive to contaminants, and complex control strategy are current major challenges of this hybrid power system. Unlike the gas turbine that has been well developed for decades and is a very mature technology, the development of the fuel cell needs a substantial research and development to reduce cost and increase flexibility. Advanced standalone fuel cell power generation for distributed generation is still very limited worldwide. Moreover, using syngas generated from MSW may subject fuel cell to harmful pollutants (such as H<sub>2</sub>S) that can poison and accelerate degradation of the fuel cell.

## References

1. IEA., *World Energy Outlook 2017*. 2017: Organisation for Economic Co-operation and Development, OECD.
2. Peters, G.P., et al., *Towards real-time verification of CO<sub>2</sub> emissions*. *Nature Climate Change*, 2017. **7**(12): p. 848-850.
3. Hausfather, Z. *Analysis: Global CO<sub>2</sub> emissions set to rise 2% in 2017 after three-year 'plateau'*. 2017 [cited 2018 February 14]; Available from: <https://www.carbonbrief.org/analysis-global-co2-emissions-set-to-rise-2-percent-in-2017-following-three-year-plateau>.
4. IEA, *World Energy Outlook 2017*. 2017, International Energy Agency: Paris.
5. Fair, D. *Gasification - Positioning for Growth*. in *2015 Gasification Technologies Conference*. 2015. Colorado Springs: Gasification Technology Council.
6. Tennant, J.B. *Gasification Systems Program - Slide Library*. 2015.
7. Denton, D. *Advanced energy technology development at RTI International*. in *2017 Syngas Technologies Conference*. 2017. Colorado Springs: Global Syngas Technologies Council
8. Denton, D. *Update on Clean Energy R&D Projects and Programs at RTI International*. in *2015 Gasification Technologies Conference*. 2015. Colorado Springs: Global Syngas Technologies Council.
9. Arthur R. Seder, J., *Building the Nation's First Coal Gasification Plant*. *Technology in Society*, 1988. **10**: p. 131-143.
10. NETL *Great Plains Synfuels Plant*.
11. Reed, T.B.D., A., *Handbook of Biomass Downdraft Gasifier Engine Systems*. 1988, Golden: Solar Energy Research Institute.
12. Bank, T.W., *What a waste: A global review of solid waste management*. 2012: Washington D.C.
13. EIA *Total Capacity of Distributed and Dispersed Generators by Technology Type*. 2017.
14. Onderdonk, T. *2017 Outlook for Energy: A View to 2040*. in *2017 Syngas Technologies Conference*. 2017. Colorado Springs.
15. EIA *International Energy Outlook 2017*. 2017.
16. Zogg, R.S., Chad; Roth, Kurt; Brodrick, James, *Using Internal-Combustion Engines For Distributed Generation*. 2007: p. 76-80.
17. Robb, D. *CCGT: Breaking the 60 per cent efficiency barrier*. 2010.
18. Ratafia-Brown, J., et al., *Major environmental aspects of gasification-based power generation technologies*. 2002, National Energy Technology Laboratory (NETL): Morgantown.
19. Seltenrich, N., *Emerging Waste-to-Energy Technologies: Solid Waste Solution or Dead End?* *Environ Health Perspect*, 2016. **124**(6): p. A106-11.
20. Verma, R., et al., *Toxic Pollutants from Plastic Waste-A Review*. *Procedia Environmental Sciences*, 2016. **35**: p. 701-708.
21. Jenkins, S. *Environmental Advantages of Gasification: Public and Agency Awareness*. in *2015 Gasification Technologies Conference*. 2015. Colorado Springs: Global Syngas Technologies Council.

22. Higman, C. *GSTC Syngas Database: 2017 Update*. in *2017 Syngas Technologies Conference*. 2017. Colorado Springs.
23. Moliere, M. *From pyrolysis to electric power An insight*. in *21th International Symposium on Analytical and Applied Pyrolysis*. 2016. Nancy.
24. Adams, T.A., et al., *Energy Conversion with Solid Oxide Fuel Cell Systems: A Review of Concepts and Outlooks for the Short- and Long-Term*. *Industrial & Engineering Chemistry Research*, 2012. **52**(9): p. 3089-3111.
25. Kumar, A., D. Jones, and M. Hanna, *Thermochemical Biomass Gasification: A Review of the Current Status of the Technology*. *Energies*, 2009. **2**(4): p. 556-581.
26. Hands, R. *Market drivers for the syngas industry*. in *2017 Syngas Technologies Conference*. 2015. Colorado Springs: Global Syngas Technologies Council.
27. La Villetta, M., M. Costa, and N. Massarotti, *Modelling approaches to biomass gasification: A review with emphasis on the stoichiometric method*. *Renewable and Sustainable Energy Reviews*, 2017. **74**: p. 71-88.
28. Nussbaumer, T., *Combustion and co-combustion of biomass: fundamentals, technologies, and primary measures for emission reduction*. *Energy & fuels*, 2003. **17**(6): p. 1510-1521.
29. Indrawan, N., et al., *Engine power generation and emission performance of syngas generated from low-density biomass*. *Energy Conversion and Management*, 2017. **148**: p. 593-603.
30. Arena, U., *Process and technological aspects of municipal solid waste gasification. A review*. *Waste Manag*, 2012. **32**(4): p. 625-39.
31. Qian, K., et al., *Recent advances in utilization of biochar*. *Renewable and Sustainable Energy Reviews*, 2015. **42**: p. 1055-1064.
32. Lopes, E.J., L.A. Okamura, and C.I. Yamamoto, *Formation of Dioxins and Furans during Municipal Solid Waste Gasification*. *Brazilian Journal of Chemical Engineering*, 2015. **32**(1): p. 87-97.
33. Indrawan, N.K., Ajay; Kumar, Sunil, *Recent Advances in Power Generation Through Biomass and Municipal Solid Waste Gasification*, in *Coal and Biomass Gasification: Recent Advances and Future Challenges*, S.D.A.K.A.V.S.M.B. Thallada, Editor. 2018, Springer: Singapore. p. 369-402.
34. Psomopoulos, C.S., A. Bourka, and N.J. Themelis, *Waste-to-energy: A review of the status and benefits in USA*. *Waste Manag*, 2009. **29**(5): p. 1718-24.
35. Isaksson, J. *Commercial CFB Gasification of Waste and Biofuels - Operational Experiences in Large Scale*. in *2015 Gasification Technologies Conference*. 2015. Colorado Springs: Global Syngas Technologies Council.
36. Mountouris, A., E. Voutsas, and D. Tassios, *Solid waste plasma gasification: Equilibrium model development and exergy analysis*. *Energy Conversion and Management*, 2006. **47**(13-14): p. 1723-1737.
37. Ruiz, J.A., et al., *Biomass gasification for electricity generation: Review of current technology barriers*. *Renewable and Sustainable Energy Reviews*, 2013. **18**: p. 174-183.
38. Tame, N.W., B.Z. Dlugogorski, and E.M. Kennedy, *Formation of dioxins and furans during combustion of treated wood*. *Progress in Energy and Combustion Science*, 2007. **33**(4): p. 384-408.
39. Sikarwar, V.S., et al., *An overview of advances in biomass gasification*. *Energy & Environmental Science*, 2016. **9**(10): p. 2939-2977.

40. McKendry, P., *Energy production from biomass (part 3): gasification technologies*. Bioresource Technology, 2003. **83**: p. 55-63.
41. Ong, Z., et al., *Co-gasification of woody biomass and sewage sludge in a fixed-bed downdraft gasifier*. AIChE Journal, 2015. **61**(8): p. 2508-2521.
42. Robinson, T., et al., *Air-blown bubbling fluidized bed co-gasification of woody biomass and refuse derived fuel*. The Canadian Journal of Chemical Engineering, 2017. **95**(1): p. 55-61.
43. Hands, R. *Market drivers for the syngas industry*. in *Gasification and Syngas Technology Council*. 2017. Colorado Springs.
44. Willquist, K., et al. *Critical metal extraction from municipal solid waste incineration ashes and the impact on a circular economy*. in *Proceedings of the 5th International Slag Valorisation Symposium, Leuven, Belgium*. 2017.
45. Kim, J.-w. *Current Review of DOE's Syngas Technology Development*. in *2017 Syngas Technologies Conference*. 2017. Colorado Springs.
46. Bocci, E., et al., *State of Art of Small Scale Biomass Gasification Power Systems: A Review of the Different Typologies*. Energy Procedia, 2014. **45**: p. 247-256.
47. WPC. *Westinghouse Plasma Gasification is the Next Generation of Energy from Waste Technology*. in *USEA Annual Meeting*. 2013. Washington D.C.
48. Wnukowski, M., *Decomposition of tars in microwave plasma - preliminary results*. Ecological Engineering, 2014. **15**(3): p. 23-28.
49. Messenger, B. *Air Products to Ditch Plasma Gasification Waste to Energy Plants in Teesside*. 2016 May 4.
50. Cothran, C. *Identifying Likely Late-stage UK WTE Projects*. in *2015 Syngas Technologies Conference*. 2015. Colorado Springs: Global Syngas Technologies Conference.
51. E4tech, *Review of technologies for gasification of biomass and wastes*. 2009: Lausanne.
52. Heidenreich, S. and P.U. Foscolo, *New concepts in biomass gasification*. Progress in Energy and Combustion Science, 2015. **46**: p. 72-95.
53. Sentis, L.R., Marco; Barisano, Donatella; Bocci, Enrico; Hamedani, Sara Rajabi; Pallozzi, Vanessa; Tascioni, Roberto, *Techno-economic analysis of UNIFHY hydrogen*. 2016, The Fuel Cells and Hydrogen Joint Undertaking (FCH JU): Brussels.
54. van der Meijden, C.M., H.J. Veringa, and L.P. Rabou, *The production of synthetic natural gas (SNG): A comparison of three wood gasification systems for energy balance and overall efficiency*. Biomass and bioenergy, 2010. **34**(3): p. 302-311.
55. Könemann, J.-W. *Development of biomass and waste gasification towards green chemicals*. in *2017 Syngas Technologies Conference*. 2017. Colorado Springs: Global Syngas Technologies Council.
56. Bhoi, P.R., et al., *Scale-up of a downdraft gasifier system for commercial scale mobile power generation*. Renewable Energy, 2018. **118**: p. 25-33.
57. Henriksen, U., et al., *The design, construction and operation of a 75kW two-stage gasifier*. Energy, 2006. **31**(10-11): p. 1542-1553.
58. Rauch, R., *Steam gasification of biomass at CHP plant Guessing- Status of the demonstration plant*.
59. Burg, R.P.v.d. *Torrefaction and gasification: The alternative by Torrgas: 100% sustainable and technological, economical viable*. in *2015 Gasification Technologies Conference*. 2015. Colorado Springs: Global Syngas Technologies Council.

60. Indrawan, N., et al., *Electricity power generation from co-gasification of municipal solid wastes and biomass: Generation and emission performance* Energy, 2018.
61. Woolcock, P.J. and R.C. Brown, *A review of cleaning technologies for biomass-derived syngas*. Biomass and Bioenergy, 2013. **52**: p. 54-84.
62. Thapa, S., et al., *Effects of syngas cooling and biomass filter medium on tar removal*. Energies, 2017. **10**(3): p. 349.
63. Haga, K., et al., *Poisoning of SOFC anodes by various fuel impurities*. Solid State Ionics, 2008. **179**(27-32): p. 1427-1431.
64. Raman, P. and N.K. Ram, *Performance analysis of an internal combustion engine operated on producer gas, in comparison with the performance of the natural gas and diesel engines*. Energy, 2013. **63**: p. 317-333.
65. Milne, T.A., R.J. Evans, and N. Abatzoglou, *Biomass Gasifier "Tars": Their Nature, Formation, and Conversion*. 1998, National Renewable Energy Laboratory, Golden, CO (US).
66. Belgiorno, V., et al., *Energy from gasification of solid wastes*. Waste Management, 2003. **23**(1): p. 1-15.
67. Baratieri, M., et al., *The use of biomass syngas in IC engines and CCGT plants: A comparative analysis*. Applied Thermal Engineering, 2009. **29**(16): p. 3309-3318.
68. van Biert, L., et al., *A review of fuel cell systems for maritime applications*. Journal of Power Sources, 2016. **327**: p. 345-364.
69. Zobaa, A. and C. Cecati. *A comprehensive review on distributed power generation*. in *Power Electronics, Electrical Drives, Automation and Motion, 2006. SPEEDAM 2006. International Symposium on*. 2006. IEEE.
70. Robb, D. *Flexibility, footprint and reliability advance aeroderivative turbines in a challenging market*. 2017; Available from: <https://www.turbomachinerymag.com/aeroderivative-gas-turbines/>.
71. Caeiro, J.P., Mark; Simmons, John; Tzelepi, Nassia. *Technical Review: Combined Heat and Power System*. 2000; Available from: [http://www.esru.strath.ac.uk/EandE/Web\\_sites/99-00/bio\\_fuel\\_cells/groupproject/library/chp/pageframe.htm](http://www.esru.strath.ac.uk/EandE/Web_sites/99-00/bio_fuel_cells/groupproject/library/chp/pageframe.htm).
72. DOE, U.S., *An Integrated Strategic Plan for the Research, Development, and Demonstration of Hydrogen and Fuel Cell Technologies*. 2011, U.S. Department of Energy: Washington D.C.
73. Hernandez, J.J.B., J.; Aranda, G., *Combustion characterization of producer gas from biomass gasification*. Global Nest, 2012: p. 125-132.
74. EIA. *Natural Gas*. 2016; Available from: [https://www.eia.gov/dnav/ng/ng\\_cons\\_heat\\_a\\_EPG0\\_VGTH\\_btucf\\_a.htm](https://www.eia.gov/dnav/ng/ng_cons_heat_a_EPG0_VGTH_btucf_a.htm).
75. Yang, L., et al., *Premixed jet flame characteristics of syngas using OH planar laser induced fluorescence*. Chinese Science Bulletin, 2011. **56**(26): p. 2862-2868.
76. Davis, L.B.B., S.H., *Dry Low NO<sub>x</sub> Combustion Systems for GE Heavy-Duty Gas Turbines*. GE Power Systems: Schenectady.
77. Gobato, P., M. Masi, and M. Benetti, *Performance Analysis of a Producer Gas-fuelled Heavy-duty SI Engine at Full-load Operation*. Energy Procedia, 2015. **82**: p. 149-155.
78. Bates, R. and K. Dölle, *Syngas Use in Internal Combustion Engines - A Review*. Advances in Research, 2017. **10**(1): p. 1-8.

79. Akansu, S., *Internal combustion engines fueled by natural gas/hydrogen mixtures*. International Journal of Hydrogen Energy, 2004. **29**(14): p. 1527-1539.
80. Sierens, R. and E. Rosseel, *Variable composition hydrogen/natural gas mixtures for increased engine efficiency and decreased emissions*. Journal of engineering for gas turbines and power, 2000. **122**(1): p. 135-140.
81. Bauer, C. and T. Forest, *Effect of hydrogen addition on the performance of methane-fueled vehicles. Part I: effect on SI engine performance*. International Journal of Hydrogen Energy, 2001. **26**(1): p. 55-70.
82. Swain, M.R., et al. *The effects of hydrogen addition on natural gas engine operation*. in *Fall Fuels and Lubricants Meeting and Exposition*. 1993.
83. Caton, J.A., *Combustion phasing for maximum efficiency for conventional and high efficiency engines*. Energy Conversion and Management, 2014. **77**: p. 564-576.
84. Przybyła, G., S. Postrzednik, and Z. Żmudka, *The impact of air-fuel mixture composition on SI engine performance during natural gas and producer gas combustion*. IOP Conference Series: Materials Science and Engineering, 2016. **148**: p. 012082.
85. Korakianitis, T., A.M. Namasivayam, and R.J. Crookes, *Natural-gas fueled spark-ignition (SI) and compression-ignition (CI) engine performance and emissions*. Progress in Energy and Combustion Science, 2011. **37**(1): p. 89-112.
86. Tsiakmakis, S., et al., *Experimental study of combustion in a spark ignition engine operating with producer gas from various biomass feedstocks*. Fuel, 2014. **122**: p. 126-139.
87. Shah, A., et al., *Performance and emissions of a spark-ignited engine driven generator on biomass based syngas*. Bioresour Technol, 2010. **101**(12): p. 4656-61.
88. Homdoun, N., N. Tippayawong, and N. Dussadee, *Performance and emissions of a modified small engine operated on producer gas*. Energy Conversion and Management, 2015. **94**: p. 286-292.
89. Sridhar, G., et al., *Development of producer gas engines*. Proceedings of the Institution of Mechanical Engineers, Part D: Journal of Automobile Engineering, 2005. **219**(3): p. 423-438.
90. Nataraj, K.M., et al., *Development of cooling and cleaning systems for enhanced gas quality for 3.7 kW gasifier-engine integrated system*. International Journal of Engineering, Science and Technology, 2016. **8**(1): p. 43.
91. Mustafi, N., et al., *Spark-ignition engine performance with 'Powergas' fuel (mixture of CO/H<sub>2</sub>): A comparison with gasoline and natural gas*. Fuel, 2006. **85**(12-13): p. 1605-1612.
92. Pareek, D., et al., *Operational experience of agro-residue briquettes based power generation system of 100 kW capacity*. International Journal of Renewable Energy Research (IJRER), 2012. **2**(3): p. 477-485.
93. IEA. *Heat Values of Various Fuels*. 2016; Available from: <http://www.world-nuclear.org/information-library/facts-and-figures/heat-values-of-various-fuels.aspx>.
94. Martínez, J.D., et al., *Syngas production in downdraft biomass gasifiers and its application using internal combustion engines*. Renewable Energy, 2012. **38**(1): p. 1-9.
95. Asadullah, M., *Barriers of commercial power generation using biomass gasification gas: A review*. Renewable and Sustainable Energy Reviews, 2014. **29**: p. 201-215.
96. EPA, U., *Technology characterization: reciprocating engines*. 2008.
97. Energy and Environmental Analysis (EEA), I., *Technology Characterization: Reciprocating Engines*. 2008, Energy and Environmental Analysis (EEA), Inc.: Arlington.

98. Van Basshuysen, R. and F. Schäfer, *Internal combustion engine handbook-basics, components, systems and perspectives*. Vol. 345. 2004.
99. Margaritis, N.K., et al., *Assessment of operational results of a downdraft biomass gasifier coupled with a gas engine*. Procedia-Social and Behavioral Sciences, 2012. **48**: p. 857-867.
100. Heywood, J.B., *Internal combustion engine fundamentals*. 1988.
101. Lee, U., E. Balu, and J.N. Chung, *An experimental evaluation of an integrated biomass gasification and power generation system for distributed power applications*. Applied Energy, 2013. **101**: p. 699-708.
102. Wright, I.G. and T. Gibbons, *Recent developments in gas turbine materials and technology and their implications for syngas firing*. International Journal of Hydrogen Energy, 2007. **32**(16): p. 3610-3621.
103. Dennis, R. *DOE FE Advanced Turbines Program*. in *2017 University Turbine Systems Research Project Review Meeting*. 2017. Pittsburgh: National Energy Technology Laboratory.
104. Karg, J. *Is IGCC a Viable Option for Biomass?* in *Workshop IEA Bioenergy Task 33*. 2016. Lucerne: IEA.
105. Rahm, S., et al., *Addressing gas turbine fuel flexibility*. GER4601, General Electric, 2009.
106. Bierdel, T.B., Patrick; Hagedorn, Thomas. *Life Cycle Value for Combined Cycle Power Plants*. in *PowerGen Asia*. 2013. Bangkok.
107. Fortunato, B., S.M. Camporeale, and M. Torresi, *A Gas-Steam Combined Cycle Powered by Syngas Derived from Biomass*. Procedia Computer Science, 2013. **19**: p. 736-745.
108. Delattin, F., et al., *Combustion of syngas in a pressurized microturbine-like combustor: Experimental results*. Applied Energy, 2010. **87**(4): p. 1441-1452.
109. Cadorin, M., et al., *Analysis of a micro gas turbine fed by natural gas and synthesis gas: MGT test bench and combustor CFD analysis*. Journal of engineering for gas turbines and power, 2012. **134**(7): p. 071401.
110. Rabou, L., et al. *Micro gas turbine operation with biomass producer gas*. in *15th European Biomass Conference & Exhibition*. 2007.
111. Cotana, F., et al., *Comparison of ORC Turbine and Stirling Engine to Produce Electricity from Gasified Poultry Waste*. Sustainability, 2014. **6**(12): p. 5714-5729.
112. Leu, J.-H., *Biomass Power Generation through Direct Integration of Updraft Gasifier and Stirling Engine Combustion System*. Advances in Mechanical Engineering, 2015. **2**: p. 256746.
113. Pop, T.O., I. Vădan, and A. Ceclan. *The cogeneration system based on solid biomass using Stirling engine*. in *Power Engineering Conference (UPEC), 2014 49th International Universities*. 2014. IEEE.
114. Boubaker, K., et al., *Optimizing the energy conversion process: an application to a biomass gasifier-Stirling engine coupling system*. Applied Mathematical Sciences, 2013. **7**: p. 6931-6944.
115. Ferreira, A.C., et al. *Modelling and cost estimation of stirling engine for CHP applications*. in *Proceedings of the 2014 International Conference on Power Systems, Energy, Environment*. ISBN. 2014.
116. Vélez, F., et al., *A technical, economical and market review of organic Rankine cycles for the conversion of low-grade heat for power generation*. Renewable and Sustainable Energy Reviews, 2012. **16**(6): p. 4175-4189.

117. Quoilin, S., et al., *Techno-economic survey of Organic Rankine Cycle (ORC) systems*. Renewable and Sustainable Energy Reviews, 2013. **22**: p. 168-186.
118. Algeri, A. and P. Morrone, *Techno-economic Analysis of Biomass-fired ORC Systems for Single-family Combined Heat and Power (CHP) Applications*. Energy Procedia, 2014. **45**: p. 1285-1294.
119. Nur, T.B., Z. Pane, and M.N. Amin, *Application of Biomass from Palm Oil Mill for Organic Rankine Cycle to Generate Power in North Sumatera Indonesia*. IOP Conference Series: Materials Science and Engineering, 2017. **180**: p. 012035.
120. Buonomano, A., et al., *Hybrid solid oxide fuel cells–gas turbine systems for combined heat and power: A review*. Applied Energy, 2015. **156**: p. 32-85.
121. Kalina, J., *Integrated biomass gasification combined cycle distributed generation plant with reciprocating gas engine and ORC*. Applied Thermal Engineering, 2011. **31**(14-15): p. 2829-2840.
122. Tartière, T. and M. Astolfi, *A World Overview of the Organic Rankine Cycle Market*. Energy Procedia, 2017. **129**: p. 2-9.
123. Chisholm, C. *Syngas Management using Solid Acid Electrochemical Systems: Power/Hydrogen Co-production for Improved Economics*. in *2017 Syngas Technologies Conference*. 2017. Colorado Springs: Global Syngas Technologies Council.
124. Sharaf, O.Z. and M.F. Orhan, *An overview of fuel cell technology: Fundamentals and applications*. Renewable and Sustainable Energy Reviews, 2014. **32**: p. 810-853.
125. Doherty, W., A. Reynolds, and D. Kennedy, *Process simulation of biomass gasification integrated with a solid oxide fuel cell stack*. Journal of Power Sources, 2015. **277**: p. 292-303.
126. Dodds, P.E., et al., *Hydrogen and fuel cell technologies for heating: A review*. International Journal of Hydrogen Energy, 2015. **40**(5): p. 2065-2083.
127. Elgowainy, A. and M. Wang, *Fuel cycle comparison of distributed power generation technologies*. 2008, Argonne National Laboratory (ANL).
128. Harun, N.F., *Fuel composition transients in solid oxide fuel cell gas turbine hybrid systems for polygeneration applications*. 2015.
129. Harun, N.F., et al. *Fuel Utilization Effects on System Efficiency and Solid Oxide Fuel Cell Performance in Gas Turbine Hybrid Systems*. in *ASME Turbo Expo 2017: Turbomachinery Technical Conference and Exposition*. 2017. American Society of Mechanical Engineers.
130. Harun, N.F., D. Tucker, and T.A. Adams II, *Technical challenges in operating an SOFC in fuel flexible gas turbine hybrid systems: Coupling effects of cathode air mass flow*. Applied Energy, 2017. **190**: p. 852-867.
131. Harun, N.F., D. Tucker, and T.A. Adams, *Impact of fuel composition transients on SOFC performance in gas turbine hybrid systems*. Applied Energy, 2016. **164**: p. 446-461.
132. Abreu-Sepulveda, M.A., et al., *Accelerated Degradation for Hardware in the Loop Simulation of Fuel Cell-Gas Turbine Hybrid System*. Journal of Fuel Cell Science and Technology, 2015. **12**(2): p. 021001.
133. Tucker, D., M. Shelton, and A. Manivannan, *The role of solid oxide fuel cells in advanced hybrid power systems of the future*. The Electrochemical Society Interface, 2009. **18**(3): p. 45.

134. Von Spakovsky, M. and B. Olsommer, *Fuel cell systems and system modeling and analysis perspectives for fuel cell development*. Energy Conversion and Management, 2002. **43**(9-12): p. 1249-1257.
135. DOE, U.S. *Solid State Energy Conversion Alliance*. 2012; Available from: <https://www.nrc.gov/docs/ML1409/ML14093A257.pdf>.
136. Curtin, S.G., Jennifer, *State of the States: Fuel Cells in America 2016*. 2016, U.S. Department of Energy: Washington D.C.
137. Phillips, J., *Can Future Coal Power Plants Meet CO2 Emission Standards Without Carbon Capture & Storage?* Electric Power Research Institute, 2015. **16**.
138. EPA, U.S. *Complying with President Trump's Executive Order on Energy Independence*. 2017; Available from: <https://www.epa.gov/energy-independence>.
139. Giuffrida, A., M.C. Romano, and G. Lozza, *Efficiency enhancement in IGCC power plants with air-blown gasification and hot gas clean-up*. Energy, 2013. **53**: p. 221-229.
140. Bang-Møller, C., M. Rokni, and B. Elmegaard, *Exergy analysis and optimization of a biomass gasification, solid oxide fuel cell and micro gas turbine hybrid system*. Energy, 2011. **36**(8): p. 4740-4752.
141. Wirth, S. and J. Markard, *Context matters: How existing sectors and competing technologies affect the prospects of the Swiss Bio-SNG innovation system*. Technological Forecasting and Social Change, 2011. **78**(4): p. 635-649.
142. Narvaez, A., D. Chadwick, and L. Kershenbaum, *Small-medium scale polygeneration systems: Methanol and power production*. Applied Energy, 2014. **113**: p. 1109-1117.
143. Haro, P., et al., *Thermochemical biorefinery based on dimethyl ether as intermediate: Technoeconomic assessment*. Applied Energy, 2013. **102**: p. 950-961.
144. Indrawan, N., et al., *Palm biodiesel prospect in the Indonesian power sector*. Environmental Technology & Innovation, 2017. **7**: p. 110-127.
145. Indrawan, N., et al., *The biogas development in the Indonesian power generation sector*. Environmental Development, 2017.
146. Rong, A. and R. Lahdelma, *Role of polygeneration in sustainable energy system development challenges and opportunities from optimization viewpoints*. Renewable and Sustainable Energy Reviews, 2016. **53**: p. 363-372.
147. Evans, A., V. Strezov, and T.J. Evans, *Sustainability considerations for electricity generation from biomass*. Renewable and Sustainable Energy Reviews, 2010. **14**(5): p. 1419-1427.
148. Kirkels, A.F. and G.P.J. Verbong, *Biomass gasification: Still promising? A 30-year global overview*. Renewable and Sustainable Energy Reviews, 2011. **15**(1): p. 471-481.
149. Worley, M. and J. Yale, *Biomass Gasification Technology Assessment: Consolidated Report*. 2012, National Renewable Energy Laboratory (NREL), Golden, CO.
150. Parks, G.D., et al., *Hydrogen production cost estimate using biomass gasification*. National Renewable Energy Laboratory, Golden, CO, 2011.
151. Tomberlin, G. and G. Mosey, *Feasibility Study of Economics and Performance of Biomass Power Generation at the Former Farmland Industries Site in Lawrence, Kansas. A Study Prepared in Partnership with the Environmental Protection Agency for the RE-Powering America's Land Initiative: Siting Renewable Energy on Potentially Contaminated Land and Mine Sites*. 2013, National Renewable Energy Lab.(NREL), Golden, CO (United States).

152. Murray, B.C., C.S. Galik, and T. Vegh, *Biogas in the United States: estimating future production and learning from international experiences*. Mitigation and Adaptation Strategies for Global Change, 2017. **22**(3): p. 485-501.
153. WPC. *Commercialized and Industrial Scale Plasma Gasification Technology for the Conversion of Various Waste Feedstocks into Clean Energy*. in *Power Gen Asia*. 2015. Bangkok.
154. Faaij, A., et al., *Gasification of biomass wastes and residues for electricity production*. Biomass and Bioenergy, 1997. **12**(6): p. 387-407.
155. Hamelinck, C.N., R.A.A. Suurs, and A.P.C. Faaij, *International bioenergy transport costs and energy balance*. Biomass and Bioenergy, 2005. **29**(2): p. 114-134.
156. McKendry, P., *Energy production from biomass (part 1): overview of biomass*. Bioresource technology, 2002. **83**(1): p. 37-46.
157. Ruiz, J., et al., *Biomass gasification or combustion for generating electricity in Spain: Review of its current situation according to the opinion of specialists in the field*. Journal of Renewable and Sustainable Energy, 2013. **5**(1): p. 012801.
158. Wei, L., et al., *Evaluation of micro-scale electricity generation cost using biomass-derived synthetic gas through modeling*. International Journal of Energy Research, 2011. **35**(11): p. 989-1003.
159. Hite, D., et al., *Consumer willingness-to-pay for biopower: Results from focus groups*. Biomass and bioenergy, 2008. **32**(1): p. 11-17.
160. Elliott, P., *Biomass-energy overview in the context of Brazilian biomass-power demonstration*. Bioresource Technology, 1993. **46**(1-2): p. 13-22.
161. Bridgwater, A.V., *The technical and economic feasibility of biomass gasification for power generation*. Fuel, 1995. **74**(5): p. 631-653.
162. Craig, K.R. and M.K. Mann, *Cost and performance analysis of biomass-based integrated gasification combined-cycle (BIGCC) power systems*. 1996, National Renewable Energy Lab., Golden, CO (United States).
163. Faaij, A., et al., *Externalities of biomass based electricity production compared with power generation from coal in the Netherlands*. Biomass and Bioenergy, 1998. **14**(2): p. 125-147.
164. Gan, J. and C.T. Smith, *A comparative analysis of woody biomass and coal for electricity generation under various CO2 emission reductions and taxes*. Biomass and Bioenergy, 2006. **30**(4): p. 296-303.
165. Bain, R.L., et al., *Biopower technical assessment: State of the industry and the technology*. 2003, National Renewable Energy Lab., Golden, CO.(US).
166. Marbe, Å., S. Harvey, and T. Berntsson, *Biofuel gasification combined heat and power—new implementation opportunities resulting from combined supply of process steam and district heating*. Energy, 2004. **29**(8): p. 1117-1137.
167. Börjesson, M. and E.O. Ahlgren, *Biomass gasification in cost-optimized district heating systems—A regional modelling analysis*. Energy Policy, 2010. **38**(1): p. 168-180.
168. Afgan, N.H., M.G. Carvalho, and M. Jovanovic, *Biomass-fired power plant: the sustainability option*. International journal of sustainable energy, 2007. **26**(4): p. 179-193.
169. Susanto, H., T. Suria, and S. Pranolo. *Economic analysis of biomass gasification for generating electricity in rural areas in Indonesia*. in *IOP Conference Series: Materials Science and Engineering*. 2018. IOP Publishing.

170. Arena, U., F. Di Gregorio, and M. Santonastasi, *A techno-economic comparison between two design configurations for a small scale, biomass-to-energy gasification based system*. Chemical Engineering Journal, 2010. **162**(2): p. 580-590.
171. Buchholz, T., I. Da Silva, and J. Furtado, *Power from wood gasifiers in Uganda: a 250 kW and 10 kW case study*. Proceedings of the Institution of Civil Engineers-Energy, 2012. **165**(4): p. 181-196.
172. EPA, U.S. *Municipal Solid Waste*. 2016; Available from: <https://archive.epa.gov/epawaste/nonhaz/municipal/web/html/>.
173. Tanigaki, N., K. Manako, and M. Osada, *Co-gasification of municipal solid waste and material recovery in a large-scale gasification and melting system*. Waste Manag, 2012. **32**(4): p. 667-75.
174. Patil, K., R. Huhnke, and D. Bellmer. *Performance of a unique downdraft gasifier*. in *ASABE annual international meeting. Portland*. 2006.
175. Gershman, B., *Gasification of Non-Recycled Plastics From Municipal Solid Waste In the United States*. 2013.
176. Agon, N., *Development and study of different numerical plasma jet models and experimental study of plasma gasification of waste*. 2015, Ghent University.
177. Willis, K.P., S. Osada, and K.L. Willerton. *Plasma gasification: lessons learned at Eco-Valley WTE facility*. in *18th Annual North American Waste-to-Energy Conference*. 2010. American Society of Mechanical Engineers.
178. EREF, *Analysis of MSW Landfill Tipping Fees 2018*, Environmental Research and Education Foundation: Raleigh. p. 1-5.
179. Heberlein, J. and A.B. Murphy, *Thermal plasma waste treatment*. Journal of Physics D: Applied Physics, 2008. **41**(5): p. 053001.
180. Arsalis, A., *Thermoeconomic modeling and parametric study of hybrid SOFC–gas turbine–steam turbine power plants ranging from 1.5 to 10 MWe*. Journal of Power Sources, 2008. **181**(2): p. 313-326.
181. Zhou, N., V. Zaccaria, and D. Tucker, *Fuel composition effect on cathode airflow control in fuel cell gas turbine hybrid systems*. Journal of Power Sources, 2018. **384**: p. 223-231.
182. Wilson, B., *Comparative assessment of gasification and incineration in integrated waste management systems*. EnviroPower Renewable, Boca Raton, 2014.
183. Management, W., *Leading Change: 2016 Sustainability Report*. 2016, Waste Management (WM): Houston.
184. Cox, S., et al., *Distributed generation to support development-focused climate action*. 2016, National Renewable Energy Lab.(NREL), Golden, CO (United States).
185. Cody, B. *Roll-out of commercial biorefineries*. in *2017 Syngas Technologies Conference*. 2017. Colorado Springs: Global Syngas Technologies Council.
186. Cody, B. *Think Smaller: microchannel Fischer-Tropsch enables biomass-to-liquids*. in *2015 Syngas Technologies Conference*. 2015. Colorado Springs: Global Syngas Technologies Council.
187. Mustapha, Z., C. Aigbavboa, and W.D. Thwala, *Assessment of atmospheric pollution reduction: challenging issue for developing countries*. 2015.
188. Ruth, L.A., *Energy from municipal solid waste: a comparison with coal combustion technology*. Progress in Energy and Combustion Science, 1998. **24**(6): p. 545-564.

189. Lonati, G. and F. Zanoni, *Probabilistic health risk assessment of carcinogenic emissions from a MSW gasification plant*. Environ Int, 2012. **44**: p. 80-91.
190. Taylor, M.R., E.S. Rubin, and D.A. Hounshell, *Control of SO<sub>2</sub> emissions from power plants: A case of induced technological innovation in the U.S.* Technological Forecasting and Social Change, 2005. **72**(6): p. 697-718.
191. EPA, U.S. *Mercury and Air Toxics Standards: Cleaner Power Plant*. 2016; Available from: <https://www.epa.gov/mats/cleaner-power-plants>.
192. Brown, T.D., et al., *Control of mercury emissions from coal-fired power plants: a preliminary cost assessment and the next steps for accurately assessing control costs*. Fuel Processing Technology, 2000. **65**: p. 311-341.
193. Zaman, A.U., *Comparative study of municipal solid waste treatment technologies using life cycle assessment method*. International Journal of Environmental Science & Technology, 2010. **7**(2): p. 225-234.
194. Center, C.A.T., *Nitrogen oxides (NO<sub>x</sub>), why and how they are controlled*. 1999, U.S. Environmental Protection Agency Research Triangle Park.
195. Caton, J.A., *The thermodynamic characteristics of high efficiency, internal-combustion engines*. Energy Conversion and Management, 2012. **58**: p. 84-93.
196. Pereira, M.d.S., *Polychlorinated dibenzo-p-dioxins (PCDD), dibenzofurans (PCDF) and polychlorinated biphenyls (PCB): main sources, environmental behaviour and risk to man and biota*. Química Nova, 2004. **27**(6): p. 934-943.
197. Dyke, P., P. Coleman, and R. James, *Dioxins in ambient air, bonfire night 1994*. Chemosphere, 1997. **34**(5-7): p. 1191-1201.
198. Kulkarni, P.S., J.G. Crespo, and C.A. Afonso, *Dioxins sources and current remediation technologies--a review*. Environ Int, 2008. **34**(1): p. 139-53.
199. Dopico, M. and A. Gomez, *Review of the current state and main sources of dioxins around the world*. J Air Waste Manag Assoc, 2015. **65**(9): p. 1033-49.
200. Addink, R. and K. Olie, *Role of oxygen in formation of polychlorinated dibenzo-p-dioxins/dibenzofurans from carbon on fly ash*. Environmental science & technology, 1995. **29**(6): p. 1586-1590.
201. Buekens, A., et al., *Fingerprints of dioxin from thermal industrial processes*. Chemosphere, 2000. **40**(9-11): p. 1021-1024.
202. UCR, *Evaluation of Emissions from Thermal Conversion Technologies Processing Municipal Solid Waste and Biomass*. 2009, University of California, Riverside: Los Angeles.
203. Wielgosiński, G., *The Reduction of Dioxin Emissions from the Processes of Heat and Power Generation*. Journal of the Air & Waste Management Association, 2011. **61**(5): p. 511-526.
204. Lundin, L. and S. Jansson, *The effects of fuel composition and ammonium sulfate addition on PCDD, PCDF, PCN and PCB concentrations during the combustion of biomass and paper production residuals*. Chemosphere, 2014. **94**: p. 20-6.
205. Łechtańska, P. and G. Wielgosiński, *The use of ammonium sulfate as an inhibitor of dioxin synthesis in iron ore sintering process*. Ecological Chemistry and Engineering S, 2014. **21**(1).
206. UNEP, *Guidelines on best available techniques and provisional guidance on best environmental practices relevant to Article 5 and Annex C of the Stockholm Convention on Persistent Organic Pollutants*. 2008, United Nations Environment Programme: Geneva.

207. Yoshida, K., et al., *Pilot-Scale Experiment for Simultaneous Dioxin and NO<sub>x</sub> Removal from Garbage Incinerator Emissions Using the Pulse Corona Induced Plasma Chemical Process*. Plasma Chemistry and Plasma Processing, 2009. **29**(5): p. 373-386.
208. Kamińska-Pietrzak, N. and A. Smoliński, *Selected Environmental Aspects of Gasification and Co-Gasification of Various Types of Waste*. Journal of Sustainable Mining, 2013. **12**(4): p. 6-13.
209. Nifuku, M., et al., *A study on the decomposition of volatile organic compounds by pulse corona*. Journal of Electrostatics, 1997. **40**: p. 687-692.
210. Obata, S. and H. Fujihira, *Dioxin and NO<sub>x</sub> Control Using Pilot-Scale Pulsed Corona Plasma Technology*. Combustion Science and Technology, 1998. **133**(1-3): p. 3-11.
211. Zhou, Y.X., et al., *Application of non-thermal plasmas on toxic removal of dioxin-contained fly ash*. Powder Technology, 2003. **135-136**: p. 345-353.
212. Mitoma, Y., et al., *Approach to highly efficient dechlorination of PCDDs, PCDFs, and coplanar PCBs using metallic calcium in ethanol under atmospheric pressure at room temperature*. Environmental science & technology, 2004. **38**(4): p. 1216-1220.
213. Anis, S. and Z.A. Zainal, *Tar reduction in biomass producer gas via mechanical, catalytic and thermal methods: A review*. Renewable and Sustainable Energy Reviews, 2011. **15**(5): p. 2355-2377.
214. Stevenson, W., *Emissions from Large and Small MWC Units at MACT Compliance*. US EPA Memo to Large MWC Docket (EPA-HQ-OAR-2005-0117), Research Triangle Park, North Carolina, 2007.
215. Themelis, N.J., *Thermal treatment*. Waste Management World, 2007: p. 37.
216. Lauber, J., *Comparative Impacts of Local Waste to Energy Versus Long Distance Disposal of Municipal Waste 3 (2006)*.
217. Lauber, J., et al. *Local waste-to-energy vs. long distance disposal of municipal waste*. in *AWMA Conference, June 21, 2006, New Orleans, Louisiana*. 2006.
218. Wilson, B., et al., *A comparative assessment of commercial technologies for conversion of solid waste to energy*. EnviroPower Renewable, Boca Raton Google Scholar, 2013.
219. Pourali, M., *Application of Plasma Gasification Technology in Waste to Energy—Challenges and Opportunities*. IEEE Transactions on Sustainable Energy, 2010. **1**(3): p. 125-130.
220. Materazzi, M., et al., *Tar evolution in a two stage fluid bed–plasma gasification process for waste valorization*. Fuel Processing Technology, 2014. **128**: p. 146-157.
221. IEA, *Energy Access Outlook 2017 from Poverty to Prosperity*. 2017, International Energy Agency: Paris. p. 1-144.
222. Patil, K.N., R.L. Huhnke, and D.D. Bellmer, *Downdraft Gasifier with Internal Cyclonic Combustion Chamber*. 2014, US Patent and Trademark Office.
223. Dayton, D.C., B. Turk, and R. Gupta, *Syngas cleanup, conditioning, and utilization*. Thermochemical Processing of Biomass: Conversion into Fuels, Chemicals and Power, 2011: p. 78-123.
224. Good, J., et al., *Sampling and analysis of tar and particles in biomass producer gases*. Technical Report CEN BT/TF, 2005. **143**.
225. Tinaut, F.V., et al., *Method for predicting the performance of an internal combustion engine fuelled by producer gas and other low heating value gases*. Fuel Processing Technology, 2006. **87**(2): p. 135-142.

226. Ahrenfeldt, J., *Characterization of biomass producer gas as fuel for stationary gas engines in combined heat and power production*. MED, DTU. Kgs. Lyngby: sn, 2007: p. 127.
227. O'Rourke, N., R. Psych, and L. Hatcher, *A step-by-step approach to using SAS for factor analysis and structural equation modeling*. 2013: Sas Institute.
228. Chen, J. and B. Young, *Stress-strain curves for stainless steel at elevated temperatures*. Engineering Structures, 2006. **28**(2): p. 229-239.
229. Arroyo, J., et al., *Combustion behavior of a spark ignition engine fueled with synthetic gases derived from biogas*. Fuel, 2014. **117**: p. 50-58.
230. Szwaja, S., *Hydrogen rich gases combustion in the IC engine*. Journal of KONES, 2009. **16**: p. 447-454.
231. Kahraman, N., et al., *Investigation of combustion characteristics and emissions in a spark-ignition engine fuelled with natural gas-hydrogen blends*. International Journal of Hydrogen Energy, 2009. **34**(2): p. 1026-1034.
232. Sridhar, G., P. Paul, and H. Mukunda, *Biomass derived producer gas as a reciprocating engine fuel—an experimental analysis*. Biomass and Bioenergy, 2001. **21**(1): p. 61-72.
233. Frenkel, M., et al., *ThermoData Engine (TDE): software implementation of the dynamic data evaluation concept*. Journal of chemical information and modeling, 2005. **45**(4): p. 816-838.
234. Musculus, M.P.B., P.C. Miles, and L.M. Pickett, *Conceptual models for partially premixed low-temperature diesel combustion*. Progress in Energy and Combustion Science, 2013. **39**(2-3): p. 246-283.
235. Homdoun, N., N. Tippayawong, and N. Dussadee, *Performance and emissions of a modified small engine operated on producer gas*. Energy conversion and management, 2015: p. 286-292.
236. Sridhar, G., et al., *Development of producer gas engines*. Automobile Engineering, 2005. **219**: p. 423-438.
237. Shah, A., et al., *Performance and emissions of a spark-ignited engine driven generator on biomass based syngas*. Bioresource Technology, 2010: p. 4656-4661.
238. Bracmort, K. *Is Biopower Carbon Neutral?* 2011. Congressional Research Service, Library of Congress.
239. Abdel-Rahman, A., *On the emissions from internal-combustion engines: a review*. International Journal of Energy Research, 1998. **22**(6): p. 483-513.
240. Featherman, W.D., *Bioenergy in the Public Sector*. 2015, University of California Berkeley.
241. Suh, H.H., et al., *Criteria air pollutants and toxic air pollutants*. Environmental Health Perspectives, 2000. **108**(Suppl 4): p. 625.
242. Wark, K., C.F. Warner, and W.T. Davis, *Air Pollution Its Origin and Control* 1998, Addison Wesley Longman.
243. Yasar, A., et al., *A comparison of engine emissions from heavy, medium, and light vehicles for CNG, diesel, and gasoline fuels*. Pol. J. Environ. Stud, 2013. **22**(4): p. 1277-1281.
244. EPA, U.S., *Advancing Sustainable Materials Management: 2014 Fact Sheet*. 2016, U.S. Environmental Protection Agency: Washington, D.C.
245. Vodyanitskii, Y.N., *Biochemical processes in soil and groundwater contaminated by leachates from municipal landfills (Mini review)*. Annals of Agrarian Science, 2016. **14**(3): p. 249-256.
246. Davoli, E., et al., *Characterisation of odorants emissions from landfills by SPME and GC/MS*. Chemosphere, 2003. **51**(5): p. 357-368.

247. McKay, G., *Dioxin characterisation, formation and minimisation during municipal solid waste (MSW) incineration*. Chemical Engineering Journal, 2002. **86**(3): p. 343-368.
248. Howard, W. *Plasma Gasification for Generating Syngas to GTL*. in *2017 Syngas Technologies Conference*. 2017. Colorado Springs: Global Syngas Gasification Technologies.
249. GSTC. *Pune Waste Gasification Plant*. 2017; Available from: <http://www.gasification-syngas.org/resources/world-gasification-database/pune-waste-gasification-plant>.
250. Arafat, H.A. and K. Jijakli, *Modeling and comparative assessment of municipal solid waste gasification for energy production*. Waste Manag, 2013. **33**(8): p. 1704-13.
251. Couto, N., et al., *Numerical and experimental analysis of municipal solid wastes gasification process*. Applied Thermal Engineering, 2015. **78**: p. 185-195.
252. Cormos, C.-C., *Hydrogen and power co-generation based on coal and biomass/solid wastes co-gasification with carbon capture and storage*. International Journal of Hydrogen Energy, 2012. **37**(7): p. 5637-5648.
253. Eghtedaei, R., et al., *Co-gasification of biomass and municipal solid waste for hydrogen-rich gas production*. Energy Sources, Part A: Recovery, Utilization, and Environmental Effects, 2017. **39**(14): p. 1491-1496.
254. Couto, N.D., V.B. Silva, and A. Rouboa, *Assessment on steam gasification of municipal solid waste against biomass substrates*. Energy Conversion and Management, 2016. **124**: p. 92-103.
255. Patil, K., et al., *Biomass downdraft gasifier with internal cyclonic combustion chamber: design, construction, and experimental results*. Bioresour Technol, 2011. **102**(10): p. 6286-90.
256. Mahinpey, N. and A. Gomez, *Review of gasification fundamentals and new findings: Reactors, feedstock, and kinetic studies*. Chemical Engineering Science, 2016. **148**: p. 14-31.
257. Onar, O.C., M. Uzunoglu, and M.S. Alam, *Modeling, control and simulation of an autonomous wind turbine/photovoltaic/fuel cell/ultra-capacitor hybrid power system*. Journal of Power Sources, 2008. **185**(2): p. 1273-1283.
258. Cho, H.M. and B.-Q. He, *Spark ignition natural gas engines—A review*. Energy Conversion and Management, 2007. **48**(2): p. 608-618.
259. Trapp, C. *Lean-burn or rich-burn?* 2013.
260. Raptotasios, S.I., et al., *Application of a multi-zone combustion model to investigate the NOx reduction potential of two-stroke marine diesel engines using EGR*. Applied Energy, 2015. **157**: p. 814-823.
261. Whitty, K.J., H.R. Zhang, and E.G. Eddings, *Emissions from Syngas Combustion*. Combustion Science and Technology, 2008. **180**(6): p. 1117-1136.
262. Obama, B., *The irreversible momentum of clean energy*. Science, 2017. **355**(6321): p. 126-129.
263. Henze, V., *Runaway 53GW Solar Boom in China Pushed Global Clean Energy Investment Ahead in 2017*. 2018, Bloomberg New Energy Finance.
264. Donohoo-Vallett, P., *Revolution... Now The Future Arrives for Five Clean Energy Technologies—2016 Update*. 2016, DOE, EERE.
265. Ahmad, A.A., et al., *Assessing the gasification performance of biomass: A review on biomass gasification process conditions, optimization and economic evaluation*. Renewable and Sustainable Energy Reviews, 2016. **53**: p. 1333-1347.

266. Ong, K.M. and A.F. Ghoniem, *Modeling of indirect carbon fuel cell systems with steam and dry gasification*. Journal of Power Sources, 2016. **313**: p. 51-64.
267. Galeno, G., M. Minutillo, and A. Perna, *From waste to electricity through integrated plasma gasification/fuel cell (IPGFC) system*. International Journal of Hydrogen Energy, 2011. **36**(2): p. 1692-1701.
268. Zaccaria, V., D. Tucker, and A. Traverso, *A distributed real-time model of degradation in a solid oxide fuel cell, part I: Model characterization*. Journal of Power Sources, 2016. **311**: p. 175-181.
269. Zaccaria, V., D. Tucker, and A. Traverso, *A distributed real-time model of degradation in a solid oxide fuel cell, part II: Analysis of fuel cell performance and potential failures*. Journal of Power Sources, 2016. **327**: p. 736-742.
270. Edenhofer, O., et al., *Renewable energy sources and climate change mitigation: Special report of the intergovernmental panel on climate change*. 2011: Cambridge University Press.
271. Moriarty, K., *Feasibility Study of Biopower in East Helena, Montana. A Study Prepared in Partnership with the Environmental Protection Agency for the RE-Powering America's Land Initiative: Siting Renewable Energy on Potentially Contaminated Land and Mine Sites*. 2013, National Renewable Energy Lab.(NREL), Golden, CO (United States).
272. Nderitu, D.G.P., Paul V.; Gotham, Douglas J.; Dobis, Elizabeth A., *Assessment of the National Prospects for Electricity Generation from Biomass*. 2014, U.S. Department of Agriculture: West Lafayette.
273. Office of Energy Efficiency & Renewable Energy (EERE), U.S.D.o.E. *Feed-in Tariff Resources*. 2018; Available from: <https://www.energy.gov/eere/slsc/feed-tariff-resources>.
274. Roddy, D.J., *A syngas network for reducing industrial carbon footprint and energy use*. Applied Thermal Engineering, 2013. **53**(2): p. 299-304.
275. Simkins, B. and R. Simkins, *Energy finance and economics: Analysis and valuation, risk management, and the future of energy*. Vol. 606. 2013: John Wiley & Sons.
276. Besley, S. and E.F. Brigham, *Essentials of managerial finance*. 2000: South-Western Pub.
277. Minimum-Wage. *Oklahoma Minimum Wage for 2017, 2018* 2018; Available from: <https://www.minimum-wage.org/oklahoma>.
278. County, H.M.M.F.o.B. *Hazardous Waste Disposal Costs for Businesses*. 2018 [cited 2018 Oct 25th]; Available from: <https://www.bouldercounty.org/environment/hazardous-waste/disposal-costs-for-businesses/>.
279. Langholtz, M.H., et al., *2016 Billion-ton report: Advancing domestic resources for a thriving bioeconomy, volume 1: Economic availability of feedstocks*. 2016, Oak Ridge National Lab.(ORNL), Oak Ridge, TN (United States).
280. Kenney, K. *Idaho Researchers Slash Cost of Providing Biomass for Biofuels Production*. 2018; Available from: <https://www.energy.gov/eere/bioenergy/articles/idaho-researchers-slash-cost-providing-biomass-biofuels-production>.
281. Investopedia. *Weighted Average Cost of Capital (WACC)*. 2018 Sept 25, 2018]; Available from: <https://www.investopedia.com/walkthrough/corporate-finance/5/cost-capital/wacc.aspx>.
282. L.P., B.F., *Cost of Capital - Current Market Value*. 2018, Bloomberg Finance L.P.
283. Energy, U.S.D.o. *Modified Accelerated Cost-Recovery System (MACRS)*. 2018 [cited 2018; Available from: <https://www.energy.gov/savings/modified-accelerated-cost-recovery-system-macrs>.

284. IRS. *Publication 946 (2017), How To Depreciate Property*. 2018 [cited 2018; Available from: <https://www.irs.gov/publications/p946>].
285. EIA. *Electricity*. 2018 [cited 2018 Sept 25]; Available from: <https://www.eia.gov/electricity/data.php>.
286. Couture, T. and K. Cory, *State Clean Energy Policies Analysis (SCEPA) Project: An Analysis of Renewable Energy Feed-in Tariffs in the United States (Revised)*. 2009, National Renewable Energy Laboratory (NREL), Golden, CO.
287. Ruiz, J.A., et al., *Biomass gasification for electricity generation: Review of current technology barriers*. *Renewable and Sustainable Energy Reviews*, 2013. **18**: p. 174-183.
288. Gomez, E., et al., *Thermal plasma technology for the treatment of wastes: a critical review*. *J Hazard Mater*, 2009. **161**(2-3): p. 614-26.
289. Simkins, G. and L. Walsh, *Reasons for TVI failure revealed*. 2016, ENDS Report: Twickenham.
290. Fridman, A., *Plasma chemistry*. 2008: Cambridge university press.
291. Minutillo, M., A. Perna, and D. Di Bona, *Modelling and performance analysis of an integrated plasma gasification combined cycle (IPGCC) power plant*. *Energy Conversion and Management*, 2009. **50**(11): p. 2837-2842.
292. Janajreh, I., S.S. Raza, and A.S. Valmundsson, *Plasma gasification process: Modeling, simulation and comparison with conventional air gasification*. *Energy Conversion and Management*, 2013. **65**: p. 801-809.
293. Roth, J.R., *Industrial Plasma Engineering: Volume 2-Applications to Nonthermal Plasma Processing*. Vol. 2. 2001: CRC press.
294. Mountouris, A., E. Voutsas, and D. Tassios, *Solid waste plasma gasification: Equilibrium model development and exergy analysis*. *Energy Conversion and Management*, 2006. **47**: p. 1723-1737.
295. Altafini, C.R. and R.M.B. P.R. Wander, *Prediction of the working parameters of a wood waste gasifier through an equilibrium model*. *Energy Conversion and Management*, 2003. **44**: p. 2763-2777.
296. Calaminus, B. and R. Stahlberg, *Continuous in-line gasification/vitrification process for thermal waste treatment: process technology and current status of projects*. *Waste Management*, 1998. **18**(6-8): p. 547-556.
297. Chen, G., et al., *Biomass pyrolysis/gasification for product gas production: the overall investigation of parametric effects*. *Energy conversion and management*, 2003. **44**(11): p. 1875-1884.
298. Benilov, M. and G. Naidis, *Modeling of hydrogen-rich gas production by plasma reforming of hydrocarbon fuels*. *International Journal of Hydrogen Energy*, 2006. **31**(6): p. 769-774.
299. Bhoi, P.R., et al., *Co-gasification of Municipal Solid Waste and Biomass in a Commercial Scale Downdraft Gasifier*. *Energy*, 2018.
300. IEA, *Power Generation from Coal*. International Energy Agency, 2010.
301. Han, J. and H. Kim, *The reduction and control technology of tar during biomass gasification/pyrolysis: an overview*. *Renewable and sustainable energy reviews*, 2008. **12**(2): p. 397-416.
302. Zhang, Y., et al., *Tar destruction and coke formation during rapid pyrolysis and gasification of biomass in a drop-tube furnace*. *Fuel*, 2010. **89**(2): p. 302-309.

303. Benilov, M.S. and G.V. Naidis, *Modeling of hydrogen-rich gas production by plasma reforming of hydrocarbon fuels*. International Journal of Hydrogen Energy, 2006. **31**: p. 769–774.
304. Panopoulos, K.D., et al., *High temperature solid oxide fuel cell integrated with novel allothermal biomass gasification*. Journal of Power Sources, 2006. **159**(1): p. 570-585.
305. Olson, A., U.N.: *World population to reach 8.1B in 2025*. 2013.
306. EPA, U.S., *Historic Tipping Fees and Commodity Values U.S. Environmental Protection Agency Office of Resource Conservation and Recovery*. 2015, U.S. Environmental Protection Agency.
307. Gomez, E., et al., *Thermal plasma technology for the treatment of wastes: A critical review*. Hazardous Materials, 2009. **161**: p. 614-626.
308. Cothran, C., *Identifying Likely Late-stage UK WTE Projects*. 2015, Gasification Technology Council: Colorado Springs, Colorado, USA.
309. Zogg, R., et al., *Using Internal-Combustion Engines For Distributed Generation*. ASHRAE Journal, 2007: p. 76-80.
310. Proctor, D., *PowerMag*. 2018, Power Magazine.
311. EG&G Technical Services, I., *Fuel Cell Handbook DEAM26-99FT40575*, US Department of Energy, Office of Fossil Energy, National Energy Technology Laboratory, Morgantown, West Virginia, USA, 2004.
312. Harun, N.F., D. Tucker, and T.A.A. II, *Impact of fuel composition transients on SOFC performance in gas turbine hybrid systems*. Applied Energy, 2016. **164**: p. 446-461.
313. Minutillo, M., A. Perna, and D.D. Bona, *Modelling and performance analysis of an integrated plasma gasification combined cycle (IPGCC) power plant*. Energy Conversion and Management, 2009: p. 2837-2842.
314. Janajreh, I., S.S. Raza, and A.S. Valmundsson, *Plasma gasification process: Modelling, simulation and comparison with conventional air gasification*. Energy Conversion and Management, 2013: p. 801-809.
315. Galeno, G., M. Minutillo, and A. Perna, *From waste to electricity through integrated plasma gasification/fuel cell (IPGFC) system*. Hydrogen Energy, 2011: p. 1692-1701.
316. Ali, A., *ce25 Overview mobile energy and detoxification system*. 2015, ARC Southern Energy, LLC: Houston. p. 1-22.
317. Boldrin, P., M. Millan-Agorio, and N.P. Brandon, *Effect of sulfur-and tar-contaminated syngas on solid oxide fuel cell anode materials*. Energy & Fuels, 2014. **29**(1): p. 442-446.
318. Hughes, D., et al. *A real-time spatial SOFC model for hardware-based simulation of hybrid systems*. in *ASME 2011 9th International Conference on Fuel Cell Science, Engineering and Technology collocated with ASME 2011 5th International Conference on Energy Sustainability*. 2011. American Society of Mechanical Engineers.
319. McLarty, D., J. Brouwer, and S. Samuelsen, *Fuel cell–gas turbine hybrid system design part II: Dynamics and control*. Journal of Power Sources, 2014. **254**: p. 126-136.
320. Gunji, A., et al., *Carbon deposition behaviour on Ni–ScSZ anodes for internal reforming solid oxide fuel cells*. Journal of power sources, 2004. **131**(1-2): p. 285-288.
321. Murray, E.P., T. Tsai, and S. Barnett, *A direct-methane fuel cell with a ceria-based anode*. Nature, 1999. **400**(6745): p. 649.

## Appendices

**Appendix 1.** Example of electrical efficiency calculation:

Electrical efficiency = electrical power output / (LHV x  $Q_m$ )

Where: LHV is low heating value of syngas (MJ/Nm<sup>3</sup>), and  $Q_m$  is the flow rate of air-fuel mixture (m<sup>3</sup>/h).

If the electrical load was 5 kW, with syngas flowrate of 8.92 scfm (~15.1 m<sup>3</sup>/h), and syngas LHV of 6.2 MJ/Nm<sup>3</sup> (~168 Btu/ft<sup>3</sup>), therefore, the electrical efficiency:

$$= (5 \text{ kW} / (8.92 \text{ ft}^3/\text{min} \times 168 \text{ Btu}/\text{ft}^3 \times 60 \text{ min}/\text{h})) \times 3412.1 \text{ Btu}/\text{kWh}$$

$$= 0.1897 \text{ (~18.97\%)}$$

## VITA

NATARIANTO INDRAWAN

Candidate for the Degree of  
Doctor of Philosophy

Thesis: ADVANCED BIOPOWER GENERATION VIA GASIFICATION OF  
BIOMASS AND MUNICIPAL SOLID WASTE

Major Field: Environmental Science

### **Biographical:**

#### Education:

Completed the requirements for the Doctor of Philosophy in Environmental Science at Oklahoma State University, Stillwater, Oklahoma in December, 2018.

Completed the requirements for the Master of Engineering in Interdisciplinary Program of Bioenergy and Biomaterials Engineering at Chonnam National University, Gwangju, South Korea in 2012.

Completed the requirements for the Bachelor of Engineering in Gas and Petrochemical Engineering at Universitas Indonesia, Depok, Indonesia in 2002.

#### Experience:

Research Assistant, Gasification and Thermochemical Conversion Laboratory, Oklahoma State University, Stillwater, Oklahoma, May 2015 to Present.

Research Assistant, Bioenergy and Biomaterials Engineering, Chonnam National University, Gwangju, South Korea, February 2011 to August 2012.

#### Professional Memberships:

American Institute of Chemical Engineers (AIChE)